



**TECHNICAL UNIVERSITY OF CRETE**  
**DEPARTMENT OF ENVIRONMENTAL ENGINEERING**  
**POST GRADUATE STUDIES PROGRAME:**  
**“ENVIRONMENTAL AND SANITARY ENGINEERING”**

**LABORATORY OF HYDROGEOCHEMICAL ENGINEERING AND  
REMEDICATION OF SOILS**

**Ph.D. DISSERTATION**

**CARBON AND NITROGEN CYCLING IN AGRICULTURAL LANDS**

**FOTINI E. STAMATI**

**ENVIRONMENTAL ENGINEER, MSc**

**CHANIA**

**APRIL 2012**



**Defense committee members:**

1. Prof. Nikolaos P. Nikolaidis, Technical University of Crete (supervisor)
  
2. Prof. Nicolas Kalogerakis, Technical University of Crete (advisory committee)
  
3. Assoc. Prof. Eleftheria Psillakis, Technical University of Crete (advisory committee)
  
4. Prof. George Karatzas, Technical University of Crete
  
5. Lect. Nikolaos Paranychianakis, Technical University of Crete
  
6. Ass. Prof. Marina Pantazidou, National Technical University of Athens
  
7. Prof. Jerald P. Schnoor, The University of Iowa



## ACKNOWLEDGEMENTS

I would like to express my gratitude and thanks to all people who made this thesis possible.

First and foremost I would like to express my deep and sincere gratitude to my supervisor, Professor Nikolaos Nikolaidis, Director of the Hydro-geochemical Engineering and Remediation of Soils Laboratory (HERS LAB), Environmental Engineering Department, Technical University of Crete (TUC). His wide knowledge and his holistic way of thinking have been of great value to me. I appreciate all his contributions of time, ideas, guidance, support, and funding to make my Ph.D. experience productive and stimulating.

I would like to express my gratitude to the members of the advisory committee Assoc. Prof. Eleftheria Psillakis, TUC and Prof. Nicolas Kalogerakis, TUC for their advice and their time to evaluate the thesis. I also owe my deepest gratitude to Prof. Jerald P. Schnoor, The University of Iowa, member of my defense committee for his kind hospitality, good advising and insightful discussions during my time at The University of Iowa (November 2008 to May 2009). I would also like to thank the members of my defense committee, Prof. George Karatzas, TUC and Lect. Nikolaos Paranychianakis, TUC for their time to evaluate the thesis and insightful questions and discussions. Finally, I owe my gratitude to the external member of my defense committee Ass. Prof. Marina Pantazidou, National Technical University of Athens for the specific comments she made on the text of the thesis.

I am also grateful to the colleagues working or have worked in the HERS LAB for their collaboration all these years. I would like to thank Dr. Daniel Moraetis and Manolis Kotronakis as well as Tasoula Fragia and Tzina Kaliakatsou for their valuable help on soil sampling in Koiliaris River Basin and the insightful discussions we had. My gratitude is also expressed to Pantelis Karagiannakis for his kind help on finding fallow fields and soil sampling in Koiliaris River Basin. I would like also to thank Lect. Danae Venieri, TUC and Ariadni Pantidou, TUC for their help in microbiological analysis. I would also like to express my gratitude to Collin Just, Aaron Gwinnup, and Prof. Thanos Papanikolaou from the University of Iowa for their help during the soil sampling and laboratory work in

Iowa. I also wish to thank all the colleagues of the research project SoilTREC (<http://www.soiltrec.eu/>) and especially Prof. Steve Banwart, Prof. Winfried Blum, Dr. Panos Panagos, and Dr. Ece Aksoy for their collaboration and insightful discussions. I would like also to mention that this thesis has been greatly improved thanks to the comments of the anonymous reviewers and editors of the articles published with contributions of this dissertation.

I gratefully acknowledge the funding sources that made my Ph.D. work possible. I was funded by the Technical University of Crete (Soil Critical Zone and SoilTREC research projects) and the University of Iowa. My work was also supported by the Bodossakis Foundation.

I owe loving thanks to my friends for their encouragement, understanding, and support all these years. I would like to thank my friends Prof. Takis Poulakos, Sofia Karatza and Dimitris Dermisis for making my stay in Iowa City enjoyable. My gratitude is due also to Crysoula Zaxariadi, Katerina Valta, Nikos Chalkias, Manolis Kotronakis, Pamela Sklepa, Alekos Michailidis, Joseph Psistakis, and Mirto Tsiknia for their endless friendship. My special gratitude is also due to Panagiotis Amitzoglou and Thanasis Papadopoulos for the great will and strength they show in their personal 'fight', being an example for us.

Lastly, I would like to thank my Grandfather Kostas Charitakis, my Aunts Areti Charitaki and Nikoleta Stamati, my Uncle Andreas Andreopoulos for being close to my family and supporting us, more than ever the last year in which my mom passed away.

Fotini E. Stamati  
February, 2012-02-01  
Technical University of Crete

*DEDICATION*

*This thesis is dedicated to my Father Evangelos Stamatis, my Brother Kostas Stamatis and to the holy memory of my mother Aglaia*



## ABSTRACT

Current management of soil has been recognized to be unsustainable. In the next 20-50 years, the pressures on soil and its core service functions are predicted to further increase, due to climate change (droughts, extreme precipitation events) and competing demands from production systems to provide food, biofuel and timber. It is of prime importance to re-evaluate current agricultural practices and develop alternative sustainable soil farming management systems that protect ecological functions of soil. There is urgent need for tools and methodologies that will give reliable predictions for climate change effects and restoration management to evaluate alternatives. The objective of this dissertation was to improve our understanding of the mechanisms of nutrient cycling and organic matter (SOM) protection/loss in soils and provide tools that can be used to assist the sustainable functioning of soil critical zone.

The scientific issues researched in this thesis can be summarized in the following objectives:

- **Assessment methodology for soil carbon simulation**: Develop and validate with field data a methodology for RothC model parameter estimation, through initialization and calibration with field derived physical fractionation data, assessment of the uniqueness of solution, sensitivity analysis and quantification of uncertainties in modeling results.
- **Testing of soil model across climatic gradient**: Apply the developed methodology to native land to cropland conversions along an international climatic gradient to assess the pattern of carbon loss and the effectiveness of carbon addition, sensitivity analysis and quantify the uncertainties.
- **Develop soil structure model**: Develop and validate with field data a coupled soil carbon (RothC), aggregation, and structure turnover model, based on the current knowledge of the proposed mechanism in the relevant scientific literature that suggests that macro-aggregates are formed around particulate organic matter, followed by the release of micro-aggregates.
- **Assess soil status of Koiliaris River Basin Critical Zone Observatory**: Assess the soil status by selecting with sophisticated statistics the appropriate soil parameters and quantify the effects of livestock grazing, landuse changes and climate change on soil biochemical quality and water quality.



## ΕΚΤΕΝΗΣ ΠΕΡΙΛΗΨΗ

### *Οι λειτουργίες του εδάφους και η Εδαφική Οργανική Ύλη (ΕΟΥ)*

Το έδαφος αποτελεί τον δεύτερο πιο σημαντικό φυσικό πόρο μετά το νερό στον οποίο εκτελούνται βασικές περιβαλλοντικές, κοινωνικές και οικονομικές λειτουργίες: α. παραγωγή τροφίμων και βιομάζας, β. αποθήκευση, διήθηση, μετατροπή ανόργανων και οργανικών συστατικών, νερού και ενέργειας, γ. εξασφάλιση οικολογικού ενδιαφέροντος για διάφορους οργανισμούς (διατήρηση βιοποικιλότητας), δ. πηγή πρώτων υλών και ε. διασφάλιση φυσικού και πολιτιστικού περιβάλλοντος (COM(2002) 179; COM(2006)232). Το έδαφος αποτελεί ένα συνδυασμό ορυκτών σωματιδίων, οργανικής ουσίας, νερού, αέρα, και ζωντανών οργανισμών και είναι στην πραγματικότητα ένα πολύ πολύπλοκο, ετερογενές και ζωντανό μέσο. Η Εδαφική Οργανική Ύλη (ΕΟΥ) διαδραματίζει ένα σημαντικό ρόλο στις λειτουργίες και υπηρεσίες που προσφέρει το έδαφος (COM (2002) 179); αποτελώντας πηγή θρεπτικών για τα φυτά, υπόστρωμα για την μικροβιακή δραστηριότητα, δρώσα δύναμη για την αποσάθρωση των ορυκτών (παραγωγή μικρο-θρεπτικών) και ρυθμιστή του κλίματος, καθώς είναι δεξαμενή συσσώρευσης του CO<sub>2</sub> (Lal, 2004). Η σταθεροποίηση της ΕΟΥ στα εδάφη ελέγχει την μικροβιακή κοινότητα, την γονιμότητα και την δομή (π.χ. μέγεθος και σταθερότητα των συσσωματωμάτων) του εδάφους, η οποία εν τέλει επηρεάζει τον ρυθμό διηθητικότητας, την υγρασία, την διάχυση του οξυγόνου, την απορροή και την διάβρωση (Arias et al., 2005; Six et al., 2004). Συνολικά, στα εδάφη συγκρατείται πάνω από δύο φορές περισσότερος άνθρακας από ότι στη βλάστηση και την ατμόσφαιρα (Batjes, 1996). Η ποσότητα του άνθρακα που δεσμεύεται ετησίως στα εδάφη είναι τέσσερις φορές λιγότερη από τους 8 Gt άνθρακα που εκπέμπονται στην ατμόσφαιρα από ανθρωπογενείς δραστηριότητες- αναδεικνύοντας τη σημασία της ΕΟΥ σε σχέση με τις κλιματικές αλλαγές (Lal, 2000).

Οι αγροτικές πρακτικές που χρησιμοποιούνται στην κτηνοτροφία και τη γεωργία και η εντατικοποίηση της γεωργικής παραγωγής κατά τη διάρκεια των τελευταίων 60 χρόνων έχουν επηρεάσει τις λειτουργίες του εδαφικού οικοσυστήματος, προκαλώντας πολλές φορές μάλιστα την κατάρρευση της λειτουργικότητάς τους και δυσμενείς επιπτώσεις στην ποιότητα του νερού και του εδάφους. Αλλαγές στις χρήσεις γης όπως η μετατροπή εδαφών με φυσική βλάστηση σε καλλιεργήσιμες εκτάσεις, η μείωση της υπέργειας βιοποικιλότητας εξαιτίας των καλλιεργητικών πρακτικών και την υπερβόσκηση, καθώς και οι κλιματικές

αλλαγές μπορούν να οδηγήσουν σε απότομες αλλαγές στο εδαφικό οικοσύστημα και να καταλήξουν σε μακράς διάρκειας μεταβολές τόσο στο τοπίο όσο και στην βιοτική και αβιοτική δομή του εδάφους (Nikolaidis, 2011). Η μετατροπή εδαφών με φυσική βλάστηση σε καλλιεργήσιμα εδάφη ή βοσκοτόπια έχει ως αποτέλεσμα την μείωση της φυτικής κάλυψης και ως εκ τούτου τη μείωση του φυτικού υπολειμματικού υλικού που εισέρχεται και ενσωματώνεται στο έδαφος, μεγαλύτερη διάβρωση και συμπίεση του εδάφους (Bastida et al., 2006; Li et al., 2007), και εν τέλει καταστροφή της δομής του επιφανειακού εδάφους (βάθος 30 cm) και απώλεια μεγάλου ποσοστού της ΕΟΥ ή/και υποβάθμιση της ποιότητάς της. Εξαιτίας του οργώματος τα συσσωματώματα του εδάφους καταστρέφονται με αποτέλεσμα ΕΟΥ που προηγουμένως ήταν προστατευμένη να μπορεί να οξειδωθεί μικροβιακά. Στην Ευρώπη συνολικά το ποσοστό των εδαφών με ΕΟΥ λιγότερη από 2.6% ανήλθε από 35% σε 42% κατά τη διάρκεια της περιόδου 1980-1995. Η υπερβόσκηση από μόνη της, η οποία είναι ιδιαίτερα έντονη στην περιοχή της Μεσογείου, είναι υπεύθυνη για το 23% της υποβάθμισης των εδαφών στην Ευρώπη (RCEP, 1996). Το 75% της περιοχής της Μεσογείου παρουσιάζει χαμηλά (3.4%) ή πολύ χαμηλά (1.7%) ποσοστά ΕΟΥ (Van-Camp et al., 2004). Αξιοσημείωτο είναι ότι οι αγρονόμοι θεωρούν ότι εδάφη με ΕΟΥ μικρότερη από το ποσοστό 1.7% βρίσκονται στο στάδιο της προ-ερημοποίησης. Η διάβρωση, η μείωση της ΕΟΥ, η μείωση της βιοποικιλότητας και η συμπίεση του εδάφους αποτελούν αλληλοσυσχετιζόμενες απειλές των λειτουργιών του εδάφους που ζημιώνουν την γονιμότητα του και το καθιστούν ευαίσθητο στην ερημοποίηση (COM (2002) 179), με συνέπειες σχετικά με την ασφάλεια και διασφάλιση της ποιότητας των τροφίμων, τις κλιματικές αλλαγές, την ποιότητα του νερού, και την οικονομία (Lal, 2004), απειλώντας εν τέλει τη βιώσιμη ανάπτυξη (COM (2001) 264).

Έχει πλέον αναγνωριστεί ότι η τρέχουσα διαχείριση των εδαφών είναι μη βιώσιμη και απειλεί το μέλλον της ανθρωπότητας και ολόκληρης της βιόσφαιρας. Στα επόμενα 20-50 έτη, οι πιέσεις στις λειτουργίες και υπηρεσίες που προσφέρουν τα εδάφη προβλέπεται να αυξηθούν, λόγω των κλιματικών αλλαγών (ξηρασίες, ακραία γεγονότα βροχοπτώσεων) και τις ανταγωνιστικές απαιτήσεις των συστημάτων παραγωγής να παρέχουν τρόφιμα, βιοκαύσιμα και ξυλεία. Είναι επομένως πρωταρχικής σπουδαιότητας να επαναξιολογηθούν οι πρακτικές που χρησιμοποιούνται στη γεωργία και να αναπτυχθούν εναλλακτικά βιώσιμα συστήματα διαχείρισης των γεωργικών εδαφών που θα προστατεύουν παρά να υποβαθμίζουν τα εδάφη. Το κύριο ερώτημα είναι: ποια είναι η μεθοδολογία που μπορεί να αναπτυχθεί για να αυξήσει την ΕΟΥ, να μειώσει το φαινόμενο του θερμοκηπίου και συγχρόνως να αυξήσει τη γονιμότητα των εδαφών; Υπάρχει επείγουσα ανάγκη για νέα

εργαλεία και μεθοδολογίες που θα είναι σε θέση να δώσουν αξιόπιστες προβλέψεις για τις επιπτώσεις των κλιματικών αλλαγών και τη πρακτικές αποκατάστασης των εδαφών, ώστε να αξιολογηθούν οι εναλλακτικές λύσεις. Τα τελευταία χρόνια έχουν συγγραφεί πολλά επιστημονικά άρθρα σχετικά με τον κύκλο του άνθρακα και του αζώτου στα χερσαία περιβάλλοντα. Στη βιβλιογραφική ανασκόπηση που πραγματοποιείται στην παρούσα διατριβή επιχειρείται μια σύνθεση της βιβλιογραφίας με έμφαση στο γεφύρωμα του χάσματος μεταξύ της πρόσφατης επιστημονικής γνώσης σχετικά με τις διεργασίες που συμμετέχουν στον κύκλο του άνθρακα και του αζώτου στα εδάφη και τον τρόπο με τον οποίο αυτές μοντελοποιούνται.

#### *Σταθεροποίηση της οργανικής ύλης στα εδάφη*

Οι χουμικές ουσίες που απομονώνονται από τα εδάφη αποτελούν πιθανότατα προϊόν της διαδικασίας απομόνωσής τους παρά πραγματικά συστατικά της ΕΟΥ (Adams et al., 2011; Kleber and Johnson, 2011). Οι αρωματικές δομές που βρίσκονται στα σταθερά υλικά της ΕΟΥ είναι προϊόντα της ατελούς καύσης της βιομάζας (βιοκάρβουνο), με μεταβλητότητα στην αποδόμησή τους, και δεν αποτελούν αποτέλεσμα της φυσικής αποδόμησης της ΕΟΥ ούτε διατηρούνται επιλεκτικά στα εδάφη (Gleixner et al., 2002; Knicker, 2007; Baldock, 2007; Kleber and Johnson, 2010, Adams et al., 2011). Σημαντικά οργανικά μόρια όπως η λιγνίνη, η κυτταρίνη, η ημικυτταρίνη, τα λιπίδια και οι πρωτεΐνες, καθώς και ο 'μαύρος' άνθρακας (black carbon) θεωρούνται πλήρως βιοαποδομήσιμα κάτω από 'ιδανικές' συνθήκες, όπως η ικανοποιητική παροχή οξυγόνου (Adams et al., 2011). Η λιγνίνη συνδέεται με την ελεύθερη οργανική ουσία και βρίσκεται στα αδρομερή κλάσματα (μεγέθους άμμου) υπό τη μορφή σχεδόν αναλλοίωτων πολυμερών λιγνίνης (Bahri et al., 2008), αλλά καθώς βιοδιασπάται μειώνεται η παρουσία της στα κλάσματα μεγέθους ιλύος-αργίλου και τα μικρο-συσσωματώματα (Christensen, 1992; Dignae et al., 2005; Grandy and Neff, 2008). Στα αδρομερή κλάσματα του εδάφους μειωμένη είναι επίσης η παρουσία των φυτικών υδατανθράκων καθώς αυτά αποδομούνται επιλεκτικά. Πιο λεπτόκοκκα συσσωματώματα και ιδιαίτερα τα αργιλικά σωματίδια (<2 μm) είναι εμπλουτισμένα σε προϊόντα μικροβιακού μεταβολισμού (Alkyl C ή και O/N alkyl C), ενώσεις που περιέχουν άζωτο (πρωτεΐνες, αμινοξέα), and υδρογονάνθρακες όπως οι κηροί και τα λιπίδια (Schoning et al., 2005; von Lutzow et al., 2007; Grandy and Neff, 2008). Μεγάλος χρόνος ζωής έχει παρατηρηθεί για ενώσεις που περιέχουν άζωτο (~49 έτη) και ενώσεις προερχόμενες από

πολυσακχαρίτες (~54 έτη) (Gleixner et al., 2002). Η πρόσφατη εννοιολογική προσέγγιση σχετικά με τη σταθεροποίηση της ΕΟΥ προτείνει ότι η προσβασιμότητα της από τους μικροοργανισμούς (φυσική προστασία της ΕΟΥ σε μακρο-συσσωματώματα και μικρο-συσσωματώματα) και η προσρόφσή της στις ορυκτές επιφάνειες του εδάφους (συσχέτιση της με την ιλύ και την άργιλο) διαδραματίζουν καθοριστικό ρόλο στην προστασία του οργανικού υλικού ενάντια στην αποδόμηση, ρητά συμπεριλαμβανομένων των υδατανθράκων, πρωτεϊνών και άλλων θεωρούμενων 'ασταθών' (labile, εύκολα αποδομήσιμα) υλικών που προέρχονται από αποσυντιθέμενα φυτικά υλικά ή/και υπολείμματα μικροβίων και μυκήτων (Kleber and Johnson, 2010; Adams et al., 2011). Οι διαδικασίες του σχηματισμού/διάσπασης των συσσωματωμάτων και της προσρόφησης/εκρόφησης είναι οι βασικοί μηχανισμοί προστασίας και απελευθέρωσης της ΕΟΥ (Six et al., 2002a, 2002b). Η πιο περιεκτική προσέγγιση της αλληλεπίδρασης των οργανικών και των ορυκτών στα εδάφη είναι το μοντέλο τριών στοιβάδων (κινητική ζώνη, υδροφοβική ζώνη, και ζώνη επαφής) που πρότειναν οι Kleber et al. (2007). Έχουν αναγνωριστεί δύο βασικά μοντέλα σχετικά με τον σχηματισμό των συσσωματωμάτων (Plante and McGill, 2002; Nikolaidis and Bidoglio, 2011): i) το ιεραρχικό μοντέλο που προτείνει το σχηματισμό των μικρο-συσσωματωμάτων και εν συνεχεία τον σχηματισμό των μακρο-συσσωματωμάτων από τον συνδυασμό των μικρο-συσσωματωμάτων, ii) και το μοντέλο που προτείνει ότι πρωτίστως λαμβάνει χώρα ο σχηματισμός των μακρο-συσσωματωμάτων γύρω από το σωματιδιακό φυτικό υλικό και έπειτα ακολουθεί η απελευθέρωση των μικρο-συσσωματωμάτων καθώς τα υλικά αποσυντίθενται. Η σταθερότητα των συσσωματωμάτων και κύκλος ζωής τους κυρίως εξαρτάται από την ποσότητα και τη χημική σύσταση της οργανικής ουσίας και του φυτικού υλικού που εισέρχεται στο έδαφος, το pH και την αγωγιμότητα, την περιεκτικότητα σε οργανικό άνθρακα, άζωτο, και ανθρακικά, την ιοντο-ανταλλακτική ικανότητα του εδάφους, τα οξείδια του σιδήρου, τη περιεκτικότητα σε άργιλο και τον τύπο των αργίλων, τη μικροχλωρίδα (π.χ. γαιοσκώληκες), τις ρίζες, ριζικά τριχίδια και μυκόρριζα, τους μύκητες, τη μικροβιακή δραστηριότητα, τις κλιματικές συνθήκες, τις καλλιεργητικές πρακτικές: είδος καλλιέργειας, τύπος οργώματος, διαχείριση των φυτικών υπολειμμάτων, εφαρμογή εδαφοβελτιωτικών, λιπάσματα, άρδευση.

### *Μοντέλα προσομοίωσης του οργανικού άνθρακα στα εδάφη*

Τα μοντέλα προσομοίωσης της ΕΟΥ έχουν χρησιμοποιηθεί ευρέως ως εργαλείο για την πρόβλεψη της περιεκτικότητας των εδαφών σε οργανικό άνθρακα, σε διαφορετικούς τύπους εδαφών, καλλιεργητικές πρακτικές και κλιματικές συνθήκες όπως επίσης και για να προβλέψουν τις επιπτώσεις των αλλαγών χρήσης γης και των κλιματικών αλλαγών (Battle-Aguilar et al 2010). Τα τελευταία χρόνια σε πολλές εργασίες έχει πραγματοποιηθεί ανασκόπηση της μοντελοποίησης τόσο του άνθρακα όσο και του αζώτου στα χερσαία οικοσυστήματα (π.χ. Falloon and Smith, 2000; Shibu et al., 2006; Minasny et al., 2008; Manzoni and Porporato, 2009; Battle-Aguilar et al., 2010; Adams et al., 2011; Nikolaidis and Bidoglio, 2011; Adams et al., 2011). Τα διεργασιοστρεφή (process-oriented) μοντέλα έχουν προτιμηθεί στην επιστημονική βιβλιογραφία σε σχέση με τα οργανισμοστρεφή (organism-oriented) μοντέλα και τα μοντέλα κλάσεων οργανικού άνθρακα (cohort), καθώς απαιτούν λιγότερα δεδομένα εισαγωγής, περιέχουν λιγότερες παραμέτρους προς ρύθμιση, έχουν μικρότερο υπολογιστικό κόστος, και για άλλους λόγους που αναφέρονται από τους Adams et al. (2011) και τους Post et al. (2007). Γενικά, τα μοντέλα προσομοίωσης του κύκλου του άνθρακα στα εδάφη περιλαμβάνουν πολλές δεξαμενές άνθρακα με διαφορετικά χαρακτηριστικά τα οποία αποδομούνται με κινητική πρώτου βαθμού. Τα διεργασιοστρεφή μοντέλα που συμπεριλαμβάνουν με μεγάλη λεπτομέρεια και πολυπλοκότητα τις αλληλεπιδράσεις των μικροβιακών πληθυσμών και την ανάπτυξη των φυτών, απαιτούν περισσότερα δεδομένα πεδίου για την εφαρμογή τους και εισάγουν μεγαλύτερο βαθμό λάθους και αβεβαιότητας (Smith et al., 1997). Το μοντέλα RothC, Century, και DNDC είναι τα πιο διαδεδομένα διεργασιοστρεφή μοντέλα. Η ικανότητα πρόβλεψης των μοντέλων ΕΟΥ μπορεί να ενισχυθεί μέσω α) της βαθμονόμησης των σταθερών του ρυθμού αποδόμησης και β) με τη χρήση δεδομένων μετρούμενων στο πεδίο σχετικά με το υπολειμματικό φυτικό υλικό που εισέρχεται στο έδαφος και τις αρχικές συνθήκες, δηλαδή την κατανομή του άνθρακα σε διάφορες δεξαμενές που σχετίζονται με τις δεξαμενές προσομοίωσης του μοντέλου, με χρήση μεθόδων διαχωρισμού της ΕΟΥ σε διάφορα φυσικά κλάσματα (Knull et al., 2005; Zimmermann et al., 2007). Οι προσομοιώσεις της ΕΟΥ με μοντέλα δεν λαμβάνουν υπόψη τους τις έμφυτες αβεβαιότητες που οφείλονται στα δεδομένα εισαγωγής, στις αρχικές συνθήκες, καθώς επίσης και στις παραμέτρους του μοντέλου, με ελάχιστες εξαιρέσεις (Juston et al., 2010; Paul et al., 2003). Έχει αναγνωριστεί ότι ένα από τα σημαντικότερα κενά στην επιστημονική γνώση που αποτελεί σημαντική ερευνητική προτεραιότητα είναι η σταθεροποίηση της ΕΟΥ (Lal, 2008) και η εξήγηση του επιπέδου κορεσμού της στα εδάφη (Six et al., 2002a). Οι Van Veen και Paul (1981), ήδη τρεις

δεκαετίες πριν είχαν αναγνωρίσει ότι το επίπεδο της ΕΟΥ σε ισορροπία εξαρτάται πολύ περισσότερο από τον βαθμό προστασίας του άνθρακα (π.χ ποσοστό μακρο-συσσωματωμάτων) παρά από τον ρυθμό αποδόμησης των φυτικών υπολειμμάτων που προστίθενται στο έδαφος από τη βλάστηση.

Τα υπάρχοντα μοντέλα προσομοίωσης του κύκλου του οργανικού άνθρακα στα εδάφη δεν είναι πάντα ικανά να προσομοιώσουν την συγκέντρωση του άνθρακα σε ισορροπία ή μόνιμες συνθήκες (Powlson et al., 2011) και να δώσουν αξιόπιστες προβλέψεις όσον αφορά στις αλλαγές σε χρήσεις γης, καλλιεργητικές πρακτικές και επιρροές από τις κλιματικές αλλαγές, καθώς δεν λαμβάνουν υπόψη περιβαλλοντικούς περιοριστικούς παράγοντες, όπως είναι η φυσική προστασία του άνθρακα στα εδάφη εξαιτίας της δημιουργίας συσσωματωμάτων κατά ντετερμινιστικό-αιτιοκρατικό τρόπο –π.χ. τη δημιουργία συσσωματωμάτων (Davidson and Janssens, 2006, Kleber and Johnson, 2010). Το μοντέλο STRUC-C (Malamoud et al., 2008), μια τροποποιημένη έκδοση του μοντέλου RothC – υποθέτει ότι οι αρχικές αλληλεπιδράσεις συμβαίνουν μεταξύ των αργλικών σωματιδίων και των οργανικών, τα οποία στη συνέχεια συνδέονται μεταξύ τους και σχηματίζουν συσσωματώματα – αποτελεί την πρώτη επιστημονική προσπάθεια για τη δημιουργία μοντέλων ΕΟΥ επόμενης γενιάς και είναι το πιο εμπειριστατωμένο μοντέλο που υπάρχει σήμερα στην διεθνή βιβλιογραφία για την μοντελοποίηση του οργανικού άνθρακα, των συσσωματωμάτων και της δομής του εδάφους, παρά τις ελλείψεις του (Adams et al., 2011, Nikolaidis and Bidoglio, 2011). Ο σημαντικότερος περιορισμός του μοντέλου STRUC-C είναι το γεγονός ότι εξετάζει κάθε τύπο συσσωματωμάτων ως μια ενιαία δεξαμενή άνθρακα και δεν λιμνάζει υπόψη του το σωματιδιακό φυτικό υλικό στην διεργασία της συσσωμάτωσης. Το εννοιικό μοντέλο το οποίο προτείνει ότι τα μακρο-συσσωματώματα σχηματίζονται γύρω από το σωματιδιακό φυτικό οργανικό υλικό που εισέρχεται στα εδάφη και κατά την διάσπασή τους απελευθερώνονται μικρο-συσσωματώματα (Golchin 1994; Balesdent et al., 2000; Puget et al., 2000; Plante and McGill, 2002; Six et al., 2002a; Six et al., 2002b; Six et al., 2004; Bronick and Lal, 2005, Helfrich et al., 2008; Nikolaidis and Bidoglio, 2011) δεν έχει ακόμη μοντελοποιηθεί.

## Σκοπός της εργασίας

Σκοπός της παρούσας διατριβής είναι να συμβάλει στην βελτίωση της κατανόησης των μηχανισμών που εμπλέκονται στον κύκλο των θρεπτικών και της οργανικής ύλης στα εδάφη και να παράσχει εργαλεία τα οποία μπορούν να βοηθήσουν ως προς την βιώσιμη λειτουργικότητα της κρίσιμης ζώνης του εδάφους. Πιο συγκεκριμένα, τα επιστημονικά ζητήματα που ερευνώνται στην παρούσα εργασία μπορούν να συνοψιστούν στα παρακάτω:

- **Ανάπτυξη μεθοδολογίας για την προσομοίωση του άνθρακα στα εδάφη:** Ανάπτυξη και αξιολόγηση με δεδομένα πεδίου μεθοδολογίας για την εκτίμηση της τιμής των παραμέτρων του μοντέλου RothC, μέσω της χρήσης δεδομένων πεδίου που προκύπτουν από μεθόδους διαχωρισμού της ΕΟΥ σε διάφορα φυσικά κλάσματα που σχετίζονται με τις δεξαμενές προσομοίωσης του μοντέλου για την αρχικοποίηση και βαθμονόμηση του μοντέλου, αξιολόγηση της μοναδικότητας της βέλτιστης λύσης, ανάλυση ευαισθησίας και ποσοτικοποίηση της αβεβαιότητας στα αποτελέσματα του μοντέλου.
- **Δοκιμή σε διαφορετικά κλίματα (κλιματική διαβάθμιση):** Μοντελοποίηση με χρήση της αναπτυχθείσας μεθοδολογίας των αλλαγών των αποθεμάτων του οργανικού άνθρακα σε εδάφη με φυσική βλάστηση που έχουν μετατραπεί σε καλλιεργήσιμα σε διαφορετικά κλίματα ανά τον κόσμο, ανάλυση ευαισθησίας και ποσοτικοποίηση της αβεβαιότητας στα αποτελέσματα του μοντέλου.
- **Ανάπτυξη μοντέλου για την προσομοίωση της δομής των εδαφών:** Ανάπτυξη και αξιολόγηση με δεδομένα πεδίου συνδυαστικού μοντέλου για τον οργανικό άνθρακα, τα συσσωματώματα και τη δομή του εδάφους, βάσει της υπάρχουσας επιστημονικής γνώσης στην σχετική βιβλιογραφία αναφορικά με τον προτεινόμενο μηχανισμό σχηματισμού των μακρο-συσσωματωμάτων γύρω από το σωματιδιακό φυτικό οργανικό υλικό που εισέρχεται στα εδάφη και κατά την διάσπασή τους απελευθερώνονται μικρο-συσσωματώματα.
- **Αξιολόγηση της κατάστασης των εδαφών της λεκάνης απορροής του ποταμού Κοιλιάρη, ένα από τα διεθνή παρατηρητήρια της κρίσιμης ζώνης του εδάφους:** Αξιολόγηση της κατάστασης των εδαφών με την επιλογή των κατάλληλων εδαφικών παραμέτρων έπειτα από στατιστική επεξεργασία και ποσοτικοποίηση των επιπτώσεων της υπερβόσκησης, των αλλαγών χρήσης γης και των κλιματικών αλλαγών στην βιοχημική ποιότητα των εδαφών και την ποιότητα των υδάτων.

*Μοντελοποίηση με το μοντέλο RothC της δέσμευσης του οργανικού άνθρακα σε δύο διαφορετικά επιφανειακά εδάφη που δεν έχουν καλλιεργηθεί για δεκαετίες– ζητήματα βαθμονόμησης και ανάλυσης αβεβαιότητας*

Ο σκοπός αυτής της μελέτης ήταν διττός: α) η ανάπτυξη μιας μεθοδολογίας για την εκτίμηση των τιμών των παραμέτρων του μοντέλου όταν αυτό εφαρμόζεται σε περιπτώσεις αλλαγής χρήσης γης από καλλιεργήσιμη έκταση σε αγρανάπαυση για δεκαετίες με ανάπτυξη φυσικής βλάστησης (αρχικοποίηση και βαθμονόμηση του μοντέλου με δεδομένα πεδίου προερχόμενα από την εφαρμογή μεθόδων διαχωρισμού της ΕΟΥ σε διάφορα φυσικά κλάσματα που σχετίζονται με τις δεξαμενές προσομοίωσης του μοντέλου) κι όπου το φυτικό υλικό/κοπριά που ενσωματώνεται στο έδαφος δεν έχει μετρηθεί και β) η ποσοτικοποίηση της αβεβαιότητας στα αποτελέσματα του μοντέλου. Μια έκδοχή του Rothamsted μοντέλου-έκδοση RothC-26.3 (Coleman and Jenkinson, 1999) σε Microsoft Excel έκδοση αναπτύχθηκε και χρησιμοποιήθηκε σε συνεργασία με το στατιστικό πακέτο @RISK (PALISADES Corp.) ώστε να εξεταστεί η μοναδικότητα της βέλτιστης λύσης και να προσομοιωθεί η αβεβαιότητα στα αποτελέσματα του μοντέλου εξαιτίας των δεδομένων εισαγωγής, τις αρχικές συνθήκες, καθώς επίσης και τις παραμέτρους του μοντέλου. Η μεθοδολογία εφαρμόστηκε σε δεδομένα που προήλθαν από εδάφη της λεκάνης απορροής του ποταμού Αϊόβα στην πόλη της Αϊόβας (Υγρό ηπειρωτικό κλίμα, αδρομερή εδάφη) και της λεκάνης απορροής του ποταμού Κουλιάρη στην Κρήτη (Μεσογειακό κλίμα, λεπτόκκοκα εδάφη). Και οι δύο περιοχές ανήκουν στο διεθνές δίκτυο των παρατηρητήριων της κρίσιμης ζώνης του εδάφους.

- Τα δεδομένα της περιεκτικότητας των εδαφών σε ολικό οργανικό άνθρακα και σε άνθρακα που σχετίζεται με το σωματιδιακό φυτικό οργανικό υλικό που προέκυψαν από την επεξεργασία του εδάφους με φυσικές μεθόδους κλασμάτωσης χρησιμοποιήθηκαν επιτυχώς για την αρχικοποίηση και βαθμονόμηση του μοντέλου και παρείχαν τις οριακές συνθήκες για τον αποτελεσματικό περιορισμό της λύσης. Οι βαθμονομημένες τιμές για τους λειμώνες της Αϊόβας, όσον αφορά τα φυτικά υπολείμματα τα οποία εισέρχονται στο έδαφος ήταν 5.05 t C/ha και όσον αφορά τη σταθερά του ρυθμού αποδόμησης ήταν 0.34 1/y για το ανθεκτικό φυτικό υλικό (RPM), ενώ για το χούμο (HUM) ήταν 0.27 1/y. Ενώ, αντίστοιχα, για τις θαμνώδεις εκτάσεις της Ελλάδας, οι τιμές για τα φυτικά υπολείμματα ήταν 3.79 t C/ha και για τη σταθερά του ρυθμού αποδόμησης ήταν 0.21 1/y (RPM) και 0.0041 1/y (HUM).

- Η βαθμονομημένη σταθερά του ρυθμού αποδόμησης του ανθεκτικού φυτικού υλικού (RPM) βρέθηκε ότι ήταν στην Αϊόβα μεγαλύτερη (13.3 %) και στην Ελλάδα μικρότερη (31%) σε σχέση με την προεπιλεγμένη τιμή του μοντέλου (0.3 1/y) αποτελώντας ένδειξη ότι η συνάρτηση που χρησιμοποιείται από το RothC για την διόρθωση του ρυθμού αποδόμησης σε σχέση με τη θερμοκρασία συστηματικά υποεκτιμά τον ρυθμό σε χαμηλές θερμοκρασίες και τον υπερεκτιμά σε μεγάλες θερμοκρασίες.
- Η βαθμονομημένη σταθερά του ρυθμού αποδόμησης του χούμου (HUM) ήταν πολύ διαφορετική από την προεπιλεγμένη τιμή του μοντέλου (0.02 1/y) τόσο στην Αϊόβα (13.5 φορές μεγαλύτερη) όσο και στην Ελλάδα (48.8 φορές μικρότερη). Η πολύ μεγάλη διαφορά ανάμεσα στις δύο περιοχές οφείλεται στις διαφορές τους στο περιεχόμενο αργίλου. Η πιο λεπτόκοκκη υφή του εδάφους στην Ελλάδα είχε ως αποτέλεσμα μεγαλύτερη προστασία του χούμου και πιθανότατα μικρότερη φαινομενική ευαισθησία στην επίδραση της θερμοκρασίας ή/και της υγρασίας στον ρυθμό αποδόμησης, σε αντίθεση με το πιο χονδρόκοκκο έδαφος της Αϊόβας, όπου παρατηρήθηκε το αντίθετο φαινόμενο.
- Η ανάλυση ευαισθησίας υπέδειξε ότι το υπολειμματικό φυτικό υλικό που εισέρχεται στα εδάφη και η σταθερά του ρυθμού αποδόμησης της δεξαμενής άνθρακα 'RPM' παρουσίασαν την μεγαλύτερη ευαισθησία στις τιμές της ΕΟΥ που προβλέφθηκαν από το μοντέλο και στις δυο υπό εξέταση περιοχές.
- Το έδαφος στην Αϊόβα μετά από 100 χρόνια παύσης της καλλιέργειας και ανάπτυξης της φυσικής βλάστησης προβλέφθηκε ότι συγκράτησε οργανικό άνθρακα ποσότητας 17.5 t C/ha ενώ στην Ελλάδα 54 t C/ha. Η ανάλυση αβεβαιότητας φανέρωσε ότι η ολική αβεβαιότητα στις παραπάνω τιμές ήταν έως και 70% της συνολικής ποσότητας του οργανικού άνθρακα που δεσμεύτηκε στα εδάφη. Τόσο στην Αϊόβα όσο και στην Ελλάδα το υπολειμματικό φυτικό υλικό που εισέρχεται στα εδάφη αποτέλεσε την μεγαλύτερη πηγή αβεβαιότητας στις προβλέψεις. Η αβεβαιότητα που υπολογίστηκε είναι πολύ σημαντική, καθώς παρεμποδίζει τελικά την δυνατότητά μας να προβλέψουμε τη δέσμευση του άνθρακα με ακρίβεια υπό συνθήκες αγρανάπαυσης. Τα αποτελέσματα της ανάλυσης αβεβαιότητας υποδεικνύουν την αναγκαιότητα που υπάρχει για την απόκτηση αξιόπιστων δεδομένων της ποσότητας του άνθρακα που εισέρχεται από το φυτό με μετρήσεις στο πεδίο σε διαφορετικές χρήσεις γης και κλιματικές συνθήκες προκειμένου να ελαχιστοποιηθούν οι αβεβαιότητες και να καθοριστούν ακριβέστερα οι σταθερές των ρυθμών αποδόμησης συναρτήσει των κλιματικών συνθηκών.

Η μεθοδολογία που αναπτύχθηκε σε αυτή την εργασία μπορεί να χρησιμοποιηθεί για την αξιολόγηση των παραγόντων που επηρεάζουν την δέσμευση του οργανικού άνθρακα στα γεωργικά εδάφη, την ποσοτικοποίηση της αβεβαιότητας στις προβλέψεις, όπως επίσης και στο σχεδιασμό υπαίθριων πειραμάτων και μετρήσεων, ώστε να ελαχιστοποιηθούν οι αβεβαιότητες και να βελτιωθούν οι προβλέψεις οι οποίες σχετίζονται με τη γονιμότητα του εδάφους.

*Μοντελοποίηση και ανάλυση αβεβαιότητας των αλλαγών των αποθεμάτων του οργανικού άνθρακα σε εδάφη με φυσική βλάστηση που έχουν μετατραπεί σε καλλιεργήσιμα σε διαφορετικά κλίματα*

Σε αυτή την εργασία η μεθοδολογία που αναπτύχθηκε και περιγράφεται στην προηγούμενη παράγραφο χρησιμοποιήθηκε για τη μοντελοποίηση (βαθμονόμηση, ανάλυσης ευαισθησίας και ανάλυση αβεβαιότητας) των αλλαγών των αποθεμάτων του οργανικού άνθρακα σε εδάφη με φυσική βλάστηση που έχουν μετατραπεί σε καλλιεργήσιμα σε διαφορετικά κλίματα, όπου ο δείκτης ξηρότητας 'Budgco's Radiative Index of Dryness, RID' κυμαινόταν από 3.94 (Ερημος) έως 0.96 (Δάσος). Χρησιμοποιήθηκαν δεδομένα χρονοσειρών από σχετικές μελέτες της διεθνούς βιβλιογραφίας. Αξιολογήθηκε ακόμη, η αποτελεσματικότητα της προσθήκης εδαφοβελτιωτικών διαφόρων ποιοτήτων στις διαφορετικές κλιματικές συνθήκες και τύπους εδαφών. Η φαινομενική ευαισθησία στην επίδραση της θερμοκρασίας των δεξαμενών άνθρακα RPM και HUM του μοντέλου RothC εκτιμήθηκε με τον υπολογισμό της τιμής του συντελεστή θερμοκρασίας Q10.

- Η ανάλυση ευαισθησίας υπέδειξε ότι οι παράμετροι που έδειξαν τη μεγαλύτερη ευαισθησία στην προσομοίωση ήταν οι σταθερές του ρυθμού αποδόμησης των δεξαμενών άνθρακα RPM και HUM, η ποσότητα του άνθρακα που εισέρχεται στο έδαφος ως υπολειμματικό φυτικό υλικό, και η αρχική ποσότητα σε άνθρακα της δεξαμενής RPM στις περιπτώσεις που αυτή δεν είχε μετρηθεί με κάποια μέθοδο φυσικής κλασμάτωσης. Η ευαισθησία εξαρτάται ακόμη από τα διαθέσιμα δεδομένα για τη βαθμονόμηση των παραμέτρων.
- Η αβεβαιότητα στις προβλέψεις της προσομοίωσης αναφορικά με την μείωση του άνθρακα στα εδάφη μετά από 100 χρόνια καλλιέργειας ήταν στις έξι περιοχές ως εξής: 26.9% -Θιβέτ, 122.5% -Ντακότα, 21.9% -Κίνα, 48.9% -Τουρκία, 108% -Αιθιοπία, και 31.6%-Μαδαγασκάρη (τα ποσοστά είναι ως προς τη συνολική ποσότητα άνθρακα που

χάθηκε). Η αβεβαιότητα ήταν μικρότερη στις περιοχές για τις οποίες υπήρχαν διαθέσιμα δεδομένα σχετικά με το σωματιδιακό φυτικό υλικό και πληροφορία σχετικά με τη ποσότητα του άνθρακα που εισέρχεται από το φυτικό υλικό.

- Η αβεβαιότητα που υπολογίστηκε είναι πολύ σημαντική, καθώς παρεμποδίζει τελικά την δυνατότητά μας να προβλέψουμε με ακρίβεια τις επιπτώσεις της αλλαγής χρήσης γης (φυσική βλάστηση σε καλλιεργήσιμη έκταση) στα αποθέματα του άνθρακα. Τα αποτελέσματα της ανάλυσης αβεβαιότητας υποδεικνύουν σε συμφωνία με τη μελέτη που παρουσιάστηκε στην προηγούμενη παράγραφο την αναγκαιότητα που υπάρχει για την απόκτηση αξιόπιστων δεδομένων με μετρήσεις της ποσότητας του άνθρακα που εισέρχεται από το φυτό και των αρχικών συνθηκών προκειμένου να ελαχιστοποιηθούν οι αβεβαιότητες.
- Η μέσος ρυθμός απώλειας οργανικού άνθρακα –ως ποσοστό του αρχικού αποθέματος- κατά την καλλιέργεια εδάφους που είχε φυσική βλάστηση στις έξι περιοχές κυμαινόταν από 1% έως 10% τον πρώτο χρόνο καλλιέργειας και από 0.32 %/γ έως 0.77 %/γ έπειτα από 100 χρόνια. Ως ποσότητα άνθρακα που χάθηκε από τα εδάφη κυμαινόταν από 1 έως 11 t C/ha τον πρώτο χρόνο και από 0.27 έως 0.85 t C/ha γ μετά από 100 χρόνια καλλιέργειας. Οι μέσοι ρυθμοί μειώνονταν με το χρόνο κατά λογαριθμικό τρόπο. Οι απώλειες του σωματιδιακού (φυτικού) άνθρακα ήταν πιο σημαντικές τα πρώτα χρόνια μετά την αλλαγή της χρήσης γης και οι απώλειες του άνθρακα που σχετίζεται με το κλάσμα αργίλου-ιλύος, τις δεξαμενές δηλαδή της βιομάζας (BIO) και του χούμου (HUM) του μοντέλου RothC τα επόμενα χρόνια. Ο λόγος του σωματιδιακού άνθρακα προς τον ολικό άνθρακα που είχε το έδαφος πριν καλλιεργηθεί φάνηκε να παίζει καθοριστικό ρόλο στην ποσοστιαία απώλεια του οργανικού άνθρακα μακροπρόθεσμα. Ο χρόνος που χρειάστηκαν τα εδάφη για να φτάσουν σε μια νέα σταθερή συγκέντρωση άνθρακα παρουσίασε μεγάλη διακύμανση υπό τις διαφορετικές κλιματικές συνθήκες και ήταν περισσότερο από 100 years (Θιβέτ, Έρημος) έως 20-30 χρόνια (Αιθιοπία, Δάσος)
- Ο λόγος του άνθρακα που μπορεί να δεσμευτεί στα εδάφη κατά την προσθήκη άνθρακα με τη μορφή εδαφοβελτιωτικού ή οργανικού λιπάσματος προς την ποσότητα άνθρακα που προστίθεται (Net C/C amended) παρουσίασε μεγάλη διακύμανση στις έξι περιοχές. Για παράδειγμα ο λόγος αυτός κατά την ετήσια εφαρμογή για 100 χρόνια ποσότητας 2.5 t C/ha υλικού με σύσταση 30/60/10 (DPM/RPM/HUM, οι αντίστοιχες δεξαμενές άνθρακα του μοντέλου RothC) βρέθηκε να είναι στη Ντακότα 0.39, στο Θιβέτ 0.32, στην Αιθιοπία 0.21, στην Κίνα και τη Μαδαγασκάρη 0.08, και στην Τουρκία 0.07. Ο άνθρακας που εν τέλει σταθεροποιήθηκε στο χούμο του εδάφους (κλάσμα αργίλου-

ιλύος) σε σχέση με τη συνολική ποσότητα που δεσμεύτηκε κατά την προσθήκη του υλικού ήταν 40.8% στο Θιβέτ, 39.8% στη Ντακότα, 60.6% στην Κίνα, 64.2% στην Τουρκία, 78% στην Αιθιοπία και 83.1% στη Μαδαγασκάρη. Στις περιοχές όπου ο ρυθμός αποδόμησης του χούμου ήταν μικρότερος, η αποτελεσματικότητα της προσθήκης ήταν μεγαλύτερη και περισσότεροι άνθρακας σταθεροποιούταν στο χούμο του εδάφους. Σε όλες τις περιπτώσεις ο λόγος Net C /C amended ratio μειώνεται λογαριθμικά με τα χρόνια εφαρμογής. Οι αξιόπιστες προσομοιώσεις είναι σημαντικές για το σχεδιασμό μακροπρόθεσμων βιώσιμων καλλιεργητικών πρακτικών, ώστε να μπορεί να προβλεφθεί η κατάλληλη ποσότητα και ποιότητα των εδαφοβελτιωτικών που χρειάζεται να προστεθούν σε διαφορετικούς τύπους εδαφών και κλιματικές συνθήκες για την αποτελεσματική δέσμευση του οργανικού άνθρακα και την αύξηση του χούμου.

- Ο συντελεστής θερμοκρασίας Q10 της δεξαμενής RPM (1.75, διακύμανση 1.66-1.88) βρέθηκε να είναι μικρότερος από αυτόν που προκύπτει με την προεπιλεγμένη σταθερά αποδόμησης στο μοντέλο RothC (2.00) στο θερμοκρασιακό εύρος 15-25 °C και μεγαλύτερος στο θερμοκρασιακό εύρος 5-15 °C (4.04, διακύμανση 2.96-8.7, και στο RothC 3.88). Ο συντελεστής θερμοκρασίας Q10 της δεξαμενής HUM ήταν 5% (0.7% έως 9.2%) μικρότερος από αυτόν της δεξαμενής RPM στο εύρος 15-25 °C και 26.1% (4.8% έως 45.5%) μικρότερος στο εύρος 15-25 °C, καταδεικνύοντας ότι η ευαισθησία του ρυθμού αποδόμησης στη θερμοκρασία διαφέρει μεταξύ των διαφορετικών δεξαμενών άνθρακα και θα πρέπει να συμπεριληφθεί στα μοντέλα άνθρακα. Επιπλέον επιβεβαιώθηκε η παρατήρηση που έχει γίνει και από άλλους μελετητές ότι η συνάρτηση που χρησιμοποιείται από το RothC για την διόρθωση του ρυθμού αποδόμησης σε σχέση με τη θερμοκρασία συστηματικά υποεκτιμά τον ρυθμό σε χαμηλές θερμοκρασίες και τον υπερεκτιμά σε μεγάλες θερμοκρασίες. Το αξιοσημείωτο είναι ότι σε αντίθεση με τη δεξαμενή RPM, ο συντελεστής θερμοκρασίας Q10 της δεξαμενής HUM σε χαμηλές θερμοκρασίες σε αυτό το σετ δεδομένων ήταν μικρότερος από αυτόν του RothC, οπότε και με τις προεπιλεγμένες τιμές υπερεκτιμάται ο ρυθμός αποδόμησης.

## *Συνδυαστικό μοντέλο για τον οργανικό άνθρακα, τα συσσωματώματα και τη δομή των επιφανειακών εδαφών (Carbon, Aggregation, and Structure, CAST)*

Σε αυτή την εργασία αναπτύχθηκε ένα συνδυαστικό μοντέλο για τον οργανικό άνθρακα, τα συσσωματώματα και τη δομή των επιφανειακών εδαφών (CAST), όπως επίσης και ένα απλό μηχανιστικό μοντέλο για το οργανικό άζωτο. Το μοντέλο προσομοιώνει τον προτεινόμενο, στη διεθνή βιβλιογραφία, μηχανισμό σχηματισμού των μακρο-συσσωματωμάτων γύρω από το σωματιδιακό φυτικό οργανικό υλικό που εισέρχεται και ενσωματώνεται στα εδάφη και κατά την διάσπασή τους απελευθερώνονται μικρο-συσσωματώματα. Οι δεξαμενές άνθρακα του μοντέλου RothC συνδυάστηκαν με υπορουτίνες προσομοίωσης της συσσωμάτωσης και της δομής του εδάφους και συνολικά το μοντέλο αξιολογήθηκε με την εφαρμογή του σε δύο περιοχές όπου υπήρχε αλλαγή χρήσης γης από καλλιεργήσιμη έκταση σε αγρανάπαυση για δεκαετίες με ανάπτυξη φυσικής βλάστησης, στην Αϊόβα και την Ελλάδα.

- Το μοντέλο προσομοίωσε επιτυχώς το περιεχόμενο σε οργανικό άνθρακα όπως επίσης και το λόγο C προς N της κάθε δεξαμενής άνθρακα από τις οποίες αποτελούνται οι τρεις τύποι συσσωματωμάτων (μακρο-συσσωματώματα: >250 μm, μικρο-συσσωματώματα: 53-250 μm, συσσωματώματα μεγέθους ιλύος-αργίλου: <53 μm) και στις δύο περιοχές.
- Ακόμη προέκυψε μια πιο αιτιοκρατική εξήγηση του επιπέδου συγκέντρωσης σε άνθρακα των διαφορετικών δεξαμενών του άνθρακα όπως επίσης και της δομής του εδάφους (πορώδες και φαινομενική πυκνότητα). Η μακρο-συσσωμάτωση και το πορώδες του εδάφους έφτασαν σε μια μέγιστη τιμή και η πυκνότητα σε μια ελάχιστη έπειτα από 7 και 14 έτη παύσης της καλλιέργειας στην Ελλάδα και τη Αϊόβα, αντίστοιχα. Κατόπιν, η διάσπαση των μακρο-συσσωματωμάτων παρουσίασε μια σταθερή εποχιακή τάση και κάθε περαιτέρω αύξηση της ΕΟY οφειλόταν στην μικρο-συσσωμάτωση, με συνέπεια την αύξηση της πυκνότητας και τη μείωση του πορώδους και εν τέλει τη σταθεροποίησή τους σε μια σταθερή τιμή.
- Τα αποτελέσματα που προέκυψαν από τον υπολογισμό της ροής των κλασμάτων αργίλου-ιλύος μεταξύ των συσσωματωμάτων και της συγκέντρωσής τους σε άνθρακα συμφωνούν με τα πρόσφατα επιστημονικά συμπεράσματα που προτείνουν ότι μεγάλη επιφάνεια των ορυκτών δεν καλύπτεται από οργανική ουσία καταδεικνύοντας ωστόσο και την πιθανή ύπαρξη περιοχών στην επιφάνεια της αργίλου-ιλύος ιδιαίτερα υψηλής συγκέντρωσης οργανικού άνθρακα, και οι οποίες παίζουν σημαντικό ρόλο στη μικρο-συσσωμάτωση.

- Το απλό μηχανιστικό μοντέλου του αζώτου που αναπτύχθηκε έδειξε ότι λόγος C προς N της βιομάζας ήταν μεγαλύτερος στο αδρομερές έδαφος της Αϊόβας σε σχέση με το λεπτόκοκκο έδαφος στην Ελλάδα και μάλιστα φάνηκε ότι υπάρχει συσχέτιση μεταξύ της παρουσίας των μυκήτων και της μακρο-συσσωμάτωσης.

Το μοντέλο CAST μπορεί να βοηθήσει στη διερεύνηση των παραγόντων που καθορίζουν την ΕΟΥ, τη συσσωμάτωση, και τη δομή του εδάφους σε διαφορετικά οικοσυστήματα και να προβλέψει την απόκριση του εδαφικού συστήματος σε διαφορετικές αγροτικές και καλλιεργητικές πρακτικές, αλλαγές χρήσης γης, και τις κλιματικές αλλαγές προκειμένου να σχεδιαστούν και να βελτιστοποιηθούν τα κατάλληλα μέτρα και πρακτικές.

*Η κατάσταση των εδαφών της λεκάνης απορροής του ποταμού Κοιλιάρη παρατηρητηρίου της κρίσιμης ζώνης του εδάφους*

Η τελευταία εργασία αυτής της διατριβής αφιερώθηκε στην εκτίμηση της κατάστασης των εδαφών του Κοιλιάρη. Πραγματοποιήθηκε μελέτη για τον καθορισμό των βασικών παραγόντων που επηρεάζουν την συσσωμάτωση των εδαφών. Ακόμη ποσοτικοποιήθηκαν οι επιπτώσεις των αλλαγών χρήσης γης όπως επίσης και των κλιματικών αλλαγών στα αποθέματα του οργανικού άνθρακα στα εδάφη. Πραγματοποιήθηκε εκτενής δειγματοληψία εδαφών (29 δείγματα) βάσει της τυπολογίας των εδαφών με τη χρήση θεματικών χαρτών GIS (γεωλογικό υπόβαθρο, τύποι εδαφών, χρήσεις γης, και υψομετρική ζώνη). Τα δείγματα εδαφών χαρακτηρίστηκαν για περισσότερες από 30 παραμέτρους οι οποίες σύμφωνα με τη βιβλιογραφία σχετίζονται με τη συσσωμάτωση των εδαφών. Η ανάλυση κύριων συνιστωσών (principal component analysis) υπέδειξε ότι στη λεκάνη υπάρχουν δύο βασικές ομάδες εδαφών οι οποίες μπορούν να περιγραφούν επαρκώς με 15 εδαφικές παραμέτρους. Τα εδάφη της πρώτης ομάδας προέρχονταν κυρίως από περιοχές όπου το γεωλογικό υπόβαθρο αποτελούνταν από σχιστολίθους και μάργες με αδρομερή υφή και όξινο pH και το υψόμετρο ήταν μικρότερο από 550 m. Τα εδάφη της δεύτερης ομάδας προέρχονταν από την αλλουβιακή πεδιάδα και από ημιορεινές περιοχές με ασβεστομάργες και μάργες με αλκαλικό pH. Τα περισσότερα εδάφη ήταν καλλιέργειες με ελιές (υψόμετρο 9-383 m) και μια υπο-ομάδα αποτελούνταν από θαμνώδεις εκτάσεις σε ασβεστόλιθους (υψόμετρο 592-1098 m). Η πρώτη ομάδα εδαφών σε σχέση με τη δεύτερη χαρακτηριζόταν από σημαντικά μικρότερο ποσοστό μακρο-συσσωματωμάτων τα οποία βρέθηκε ότι σχετίζονται κυρίως από τη μικρότερη ικανότητα ανταλλαγής κατιόντων (IAK) του εδάφους και την πιο αδρομερή υφή τους (περισσότερη χονδρόκοκκη άμμος και μικρότερο ποσοστό αργίλου και ιλύος). Το

ποσοστό των μακρο-συσσωματωμάτων στο έδαφος περιγράφηκε με πολυκριτηριακή ανάλυση παλινδρόμησης από 7 παραμέτρους στην πρώτη ομάδα εδαφών: ξηρή πυκνότητα, pH, ολικό άζωτο, κόκκοι >1000μm, ΙΑΚ, δυναμικά ανοργανοποιήσιμο άζωτο (ΔΑΑ) και βαθμός κορεσμού σε Νάτριο και από 11 παραμέτρους στη δεύτερη ομάδα: ξηρή πυκνότητα, pH, ολικό άζωτο, κόκκοι >1000 μm, κόκκοι <53 μm, κόκκοι <2 μm, ΙΑΚ, ΔΑΑ, ανταλλάξιμο άζωτο, Κάλιο που εκχυλίστηκε με BaCl<sub>2</sub> και βαθμός κορεσμού σε Νάτριο.

Οι επιπτώσεις των κλιματικών αλλαγών, όπως αυτές προβλέπονται να λάβουν χώρα σύμφωνα με το σενάριο IPCC-A1B (IPCC, 2007) –το οποίο θέτει ισορροπημένη έμφαση σε όλες τις πηγές ενέργειας- στα αποθέματα του οργανικού άνθρακα στα καλλιεργήσιμα εδάφη του Κοιλιάρη σε τρεις διαφορετικές λιθολογίες (Σχιστόλιθοι, Μάργες, Ασβεστόλιθοι Τρυπαλίου) εκτιμήθηκαν με το μοντέλο άνθρακα RothC. Τα αποτελέσματα του παρόντος σεναρίου (1990-2010) συγκρίθηκαν με αυτά των δεκαετιών 2010-2030 και 2030-2050 ώστε να ληφθεί υπόψη η δεκαετής διακύμανση των κλιματικών συνθηκών. Βρέθηκε ότι ο λιγότερος άνθρακας που θα δεσμευτεί στα εδάφη εξαιτίας των κλιματικών αλλαγών αντιστοιχεί στο 1.4% με 1.7% των αρχικών αποθεμάτων των εδαφών (ταυτόχρονη προσομοίωση αλλαγής χρήσης γης από θαμνότοπο σε καλλιέργεια ελιάς). Η αλλαγή χρήσης γης από μόνη της (1990-2010) ευθύνεται για 12% με 28% μείωση των αρχικών αποθεμάτων. Από την άλλη πλευρά, οι επιπτώσεις των κλιματικών αλλαγών στα εδάφη που καλλιεργούνται ήδη 50 χρόνια με ελιές εκτιμήθηκε να είναι 2-3% του αρχικού άνθρακα (για 20 χρόνια προσομοίωση), ενώ δίχως τις κλιματικές αλλαγές, η καλλιέργεια από μόνη της προκαλεί μεταβολή του αποθέματος του εδάφους κατά 1.7% με 8.9%. Η ποσότητα του άνθρακα που δεν θα δεσμευτεί στα εδάφη εξαιτίας των κλιματικών εδαφών προβλέφθηκε να είναι 1.5-3 t/ha την 20ετία. Τα αποτελέσματα καταδεικνύουν ότι η απώλειες οργανικού άνθρακα που λαμβάνουν χώρα εξαιτίας αλλαγών χρήσης γης και καλλιεργητικών πρακτικών είναι τόσο μεγάλες που μειώνουν την ικανότητα μας να ανιχνεύσουμε τις αντίστοιχες επιπτώσεις των κλιματικών αλλαγών.

Τέλος, ελέγχθηκε η υπόθεση ότι η υπερβόσκηση που λαμβάνει χώρα στις ορεινές περιοχές της λεκάνης υποβαθμίζει την ποιότητα του εδάφους και επιβαρύνει ακόμη τα υπόγεια και επιφανειακά νερά με υψηλές συγκεντρώσεις διαλυτού οργανικού αζώτου (DON) με διερεύνηση σε τρία επίπεδα. Από τη μελέτη προέκυψε ότι υπάρχει συσχέτιση του φορτίου του DON στα ποτάμια με το φορτίο που εισέρχεται στη λεκάνη του ποταμού από την βόσκηση, όπως φάνηκε από τη γραμμική συσχέτιση που προέκυψε για πέντε χαρακτηριστικές λεκάνες απορροής στην Ελλάδα. Ο υπολογισμός του ισοζυγίου μάζας

υπέδειξε ότι το DON συμπεριφέρεται ως 'συντηρητικός' ρύπος. Στα εδάφη που δεν υπήρχε βλάστηση συγκριτικά με αυτά που είχαν βλάστηση βρέθηκε χαμηλότερη περιεκτικότητα σε άνθρακα και άζωτο, μικρότερη μικροβιακή και μικρότερη ικανότητα ανοργανοποίησης αζώτου. Το DON ήταν η βασική μορφή αζώτου που εκχυλίστηκε από τα εδάφη. Η ανοργανοποίηση και η άμεση πρόσληψη από τα φυτά φαίνεται να είναι περιορισμένη και η εκχύλιση οργανικού υλικού με χαμηλή αρωματικότητα να ευνοείται. Το DON φάνηκε είναι ένας δείκτης των επιπτώσεων της υπερβόσκησης στα εδάφη.

# Table of Contents

1.	LITERATURE REVIEW .....	33
1.1	INTRODUCTION .....	33
1.1.1	<i>Soil Quality and Ecosystem Functions</i> .....	33
1.1.2	<i>Soil Threats and Soil Degradation in Agricultural Lands</i> .....	36
1.1.3	<i>Soil Restoration and Management Tools</i> .....	41
1.2	SOIL ORGANIC MATTER DYNAMICS IN TERRESTRIAL ENVIROMENTS .....	41
1.2.1	<i>Components of decomposing SOM</i> .....	41
1.2.2	<i>SOM chemical composition and protection mechanisms</i> .....	43
1.2.3	<i>Conceptual Model of Organo-Mineral Interactions (Kleber Zonal Model)</i> .....	49
1.2.4	<i>Conceptual Model for Soil Aggregation</i> .....	51
1.2.5	<i>Factors Affecting Soil Aggregation and Structure</i> .....	54
1.2.6	<i>Summary on SOM Stabilization</i> .....	58
1.3	SOM TURNOVER MODELING.....	59
1.3.1	<i>Model Categories and Characteristics</i> .....	59
1.3.2	<i>Process-oriented models</i> .....	62
1.3.3	<i>Summary on SOM Turnover Modeling</i> .....	72
1.4	THESIS OBJECTIVE .....	73
1.5	LITERATURE CITED.....	74
2.	RothC-CALIBRATION ISSUES AND UNCERTAINTY ANALYSIS .....	83
2.1	INTRODUCTION .....	84
2.2	METHODOLOGY .....	85
2.2.1	<i>Study sites</i> .....	86
2.2.2	<i>Physical fractionation</i> .....	88
2.2.3	<i>Carbon turnover modeling</i> .....	92
2.3	RESULTS AND DISCUSSION .....	96
2.3.1	<i>Soil Characterization</i> .....	96
2.3.2	<i>Carbon turnover modeling</i> .....	104
2.4	CONCLUSIONS .....	114
2.5	LITERATURE CITED.....	115
3.	CARBON LOSS DUE TO LANDUSE CHANGE ALONG A CLIMATIC GRADIENT .....	118
3.1	INTRODUCTION .....	119
3.2	METHODOLOGY .....	121
3.2.1	<i>Study sites</i> .....	121
3.2.2	<i>RothC modeling-methodological approach</i> .....	124
3.3	RESULTS AND DISCUSSION .....	127
3.4	CONCLUSIONS .....	145
3.5	LITERATURE CITED.....	147
4.	DEVELOPMENT OF A COUPLED CARBON, AGGREGATION AND STRUCTURE TURNOVER (CAST) MODEL FOR TOPSOILS.....	150
4.1	INTRODUCTION .....	151
4.2	METHODOLOGY .....	153
4.2.1	<i>Model conceptualization and description</i> .....	153
4.2.2	<i>Field data used for model evaluation</i> .....	163
4.2.3	<i>Methodological approach for initialization and calibration of the model</i> .....	164
4.3	RESULTS AND DISCUSSION .....	166

4.4	CONCLUSIONS .....	177
4.5	LITERATURE CITED.....	179
5.	SYNTHESIS: SOIL DEGRADATION IN KOILIARIS RIVER BASIN CRITICAL ZONE ONBSERVATORY ..	181
5.1	INTRODUCTION- KOILIARIS RIVER BASIN DESCRIPTION.....	182
5.2	SOIL THREATS AND SOIL DEGRADATION IN KOILIARIS RIVER BASIN.....	189
5.3	PRIMARY FACTORS CONTROLING AGGREGATION OF KOILIARIS SOILS .....	193
5.4	LANDUSE AND CLIMATE CHANGE IMPACTS: MODELING OF SOC CHANGE IN SHRUBLAND TO CROPLAND CONVERSIONS.....	206
5.5	DISSOLVED ORGANIC NITROGEN AS AN INDICATOR OF LIVESTOCK IMPACTS ON SOIL BIOCHEMICAL QUALITY .....	216
5.5.1	<i>Introduction</i> .....	216
5.5.2	<i>Methodology</i> .....	217
5.5.3	<i>Results</i> .....	220
5.6	LITERATURE CITED.....	227
6.	CONCLUSIONS.....	231
7.	APPENDIX.....	237

## Table of Figures

Figure 1.1 Schematic depiction of the soil critical zone (taken from Brantley, 2007).....	33
Figure 1.2 Terrestrial ecosystem pathways and processes to determine carbon cycling (taken from Dawson and Smith, 2007).....	36
Figure 1.3 Relationship between soil ecosystem shift drivers (the 4th driver fertilization, is not depicted) with soil functions and threats (taken from Nikolaidis, 2011).....	37
Figure 1.4 Pattern of average rate of SOC decline after the conversion of an uncultivated native land to cultivated (Data taken from Mann, 1986).....	38
Figure 1.5 Effect of stocking rate (animal density) on a) green biomass (herbaceous plants + shrub leaves) under current climate conditions in five climatic regions (open circle arid, open triangle semiarid, open diamond dry Mediterranean, inverted triangle typical Mediterranean, star mesic Mediterranean) in each habitat. Black dots indicate the mean stocking capacity (number of animals for which there is enough food in 9/10 years) of the habitat, b) on shrub cover under the five climatic regions (taken from Kochy et al., 2008).....	40
Figure 1.6 Effect of grazing on the patch-size distribution of vegetation in a Mediterranean ecosystem (Greece) (taken from Kefi et al., 2007) .....	40
Figure 1.7 Carbon structure associated with different soil size classes. The black regions indicate plant-derived compounds and the shaded regions indicate microbially-derived compounds (taken from Grandy and Neff, 2008). .....	45
Figure 1.8 Typical allocation of organic carbon in particle size fractions of temperate top soils: Abundance, composition, dynamics and relationship to microbial parameters (GA =galactose, MA =mannose, Ar =arabiose, Xy =xylose) (taken from Lutzow et al., 2007).....	46
Figure 1.9 Zonal model of organo-mineral interactions (taken from Klebel et al, 2007). .....	50
Figure 1.10 Macro-aggregate turnover: formation and degradation process (taken from Grandy and Neff, 2008).....	52
Figure 1.11 Change in aggregate turnover and mineralization rate of a) stabilized and b) newly added C input across ecosystems (taken from Plante and McGill, 2002).....	53
Figure 1.12 Changes in percentage of macro-aggregates and accumulation of SOC with time since cultivation (taken from Krull et al., 2004, modified from Jastrow, 1996).....	53
Figure 1.13 a) Effect of increasing SOC content on aggregate stability, measured by wet-sieving (MWD, mm), using air-dried (●) and field moist (○) samples (R = 0.98) (taken from Krull et al., 2004, original data Haynes, 2000), b) Relationship between wet sieving stability index and OM content in the 5th year of experiments in 3 sites with different texture (taken from Douglas and Goss, 1982). .....	54
Figure 1.14 Relationship between microbial biomass and aggregate stability in terms of the mean weight diameter in a Mollisol dominated by 2:1 minerals and an Oxisol by 1:1 minerals and oxides (taken from Six et al., 2004, original data Denef and Six, 2003). .....	55
Figure 1.15 A diagram describing the effect of climate on soil aggregation under natural ecosystems (taken from Dalal and Bridge, 1996) .....	57
Figure 1.16 Structure of an organism-oriented model (taken from Smith et al., 1998). .....	62
Figure 1.17 Structure of the Rothamsted Carbon Model (taken from Coleman and Jenkinson, RothC-26.3, Model description and users guide).....	65
Figure 1.18 Structure of the CENTURY model (taken from CENTURY Model Version 5, User's guide). ..	65
Figure 1.19 Concept of SOC fractions and that relates measureable SOC fractions to conceptual pools used in the RothC model (taken from Adams, 2011, based on Zimmermann et al., 2007), (dissolved organic matter (DOC), particulate organic matter (POM), sand and stable aggregates (S+A), silt and clay particles (s+c) and oxidation-resistant carbon (rSOC)).....	67
Figure 1.20 Structure of the STRUC-C model (taken from Malamoud et al., 2008).....	70
Figure 2.1 Soil organic carbon content in topsoil (0-15 cm) and subsoil (15-30 cm) of tilled and no-tilled olive grove fields (samples taken from the area between the trees) in the alluvial plain of Koiliaris River Basin (average and standard deviation derived by three spatial samples). (Details about these data are given in Chapter 5).....	88
Figure 2.2 Physical fractionation scheme used in the study. cPOM = coarse particulate organic matter, mM = micro-aggregates within macro-aggregates, sc-M = easily dispersed silt-clay fraction, fPOM =	

*fine particulate organic matter, sc-mM = silt-clay fraction of the microaggregate. POM fractions correspond to sand sized fractions and free POM.*..... 90

Figure 2.3 a) Soil water stable (sand free) aggregate distribution, b) C distribution among aggregates fractions, and c) N distribution among aggregates fractions. .... 99

Figure 2.4 a) C and b) N concentration of the sand free aggregate fractions ( $\text{g kg}^{-1}$ ). Values are shown as means ( $n=3$ ). Standard deviation was lower than 1-3% for OC and 1-4% for N. Mean values followed by the same lowercase letter under the same series label are not significantly different ( $p<0.05$ ). Mean values followed by the same uppercase letter under the same x-axis legend are not significantly different ( $p<0.05$ ). .... 101

Figure 2.5 a) Carbon and b) Nitrogen concentration in fractions (related with particulate organic matter and the minerals) of composite microaggregates ( $>250 \mu\text{m}$ ) and small macroaggregates (250-1000  $\mu\text{m}$ ). .... 102

Figure 2.6 Carbon and Nitrogen distribution among the fractions of composite microaggregates ( $>250 \mu\text{m}$ ) and small macroaggregates (250-1000  $\mu\text{m}$ ). .... 103

Figure 2.7 RothC simulation results under optimum solution for Iowa and Greece (carbon pools: RPM=resistant plant material, DPM=decomposable plant material, HUM=humus, BIO= biomass, IOM= inert organic matter, SOC= soil organic carbon, POC particulate organic carbon). DPM in both graphs is very low and coincides with the x-axis. .... 108

Figure 2.8 Tornado Graphs for 10% (black indicated) and 50% (grey indicated) sensitivity analysis. RPM=resistant plant material decomposition rate constant, DPM=decomposable plant material decomposition rate constant, HUM=humus decomposition rate constant, BIO= biomass decomposition rate constant, DPM/RPM ratio=the apportionment ratio of plant litter input DPM and RPM carbon pools, BIO%=the proportion that goes to BIO (100-BIO% is the proportion that goes to HUM). The x-axis of the graphs corresponds to the model predicted SOC content ( $\text{t C/ha}$ ) in the set-aside fields the 20<sup>th</sup> and 35<sup>th</sup> year of the simulation in Iowa and Greece respectively. .... 110

Figure 2.9 Uncertainty of soil organic carbon (SOC) and particulate organic carbon (POC) due to model parameters, input data, and initial conditions, as well as the total uncertainty, compared with the optimum solution (calibration). .... 111

Figure 2.10 The output distributions by the Monte-Carlo simulations for the calculation of the total uncertainty for 100 y of simulation in Greece and Iowa for soil organic carbon (SOC) and Particulate organic carbon (POC). The x-axis indicates the SOC or POC content in  $\text{t C/ha}$ . The value of the optimum solution for SOC and POC is indicated in the top of the plot separating the distribution in two parts: the left part (light shaded histogram bars) indicates the area of the distribution below the value of the optimum solution and the right (dark shaded histogram bars) indicates the area of the distribution below the value of the optimum solution. The percentage covered in each area is given in the bars at the top of each plot. .... 113

Figure 3.1 Tornado Graphs for 10% (left) and 50% (right) sensitivity analysis. Decomposition rate constants for RPM=resistant plant material, DPM=decomposable plant material, HUM=humus, and BIO=biomass, DPM/RPM ratio=the apportionment ratio of plant litter input DPM and RPM carbon pools, BIO%=the proportion that goes to BIO (100-BIO% is the proportion that goes to HUM), and RPM initial=the initial RPM carbon pool. .... 130

Figure 3.2 Total uncertainty of total organic carbon (SOC) and particulate organic carbon (POC) due to model parameters, input data, and initial conditions compared with the optimum solution (calibration) for the six sites. .... 132

Figure 3.3 a) Carbon loss in terms of average SOC loss, b) The cumulative loss of SOC proportional to the initial stocks, c) the ratio of the POC loss to the SOC loss. .... 135

Figure 3.4 Carbon loss in terms of a) average rate of SOC loss, b) and as proportional to initial SOC amount. The data of Mann (1986) are also drawn in the inserts within the figures, soil depth 30 cm. .... 137

Figure 3.5 a) The effectiveness of carbon addition by the application of amendments of different quality at annually doses of 2.5  $\text{t C/ha}$  (carbon amended: the cumulative load of the carbon amended to soil, Net C: the extra carbon sequestered as compared with the soil where no amended was applied), b) the proportion of the carbon sequestered that is stabilized in the silt-clay fraction. .... 140

Figure 3.6 Linear correlations of the annual RPM and HUM decomposition rates with climatic indexes, the soil clay content and the Particulate Organic Carbon (POC) initial pool. .... 142

Figure 4.1 Schematic overview of macro-aggregation. .... 154

Figure 4.2 Schematic representation of the carbon and aggregate turnover in the CAST model. .... 155

Figure 4.3 Simulated evolution of carbon content of modeled pools in the A) Greek and the B) Iowa cropland (initial conditions) to set-aside conversion (data used for calibration), a) soil (SOC), aggregate type 1 (AC1), type 2 (AC2), and type 3 (AC3) plus the coarse POM of the non aggregated pools (cPOM), b) the different pools contained in the aggregate type 3: silt-clay sized aggregates (AC1 in AC3), silt-clay related carbon of the micro-aggregates (silt-clay AC2inAC3), fine POM of the micro-aggregates (fPOM AC2inAC3) plus the intra macro-aggregated fPOM (fPOM inAC3), macro-aggregated cPOM (cPOM inAC3) plus the cPOM of the non aggregated pools. Points indicate the field measurements of the same colored line..... 167

Figure 4.4 Seasonal pattern of emissions of a) the coarse RPM litter pool and b) the soil (in the right up corner the small figure indicates the annual emissions for 20 years). ..... 168

Figure 4.5 Simulated evolution in the A) Greek and the B) Iowa cropland to set-aside conversion of a) silt-clay mass and b) carbon content (%) of the silt-clay fraction, related to aggregate type 1 (AC1), type 2 (AC2), silt-clay sized aggregates within the type 3 (AC1 in AC3), and micro-aggregates within the type 3 (AC2 in AC3). ..... 173

Figure 4.6 Simulated evolution in the A) Greek and the B) Iowa cropland to set-aside conversion of porosity (%) and bulk density (g/cm<sup>3</sup>). Points indicate the field measurements of the same colored line. .... 174

Figure 4.7 Simulated evolution of C-to-N ratio in the A) Greek and B) Iowa cropland to set-aside conversion, of soil, aggregate type 1 (AC1), type 2 (AC2), and type 3 (AC3) plus the coarse particulate organic matter of the non aggregated pools (cPOM). Points indicate the field measurements. .... 176

Figure 5.1 Classification of elevation-contour mapping (digital data sets were obtained from the data base of the Region of Crete. The respective data derive from the topographic diagrams (1:50000 scale) of the Geographic Service of the Army). ..... 182

Figure 5.2 Classification of geologic formations classes (Digital data sets were obtained from the data base of the Region of Crete. The respective data derive from the maps (1:50000 scale) of the Institute of Geology and Mineral Exploration (IGME)). ..... 183

Figure 5.3 a) Classification of soil types according to FAO - Calcaric Lithosols (Ic), Eutric Lithosols (Ie), and Calcaric Regosols (Rc), b) Greek classification for soil types - 4) Calcareous rendzines soil and mediterranean brown soil, 6) Brown and red-brown alkaline mediterranean soil, 10) Alpine humic Ranker type, 11) Podzols mixed with forest acid red soil. .... 184

Figure 5.4 Classification of land cover classes (digital data sets were obtained from the CLC 2000 (Corine Land Cover 2000) database which is available by the European Environment Agency). ..... 185

Figure 5.5 Soil mapping typology for the Koiliaris River Watershed (excluded areas in white color), towns, roads, and riparian buffer. .... 187

Figure 5.6 Geologic formations, landuses and hydrologic and nutrient fluxes in Koiliaris River Basin. Note: Runoff from Keramianos stream is higher than the total watershed surface runoff as water is lost through a karstic gorge and only peak flows contribute to Koiliaris River (taken from Stamati et al., 2011). .... 188

Figure 5.7 Comparison of simulated flows with field data at the basin outlet (taken from Nikolaidis et al., HESSD, under revision) ..... 189

Figure 5.8 The DPSIR Framework for soils in Koiliaris CZO. .... 192

Figure 5.8 Loading plot of first versus second component of PCA analysis. .... 197

Figure 5.9 Score plot of first versus second component of PCA analysis. .... 197

Figure 5.10 Loading plot of first versus third component of PCA analysis. .... 198

Figure 5.11 Score plot of first versus third component of PCA analysis. .... 198

Figure 5.12 Multi-regression analysis for combined Group-1 and Group-2 with 11 parameters used. 204

Figure 5.13 Multi-regression analysis for Group-2 with 11 parameters used. .... 204

Figure 5.14 Multi-regression analysis for Group-1 with 7 parameters used. .... 205

Figure 5.15 Tornado Graphs for 10% (left) and 50% (right) sensitivity analysis for the three shrubland to cropland conversions simulated in the Koiliaris Reiver Basin CZO. RPM=resistant plant material decomposition rate constant, DPM=decomposable plant material decomposition rate constant, HUM=humus decomposition rate constant, BIO= biomass decomposition rate constant, DPM/RPM ratio=the apportionment ratio of plant litter input DPM and RPM carbon pools, BIO%=the proportion that goes to BIO (100-BIO% is the proportion that goes to HUM). .... 209

Figure 5.16 Total uncertainty of total organic carbon (SOC) and particulate organic carbon (POC) due to model parameters, input data, and initial conditions compared with the optimum solution (calibration) for the six sites. .... 210

<i>Figure 5.17 The average rate of the change of carbon stock and the cumulative change of carbon stock change proportional to the initial stocks. ....</i>	<i>211</i>
<i>Figure 5.18 The effectiveness of carbon addition by the application of amendments of different quality at annually doses of 2.5 tC/ha on Trypalis soils (carbon amended: the cumulative load of the carbon amended to soil, Net C: the extra carbon sequestered as compared with the soil where no amended was applied). ....</i>	<i>215</i>
<i>Figure 5.19 The average rate of carbon sequestered due to the application of amendments of different quality at annually doses of 2.5 tC/ha for 20 years on Schists, Marls and Trypalis soils. ....</i>	<i>215</i>
<i>Figure 5.20 The effectiveness of carbon addition by the application of amendments of different quality at annually doses of 2.5 tC/ha for 20 years on Schists, Marls and Trypalis soils. ....</i>	<i>215</i>
<i>Figure 5.21 Annual fluxes of Nitrogen in the karstic system discharging Stilos spring, where, P = Precipitation flux, M= Manure flux, U = Urine flux, V= Volatilization, flux D= Denitrification flux, and S= Spring flux (taken from Stamati et al., 2011). ....</i>	<i>221</i>
<i>Figure 5.22 Exchangeable Mineral Nitrogen (EMN), Potential Mineralizable Nitrogen (PMN), Potential Soluble Organic Nitrogen (PSON), and Potential Soluble Organic Carbon (PSOC) of soil samples. Values followed by the same letter or number under the same series label are not significantly different (<math>p &lt; 0.05</math>) (taken from Stamati et al., 2011). ....</i>	<i>224</i>
<i>Figure 5.23 A comparison of the annual dissolved organic nitrogen (DON) river export versus livestock DON input (normalized to the grazing land area) for five rivers of Greece (taken from Stamati et al., 2011). ....</i>	<i>225</i>
<i>Figure 5.24 River concentration of dissolved inorganic nitrogen (DIN) relatively to the DON/TDN ratio in different watershed types (See detailed data in Table A5.5 in the Appendix) (taken from Stamati et al., 2011). ....</i>	<i>225</i>
<i>Figure A2.1 The output distributions by the Monte-Carlo simulations for the calculation of the uncertainty due to initial conditions, input data, and model parameters for 100 y of simulation in a) Greece and b) Iowa for soil organic carbon (SOC) and Particulate organic carbon (POC). The x-axis indicates the SOC or POC content in t C/ha. The value of the optimum solution for SOC and POC is indicated in the top of the plot separating the distribution in two parts: the left part (light shaded histogram bars) indicates the area of the distribution below the value of the optimum solution and the right (dark shaded histogram bars) indicates the area of the distribution below the value of the optimum solution. The percentage covered in each area is given in the bars at the top of each plot. ....</i>	<i>241</i>
<i>Figure A3.1 Uncertainty of total organic carbon (SOC) and particulate organic carbon (POC) due to model parameters, input data, and initial conditions compared with the optimum solution (calibration) for a) Tibet-Desert, b) Dakota-semi-arid, c) China-steppe, d) Turkey-steppe, e) Ethiopia-steppe, and f) Madagascar-forest. ....</i>	<i>250</i>
<i>Figure A5.1 Uncertainty of total organic carbon (SOC) and particulate organic carbon (POC) due to model parameters, input data, and initial conditions compared with the optimum solution (calibration) for the shrubland to cropland conversions of a) Schists, b) Marls, and c) Trypalis geologic substrate. ....</i>	<i>257</i>

## Table of Tables

<i>Table 1.1 Components of decomposing SOM.</i>	42
<i>Table 1.2 Gross estimation of SOM chemical composition (Schnitzer, 1991).</i>	43
<i>Table 1.3 Gross estimation of chemical composition of N- containing compounds in SOM (Schulten and Schnitzer, 1998).</i>	43
<i>Table 1.4 Main characteristics of processes-oriented versus organism-oriented models (After Adams et al., 2011).</i>	60
<i>Table 1.5 Main characteristics of the most frequent referred to models in the scientific literature (After Adams et al., 2011).</i>	63
<i>Table 2.1 Study sites location and characteristics.</i>	87
<i>Table 2.2 Mean monthly meteorological data used for the application of the RothC model in the two sites (taken from the Local Climate Estimator-New LocClim 1.10, Grieser, 2006).</i>	93
<i>Table 2.3 Chemical and physical properties of IA and GR soils.</i>	97
<i>Table 2.4 Soil water stable aggregate distribution (WSA, g sand-free aggregate/100 g soil), particle recovery, and mean weight diameter (MWD) as well C and N distribution among aggregates fractions (g/kg). Values are shown as means and standard deviation is given in brackets (n=3). Mean values followed by the same lowercase letter within the same column are not significantly different at P&lt;0.05). Mean values followed by the same uppercase letter within the same row are not significantly different at P&lt;0.05).</i>	100
<i>Table 2.5 The relative absorbance of FTIR spectra at 1630 (1/cm).</i>	103
<i>Table 2.6 Ratio of fPOC-to-cPOC concentration.</i>	104
<i>Table 2.7 Distribution of C and N in the particulate organic matter (POM) and in the silt-clay fractions.</i>	105
<i>Table 3.1 Study sites location and characteristics.</i>	123
<i>Table 3.2 Statistics of the parameter distributions for the solutions fell within the <math>\pm 5\%</math> of the SOC and POC field measured stocks as well as the optimum solutions derived by the Monte-Carlo simulation.</i>	128
<i>Table 3.3 The average SOC loss (t C/ha y) by the optimum solution and the statistics derived by the total uncertainty. In the last two columns it is presented the percentage variation of the 5% and 95% from the optimum solution.</i>	133
<i>Table 3.4 Stepwise regression of the average % from the initial SOC/ y loss (for the 1<sup>st</sup>, 5<sup>th</sup>, 10<sup>th</sup>, 20<sup>th</sup>, 50<sup>th</sup>, 75<sup>th</sup>, and the 100<sup>th</sup> year after the conversion) with the POC to SOC ratio and the temperature (TEMP) and the POC to SOC ratio and the Radiational Index of Dryness (RID).</i>	138
<i>Table 3.5 Stepwise regression (Pearson correlation) of the RPM and HUM annual decomposition rates with the clay (only in the case of HUM) content, the temperature (TEMP) and the particulate organic carbon (POC) initial pool.</i>	143
<i>Table 3.6 The Q10 temperature factor ('apparent' sensitivity) for the RPM and HUM RothC model pools as calculated by the calibrated values of this study.</i>	144
<i>Table 4.1a Field measured water stable aggregates (WSA) as well as sand corrected WSA and Carbon and Nitrogen content of the field measured pools for the Greek and the Iowa cropland and set-aside fields, used for the initialization and calibration of the model, respectively.</i>	165
<i>Table 4.1b Field measured silt-clay (SC) mass (t) in bulk soil and different aggregate fractions and its concentration in carbon (t C/100 t SC mass, %), used for the initialization and calibration of the model, respectively.</i>	165
<i>Table 4.2 Calibrated values of the rate constants and turnover time (1/rate constant -corrected with the 'abc' factors, see Table 4.3) of the model for the Greek and the Iowa cropland to set-aside conversion.</i>	170
<i>Table 4.3 Monthly correction factor for rate constants; the product of the rate modifying factor for temperature (a), the topsoil moisture deficit rate modifying factor (b), and the soil cover factor (c).</i>	171
<i>Table 4.4 Calibrated values of the C-to-N ratio of the mechanistic N model for the Greek and the Iowa cropland to set-aside conversion.</i>	176
<i>Table 5.1 Class assignments for geologic substrate types.</i>	183
<i>Table 5.2 Description of Land cover levels according to the CLC 2000 database and Class assignments for land cover types.</i>	185

Table 5.3 The major types of soil mapping typology for the Koiliaris River Watershed (90% cover of the area) and the sampling design. ....	186
Table 5.4 Pearson Correlation results and P-Value in parenthesis of WSA-250 with measured soil properties; inter-correlated parameters are also indicated. ....	194
<sup>1</sup> Although it was significantly inter-correlated with the >1000 $\mu\text{m}$ fraction it was decided to keep this parameter, since it is soil type specific. ....	194
<sup>1</sup> The parameter is significantly inter-correlated with the <20 $\mu\text{m}$ fraction which has been removed, although it is correlated with the <53 $\mu\text{m}$ fraction (pearson correlation 0.768) it was decided to keep this parameter, since it is soil type specific. ....	194
Table 5.5 Pearson correlation results (R-Sq) of the 15 soil properties used in the PCA. ....	195
Yellow highlighted cells correspond to R-Sq higher than 0.5 and red highlighted cells correspond to R-Sq higher than 0.7. ....	195
Table 5.6 Eigenvalue, and proportionally and cumulative explanation of the variation of soil samples. ....	196
Table 5.7 The three major components of the principal component analysis. ....	196
Table 5.8 Mean value, standard deviation, minimum and maximum soil parameters used in PCA analysis of the two groups indicated by first component. ....	199
Table 5.9 The values for soil parameters characterizing the two soil Groups. ....	200
<sup>1</sup> It is not recommended to use this parameter to group the soils due to the low range of the differences between the two soil groups which creates uncertainties. ....	200
Table 5.10 Statistics of the multi-regression analysis of all samples together and each group separately. ....	202
Table 5.11 Statistics of the multi-regression analysis of all samples and groups separately. ....	203
Table 5.12 Soil parameters for the shrublands and olive grove fields under different lithology in the Koiliaris River Basin CZO used for the simulation with RothC. ....	206
Table 5.13 Statistics of the parameter distributions for the solutions fell within the $\pm 5\%$ of the SOC and POC field measured stocks as well as the optimum solutions derived by the Monte-Carlo simulation for the three shrubland to cropland conversions simulated in the Koiliaris River Basin CZO. ....	207
Table 5.14a The effect of climate change on SOC stocks after the conversion of a shrubland to olive grove field. ....	213
Table 5.14b The effect of climate change on SOC stocks in a 50 year old olive grove field. ....	213
Table 5.15 The effect of climate change on carbon adition effectiveness in shrubaland to cropland conversions of different lithologies (% change of the Net C to C amended ratio, negative values indicate decline). ....	214
Table 5.16 Landuse load apportionment calculations. ....	219
Table 5.17 Physicochemical characteristics of soil samples (standard deviation in parenthesis). ....	222
Table 5.18 Bacteria species richness, bacteria and fungi populations in colony forming units (CFUs), and count ratio of fungi to bacteria for soil samples. ....	223
Table A3.1 Details on natural vegetation as well crop type and crop management for the six sites. ...	242
Table A3.2 Mean monthly meteorological data used for the application of the ROTHC model in the six sites (taken from the Local Climate Estimator-New LocClim 1.10, Grieser, 2006 according to the coordinates and elevation given in the manuscripts). ....	243
Table A3.3 Sensitivity coefficients (the absolute value of the ratio: $(\Delta Y/Y)/(\Delta x/x)$ ) for ROTHC model parameters for $\pm 10\%$ and $\pm 50\%$ change of the calibrated values for the six sites. ....	244
Table A5.1 The 15 soil properties used in the PCA analysis (the 12 first samples correspond to soil Group-1 and the latter 16 in soil Group-2). ....	251
Table A5.2 Mean monthly meteorological data used for the calibration (long average 1960-2010) and the climate change scenarios for the station of Samonas. ....	252
Table A5.3 Monthly and annual decomposition rates <sup>a</sup> (1/y) for resistant plant material (RPM) and humus (HUM) soil organic pools pools of ROTHC model for the Greek and Iowa sites. ....	253
Table A5.4 Sensitivity coefficients (the absolute value of the ratio: $(\Delta Y/Y)/(\Delta x/x)$ ) for ROTHC model parameters for $\pm 10\%$ and $\pm 50\%$ change of the calibrated values for the three shrubland to cropland conversions (for the 50 year of the conversion used for the calibration in all sites) for both soil organic carbon (SOC) and particulate organic carbon (POC). ....	254
Table A5.5 Concentrations of dissolved inorganic nitrogen (DIN) and DON/TDN ratio, as well as precipitation for the rivers presented in Figure 5.10 in Chapter 5. ....	258

# 1. LITERATURE REVIEW

---

## 1.1 INTRODUCTION

### 1.1.1 Soil Quality and Ecosystem Functions

Soil critical zone is defined as the top layer of the earth's crust situated between the bedrock and the tree top (Figure 1.1) (Brantley, 2007). Soil, defined as the top layer of the earth's crust (between the bedrock and the surface, excluding the groundwater zone) is our second most important natural resource after water that performs a number of key environmental, social and economic functions (Blum, 2005).

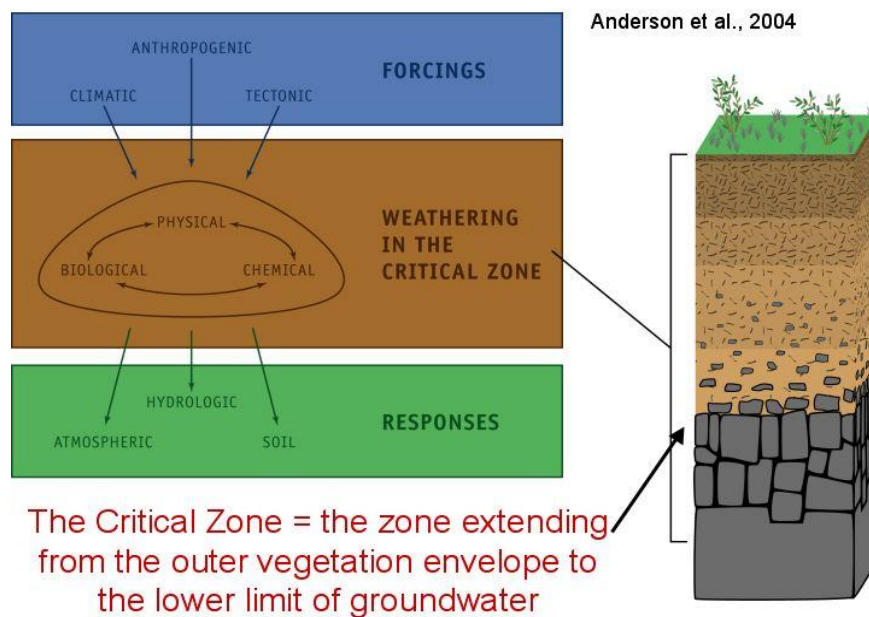


Figure 1.1 Schematic depiction of the soil critical zone (taken from Brantley, 2007).

*“Soil ecosystem functions are derived from the dynamic actions of plant, animal and microorganism communities and the non-living environment interacting as a unit” (Nikolaidis, 2011). The soil functions identified in the Communication “Thematic Strategy for Soil*

Protection” (European Commission, 2006a) and the upcoming Directive for Soil Protection (European Commission, 2006b) are: food and other biomass production, storing, filtering and transformation of many substances including water, carbon, nitrogen, habitat and gene pool, physical and cultural environment for humankind, source of raw materials. The Soil Science Society of America Ad Hoc Committee on Soil Quality (S-581) defined soil quality as *“the capacity of a reference soil to function, within natural or managed ecosystem boundaries, to sustain plant and animal productivity, maintain or enhance water and air quality, and support human health and habitation”* (Karlen et al., 1997). Understanding soil quality means reading and managing the soil so that it functions optimally now and is not degraded for future use (Lewandowski et al., 1999). Soil quality together with water and air quality correspond to Environmental quality which is a major component for agro-ecosystem sustainability (agronomic sustainability and socio-economic viability are the other two) (Andrews et al., 2002).

The scientific community has examined the factors indicating soil quality and many soil quality indicators have been proposed in response to the growing needs of evaluating and monitoring of soils worldwide. Hall (2003) reviewed 488 records of scientific publications regarding soil quality indices (static or dynamic, point, regional, farm-level or national scale, as well as catchment or riparian zone scale, applied to forest, rangeland or grassland, landuses). Field-, Farm-, or Watershed Scale indicators differ from Regional-, National-, or International Scale indicators; non point indicators are used for assessments on larger scales (Lewandowski et al., 1999). The framework of soil quality research resembles the relative water quality assessments. For example the DPSIR framework (Driver-Pressure-State-Impact-Response) which is usually used in water quality assessments can be also applicable to soil quality assessments (Jónsdóttir, 2011). The structure of an analogue approach is (Lewandowski et al., 1999): 1) management practices and systems (measures of management e.g. pesticide use, tillage methods, grazing pressure, or crop rotations - quantify the Pressures), 2) observable soil characteristics (State), 3) soil processes (Impact), and 4) the performance of soil functions (Response). Soil performance, or response, measurements include yield per unit input, erosion rates, stream flow rates and sediment levels, and levels of water contaminants. These are direct measures of the benefits we receive from soil.

There are several criteria to consider when selecting soil health and soil quality indicators. In general, appropriate indicators should be (Kinyangi, 2007; Lewandowski et al., 1999): 1) readily and economically accessible, 2) sensitive to management changes, but somewhat

stable in response to non-management changes such as weather, 3) able to reflect/measure aspects and changes of the functioning of the system both at plot and landscape scales, 4) always exist throughout a field or region but respond to temporal and spatial variation in ecosystem function to make management decisions, 5) accessible to many farmers, 6) sensitive to variations in agro-ecological zone, 7) representative of physical, biological or chemical properties of soil, 8) assessed by both qualitative and/or quantitative approaches. There is no single ideal indicator or suite of indicators of soil function. They are interrelation, and each provides different clues about the processes occurring in soil. Most research has measured the characteristics, or the state, of the soil. Using these measurements requires an understanding of how soil characteristics are linked to soil performance and to management practices. Dynamic soil characteristics are those that change on human time scales—biological activity, some structural features, and water and nutrient movements (Lewandowski et al., 1999). Practically speaking, inherent characteristics are those that change over geologic time scales—texture, slope, mineralogy, and depth. Previous assessments of soil have focused on inherent features and how they relate to potential productivity, erodibility, and determinations of appropriate landuse (Lewandowski et al., 1999).

Soil is formed by mineral particles, organic matter, water, air and living organisms, being in fact an extremely complex, variable and living medium (COM2006(231); COM2006(232)). Soil organic matter (SOM), even if minor in quantity, plays a significant role in soil functional services (COM2006(231); COM2006(232); Lal, 2004a): it is a source of nutrients for the plants, a substrate for microbial activity, a driver for mineral weathering (micronutrient production) and a regulator of the climate, as it is a sink of CO<sub>2</sub> (Figure 1.2). Soil organic matter (SOM) is a mixture of biogenic components (plant, animal, and microbial residue) in various stages of decomposition, microorganisms and non-decomposed plant materials (Arias et al., 2005). Live soil organisms and plant roots are not considered SOM until they die and begin to decay. SOM cycling and its stabilization in soils control soil microbial community, fertility and structure (size and stability of aggregation), which in turn affects infiltration rate, moisture content, oxygen diffusion, runoff, and erosion (Arias et al., 2005; Six et al., 2004). Globally, more than twice as much carbon is held in soils as in vegetation and the atmosphere, while the amount of carbon sequestered in soil organic matter annually is four times less than the 8 Gt of anthropogenic carbon emitted to the atmosphere annually—a fact that underlies the importance of SOM in relation to climate change (Lal, 2004a).

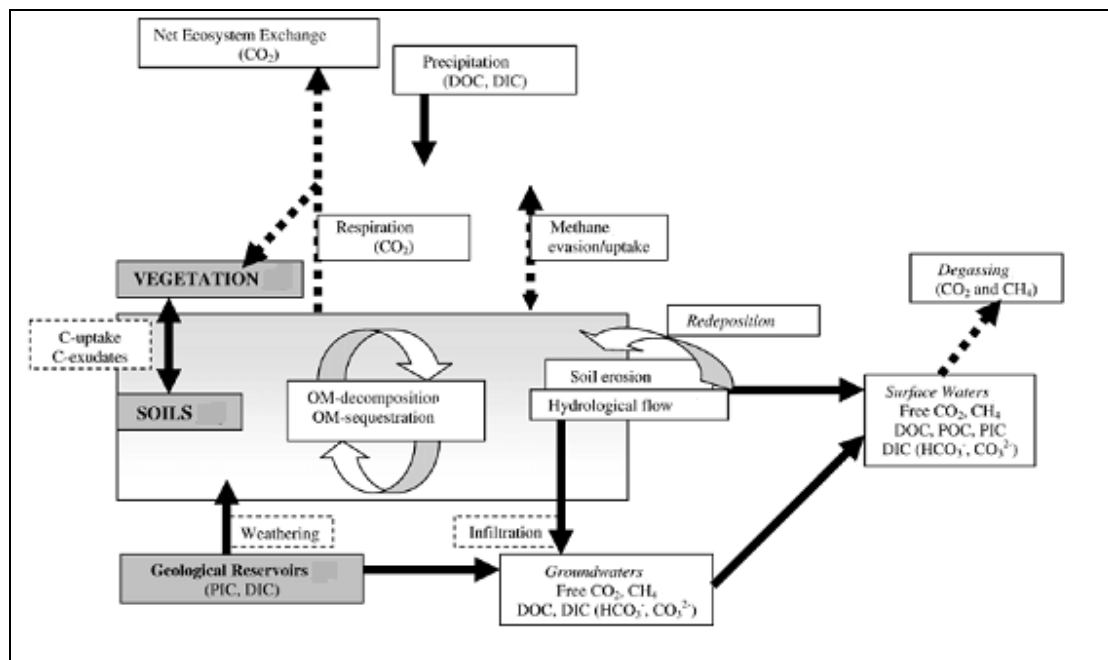
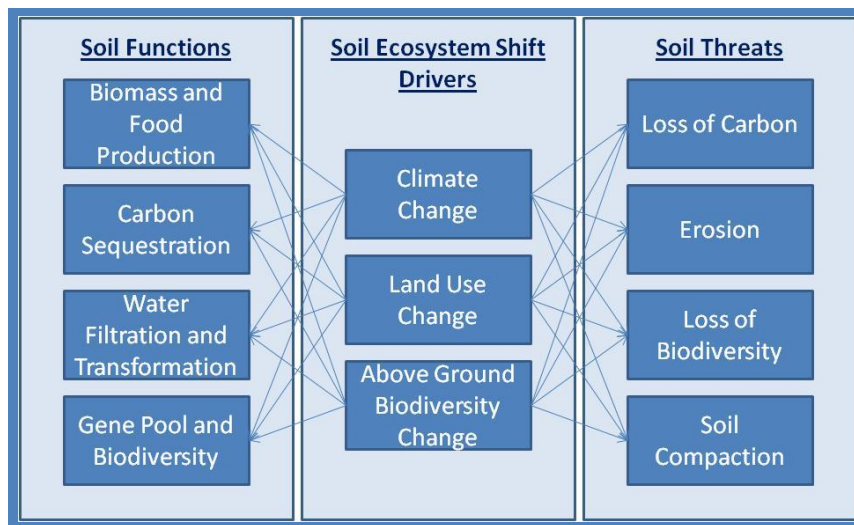


Figure 1.2 Terrestrial ecosystem pathways and processes to determine carbon cycling (taken from Dawson and Smith, 2007).

### 1.1.2 Soil Threats and Soil Degradation in Agricultural Lands

Humans have not integrated themselves in the soil ecosystem, but depended on its services, by using soil functions, for sustenance (Nikolaidis, 2011). The anthropogenic impact on soils increased substantially during the last decades due to industrial pollution, traffic and agricultural practices. Intensification of agricultural production and inappropriate agricultural practices used by human over the past 60 years aimed to maximize agricultural production, without considering soil as a system (Nikolaidis, 2011; Banwart et al., 2011). Consequently, modern agricultural systems may have become productive, but are highly dependent on external input (Altieri, 1999). However, fertilizers are rather expensive and they are not used appropriately. We use 50 times more P from the quantity we really need, sending enormous quantities of P to waste water treatment plants and finally causing eutrophication to waters, while on the other hand the P-rock deposits decline (Nikolaidis, 2011). Moreover current agricultural practices are unsustainable since require 10–57 times more energy to produce 1 unit of energy of a meat product and 7–10 units more energy for a plant product (Nikolaidis, 2011). In Greece, there are about 255000 tractors which are so heavy that cannot plow according to contours but only vertically, causing erosion (Nikolaidis, 2011). Moreover, the use of pesticides results in monoculture, destroying above ground biodiversity.

Overall, agricultural practices have severely affected soil ecosystem functions and in many cases caused soil ecosystem collapse, impacting water and soil quality. Soil ecosystem shifts, abrupt changes ('tipping point') that have long-lasting effects on the landscape and both the biotic and abiotic structure of the soil, can happen due to climate change, land use changes such as changes from native lands to cultivated lands, and decline of above ground biodiversity due to agricultural practices used in cultivation and overgrazing (Nikolaidis, 2011) (Figure 1.3).



**Figure 1.3 Relationship between soil ecosystem shift drivers (the 4th driver fertilization, is not depicted) with soil functions and threats (taken from Nikolaidis, 2011).**

A characteristic example of permanent shift due to change of climatic conditions as well as anthropogenic factors is the Sahel transition zone in Sahara where the landscape was changed permanently in a few kilometers after the drought of 1968 (Zheng, 2003; Zwarts et al., 2009). The Sahel drought was likely initiated by a change in worldwide ocean temperatures, which reduced the strength of the African monsoon, and was exacerbated by land-atmosphere feedbacks through natural vegetation and land cover change as well as anthropogenic factors, such as overgrazing and conversion of woodland to agriculture land use, all changes by humans which may have played the major role (Zheng, 2003; Zwarts et al., 2009).

Conversion of native lands to agricultural lands, arable and grazing lands, results in the reduction of plant cover and therefore of the litter input, water erosion (Bastida et al., 2006; Li et al., 2007), compaction, and eventually, destruction of soil structure and loss of SOM, and/or degrading of its quality. During plowing, the soil aggregates are rapidly destroyed; O<sub>2</sub> can now reach the previously protected OM, which can be microbially oxidized (Balesdent et al., 1998; Wagai et al., 2008; Don et al., 2009; Emadi et al., 2009). Changes can be very abrupt as can be depicted by the average rate of SOC decline after the conversion of an uncultivated native land to cultivated land in Figure 1.4 by data taken by Mann (1986).

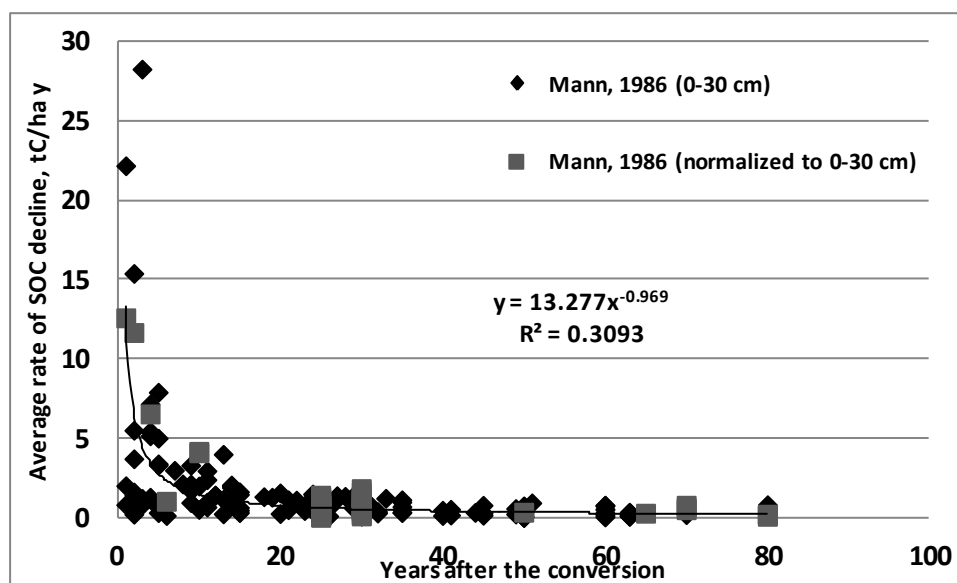


Figure 1.4 Pattern of average rate of SOC decline after the conversion of an uncultivated native land to cultivated (Data taken from Mann, 1986).

In Europe as a whole the percentage of soils with less than 2.6% organic matter rose from 35% to 42% in the period 1980-1995 (European Commission, 2000). In the same period, soils in the Beauce region south of Paris lost half of their organic matter (European Commission, 2000). Furthermore Bellamy et al., (2005) demonstrated that soil carbon loss in England and Wales over the past quarter of a century is as high as 16%. Decline of SOM constitutes also decline of nutrients in soils, since conventional agriculture only puts major nutrients into the soil in the form of N:P:K fertilizers. As a result food stuffs in the UK are up to 75% depleted in various minerals and trace metals relative to values half a century ago (Thomas, 2007). The

75% of the Mediterranean area exhibits SOM in the low (3.4%) to very low (1.7%) range (Van-Camp et al., 2004). Of note is that agronomists consider soils with less than 1.7% organic matter to be in a pre-desertification stage (European Commission, 2006a and 2006b). Mediterranean areas in contrast with northern Europe are particularly prone to erosion since they are subjected to long dry periods followed by heavy bursts of erosive rain, falling on steep slopes with fragile thin soils (Grimm et al., 2002) due to the prevalence of hard limestones substrate (Yassoglou et al., 1997).

Livestock grazing alone is responsible for 23% of soil degradation in Europe (RCEP, 1996) and is particularly intense in the Mediterranean region. Free grazing of uncontrolled length and frequency and high stocking densities are responsible for the de-vegetation of many areas within this region (Hill et al., 1998). The Greek island of Crete represents a characteristic case of land degradation resulting from intensive grazing (Hill et al., 1998). Since Greece joined the European Communities in 1981, grazing in mountainous regions has expanded due to subsidies that became available through the Common Agricultural Policy (Hill et al., 1998). Plants develop a positive interaction in order to maintain for example more water (Rietkerk et al., 2004). As the animal stocking density increases, plant productivity declines (Figure 1.5) (Kochy et al., 2008). Decline of patch size distribution due to overgrazing (Figure 1.6) diminishes the local positive interaction among plants and has been suggested as a warning signal for the onset of desertification (Kefi et al., 2007). Grazing has been also found to affect the mobility of dissolved organic matter; dissolved organic nitrogen (DON) has been found to be decoupled from the production of dissolved organic carbon (DOC) in such soils and has proportionally more labile soluble organic matter (Ghani et al., 2007; Mc Donald et al., 2007). However, detailed information on the nature, bioavailability, and fate of the mobilized dissolved OM following a change in landuse such as de-vegetation is still lacking (Akagi and Zsolnay, 2008).

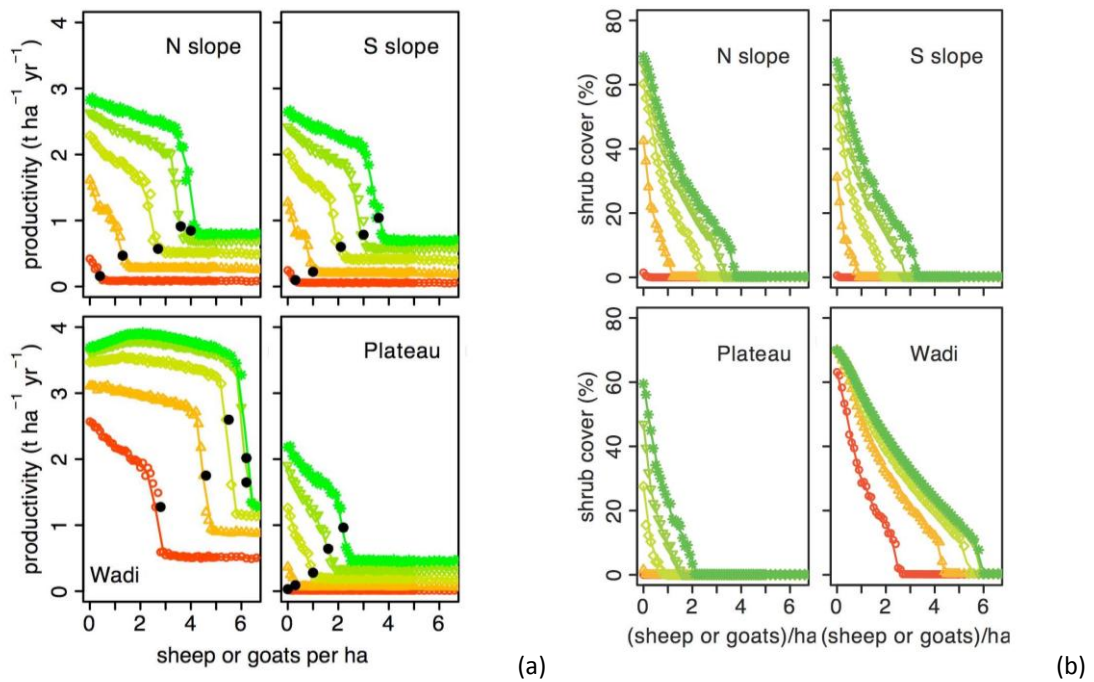


Figure 1.5 Effect of stocking rate (animal density) on a) green biomass (herbaceous plants + shrub leaves) under current climate conditions in five climatic regions (open circle arid, open triangle semiarid, open diamond dry Mediterranean, inverted triangle typical Mediterranean, star mesic Mediterranean) in each habitat. Black dots indicate the mean stocking capacity (number of animals for which there is enough food in 9/10 years) of the habitat, b) on shrub cover under the five climatic regions (taken from Kochy et al., 2008)

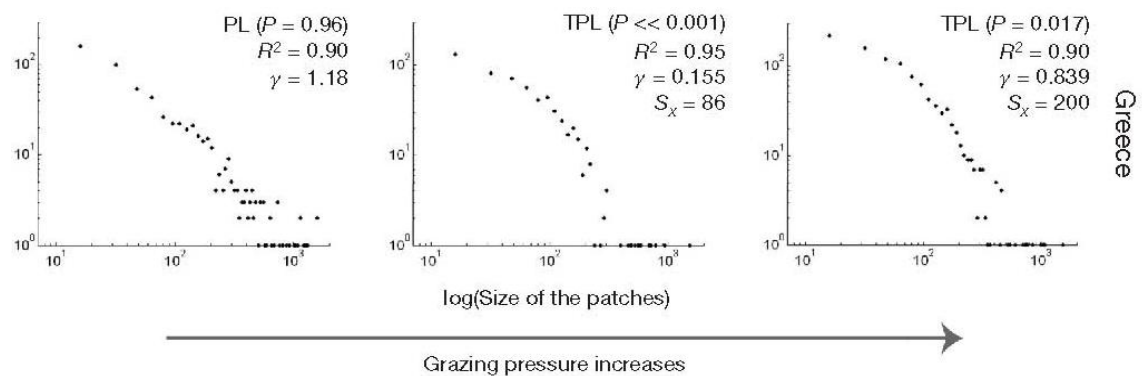


Figure 1.6 Effect of grazing on the patch-size distribution of vegetation in a Mediterranean ecosystem (Greece) (taken from Kefi et al., 2007)

### **1.1.3 Soil Restoration and Management Tools**

Current agricultural practices threaten soil functions and quality through inter-correlated threats like erosion, loss of SOM, loss of biodiversity, and compaction (Figure 1.5) which damage soil fertility and make soil susceptible to desertification (European Commission, 2006a), threatening sustainable development (European Commission, 2001) with global consequences for food security, climate change, water quality, and economy (Lal, 2004b). Soil erosion in farmlands is observed at rates up to two or three orders of magnitude faster than soil formation (Brantley et al., 2007) and therefore soil should be managed as a largely non-renewable, natural resource (European Commission, 2006a). In the next 20-50 years, the pressures on soil and its core service functions are predicted to further increase, due to climate change (droughts, extreme precipitation events), and competing demands from production systems to provide food crops, biofuel and timber (Richardson, 2010). It is therefore of prime importance to re-evaluate the methodologies we are using in agriculture and develop alternative sustainable soil farming management systems that incorporate the sustainable ecological functioning of soils and protect rather than deteriorate soils (European Commission, 2006b). The main question that emerges is: what is the methodology that can be developed to increase SOM/reduce the greenhouse effect and at the same time to increase fertility? There is urgent need for tools and methodologies that will give reliable predictions for climate change effects and restoration management to evaluate alternatives. Carbon and nitrogen dynamics in terrestrial environments have been reviewed extensively in the recent years (e.g. Nikoalidis and Bidoglio, 2011 and cited review papers therein). The literature review in this thesis attempted a synthesis of the literature with an emphasis in bridging the gap between the insights of the recent scientific knowledge in carbon and nitrogen turnover in soils and ways organic matter is modeled.

## **1.2 SOIL ORGANIC MATTER DYNAMICS IN TERRESTRIAL ENVIRONMENTS**

### **1.2.1 Components of decomposing SOM**

Carbon dynamics in soils are driven by photosynthetically derived plant litter inputs to the soil system. Components of decomposing SOM are presented in Table 1.1. Plant litter is physically fragmented into Particulate Organic Matter (POM) which is primarily composed of lignins, cellulose and hemi-cellulose (Trevenot et al., 2010). Microorganisms uptake and

decompose POM. The products of decomposition are sugars, polyphenols and quinones. The products from microorganism lysis and released exudates are amino compounds, acids and sugars. Linear chains (>250) of amino acids form proteins which are essential parts of microorganisms and plants participating in all processes within their cells. Amino acids are bonded together with peptide bonds (CO-NH amide moiety) to form the protein chains. Many proteins are enzymes with specific roles in catalyzing chemical reactions within the cell (metabolism) or outside the cell (substrate utilization by microorganisms). Other proteins are involved in signaling processes or as structural components of the cell. Rillig et al. (2007) classified proteins into two categories, the detrital proteins (released after cell lysis) and the functional proteins that include microbial surface-active proteins and extracellular enzymes. Finally, mycorrhizal fungi contribute glycoprotein complex molecules to the SOC pool through the release of exudates and products of fungal lysis. Plants and microorganisms produce enzymes to mitigate oxidative stress, detoxify phenolic compounds and utilize carbon sources. Environmental factors such as oxygen availability, soil pH, mineral and organic matter composition as well as nitrogen enrichment regulate the overall enzyme activity in soils. The interactions between the biological and environmental factors produce positive and negative feedbacks that control the content of organic matter in soils. Plant roots release exudates that can “prime” microbial activity (Kuzyakov, 2010; Blagodatskaya and Kuzyakov, 2008) and the phenomenon is especially significant in microbial hotspots where the activity is intense.

**Table 1.1 Components of decomposing SOM.**

<b>Vascular plant residues</b>	<b>% Dry matter</b>	<b>C to N ratio</b>
cellulose	15% to 60%	20 - 50 (tree leaves) 25 - 80 (herbaceous plants)
hemicellulose	10% to 30%	
Lignin, a macropolymer of phenylpropane monomers (secondary wall of woody cells in vascular plants)	5% to 30%	
N-containing compounds such as amino acids, amino sugars, pyrimidines and purines or porphyrin structures	2% to 15%	
lipids, waxes, resins, tannins and pigments		
<b>Bacterial biomass</b>		
N containing compounds (proteins, peptides and amino acids)	50% to 60%	5 - 8
lipid contents	10% to 35%	
Water soluble carbohydrates cell walls containing	5% to 30% 4% to 32%	
<b>Fungi</b>		
N containing compounds	14% to 52%	~10
lipids	1% to 42%	
water-soluble carbohydrates	8% to 60%	

### 1.2.2 SOM chemical composition and protection mechanisms

Until few decades ago, 65% (Table 1.2) of SOM was considered to be a system of polymers, called humic substances (HS), consisted of products of biologically-assisted synthesis from compounds deriving from degradation of lignin, polyphenols, cellulose, and amino acids (Schnitzer, 1991). Proteinaceous materials (proteins, peptides, amino acids) comprise 40% (Table 1.3) of N-containing components in SOM (Schulten and Schnitzer, 1998). HS were considered to be the most stable fraction of SOM due to their refractory character. This consideration led to the operational separation of soil humus according to its solubility in either acid or alkali, to humic and fulvic acids, and humin. However, the traditional alkaline (NaOH) extraction procedures used for this fractionation affected different stabilization mechanisms (organo-mineral, organo-organo, aggregation, and the SOM stabilized by polyvalent cation bridges on mineral surfaces, when  $\text{Na}_4\text{P}_2\text{O}_7$  was also used) and therefore did not yield in homogenous in terms of turnover rates or functional OM pools (von Lütow et al., 2007).

**Table 1.2 Gross estimation of SOM chemical composition (Schnitzer, 1991).**

Carbohydrates	10%
N-components (proteins, peptides, amino acids, amino sugars, purines, pyrimidines, unidentified compounds)	10%
Alkanes, fatty acids, waxes, resins, etc.	15%
Humic substances	65%

**Table 1.3 Gross estimation of chemical composition of N- containing compounds in SOM (Schulten and Schnitzer, 1998).**

Proteinaceous materials (proteins, peptides, amino acids)	40%
Amino sugars	5-6%
Heterocyclic N compounds (including purines, pyrimidines)	35%
$\text{NH}_3$ (app. $\frac{1}{4}$ of the $\text{NH}_3$ is fixed $\text{NH}_4^+$ )	19%

The prevalence of amide forms of nitrogen within humic fractions, suggested by extensive experimental evidence, was the main evidence that key synthesis reactions postulated by the “polymer model”, which suppress amide N functional groups as part of the pathway for the creation of humic substances, are not dominant processes in natural systems (Rilling et al.,

2007). Piccolo (2001) and Sutton and Sposito (2005), following on work by Wershaw et al. (1996), gathered the recent information from independent analytical techniques and suggested a new view of the molecular structure of soil humic substances, where they are considered as supramolecular associations, of chemically diverse organic molecules, including recognizable biomolecules, form dynamic associations (clusters) stabilized by hydrophobic interactions (van der Waals, a-n, CH-n) and hydrogen bonds (H-bonds) the former becoming more important with the increase of pH.

Moreover, Kleber and Johnson (2011) in their review demonstrated literature evidence that humic substances obtained by alkaline extractions are chemically and physically different from the organic materials that actually occur in soils. Alkaline extractions modify the protonation state of oxygen-containing functional groups and cleave lignin moieties. They also interfere with mineral-organic associations by modifying mineral surface reactivity through dissolution processes, releasing organic matter that was previously adsorbed on mineral surfaces and creating fresh mineral surfaces for the sorption of other organic compounds that have previously been free (Kleber and Johnson, 2011). In addition, latest technologies such as NMR and synchrotron spectroscopy did not detect evidence for discrete humic molecules in unprepared soil (Lehmann et al., 2008). Therefore the extracted humic substances are most likely a product of the extraction procedure rather than a true in-situ component of SOM (Adams et al., 2011; Kleber and Johnson, 2011).

Recent literature suggested that aromatic compounds are not selectively preserved (Gleixner et al., 2002; Knicker, 2007; Baldock, 2007). The concept of inherent chemical stability was questioned in the literature based on the theory that aromatic structures found in stable materials were the products of incomplete combustion with variability in recalcitrance and degradability (biochar) and were not the result of natural decomposition process (Knicker, 2007; Baldock, 2007; Kleber and Johnson, 2010, Adams et al., 2011). Biochar exhibits turnover time in the range of centuries to millennia (Powlson et al., 2011). The positive correlation that had been observed between the concentration of humic acids and the period of biological activity was not linked to the humification process but to the climate: summer dryness promotes vegetation fires and black carbon inputs according to Kleber and Johnson (2010). More or less almost every soil has experienced fire events (Kleber and Johnson, 2010). The higher soil carbon content implied either dry climate or high vegetation input and this could be the reason for the power pattern, site specific though, observed by Fallloon's data for the estimation of inert carbon, used in the RothC model. The authors of RothC model

recently reported that they visualized the inert organic matter (IOM) as an ancient clay-bound OM and may be ancient carbonized material such as coal (Jenkinson and Coleman, 2008).

The combination of physical fractionations (aggregate, particle size, and density fractions) with various chemical and spectroscopic methods for the chemical characterization of these fractions offered ample evidences and many insights (Figures 1.7 and 1.8) for the formulation of a more mechanistic conceptualization of SOM turnover and composition and stabilization that was suggested from many scientists today (see reviews of von Lützow et al., 2007 and Grandy and Neff, 2008).

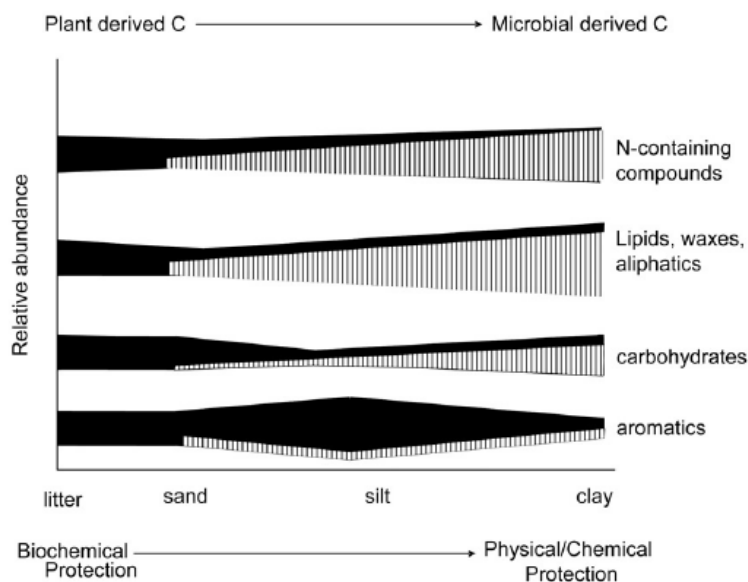


**Figure 1.7 Carbon structure associated with different soil size classes. The black regions indicate plant-derived compounds and the shaded regions indicate microbially-derived compounds (taken from Grandy and Neff, 2008).**

Major organic materials (i.e. lignin, cellulose and hemicellulose, lipids and proteins) as well as black carbon are considered fully decomposable under ‘perfect’ conditions (i.e. sufficient oxygen supply), even though some organic materials might take longer to decompose than others (i.e. wood > leaves) (Adams et al., 2011; Baldock, 2007). OM ‘recalcitrance’ has been found to be lowest in the most physically protected fractions and highest in the less protected fractions (Rovira et al., 2002). Lignin was associated with the free organic matter and was found in coarse (sand sized) fractions in the form of fairly untransformed lignin

polymer (Bahri et al., 2008), but, as it was severely biodegraded, did not contribute to the refractory pool and was depleted in silt-clay fractions and micro-aggregates where the most stabilized carbon can be found (Grandy and Neff, 2008) (Figure 1.7). Sand was depleted in (plant origin) carbohydrates as they were preferentially decomposed. Finer fractions and aggregates and especially clay (<2 μm) was significantly enriched in microbially synthesized metabolites (Alkyl C and/or O/N alkyl C), N-containing compounds (proteins, amino acids), and hydrocarbons such as waxes and lipids (Schoning et al., 2005; von Lutzow et al., 2007; Grandy and Neff, 2008). Generally, there was some evidence that the degree of decomposition increased with decreasing aggregate size as well as the C/N ratio (von Lutzow et al., 2007).

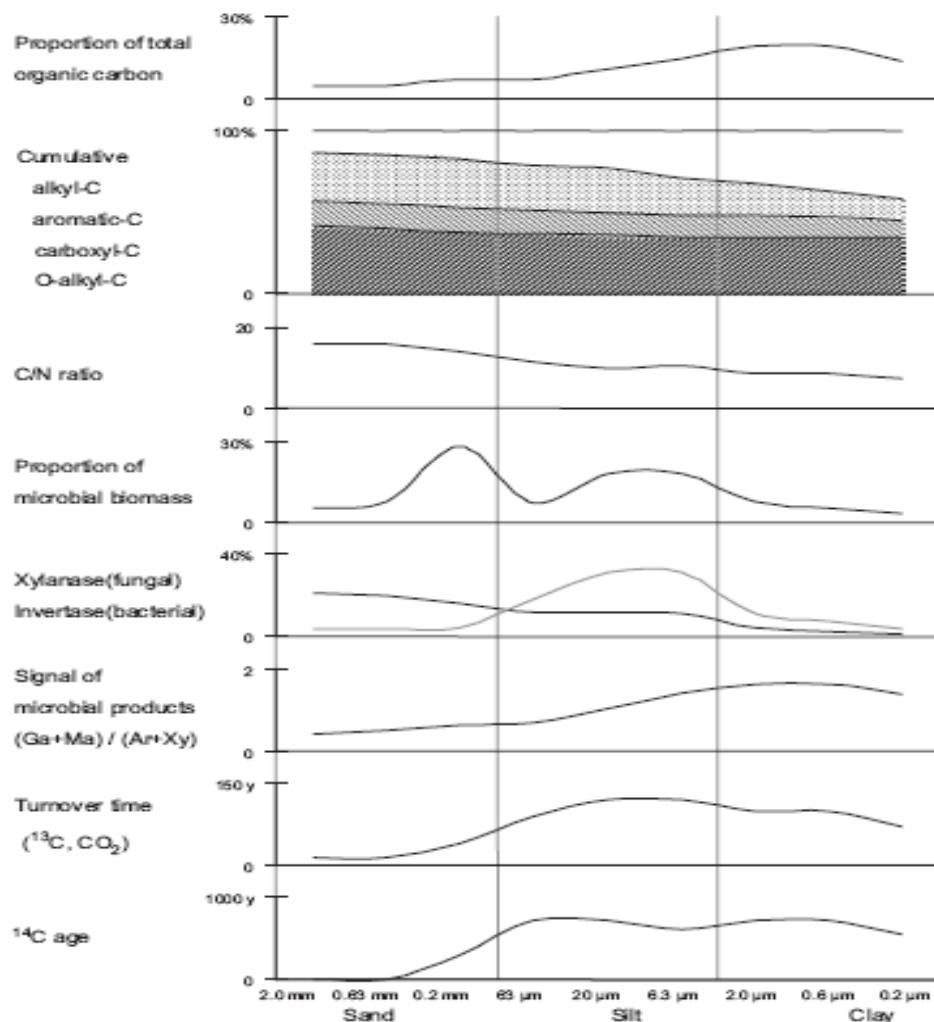


**Figure 1.8 Typical allocation of organic carbon in particle size fractions of temperate top soils: Abundance, composition, dynamics and relationship to microbial parameters (GA =galactose, MA =mannose, Ar =arabiose, Xy =xylose) (taken from Lutzow et al., 2007)**

Apparently N was much better protected than C (Hassink et al., 1993) and long life-times have been observed for N-containing (~49 years) and polysaccharide derived (~54 years) compounds (Gleixner et al., 2002). The interaction of the various nitrogen compounds with the mineral play an important role in the regulation on nitrogen transformation in soils by limiting its availability (Nikolaidis and Bidoglio, 2011). Jamtgard et al., (2010) found that the concentration of bound amino acids in unfertilized soils were 50 times higher than the free amino acids in solution as well as higher than the ammonium and nitrate concentrations suggesting the importance of soils in regulating the availability of enzymes for soil organic matter decomposition. The long term stabilized SOM by clay did not differ in quality between soils e.g. tropical and temperate soils (review of Six et al., 2002b), while in the silt and sand fraction different degrees of decomposition were found due to climatic effect. The type of clay played also a major role; 2:1 clays as they have higher cation exchange capacity (CEC) and surface areas as compared with 1:1 clays stabilized more C (reviews of Six et al., 2002a and Six et al., 2002b). It has been found a direct relationship between the silt plus clay content of soil and the amount of silt- and clay-protected soil C, indicating a saturation level for silt and clay associated C (Hassink, 1997; Six et al., 2002a; Six et al., 2002b). Worth noting was the finding of Bechtold and Naiman (2009) that century model underestimated soil N by 35%, suggesting that the model failed to detect the N enrichment of an OM pool after its initial formation.

Moreover, regarding the nitrogen cycle the traditional view was that SON is being mineralized to ammonia and ammonium ion due to microbial activity in the soils (Mineralization-Immobilization-Turnover, MIT route) (Nikolaidis and Bidoglio, 2011). Ammonium is then converted to nitrite and then to nitrate through the microbial assisted nitrification process. Denitrification converts nitrate to nitrogen gas and nitrous oxide. Microbial cell synthesis requires ammonium uptake creating an immobilization mechanism, while plants uptake nitrate and ammonium for the development of plant tissue. However recent finding suggest that SON by enzyme catalyzed de-polymerization results into light molecular weight Org-N such as amino-acids and aminosugars which plants uptake directly (Direct route) these monomeric Org-N compounds (Schimel and Bennett, 2004; Neff, 2002). Nannipieri and Eldor (2009) extending the review of Schimel and Bennett (2004), identified three pathways of org-N transformation: i) direct mineralization of org-N to ammonium by microorganisms, ii) release of org-N due to micro-organism lysis and exudates, and iii) excretion of ammonium by bacterial-grazing protozoa and nematodes. Three factors determine the relative importance of the direct route of org-N uptake versus the MIT route in

various ecosystems: the form of available N, the source of C, and the availability of N relatively to C (Geisseler et al., 2010). Two additional processes have been suggested as being important in the microbial N transformation in soils: Nitrifier denitrification (oxidation of ammonium to nitrite followed by reduction of nitrite to nitrogen gas) and anaerobic ammonia oxidation (Anammox – Oxidation of ammonium to nitrite followed by reduction of nitrite to hydroxylamine; hydroxylamine then reacts with ammonium to form hydrazine which is oxidized to nitrogen gas and the released electron are used to reduce nitrite) (Nikolaidis and Bidoglio, 2011).

Most models were designed based on the assumption that biochemically protected carbon contributing to humus, inert or passive, organic carbon pools was the product of the humification process, a very stable highly aromatic material (Kleber and Johnson, 2010). An updated concept of the dynamic nature of SOM is the realization that accessibility and sorption interactions with mineral surfaces may provide powerful protection against decomposition, explicitly including carbohydrates, proteins and other supposedly 'labile' materials (Kleber and Johnson, 2010). Decomposed plant residues and/or remnants of microbes and fungi and their sorptive interactions with mineral surfaces might be responsible for the stability of parts of SOM (Adams et al., 2011). Grandy and Neff (2008) in their review stated that SOM chemistry, turnover and its variation are due to interactions of three components: 1) deposition of chemically distinct compounds in soil from plants (as well as organic amendments and animal manure), 2) the processing by mesofaunal, bacteria and fungi of these plant-derived compounds through the action of the extracellular enzymes and through assimilation (and re-deposition) of carbon compounds as microbes die, 3) the physical redistribution and stabilization of these primary and secondary SOM sources in soils including transport, sorption, and aggregation of soil particles.

The processes of aggregate formation/degradation, adsorption/desorption are the main mechanisms of protection and release of SOM. Stabilization of SOM is thought to be due to: 1) stabilization by the organo-mineral interactions (mineral bound OM has been defined as all OM that is absorbed to minerals or entrapped in small microaggregates (Abiotic clay flocculation in micro-aggregates) association with silt and clay, and 2) physical protection by the encapsulation of organics within aggregate structures macro-aggregates and micro-aggregates, the biotic exclusion, which seems to be the major SOM stabilization mechanism in mineral depleted deposits (Six et al., 2002a, Six et al., 2002b). The most comprehensive conceptualization of organo-mineral interactions in soils, is the three layer (kinetic zone,

hydrophobic zone, and contact zone) zonal model proposed by Kleber et al., (2007). There have been recognized two basic conceptual schemes for aggregate formation (Plante and McGill, 2002; Nikolaidis and Bidoglio, 2011). The hierarchical model implied the formation of micro-aggregates followed by the formation of macro-aggregates by the combination of micro-aggregates. The second proposed mechanism of aggregate formation in the relevant scientific literature suggests that macro-aggregates are formed around particulate organic matter (POM), followed by the release of micro-aggregates as the occluded organic materials are decomposed.

### **1.2.3 Conceptual Model of Organo-Mineral Interactions (Kleber Zonal Model)**

Sorption of organic and organo-mineral compounds on clays and oxides is a significant chemical protection mechanism in the carbon cycle. Organic compounds bind to mineral surfaces through cation bridges, hydrogen bonding and van der Waals forces (i.e. Kleber et al., 2007). A number of factors such as pH, redox conditions, and the characteristics of the mineral surface and of the organic matter affect the degree of sorption and surface complexation of organics with the mineral surfaces. The negatively charged surfaces of clay minerals bind with the negatively charged organic compounds through cation bridges (Jastrow et al., 2007). The availability of multivalent cations plays an important role in the formation of clay-cation-organic complexes. Similarly, the availability of iron and aluminum oxide surfaces bind organic compounds via electrostatic forces. Kleber et al. (2007), following on work by Wershaw et al. (1996), Piccolo (2001), and Sutton and Sposito (2005), suggested a conceptual model of organo-mineral interaction in soils that consists of three layers, the contact zone, the hydrophobic zone and the kinetic zone (Figure 1.9).

According to Kleber et al. (2007), SOM is viewed as consisting of organic molecular fragments (derived from the depolymerization and oxidation of standard biomolecules, and not as large resynthesized polyaromatic structures) of varying degrees of amphiphilicity or surfactant-like properties (molecules that are solely nonpolar and hydrophobic, to those that are predominantly amphiphilic because they also contain hydrophilic, highly polar or charged functional groups) in intimate contact with mineral surfaces of variable chemical reactivity and a polar solvent (water). The second law of thermodynamics then dictates that the organic fragments and mineral surfaces will arrange themselves in structures (micellar structures) in aqueous solution that maximize entropy, which lead the authors to propose a

layered structure for mineral–organic associations. They further proposed that microbial proteins were better able to bind to mineral surfaces, as well more likely to arrive at these surfaces, than were residues of vascular plants, thus explaining the proposed existence of a particularly stably bound, N-rich inner layer of organic material (contact zone). Hydrophobic portions of these surface-bound molecules could be protected from contact with aqueous solution by the additional accumulation of amphiphiles arranged such that the polar portions point towards the aqueous phase, creating a bilayer structure with a discrete hydrophobic zone. Empirical evidence for organic surface loadings of 2–5 times the monolayer equivalent suggested that further attachment of organics in a third region or kinetic zone (controlled by exchange kinetics, similar to a phase-partitioning process) was possible, although for this outer zone or region, exchange rates of organic compounds with the soil solution were likely high, and residence times short (Klebel et al. 2007).

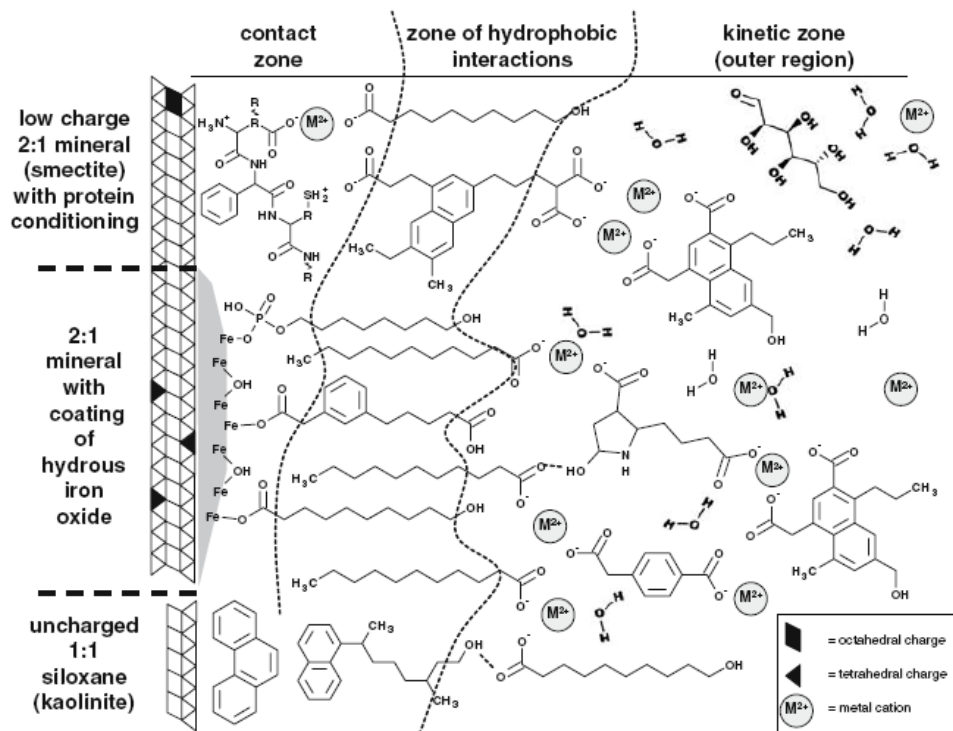
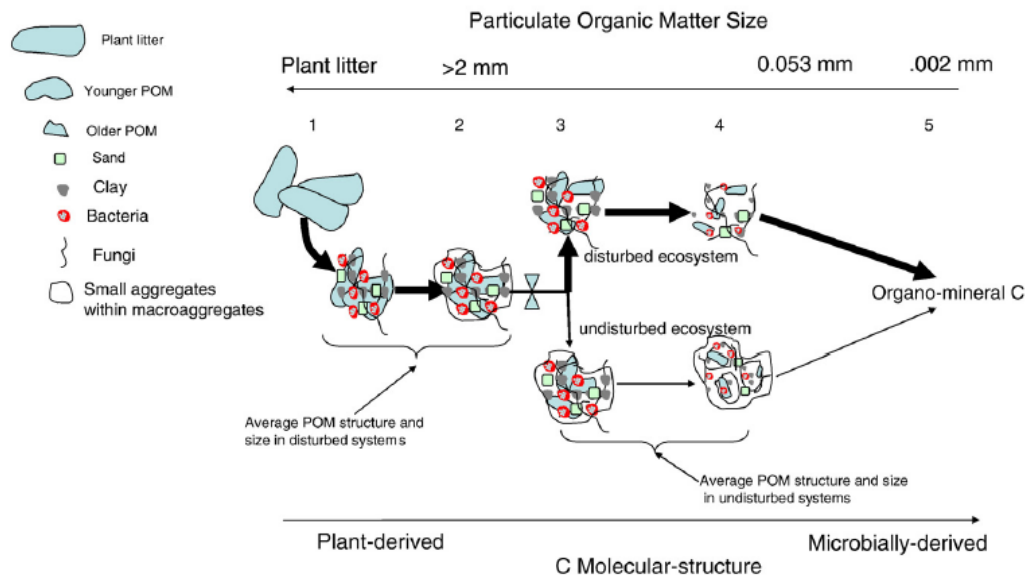


Figure 1.9 Zonal model of organo-mineral interactions (taken from Klebel et al, 2007).

#### 1.2.4 Conceptual Model for Soil Aggregation

Tisdall and Oades (1982) suggested the hierarchical aggregate model where the aggregates are sequentially formed, i.e. micro-aggregates are first formed free and then serve as the building blocks for the formation of macro-aggregates. Oades (1984) modified this concept and postulated that the roots and hyphae holding together the macro-aggregate form the nucleus for micro-aggregate formation in the center of the macro-aggregate. Since roots and hyphae are temporary binding agents, they do not persist and decompose into fragments. These fragments coated with mucilages produced during decomposition become encrusted with clays resulting in the inception of a micro-aggregate within a macro-aggregate (Six et al., 2004).

The conceptual model of Oades (1984) has been suggested by many authors today (Golchin 1994; Balesdent et al., 2000; Puget et al., 2000; Plante and McGill, 2002; Six et al., 2002a; Six et al., 2002b; Six et al., 2004; Bronick and Lal, 2005, Grandy and Nff, 2008; Helfrich et al., 2008; Nikolaidis and Bidoglio, 2011). The proposed conceptual model for the aggregate turnover (aggregate degradation and re-formation) corresponds to soils where OM serves as an intra-macro-aggregate binding agent and there is aggregate hierarchy (while this may not be the case in oxide-rich soils). A schematic overview of the conceptual model is given in Figure 1.10. Briefly, the fresh residue induces the formation of macro-aggregates because it is a C source for microbial activity and the production of microbial derived binding agents. Macro-aggregates are formed around fresh residue which then becomes coarse iPOM (intra-aggregate particulate OM) (t1). Then fine iPOM within macro-aggregates is derived from the decomposition and subsequent fragmentation of coarse iPOM (t2). Fine iPOM gradually becomes encrusted with clay particles and microbial products to form micro-aggregates within macro-aggregates (t3). The binding agents in macro-aggregates degrade, resulting in loss of macro-aggregate stability and the release of stable micro-aggregates (t4), which are the building blocks for the next cycle. Micro-aggregates and macro-aggregates provide a physical protection to the soil organic carbon and nitrogen incorporated in them from activity of decomposers and influence carbon and nitrogen turnover in soils. Decomposer activity is limited in the aggregate structures due to oxygen and water availability, and enzyme accessibility (Jastrow, 2007); consider that Bacteria, protozoa and nematodes can enter pores >3  $\mu\text{m}$ , >5  $\mu\text{m}$ , >30  $\mu\text{m}$ , respectively.



**Figure 1.10 Macro-aggregate turnover: formation and degradation process (taken from Grandy and Neff, 2008).**

### *Soil aggregate turnover rate and OM mineralization*

The conceptual representation of the relationships between soil aggregate turnover rate and OM mineralization of stabilized and newly incoming fresh OM (Plante and McGill, 2002; Six et al., 2004) is given in Fig 1.11. Regarding the stabilized (native, protected organic matter) SOM the slower the macro-aggregate turnover the higher would be the protection level. R3 is the threshold aggregate turnover rate where organic matter begins to become exposed. On the other hand, for the newly incoming fresh residue an intermediate aggregate turnover is optimum in order to have aggregate formation and occlusion and subsequent protection of C (highest sequestration rate). R1 is the threshold aggregate turnover rate where organic matter is occluded before it is mineralized and R2 is the threshold rate where incoming organic matter is re-exposed more quickly than it is occluded. This conceptualization is in accordance with Kimetu et al. (2009) findings, which indicate that SOM stabilization efficiency was highest with intermediate cultivation history of about 20 years as compared with both degraded soils and high C-containing soils. They suggested that depending on the C saturation limit of a soil, soils with high organic C have high rates of labile C mineralization possibly due to limited protection of organic matter by minerals.

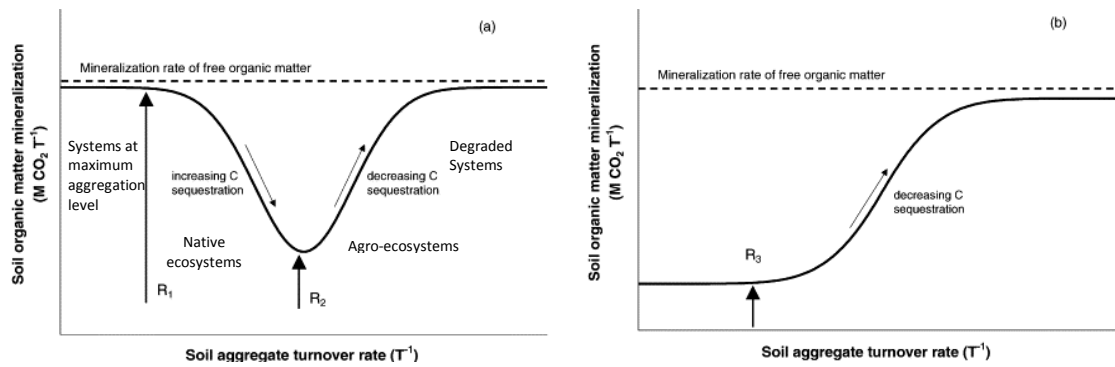


**Figure 1.11** Change in aggregate turnover and mineralization rate of a) stabilized and b) newly added C input across ecosystems (taken from Plante and McGill, 2002).

In agroecosystems, macro-aggregation exhibited great seasonal dynamics (Six et al., 2004). Macro-aggregates provided instant protection of recently added organic matter and allowed a transfer of C and N into micro-aggregates, where the new C and N may become stabilized after macro-aggregate breakdown (Helfrich et al., 2008). Jastrow (1996) found that accumulating organic matter in macro-aggregates was relatively fresh and less than 20% of the accumulated carbon occurred in the form of POM. Most of the accumulated carbon was found in the silt-clay fraction of macro-aggregates. Jastrow (1996) and Krull et al., (2004) also reported a threshold of organic carbon for aggregate formation.

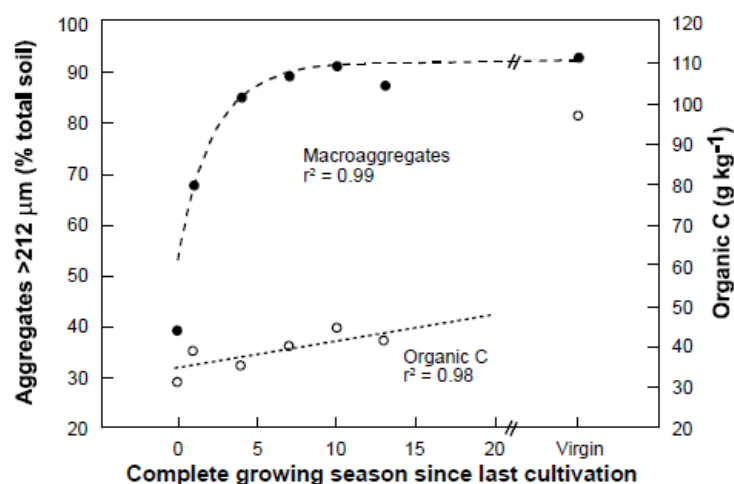


**Figure 1.12** Changes in percentage of macro-aggregates and accumulation of SOC with time since cultivation (taken from Krull et al., 2004, modified from Jastrow, 1996).

### 1.2.5 Factors Affecting Soil Aggregation and Structure

The stability of aggregates and their turnover greatly depends on the quantity and quality of plant litter residue and/or organic amendments added to the soil (Abiven et al., 2007; Abiven et al., 2009). Since SOM is central to the formation of stable soil macro-aggregates there has been found a strong positive relationship between the aggregate stability in terms of the mean weight diameter-MWD (mm) and the SOM content (%) (Figure 1.13). SOM is the property that has been mostly related with aggregation. A synopsis of studies that defined algorithms to relate aggregate stability to SOM content or failed to find a significant correlation can be found in Krull et al. (2004). Linear positive pattern has been found by Chaney and Swift (1984). However, such relationship would be significant for soils of similar mineralogy and texture (Boix-Fayos et al., 2001). Total N content has been reported to be more closely correlated with MWD (mm) compared with total SOM content (e.g. Chaney and Swift, 1984), probably because it is associated with mineral surfaces and involved in the formation and stabilization of aggregates (Williams, 1970). Moreover, studies on SOM composition have consistently shown that the C-to-N ratio decreases with decreasing aggregate size (Elliot, 1986; Gupta and Germida, 1988; Angers and Carter, 1996).

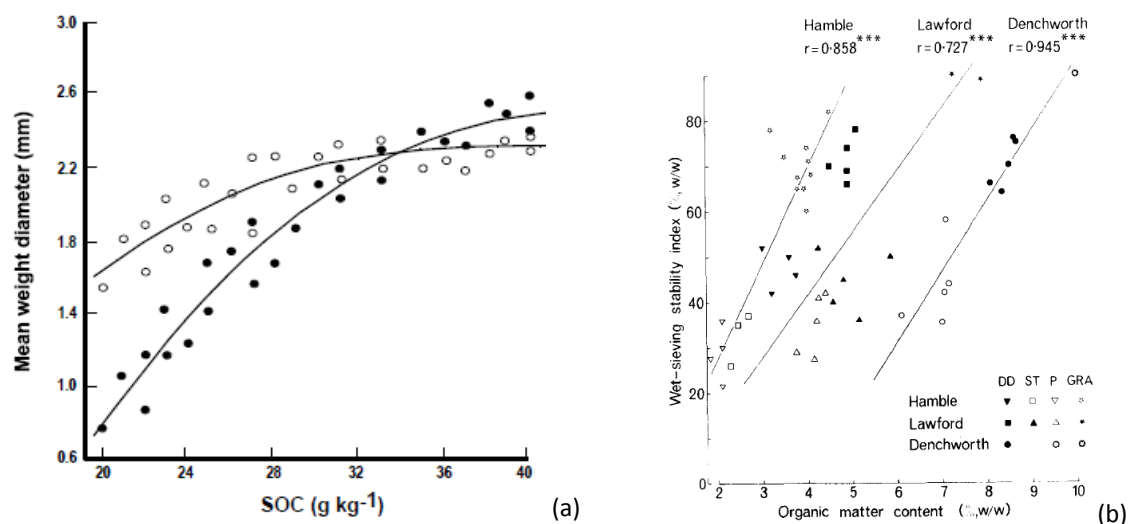
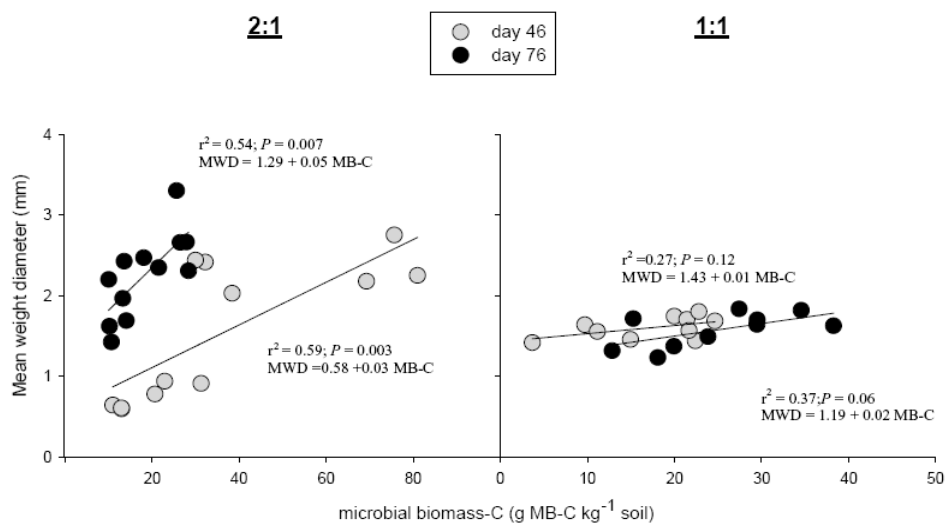


Figure 1.13 a) Effect of increasing SOC content on aggregate stability, measured by wet-sieving (MWD, mm), using air-dried (●) and field moist (○) samples ( $R = 0.98$ ) (taken from Krull et al., 2004, original data Haynes, 2000), b) Relationship between wet sieving stability index and OM content in the 5th year of experiments in 3 sites with different texture (taken from Douglas and Goss, 1982).

Other important soil properties are the pH, cation exchange capacity and calcium content through its role in the formation clay–polyvalent cation–organic matter complexes (Six et al., 2004). Addition of calcium (lime or gypsum) to field soils has been found to increase (approx. 10%), although an initial temporary decrease (1–3%) has been observed mostly in acidic soils due to the increase of soil pH and microbial activity (Six et al., 2004).

However, abiotic factors such as soil texture are more important for determining soil aggregation than biotic factors (Barto et al., 2010). With increasing clay content soils require a higher OC content in order to maintain a given aggregate stability (Douglas and Goss, 1982). In most cases, the relationship between OC and soil structural stability is modified by soil clay content (Figure 1.13). Virto et al., (2008) showed that clay aggregates were selectively formed from 2:1 clays, while quartz and kaolinite-like clays were preferentially found in the non-aggregated clay fraction (see also Figure 1.14).



**Figure 1.14 Relationship between microbial biomass and aggregate stability in terms of the mean weight diameter in a Mollisol dominated by 2:1 minerals and an Oxisol by 1:1 minerals and oxides (taken from Six et al., 2004, original data Denef and Six, 2003).**

In addition, oxides have been recognized to be very important regarding aggregation and SOM stabilization and the dominant binding agent in oxide-rich tropical soils (Six et al., 2004). The aggregating effects of oxides and calcium have been mainly related to the micro-aggregate level. However, they have been also related to macro-aggregation. Stimulation of microbial activity in acidic soils has been observed due to calcium. The role of oxides on

stabilization is manifested in three ways (Six et al., 2004): 1) organic materials adsorb on oxide surfaces, 2) an electrostatic binding occurs between the positively charged oxides and negatively charged clay minerals, and 3) a coat of oxides on the surface of minerals forms bridges between primary and secondary particles. The coating of oxides has been reported to be mostly related to the stability of macro-aggregates in oxisols compared to temperate soils with low oxide levels (Six et al., 2004). Worth noting is that in the case of a kaolinitic soil the cation exchange capacity of the kaolinite can be reduced by the binding of oxides to minerals.

Soil macrofauna also play an important role in macro-aggregation. The most significant group of macrofauna in temperate soils are earthworms and in temperate pastures their population may reach 1000-2000 per m<sup>2</sup> (Six et al., 2004). Earthworms contribute greatly to soil aggregation by utilizing plant litter together with soil, passing it through their gut and excreting casts. Casts mediate both micro-aggregate and macro-aggregate formation in soils the stability of which depends on the quality of organic material consumed by the earthworms. In addition, earthworms contribute to aggregate formation due to burrowing activities where they deposit mucus on the burrow walls which together with the soil clays can form a stable structure (Six et al., 2004). Microbial biomass (Figure 1.14), the OC light fraction or labile carbohydrates as well KCl or hot water extracted carbon (the OC light fraction) have been found to be early indicators of the change in soil OC. Especially, the 'easily extractable' fraction of soil carbohydrate appear to be closely related to aggregation in temperate soils (Haynes and Swift, 1990). Macro-aggregation has been found to be significantly delayed (28–42 days) in fungicide-treated soils compared to their untreated counterparts, highlighting the importance of the fungal biomass in macro-aggregate formation (Helfrich et al., 2008).

Roots influence soil aggregation through entanglement of soil particles with the mycorrhizal-root system as well as through root exudates (Jastrow et al., 2007; Six et al., 2004). Large amounts of OM are supplied to soils from roots (rhizodeposition), especially in warm-humid climates. Thus, a large active microbial biomass develops in the rhizosphere and therefore large amounts of organic binding agents are produced. However, it has been reported that roots, root hairs, and hyphae absorb water from the surrounding soil and thus cause localized drying, which can have stabilizing as well disrupting effects on soil macro-aggregates (Haynes and Beare, 1996).

The extent of aggregation is also related to the climate under which the soil has been formed. As the P/PET ratio increases the percentage of silt and clay aggregated also increases and reaches a maximum value between a P/PET ratio of 0.4 and 0.6 so that the extent of soil aggregation increases from Entisols to Vertisols and Mollisols (Dalal and Bridge, 1996). At higher values of P/PET ratios, however, soil aggregation may decrease as in Alfisols and especially in Ultisols or it may increase even further as in Oxisols.

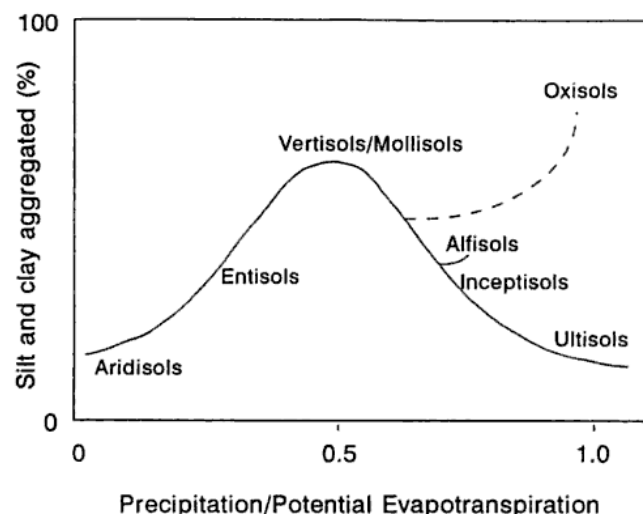


**Figure 1.15** A diagram describing the effect of climate on soil aggregation under natural ecosystems (taken from Dalal and Bridge, 1996)

Agricultural practices (e.g. crop types, fertility management, irrigation regime, insecticides and fungicides) as well as environmental variables i.e. freeze-thaw cycles, dry-wet cycles, and fires also significantly influence aggregation (see review of Six et al., 2004).

### 1.2.6 Summary on SOM Stabilization

In the following box critical points regarding the SOM stabilization are summarized in a bullet-like form.

1. The extracted humic substances are most likely the product of the extraction procedure rather than a true in-situ component of SOM.
2. Aromatic structures in stable materials are the products of incomplete combustion (biochar) with variability in recalcitrance and degradability and not the result of natural decomposition process nor selectively preserved.
3. Major organic materials (lignin, cellulose, hemicellulose, lipids, proteins) as well as black carbon are fully decomposable under sufficient oxygen supply.
4. Lignin is associated with the free organic matter found and coarse (sand sized) fractions, but severely biodegraded and depleted in finer fractions.
5. Sand sized fractions are depleted in plant originating carbohydrates.
6. Finer fractions are significantly enriched in microbial synthesized metabolites ((O/N)-Alkyl C), N-containing compounds (proteins, amino acids), waxes and lipids.
7. Long life-times for N-containing (~49 y) & polysaccharide derived (~54 y) compounds.
8. Accessibility (physical protection within aggregates) and sorbitivity interactions with mineral surfaces provide protection against decomposition, explicitly including carbohydrates, proteins, and other supposedly 'labile' materials, deriving from decomposed plant residues and/or remnants of microbes and fungi.
9. The most comprehensive conceptualization of organo-mineral interactions in soils is the three layer zonal model proposed by Kleber et al., (2007).
10. Two basic conceptual schemes for aggregate formation are proposed **i)** the hierarchical model: formation of micro-aggregates followed by the formation of macro-aggregates by the combination of micro-aggregates. **ii)** macro-aggregates formed around particulate organic matter, followed by the release of micro-aggregates as the occluded organic materials are decomposed and macro-aggregates are destroyed.
11. The stability of aggregates and their turnover depend on the quantity and quality of organic matter added to soil, SOM content, clay quantity and type (2:1 versus 1:1), iron oxides, soil macrofauna, mycorrhizal-root system, microorganisms, climatic conditions, management.

## 1.3 SOM TURNOVER MODELING

### 1.3.1 Model Categories and Characteristics

Models of soil organic matter dynamics have been widely used as a well-known tool to predict SOM stock and its distribution to different SOM pools, under different soil types, management practices and climate regimes, land-use change conditions and climate changes (Battle-Aguilar et al., 2010). Modeling of carbon and nitrogen dynamics in terrestrial environments has been reviewed extensively in recent years (i.e. Falloon and Smith, 2000; Shibu et al., 2006; Minasny et al., 2008; Manzoni and Porporato, 2009; Battle-Aguilar et al., 2010; Adams et al., 2011; Nikolaidis and Bidoglio, 2011; Adams et al., 2011). Models, other than empirical regression models, can be divided into four categories depending on their internal structure (Battle-Aguilar et al., 2008; Post et al., 2007, Adams et al., 2011):

1. process-oriented, (multi)-compartment models
2. organism-oriented (food-web) models
3. cohort models describing decomposition as a continuum and
4. a combination of model types (1) and (2).

The main characteristics of processes-oriented versus organism-oriented models and the main characteristics of the most frequent referred to models in the scientific literature are summarized in Table 1.4, after Adams et al. (2011). A detailed list of main features of SOM dynamic models can be found in the review by Manzoni and Porporato (2009). Manzoni and Porporato (2009) reviewed and classified 250 biogeochemical models in terms of their mathematical approaches to soil carbon and nitrogen dynamics. In addition, they analyzed the relationship between model structure and the temporal and spatial scale of its respective application. They identified the following theoretical gaps: i) mechanistic and scale dependent description of microbial mass and activity using dedicated state variables, ii) link decomposer activity and metabolism, nutrient availability, vegetation growth and climate dynamics using stoichiometric theory, iii) model soil food web dynamics instead of aggregated variables, iv) develop mechanistic and rigorous representations of small-scale processes that account for spatial heterogeneity, v) physical processes that affect soil structure (tillage, wetting and drying cycles and aggregate turnover) should be included in the biogeochemical models, and vi) need to develop novel modeling approaches for scaling up pore scale dynamics to observational scales.

**Table 1.4 Main characteristics of processes-oriented versus organism-oriented models (After Adams et al., 2011).**

	<b>Process-oriented models</b>	<b>Organism-oriented models</b>
<b>Model type</b>	mechanistic predictive value	mechanistic explanatory value
<b>Aim</b>	/simulate processes involved in SOM migration and transformation	/simulate SOM using functional/taxonomic groups of the soil
<b>Examples</b>	CANDY, CENTURY, DAISY, DNDC, ITE, NCSOIL, RothC, Socrates, SOILN, SOMM, Struc-C and the Verbene model	/Fungal-growth models /Models of decomposition of OM that incorporate functional groups of microbial biomass /Food web models based on taxonomic groups (mostly detrital models)
<b>Representation of SOM</b>	/different conceptual carbon pools with similar chemical or physical characteristics /differ by decomposition rates, stabilization mechanisms /generally soil biota only included in form of microbial biomass (exception: SOMM) Generally, more than one compartment of SOM degradation: a) active pool (fresh plant material, root exudates, microbial biomass) with MRT of 1 year b) slow pool (SOC that decomposes at intermediate rate) with MRT of 100 years c) passive or inert pool (SOC with physical or chemical stability) with MRT of 1000 years	SOC dynamics represented through different pools of soil biota (classified according to their taxonomy or metabolism) i.e. representation of soil biota by functional groups (food web models): microorganisms (bacteria, mycorrhizal and saprotrophic fungi) SOM and litter (represented in form of roots, detritus)
<b>Mechanism</b>	/SOC decomposition based on first-order kinetic rates	/C and N fluxes simulated through functional groups based on their specific death rates and consumption rates, applying energy conversion efficiencies and C:N ratios of the organisms
<b>Time-step</b>	/weekly or monthly	/daily
<b>Scale</b>	/include top 30 cm of the soil /small-plot to regional-scale	/small-plot
<b>Application</b>	/have been applied to a range of ecosystems (grassland, arable land, grass-arable rotations, forest)	/have been applied to arable land and grassland
<b>Others</b>	/successfully coupled with GIS software (CANDY, CENTURY, RothC)	/include changes of soil biota communities in the modeling of SOM dynamics (i.e. simulating feedback mechanisms due to changes in biota activity or characteristics)

Organism-oriented models have been successfully applied to provide understanding on C and N flows through food webs (i.e. Fig 1.16) giving many insights; e.g. role of soil biota in C and N mobilization as well as mechanisms of above and below ground linkage of food webs (Brussaard, 1998; Smith et al., 1998; Susilo et al., 2004). However, an important constraint of the wide application and validation of food web models with field data is their high cost as a wide range of parameters should be monitored; feeding preferences, nitrogen content, life cycles, assimilation efficiencies, production:assimilation ratios, decomposability and population sizes (Smith et al., 1998). Brussaard (1998) presented the main limitations of these models for predictive purposes: *(a) the quality of organic matter consumed at each trophic interaction is not well known, (b) a number of functional groups are not included in the existing models, (c) the possible spatial habitat restriction of certain functional groups is not incorporated, and (d) many biological interactions in the soil are actually of non-trophic nature.* Application and calibration tends to be more difficult in such models (Battle-Aguilar et al., 2010) and the estimation of this wide range of parameters might increase the level of model uncertainties (Adams et al., 2011).

Similar constraints present the coupled process oriented/organism-oriented models (Adams et al., 2011). The cohort models like the SOMCO (Gignoux et al. 2001) separate the soil organic matter into different cohorts with specific characteristics, like similar ages which are further divided into different pools (i.e. C and N). Decomposition in such models is simulated based on the physiology of the microbial biomass in contrast with process-oriented models where decompositions rates are simulated based on physical and biochemical processes (Battle-Aguilar et al., 2010; Adams et al., 2011).

Process-oriented models have been extensively preferred in the scientific literature over organism-oriented models since they can easier be applied to predict SOC levels under certain management practices and serve as tools to policy makers (Smith et al., 1998; Adams et al., 2011) due to a number of reasons: *(1) they have a relatively simple model structure and often larger integration time-steps (i.e. months versus days for organism-oriented models), (2) their internal parameters are easier to estimate and calibrate for specific purposes, (3) most have been applied to a variety of ecosystems, (4) have been successfully coupled to GIS software, (5) are more suitable for larger scales (landscape, regional), and (6) their computer processing time is likely to be shorter* (Adams et al., 2011; Post et al., 2007, Brussaard, 1998, Smith et al., 1998).

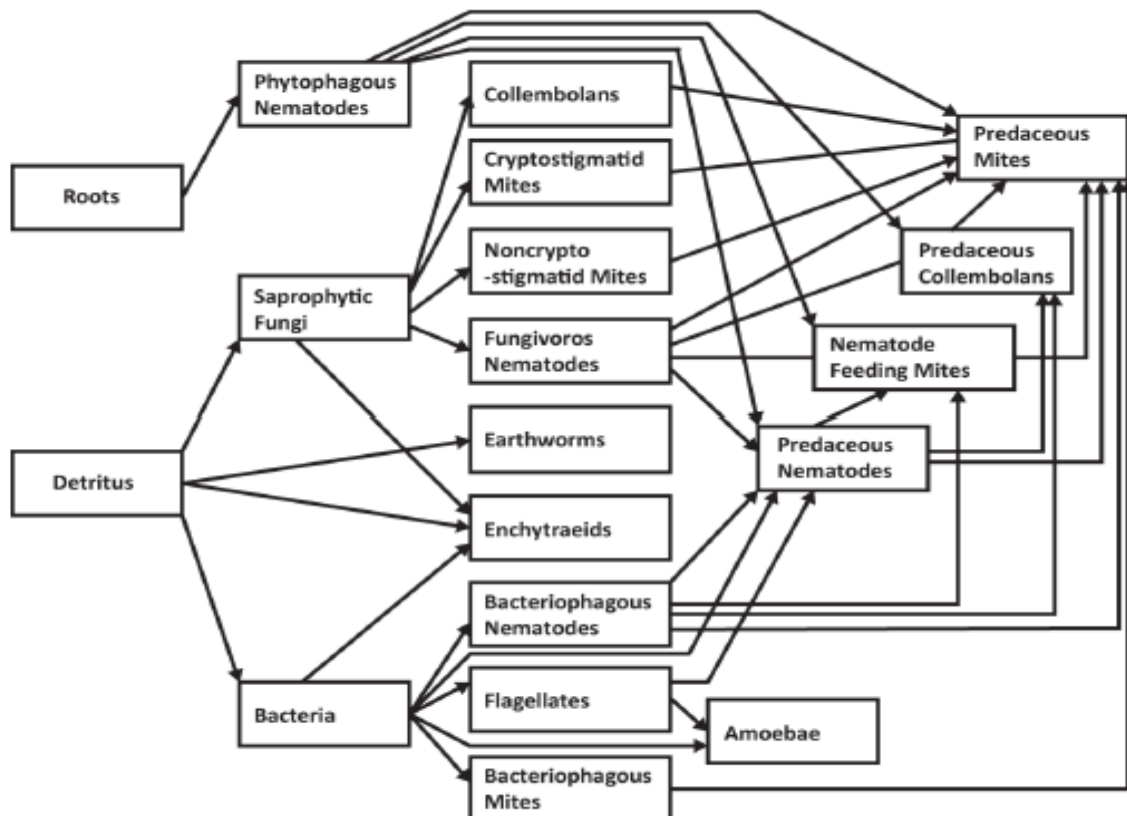


Figure 1.16 Structure of an organism-oriented model (taken from Smith et al., 1998).

### 1.3.2 Process-oriented models

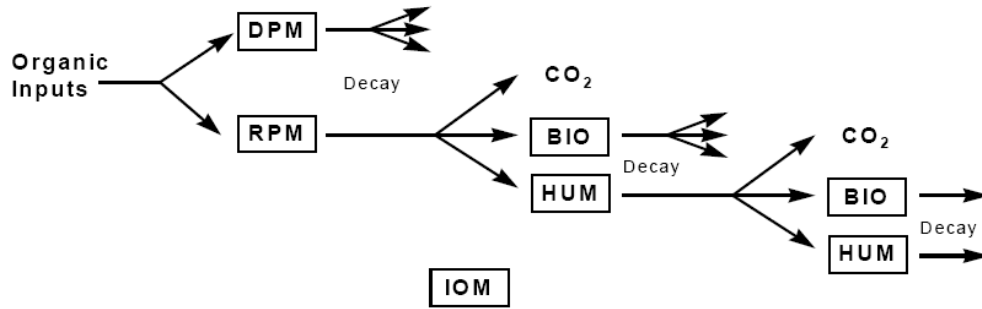
The main characteristics of the most frequent referred to process-oriented models in the scientific literature are presented in Table 1.5, after Adams et al. (2011). A schematic representation of SOM dynamics for the RothC and Century the most frequently used process-oriented models, along with the DNDC model (Viaud et al., 2010; Adams et al., 2011) to simulate SOM dynamic spatially on the small farm-scale level is displayed in Figures 1.17 and 1.18, correspondingly.

**Table 1.5 Main characteristics of the most frequent referred to models in the scientific literature (After Adams et al., 2011).**

<b>Model</b>	<b>Main characteristics</b>	<b>Reference</b>
<b>CANDY</b>	<ul style="list-style-type: none"> <li>/modular system combined with data base system for model parameters, measurement values, initial values, weather data, soil management data</li> <li>/simulates soil N, temperature and water to predict N uptake, leaching, water quality</li> <li>/uses proportion of soil particles to separate inert organic matter (IOM) (&lt;6 µm)</li> </ul>	(i.e. Franko, 1996)
<b>CENTURY</b>	<ul style="list-style-type: none"> <li>/designed for long-term (up to centuries) SOM dynamics, plant growth and N, P and S cycling</li> <li>/developed for grassland, but extended to agricultural crops, forests and savanna systems</li> <li>/monthly time step</li> <li>/implements two forms of litter: metabolic and structural</li> <li>/implements three SOM compartments: active (MRT 1-5 yr), slow (MRT 25 yr, 30-60 % of SOC) and passive (MRT 1000 yr, 30-50 % of SOC)</li> <li>/soil texture (clay content) determines separation of C from active OM pool into CO<sub>2</sub> or slow pool</li> <li>/basic ideas similar to RothC</li> <li>/biomass included</li> </ul>	(i.e. Parton, 1996)
<b>DAISY</b>	<ul style="list-style-type: none"> <li>/simulates crop production and soil water and nitrogen dynamics</li> <li>/developed as field management tool for agricultural systems</li> <li>/portioned into hydrological model, soil nitrogen model with a SOM submodel and a crop model with a nitrogen uptake model</li> <li>/clay content influences rate constants</li> <li>/semi-cohort accounting system used for litter decay</li> <li>/biomass included</li> </ul>	(i.e. Mueller et al., 1996)
<b>DNDC</b>	<ul style="list-style-type: none"> <li>/couples denitrification and decomposition processes</li> <li>/4 submodels: soil climate, decomposition, denitrification, plant growth</li> <li>/clay absorption of humads</li> <li>/biomass included</li> </ul>	(i.e. Li et al., 1992)
<b>ITE</b>	<ul style="list-style-type: none"> <li>/developed for grassland environments</li> <li>/aims to simulate N cycling</li> <li>/3 submodels: grazing-animal intake model, vegetative grass-growth model, SOM model</li> <li>/decomposition rates are function of quantity of microbial biomass</li> </ul>	(i.e. Thornley and Verbeke, 1989)
<b>NCSOIL</b>	<ul style="list-style-type: none"> <li>/simulates N and C through soil microbes and organic components</li> <li>/4 organic compartments: plant residues, microbial biomass, humads, stable organic matter (stability of SOM results from metabolism)</li> <li>/decomposition independent of microbial biomass</li> <li>/biomass included</li> </ul>	(i.e. Molina, 1996)

<b>RothC<sup>a</sup></b>	<ul style="list-style-type: none"> <li>/developed for arable land, but also applied to temperate grasslands and forest soils</li> <li>/monthly time step</li> <li>/5 compartments: decomposable plants, resistant plant material, microbial biomass, humified organic matter (MRT 50 yr 80-90 % of SOC), inert organic matter (MRT up to 10000 yr, 5-15 % of SOC)</li> <li>/decomposition rate, and ratio of humus, microbial biomass and CO<sub>2</sub> dependent on soil clay content</li> <li>/basic ideas similar to CENTURY</li> <li>/biomass included</li> </ul>	(i.e. Jenkinson and Coleman, 1994)
<b>Socrates</b>	<ul style="list-style-type: none"> <li>/weekly time step</li> <li>/5 compartments: decomposable plant material, resistant plant material, unprotected microbial biomass, protected microbial biomass, humus (stabilised pool)</li> <li>/decomposition rate (into humus, microbial materials and CO<sub>2</sub>) dependent on soil CEC</li> <li>/biomass included</li> </ul>	(Grace et al., 2006)
<b>SOMM</b>	<ul style="list-style-type: none"> <li>/developed for forest systems/process rates regulated by N and ash content of litter fall</li> <li>/3 soil litter layers: L, F, H</li> <li>/soil animals influence C fluxes (i.e. distinction into forms of humus such as mull and mor based on role of soil fauna – microarthropods and earthworms)</li> <li>/models C accumulation in soil organic horizons</li> </ul>	(i.e. Chertov and Komarov, 1996)
<b>Struc-C</b>	<ul style="list-style-type: none"> <li>/updated, modified version of the Roth-C model</li> <li>/monthly time step</li> <li>/incorporates soil structure (aggregate) hierarchies within physical protection of SOC</li> <li>/simulates formation of organo-mineral associations and aggregates (physically protected SOC)</li> </ul>	(Malamoud et al., 2009)
<b>Verbene</b>	<ul style="list-style-type: none"> <li>/developed for grasslands</li> <li>/implements a plant growth submodel</li> <li>/3 submodels: soil water, SOM (plant residues: decomposable, structural, resistant, OM: stabilized, protected, unprotected), soil N</li> <li>/ physical protection caused by soil clay</li> <li>/decomposition rate modified by temperature and soil moisture, not influenced by microbial activity</li> <li>/biomass included</li> </ul>	(i.e. Verbene et al., 1990)

<sup>a</sup>RothC has been also modified to include more soil layers (RothPC-1, Jenkinson and Coleman, 2008), combined with the CEH Biota plant model (Brown et al), and integrated with a transport and speciation of inorganic anions model, LEACHC (SoilGen1 model: The one dimensional transport equation -Richards' equation- for transient flow is coupled with heat flow and the advective-dispersive equation for solutes, major anions and cations are simulated and chemical speciation determines their precipitated and exchange phase based on thermodynamic considerations. Mass changes due to bioturbation, organic carbon and precipitates are used to calculate changes in bulk density and porosity and thus soil evolution, Finke and Hutson, 2008).



RPM : Resistant Plant Material  
 DPM : Decomposable Plant Material  
 BIO : Microbial Biomass  
 HUM : Humified OM  
 IOM : Inert Organic Matter

Figure 1.17 Structure of the Rothamsted Carbon Model (taken from Coleman and Jenkinson, RothC-26.3, Model description and users guide).

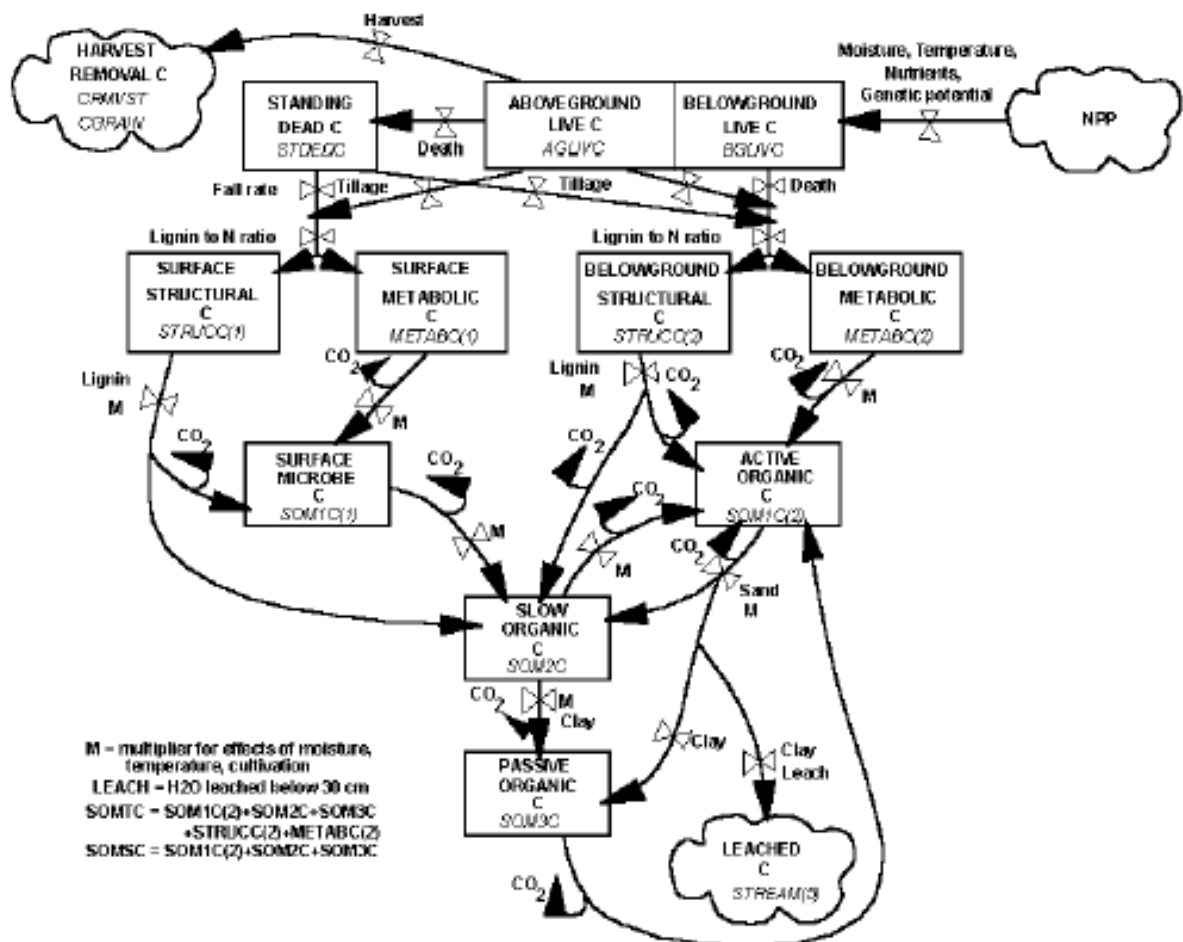
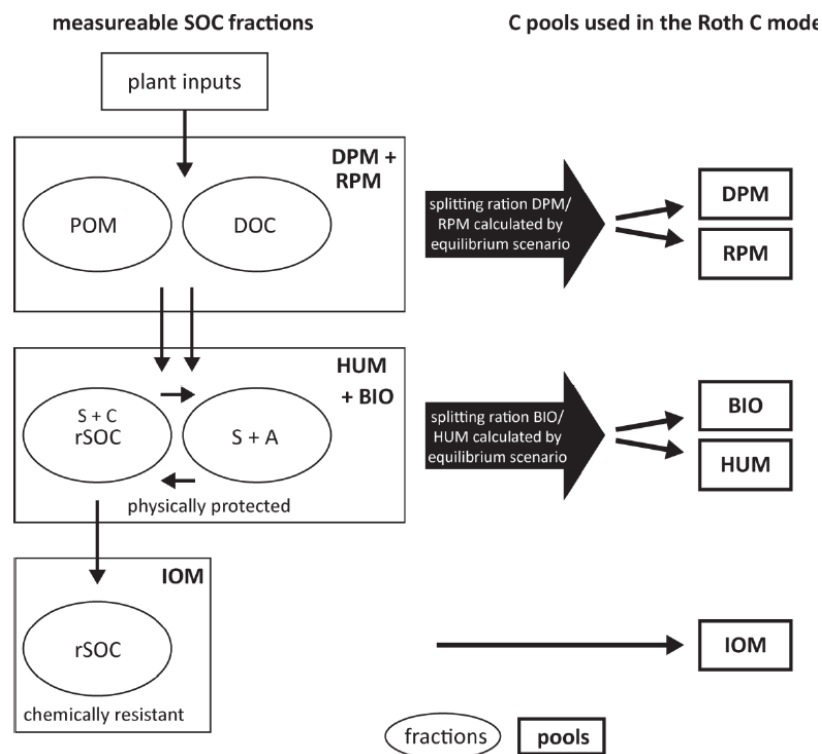


Figure 1.18 Structure of the CENTURY model (taken from CENTURY Model Version 5, User's guide).

In general, carbon models divide SOM into several pools which degrade with a first order process. One of these pools at least is the soil biomass pool, with the exceptions of the CANDY and ITE models (Table 1.5). Since microbial biomass is treated as one pool, functionality is not assessed (Chabbi and Rumpel, 2009). Lawrence et al.'s (2009) results indicated that the inclusion of exoenzyme and microbial controls in the kinetic representation of decomposition rates improved the proposed models to simulate. However, the inclusion of more defined components of soil biota dynamics requires extended modular structures and more field data for validation (Adams et al., 2011).

A study testing the performance of nine SOM models on predicting long-term changes in SOM across a range of landuses, soil types and climatic regions, using data from seven long-term (>20 years) experiments indicated the distinction of two groups according to their overall performance and similarity in modeling errors (Smith et al., 1997): (1) RothC, CANDY, DNDC, CENTURY, DAISY, and NCSOIL, (2) SOMM, ITE and Verbene. The second group of models was found to show significantly larger model errors than the first group. Their poor performance was attributed to their coupling with more complexed (physiologically based) plant growth models (such as in ITE) in contrast with simpler plant growth models used by models by the 1<sup>st</sup> group, such as DAISY and CENTURY (Smith et al., 1997; Adams et al., 2011). Much detail and complexity most likely introduced a greater degree of error and uncertainty (Smith et al., 1997), implying that specific model calibrations play a major role in influencing the predictive capacity of these models. Moreover in another comparative study (Falloon and Smith, 2002), the plant input needed by the RothC model to give similar fits as the CENTURY model was found to be even more than three times higher in some cases, which means that either the 'net' mineralization in RothC was high or that in CENTURY was low. It should not be neglected that in these models some functions have been developed by field data and some have been set arbitrarily or by only very few data; the flows between some pools in CENTURY; the split between the BIO and HUM formed in RothC (Falloon and Smith, 2002). Therefore, the applicability of SOM models for predicting carbon stocks and composition changes due to landuse or management changes is highly enhanced through calibration of the decomposition rate constants instead of the use of default values. Nevertheless, models can be greatly constrained by using field measured carbon pools to initialize and calibrate the model. For example, physical fractionation schemes like dispersing and sieving (Krull et al., 2005) as well density fractionation (Zimmermann et al., 2007) have been used to measure modeled carbon pools in RothC carbon model (Figure 1.19). It had been suggested that process-oriented models could be improved by modifying the C pools used in the models so

that they are based on measureable C fractions in contrast to identifying fractionation methods which can be used to identify existing conceptualized SOC pools (Adams et al., 2011). However, these models have been mostly used by using default decomposition rate constants and in any case without accounting for the uncertainty that arises from the initial conditions, model parameters, inputs and model structure with very few exceptions (Juston et al., 2010; Paul et al., 2003).



**Figure 1.19 Concept of SOC fractions and that relates measurable SOC fractions to conceptual pools used in the RothC model (taken from Adams, 2011, based on Zimmermann et al., 2007), (dissolved organic matter (DOC), particulate organic matter (POM), sand and stable aggregates (S+A), silt and clay particles (s+c) and oxidation-resistant carbon (rSOC)).**

The applicability of current models to predict climate change effects on distinct carbon pools, without calibration has also been questioned (Davidson and Janssens, 2006, Kleber and Johnson, 2011). Takeshi et al., (2006) optimized the Century’s model temperature and moisture dependencies to best match the observed global distribution of SOC and found out that the temperature sensitivity of decomposition at global scale should be on average

significantly lower ( $Q_{10}=1.37$ ) than it was assumed to be by many models ( $Q_{10}=2$ ). The temperature effect on the decomposition rate at equilibrium in another global study considering a single carbon pool was estimated to be  $Q_{10}=1.7$  (Yang et al., 2002). Although in both analyses there were many assumptions e.g. for the initialization of the model and the estimation of carbon inputs it is revealed that modelled temperature sensitivity is only apparent and depends on the one hand on the moisture sensitivity function used and on the other hand on the complexion of the model and the degree of protection it simulates. As it is also reported by Takeshi et al., (2006) there are indications that the temperature sensitivity of decomposition varies between different pools, while typically most soil carbon models consider that soil SOM pools are equally sensitive to temperature. Davidson and Janssens (2006) showed that although there is indefinitely intrinsic temperature sensitivity of substrate decomposition, being higher for more recalcitrant compounds due to the kinetic theory, there are also environmental constraints (drought, flooding, freezing as well physical and chemical protection) that may affect the 'apparent' temperature sensitivity, being themselves sensitive to climate. Protected and unprotected compounds, sometimes of different complexity, might be lumped together into a common pool. Davidson and Janssens (2006) suggested that protected pools might due to climate change expose SOM with high intrinsic temperature sensitivity. However, Kleber and Johnson (2011) explained that considering that the humus or slow carbon pools of models as recalcitrance due to humification process and therefore more sensitive to intrinsic temperature sensitivity (Davidson and Janssens, 2006), as they require more enzymatic steps for decomposition need to be revised (see section describing SOM composition and the new view against the humification process). Definitely, potential feedback responses of the global soil system to climate change would be much different if the carbon contained in the 'passive' pool is inherently resistant to decomposition or instead a ready substrate for decomposers stabilized only by its association with mineral surfaces (Kleber and Johnson, 2011) or occluded in micro-aggregates.

The equilibrium level of SOC has been long ago recognized to be more dependent on the extent of protection than on the decomposition rate of the plant residues added to soil (Van Veen and Paul, 1981). Carbon input is known not to be linear correlated with SOC sequestration (Six et al., 2002a; Powlson et al., 2011). The annual rate of carbon sequestration in soils is much higher the early years after the conversion of a cropland to native land and then gradually decreases; therefore initial rapid rates of SOC increase cannot be extrapolated to make estimates of the total potential carbon sequestration (Powlson et

al., 2011). In addition, Campbell et al. (1991) and Solberg et al. (1997) found no increase in soil C content with a two to three fold increase in C inputs. Relating C inputs with C content for 48 agricultural systems across 11 sites (Paul et al. 1997), resulted in an asymptotic relationship explained slightly more of the observed variability than a linear relationship. It has been acknowledged that major knowledge gaps and research priorities are the processes of carbon stabilization in soil (Lal, 2008) and the mechanistic explanation of the saturation level (Six et al., 2002a). Six et al. (2002a) conceptualized that maximum physical protection capacity for SOM is determined by the maximum micro-aggregation, which is in turn determined by clay content and type.

Physical protection in SOM turnover has been included in the past with simple manners like a reduced life-time or protection coefficient, periodically transferred to a more labile pool at cultivation events (Van Veen and Paul, 1981; Molina et al., 1983). Hassink and Whitmore (1997) developed a model where the rate at which organic matter becomes protected depends on the degree to which the protective capacity is filled, incorporating the processes of desorption and adsorption in order to model silt and clay protection of SOM. Soil texture is also used in some of the models to modify decomposition processes (i.e. texture assigned physical protection) (Trumbore, 2009). Most of the current models of SOM dynamics simply affect the decay rates of SOM pools by an empirical parameter corresponding to landuse. Existing soil aggregate models can be classified into four classes (Nikolaidis and Bidoglio, 2011): empirical (De Gryze et al., 2005; Abiven et al., 2008), mechanistic (De Gryze et al., 2006; Plante et al., 2002), deterministic soil aggregate models (De Gryze et al., 2005), and deterministic soil carbon aggregate and structure models (Malamoud et al., 2009). Empirical models represent the first attempt to model aggregate stability dynamics after the incorporation of organic residues. Mechanistic models were shown to provide valuable information on the micro- and macro-aggregate stability and turnover, indicating that micro-aggregate turnover is higher than the macro-aggregate one.

However, coupled carbon and aggregate modeling has been only utilized by Malamoud et al. (2008). Malamoud et al. (2008) in their modeling exercise with STRUC-C made the assumption that the primary interactions occur between clay particles and SOC components to form organo-mineral associations, which are then bound together to form aggregates (Figure 1.20). RothC-26.3 model was modified to accommodate the concept of size hierarchy for the physical protection of aggregates and developed aggregation and porosity sub-models in order to model aggregate fractionation and carbon content, aggregate turnover

time and changes in the porosity of the soil. The new model defined three aggregate fractions with corresponding three aggregate carbon types and complexed clay distributed in these three fractions assuming constant partitioning with soil organic carbon for each fraction. Once the organo-mineral aggregates have been calculated, the porosity submodel estimates the bulk density of each of the three aggregate types (assuming pyramidal, tetragonal and cubic packing respectively) and then the new porosity of the soil.

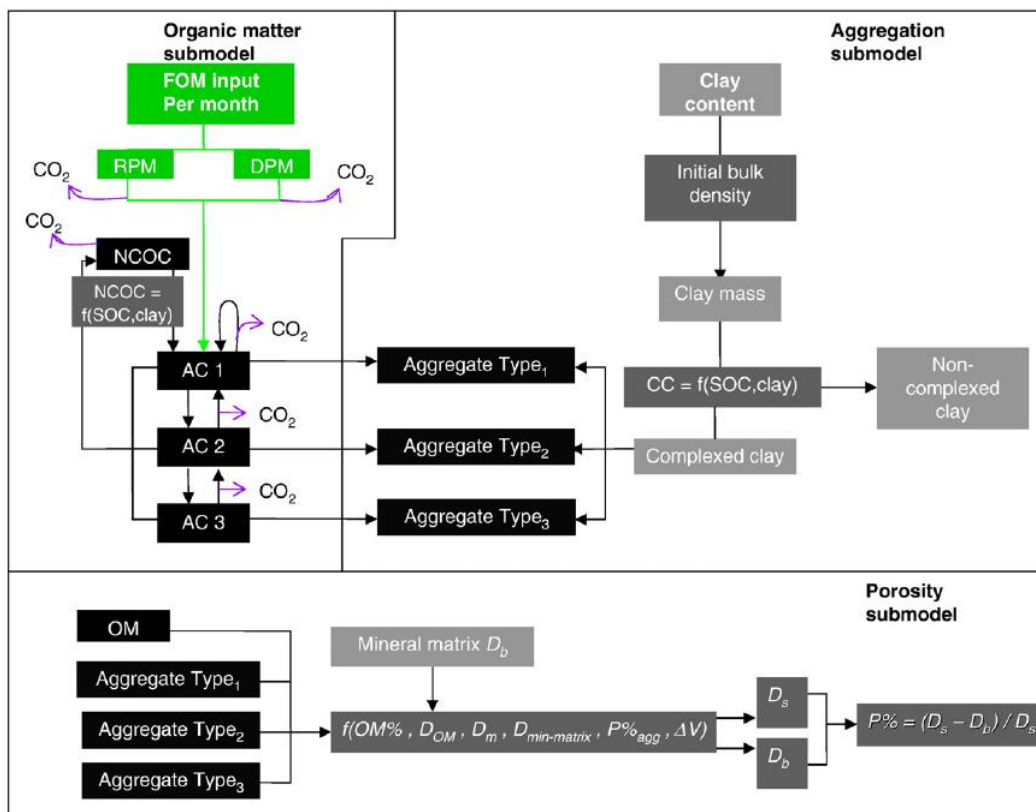


Figure 1.20 Structure of the STRUC-C model (taken from Malamoud et al., 2008).

The major limitations of STRUC-C model, as outlined by its authors, relate to the following: i) the relation between input residue and SOC is not linear and the quality of the input is not addressed, ii) geochemical factors that influence soil structure such as type of clay, iron oxide sorption, pH etc are not included in the formulation, and iii) aggregate parameters do not vary with space and time. Even though these are significant limitations, STRUC-C is considered the most comprehensive model regarding soil aggregate stability and turnover as well as soil structure in the scientific literature thus far and the first attempt towards the

next generation SOM models (Nikolaidis and Bidoglio, 2011; Adams et al., 2011). The most important constrains of STRUC-C model is that considers each aggregate type as being a single carbon pool and does not account for POM in the aggregation process, not considering the DPM and RPM pools SOC in contrast with RothC. Moreover, formation of macro-aggregates (>250  $\mu\text{m}$ ) is considered as the aggregation product of micro-aggregates (>53-250  $\mu\text{m}$ ), although macro-aggregates are known to consist of both micro-aggregates and silt-clay sized aggregates (<53  $\mu\text{m}$ ) as well POM.

It is essential to model SOM dynamics more deterministically and reproduce the processes of physical protection (Adams et al., 2011; Plante et al., 2002; Balesdent et al., 2000) as described in the conceptual model which suggest that macro-aggregates are formed around particulate organic matter (POM), followed by the release of micro-aggregates as the occluded organic materials are decomposed (Golchin 1994; Balesdent et al., 2000; Puget et al., 2000; Plante and McGill, 2002; Six et al., 2002a; Six et al., 2002b; Six et al., 2004; Bronick and Lal, 2005, Helfrich et al., 2008; Nikolaidis and Bidoglio, 2011) which has not been modeled yet. Such an attempt it is considered to move forward a more deterministic explanation of the saturation level of the different carbon pools, estimation of the rates of occlusion or release of labile organic materials and therefore their availability for mineralization or stabilization (Plante and McGill, 2002), evaluation of soil structure which is related with soil hydraulics and fertility, and optimization of the appropriate measures/practices to manage landuse changes, and climate change (Bronick and Lal, 2005; Rees et al., 2005).

### 1.3.3 Summary on SOM Turnover Modeling

In the following box critical points regarding the modeling of SOM turnover are summarized in a bullet-like form.

1. Process-oriented models have been extensively preferred in the scientific literature over organism-oriented and cohort models.
2. The inclusion of much detail and complexity in soil biota dynamics and plant growth models, in process-oriented models requires more field data for validation and introduce a greater degree of error and uncertainty.
3. RothC, Century, and DNDC are the most frequently used process-oriented models.
4. The predicting efficiency of SOM models can be highly enhanced through calibration of the decomposition rate constants, and constrained by using field measured plant input and carbon pools derived by physical fractionation schemes.
5. Most model simulations of SOM turnover do not account for the inherent uncertainties due to input data, initial conditions, and model parameters.
6. Current multi-pool SOC models are not always able to capture soil saturation capacity and give reliable predictions for climate change effects, since they do not include in a deterministic manner physical protection (e.g. aggregation).
7. The STRUC-C model, a modified version of RothC model- *assuming that primary interactions occur between clay particles and soil organic carbon components to form organo-mineral associations, which are then bound together to form aggregates-* constitutes the first attempt towards the next generation SOM models, being the most comprehensive carbon, aggregate, and structure model thus far. The most important constrains of the model is that considers each aggregate type as being a single carbon pool and does not account for POM in the aggregation process.
8. The conceptual model which suggests that macro-aggregates are formed around POM, followed by the release of micro-aggregates as the occluded organic materials are decomposed has not been modeled yet.

## 1.4 THESIS OBJECTIVE

Overall, the objective of this dissertation was to improve our understanding of the mechanisms of nutrient cycling and organic matter (SOM) protection/loss in soils and provide tools that can be used to assist the sustainable functioning of soil critical zone. The scientific issues researched in this thesis can be summarized in the following objectives:

- **Assessment methodology for soil carbon simulation**: Develop and validate with field data a methodology for RothC model parameter estimation, through initialization and calibration with field derived physical fractionation data, assessment of the uniqueness of solution, sensitivity analysis and quantification of uncertainties in modeling results.
- **Testing of soil model across climatic gradient**: Apply the developed methodology to native land to cropland conversions along an international climatic gradient to assess the pattern of carbon loss and the effectiveness of carbon addition, sensitivity analysis and quantify the uncertainties.
- **Develop soil structure model**: Develop and validate with field data a coupled soil carbon (RothC), aggregation, and structure turnover model, based on the current knowledge of the proposed mechanism in the relevant scientific literature that suggests that macro-aggregates are formed around particulate organic matter, followed by the release of micro-aggregates.
- **Assess soil status of Koiliaris River Basin Critical Zone Observatory**: Assess the soil status by selecting with sophisticated statistics the appropriate soil parameters and quantify the effects of livestock grazing, landuse changes and climate change on soil biochemical quality and water quality.

## 1.5 LITERATURE CITED

- Abiven, S., Menasseri, S., Angers, D.A., Leterme, P., 2007. Dynamics of aggregate stability and biological binding agents during decomposition of organic materials, *European Journal of Soil Science* 58, 239-247.
- Abiven, S., Menasseri, S., Angers, D.A., and Leterme, P., 2008. A model to predict soil aggregate stability dynamics following organic residue incorporation under field conditions. *Soil Science Society of America Journal* 72, 119-125.
- Abiven, S., Menasseri, S., Chenu, C., 2009. The effects of organic input over time on soil aggregate stability – a literature analysis. *Soil Biology and Biochemistry* 41, 1-12.
- Adams, M., Crawford, J., Field, D., Henakaarchchi, N., Jenkins, M., McBratney, A., de Remy de Courcelles, V., Singh, K., Stockmann, U., Wheeler, I., Compiled by Stockmann, U., 2001. Managing the soil-plant system to mitigate atmospheric CO<sub>2</sub>. Discussion paper for the Soil Carbon Sequestration Summit January 31-February 2 2011 55p.
- Andrews, S.S., Karlen, D.L., Mitchell, J.P., 2002. A comparison of soil quality indexing methods for vegetable production systems in Northern California. *Agriculture, Ecosystems and Environment* 90, 25–45.
- Angers, D.A., Carter, M.R., 1996. Aggregation and organic matter storage in cool, humid agricultural soils, M.R. Carter, B.A. Stewart, Editors, *Structure and Organic Matter Storage in Agricultural Soils. Advances in Soil Science*, Lewis-CRC Press, Boca Raton, FL (1996), pp. 193–211.
- Akagi, J., Zsolnay Á., 2008. Effects of long-term de-vegetation on the quantity and quality of water extractable organic matter: Biogeochemical implications. *Chemosphere* 72, 1462-1466.
- Altieri, M.A., 1999. The ecological role of biodiversity in agroecosystems. *Agriculture, Ecosystems and Environment* 74, 19–31
- Arias, M.E., González-Pérez, J.A., González-Vila, F.J., Ball, A.S., 2005. Soil health—a new challenge for microbiologists and chemists. *International Microbiology* 8, 13-21.
- Bahri H., Rasse D.P., Rumpel C., Dignac M.-F., Bardoux G., Mariotti A., 2008. Lignin degradation during a laboratory incubation followed by 13C isotope analysis. *Soil Biology and Biochemistry* 40, 1916-1922.
- Baldock, J.A. (2007). Composition and cycling of organic carbon in soils. P. Marschner, and et al (eds), *Nutrient Cycling in Terrestrial Ecosystems*, (Soil Biology; 10): 1-35.
- Balesdent, J., Besnard, E., Arrouays D., Chenu, C., 1998. The dynamics of carbon in particle-size fractions of soil in a forest-cultivation sequence. *Plant Soil* 201, 49–57.
- Balesdent, J., Chenu, C., Balabane, M., 2000. Relationship of soil organic matter dynamics to physical protection and tillage. *Soil and Tillage Research* 53, 215–230.
- Banwart, S., Bernasconi, S.M., Bloem, J., Blum, W., Brandao, M., Brantley, S., Chabaux, F., Duffy, C., Kram, P., Lair, G., Lundin, L., Nikolaidis, N., Novak, M., Panagos, P., Ragnarsdottir, K.V., Reynolds, B., Rousseva, S., de Ruiter, P., van Gaans, P., van Riemsdijk, W., White, T., Zhang, B., 2011. Assessing Soil Processes and Function in Critical Zone Observatories: hypotheses and experimental design. *Vadose Zone Journal* 10, 974-987.
- Barto, E.K., Alt, F., Oelmann, Y., Wilcke, W., Rillig, M.C., 2010. Contributions of biotic and abiotic factors to soil aggregation across a landuse gradient. *Soil Biology and Biochemistry* 42, 2316-2324.
- Bastida F., Moreno J.L., Hernández T., García C., 2006. Microbiological activity in a soil 15 years after its devegetation. *Soil Biology and Biochemistry* 38, 2503-2507.
- Batlle-Aguilar, J., Brovelli, A., Porporato, A., and Barry, D.A., 2010. Modeling soil carbon and nitrogen cycles during landuse change: a review. *Agronomy for Sustainable development* (<http://dx.doi.org/10.1051/agro/2010007>)
- Bechtold, J.S., Naiman, R.J., 2009. A Quantitative Model of Soil Organic Matter Accumulation During Floodplain Primary Succession. *Ecosystems* 12, 1352–1368.
- Bellamy, P.H., Loveland, P.J., Bradley, R.I., Lark, R.M., Kirk, G.J.D., 2005. Carbon losses from all soils across England and Wales 1978–2003. *Nature* 437, 245-248.

- Blagodatskaya, E., and Kuzyakov, Y., 2008. Mechanisms of real and apparent priming effects and their dependence on soil microbial biomass and community structure: critical review. *Biology and Fertility of Soils* 45, 115-131.
- Blum, W.E.H., 2005, Functions of soil for society and the environment. *Reviews in Environmental Science and Bio/Technology* 4, 75–79.
- Brantley, S.L., White, T.S., White, A.F., Sparks, D., Richter, D., Pregitzer, K., Derry, L., Chorover, J., Chadwick, O., April, R., Anderson, S., Amundson, R., 2006. *Frontiers in exploration of the Critical Zone: Report of a workshop sponsored by the National Science Foundation (NSF), October 24-26, 2005, Newark, DE, 30p.*
- Bronick, C.J., Lal, R., 2005. Soil structure and management: a review. *Geoderma* 124, 3 –22.
- Brussaard, L., 1998. Soil fauna, guilds, functional groups and ecosystem processes. *Applied Soil Ecology* 9, 123-135.
- Boix-Fayos, C., Calvo-Cases, A., Imeson, A.C., Soriano-Soto, M.D., 2001. Influence of soil properties on the aggregation of some Mediterranean soils and the use of aggregate size and stability as land degradation indicators. *Catena* 44, 47–67.
- Campbell, C.A., Bowren, K.E., Schnitzer, M., Zentner, R.P., Townley-Smith, L., 1991. Effect of crop rotations and fertilization on soil biochemical properties in a thick Black Chernozem. *Canadian Journal of Soil Science* 71, 377–387.
- Chabbi, A., RUMPEL, C., 2009. Guest Editors' Introduction. Organic matter dynamics in agro-ecosystems – the knowledge gaps. *European Journal of Soil Science* 60, 153-157.
- Chaney, K., Swift, R.S., 1984. The influence of organic matter on aggregate stability in some British soils. *Journal of Soil Science* 35, 223–230.
- Chertov, O.G., Komarov, A.S., 1996. SOMM - a model of soil organic matter and nitrogen dynamics in terrestrial ecosystems. In: Powlson, D.S., Snith, P., Smith, J.U., (eds.) *Evaluation of soil organic matter models using existing long-term datasets. NATO ASI Series I. Heidelberg: Springer-Verlag.*
- Dalal, R.C., Bridge, B.J., 1996, Aggregation and organic matter storage in sub-humid and semi-arid soils, M.R. Carter, B.A. Stewart, Editors , *Structure and Organic Matter Storage in Agricultural Soils. Advances in Soil Science, Lewis Publishers, Boca Raton, FL (1996), pp. 263–307.*
- Davidson, E. A., Janssens, I. A. 2006. Temperature sensitivity of soil carbon decomposition and feedbacks to climate change. *Nature* 440, 165–173.
- Dawson, J.J.C., Smith, P., 2007. Carbon losses from soil and its consequences for land-use management. *Science of the Total Environment* 382, 165–190.
- De Gryze, S., Six, J., Brits, C., and Merckx, R., 2005. A quantification of short-term macroaggregate dynamics: influences of wheat residue input and texture. *Soil Biology and Biochemistry* 37, 55-66.
- De Gryze, S., Six, J., and Merckx, R., 2006. Quantifying water-stable soil aggregate turnover and its implication for soil organic matter dynamics in a model study. *European Journal of Soil Science* 57, 693-707.
- Denef, K., 2004. Carbon sequestration in microaggregates of no-tillage soils with different clay mineralogy. *Soil Science Society of America Journal* 68, 1935–1944.
- Denef, K., Six, J., 2005. Clay mineralogy determines the importance of biological versus abiotic processes for macroaggregate formation and stabilization. *European Journal of Soil Science* 56, 469-479.
- Don, A., Scholten, T., Schulze E.D., 2009. Conversion of cropland into grassland: Implications for soil organic-carbon stocks in two soils with different texture. *Journal of Plant Nutrition and Soil Science* 172, 53–62.
- Douglas, J.T., Goss, M.J., 1982. Stability and organic matter content of surface soil aggregates under different methods of cultivation and in grassland. *Soil and Tillage Research* 2, 155 - 175.
- FAO, 1990. *Guideline for*
- Elliott, E.T., 1986. Aggregate structure and carbon, nitrogen, and phosphorus in native and cultivated soils. *Soil Science Society of America Journal* 50, 627–633.

- Emadi, M., Baghernejad, M., Memarian, H.R., 2009. Effect of land-use change on soil fertility characteristics within water-stable aggregates of two cultivated soils in northern Iran. *Landuse Policy* 26, 452–457.
- European Commission (2000) - Communication from the Commission to the Council and the European Parliament on EU policies and measures to reduce greenhouse gas emissions: Towards a European climate change programme (ECCP) (COM(2000)88)
- European Commission (2001) - Communication from the Commission: A Sustainable Europe for a Better World: A European Union Strategy for Sustainable Development (Commission's proposal to the Gothenburg European Council) (COM(2001)264).
- European Commission (2006a) - Thematic Strategy for Soil Protection Communication (COM(2006)231).
- European Commission (2006b) - Proposal for a Directive of the European Parliament and of the Council establishing a framework for the protection of soil and amending Directive 2004/35/EC. Directive (COM(2006)232).
- Falloon, P., and Smith, P., 2002. Simulating SOC changes in long term experiments with RothC and Century: model evaluation for a regional scale application. *Soil Use and Management* 18, 101-111.
- Finke, P.A., Hutson, J.L., 2008. Modeling soil genesis in calcareous loess. *Geoderma*, 145, 462-479.
- Franco, U., 1996. Modeling approaches of soil organic matter turnover within the CANDY system. In: POWLSON, D. S., SMITH, P. & SMITH, J. U. (eds.) Evaluation of soil organic matter models using existing long-term datasets. NATO Series I. Heidelberg: Springer-Verlag.
- Geisseler, D., Horwath, W.R., Joergensen, R.G., and Ludwig, B., 2010. Pathways of nitrogen utilization by microorganisms – A review. *Soil Biology and Biochemistry*, (Available on-line).
- Ghani, A., Dexter, M., Carran, R.A., Theobald, P.W., 2007. Dissolved organic nitrogen and carbon in pastoral soils: the New Zealand experience. *European Journal of Soil Science* 58, 832–843.
- Gignoux, J., Hall, D., House, J., Masse, D., Nacro, H.N., Abbadie, L., 2001. Design and test of a generic cohort model of soil organic matter decomposition: the SOMKO model. *Global Ecology and Biogeography* 10, 639-660.
- Gleixner, G., Poirier, N., Bol, R., Balesdent, J., 2002. Molecular dynamics of organic matter in a cultivated soil. *Organic Geochemistry* 33, 357–366.
- Grace, P.R., Ladd, J.N., Robertson, G.P., Gage, S.H., 2006. SOCRATES--A simple model for predicting long-term changes in soil organic carbon in terrestrial ecosystems. *Soil Biology and Biochemistry* 38, 1172-1176.
- Grimm, M., Jones, R.J.A., Montanarella, L., 2002. Soil erosion risk in Europe. European Soil Bureau, Institute for Environment and Sustainability, JRC, Ispra, Italy, EUR 19939 EN.
- Golchin, A., Oades, J.M., Skjemstad, J.O., Clarke, P., 1994 Study of free and occluded particulate organic matter in soils by solid state <sup>13</sup>C CP/MAS NMR spectroscopy and scanning electron microscopy. *Australian Journal of Soil Research* 32, 285–309.
- Grandy A.S., Neff J.C., 2008. Molecular C dynamics downstream: The biochemical decomposition sequence and its impact on soil organic matter structure and function. *Science of the Total Environment*, 404, 297-307.
- Gupta, V.V.S.R, Germida, J.J., 1988. Distribution of microbial activity in different soil classes as affected by biomass and its aggregate size in cultivation. *Soil Biology and Biochemistry* 10, 777-786.
- Hall, C., M.L.S., 2003. The soil quality indices literature. Compiler's Report SQI Literature Project prepared for Alberta Environmentally Sustainable Agriculture Soil Quality Monitoring Program.
- Hassink, J., Bouwman, L.A., Zwart, K.B., Bloem, J., Brussaard, L., 1993. Relationships between soil texture, physical protection of organic matter, soil biota, and C and N mineralization in grassland soils. *Geoderma* 57, 105-128.
- Hassink, J., 1997. The capacity of soils to preserve organic C and N by their association with clay and silt particles. *Plant Soil* 191, 77–87.
- Hassink, J., and Whitmore, A.P, 1997. A model of the physical protection of organic matter in soils. *Soil Science Society of America Journal* 61, 131–139.

- Haynes, R.J., Swift, R.S., 1990. Stability of soil aggregates in relation to organic constituents and soil water content. *Journal of Soil Science* 41, 73–83.
- Haynes, R.J., Beare, M.H., 1996. Aggregation and organic matter storage in meso-thermal, humid soils. In: Carter MR, Stewart BA (eds) *Advances in soil science. Structure and organic matter storage in agricultural soils*. CRC Press, Boca Raton, Fla., pp 213–262.
- Helfrich, M., Ludwig, B., Potthoff, M., Flessa, H., 2008. Effect of litter quality and soil fungi on macroaggregate dynamics and associated partitioning of litter carbon and nitrogen. *Soil Biology and Biochemistry* 40, 1823–1835.
- Hill, J., Hostert, P., Tsiourlis, G., Kasapidis, P., Udelhoven, Th., Diemer, C., 1998. Monitoring 20 years of increased grazing impact on the Greek island of Crete with earth observation satellites. *Journal of Arid Environment* 39, 165-178.
- Jamtgard, S., Nasholm, T., Huss-Danell, K., 2010. Nitrogen compounds in soil solutions of agricultural land. *Soil Biology and Biochemistry* 42, 2325-2330.
- Jastrow, J.D., 1996, Soil aggregate formation and the accrual of particulate and mineral-associated organic matter. *Soil Biology and Biochemistry* 28, 665-676.
- Jastrow, J.D., Amonette, J.E., Bailey, V.L., 2007. Mechanisms controlling soil carbon turnover and their potential application for enhancing carbon sequestration, *Climate change* 80, 5-23.
- Jenkinson, D.S., Coleman, K., 1994. Calculating the annual input of organic matter to soil from measurements of total organic carbon and radiocarbon. *European Journal of Soil Science* 45, 167-174.
- Jenkinson, D.S., Coleman, K., 2008. The turnover of organic carbon in subsoils. Part 2. Modeling carbon turnover. *European Journal of Soil Science* 59, 400–413.
- Jónsdóttir E.M. 2011. Soil Sustainability Assessment – Proposed Soil Indicators for Sustainability. MSc Thesis, Faculty of Earth Sciences, University of Iceland.
- Juston, J., André, O., Kätterer, T., Jansson, P.E., 2010. Uncertainty analyses for calibrating a soil carbon balance model to agricultural field trial data in Sweden and Kenya. *Ecological Modelling* 221, 1880-1888.
- Karlen, D.L., Mausbach, M.J., Doran, J.W., Cline, R.G., Harris, R.F., Schuman, G.E., 1997. Soil quality: A concept, definition, and framework for evaluation. *Soil Science Society of America Journal* 61, 4–10.
- Kefi, S., Rietkerk, M., Alados, C.L., Pueyo, Y., Papanastasis, V.P., ElAich, A., de Ruiter, P.C., 2007. Spatial vegetation patterns and imminent desertification in Mediterranean arid ecosystems. *Nature* 449, 213-217.
- Kimetu, J.M., Lehmann, J., Kinyangi, J.M., Cheng, C.H., Thies, J., Mugendi, D.N., Pell, A., 2009. Soil organic C stabilization and thresholds in C saturation. *Soil Biology and Biochemistry* 41, 2100–2104.
- Kinyangi, J., 2007. Soil health and soil quality: a review. Draft publication. Available on: <http://www.cornell.edu.org>; Accessed on: [www.worldagroinfo.org](http://www.worldagroinfo.org). Accessed 23 Dec 2011.
- Kleber M., Sollins P., Sutton R., 2007. A conceptual model of organo-mineral interactions in soils: self-assembly of organic molecular fragments into zonal structures on mineral surfaces. *Biogeochemistry* 85, 9–24.
- Kleber, M., and Johnson, K.J., 2010. Advances in Understanding the Molecular Structure of Soil Organic Matter: Implications for Interactions in the Environment. *Advances in Agronomy* 106, 77-142.
- Knicker, H., 2007. How does fire affect the nature and stability of soil organic nitrogen and carbon? A review. *Biogeochemistry* 85, 91–118.
- Kochy, M., Mathaj, M., Jeltsch, F., Malkinson, D., 2008. Resilience of stocking capacity to changing climate in arid to Mediterranean landscapes. *Regional Environmental Change* 8, 73-87.
- Kong, A.Y.Y., Six, J., Bryant, D.C., Denison, R.F., van Kessel, C., 2005. The Relationship between Carbon Input, Aggregation, and Soil Organic Carbon Stabilization in Sustainable Cropping Systems. *Soil Science Society of America Journal* 69, 1078–1085.
- Krull, E.S., Skjemstad, J.O., Baldock, J.A., 2004, Functions of Soil Organic Matter and the effect on soil properties. GRDC report, Project CSO 00029.

- Krull, E.S., Skjemstad, J.O., Burrows, W.H., Bray, S.G., Wynn, J.G., Bol, R. et al. 2005. Recent vegetation changes in central Queensland, Australia: Evidence from  $\delta^{13}\text{C}$  and  $^{14}\text{C}$  analyses of soil organic matter. *Geoderma* 12, 241–259.
- Kuzyakov, Y., 2010. Priming effects: Interactions between living and dead organic matter. *Soil Biology and Biochemistry* 42, 1363-1371.
- Lal, R., 2004a. Soil carbon sequestration to mitigate climate change. *Geoderma* 123, 1–22.
- Lal R., 2004b. Soil Carbon Sequestration Impacts on Global Climate Change and Food Security. *Science* 304, 1623–1627.
- Lal, R., 2008. Carbon sequestration. *Philosophical Transactions of the Royal Society* 363, 815-830.
- Lawrence, C.R., Neff, J.C., Schimel, J.P., 2009. Does adding microbial mechanisms of decomposition improve soil organic matter models? A comparison of four models using data from a pulsed rewetting experiment. *Soil Biology and Biochemistry* 41, 1923-1934.
- Lehmann, J., Solomon, D., Kinyangi, J., Dathe, L., Wirick, S., JACOBSEN, C., 2008. Spatial complexity of soil organic matter forms at nanometre scales. *Nature Geoscience* 1, 238-242.
- Lewandowski, A, Zumwinkle, M., Fish, A., 1999. Assessing the soil system: a Review of soil quality literature, Minnesota Department of Agriculture, Energy and Sustainable Agriculture, St. Paul, MN.
- Li, C., Frolking, S., Frolking, T.A., 1992. A model of nitrous oxide evolution from soil driven by rainfall events. I Model structure and sensitivity. *Journal of Geophysical Research* 97, 9759-9776.
- Li X.G., Wang Z.F., Ma Q.F., Li F.M., 2007. Crop cultivation and intensive grazing affect organic C pools and aggregate stability in arid grassland soil. *Soil and Tillage Research* 95, 172-181.
- Mc Donald, A.J., Murphy, D.V., Mahieu, N., Fillery, I.R.P., 2007. Labile soil organic matter pools under a mixed grass/lucerne pasture and adjacent native bush in Western Australia. *Australian Journal of Soil Research* 45, 333-343.
- Malamoud, K., McBratney, A.B., Minasny, B., and field, D.J., 2009. Modeling how carbon affects soil structure. *Geoderma*, 149, 19-26.
- Mann, L.K. 1986. Changes in soil carbon storage after cultivation. *Soil Science* 142(5), 279-288.
- Manzoni, S., and Porporato, A., 2009. Soil carbon and nitrogen mineralization: Theory and models across scales. *Soil Biology and Biochemistry* 41, 1355-1379.
- Minasny, B., McBratney, A.B., Salvador-Blanes, S., 2008. Quantitative models for pedogenesis – A review, *Geoderma* 144, 140-157.
- Molina, J.A.E., Clapp, C.E., Shaffer, M.J., Chichester, F.W., Larson, W.E., 1983. NCSOIL, a model of nitrogen and carbon transformation in soil: description, calibration and behaviour. *Soil Science Society of America Journal* 47, 85-91.
- Molina, J.A.E., 1996. Description of the model NCSOIL. In: Powlson, D.S., Snith, P., Smith, J.U., (eds.) *Evaluation of soil organic matter models using existing long-term datasets*. NATO ASI Series I. Heidelberg: Springer-Verlag.
- Mueller, T., Jensen, L.S., Hansen, S., Nielsen, N.E., 1996. Simulating soil carbon and nitrogen dynamics with the soil-plant-atmosphere system model DAISY. In: Powlson, D.S., Snith, P., Smith, J.U., (eds.) *Evaluation of soil organic matter models using existing long-term datasets*. NATO ASI Series I. Heidelberg: Springer-Verlag.
- Nannipieri, P., and Eldor, P., 2009. The chemical and functional characterization of soil N and its biotic component. *Soil Biology and Biochemistry* 41, 2357-2369.
- Neff, J.C., Holland, E.A., Detenter, F.J., McDowell, W.H., Russell, K.M., 2002. The origin, composition and rates of organic nitrogen deposition: A missing piece of the nitrogen cycle? *Biogeochemistry* 57/58, 99–136.
- Nikolaidis, N.P., 2011, Human impacts on soils: Tipping points and knowledge gaps. *Applied Geochemistry* 26, S230–S233.
- Nikolaidis, N.P. and Bidoglio G., 2011. Modeling of Soil Organic Matter and Structure Dynamics: A Synthesis Review. *Geoderma* (submitted revisions).

- Parton, W.J., 1996. The CENTURY model. In: Powlson, D.S., Snith, P., Smith, J.U., (eds.) Evaluation of soil organic matter models using existing long-term datasets. NATO ASI Series I. Heidelberg: Springer-Verlag.
- Paul, E.A., Paustian, K., Elliott, E.T., Cole, C.V., 1997. Soil Organic Matter in Temperate Agroecosystems. CRC Press, Boca Raton. 414 p.
- Paul, K.I., Polglase, P.J., Richards, G.P., 2003. Predicted change in soil carbon following afforestation or reforestation, and analysis of controlling factors by linking a C accounting model (CAMFor) to models of forest growth (3PG), litter decomposition (GENDEC) and soil C turnover (RothC). *Forest Ecology and Management* 177, 485-501.
- Plante, A.F., McGill, W.B., 2002. Soil aggregate dynamics and the retention of organic matter in laboratory-incubated soil with differing simulated tillage frequencies. *Soil and Tillage Research* 66, 79–92.
- Plante, A.F., Feng, Y., McGill, W.B., 2002. A modeling approach to quantifying soil macroaggregate dynamics. *Canadian Journal of Soil Science* 82, 181–190.
- Piccolo A., 2001. The supramolecular structure of humic substances. *Soil Science* 166, 810-832.
- Post, J., Krysanova, V., Suckow, F., Mirschel, W., Rogasik, J., Merbach, I., 2007. Integrated ecohydrological modeling of soil organic matter dynamics for the assessment of environmental change impacts in meso- and macro-scale river basins, *Ecological Modeling* 206, 93-109.
- Powlson, D.S., Whitmore, A.P., Goulding, K.W.T., 2011. Soil carbon sequestration to mitigate climate change: a critical re-examination to identify the true and the false. *European Journal of Soil Science* 62, 42-55.
- Puget, P., Chenu, C., Balesdent, J., 2000. Dynamics of soil organic matter associated with particle-size fractions of water-stable aggregates. *European Journal of Soil Science* 51, 595-605.
- RCEP., 1996. Sustainable Use of Soil. 19th report of the Royal Commission on Environmental Pollution. Cmnd 3165, HMSO, London.
- Rees, R.M., Bingham, I.J., Baddeley, J.A., Watson, C.A., 2005. The role of plants and land management in sequestering soil carbon in temperate arable and grassland. *Geoderma* 128, 130-154.
- Richardson, R.B., 2010. Ecosystem Services and Food Security: Economic Perspectives on Environmental Sustainability. *Sustainability* 2, 3520-3548.
- Rietkerk, M., Dekker, S.C., de Ruiter, P.C., van de Koppel, J., 2004. Self-Organized Patchiness and Catastrophic Shifts in Ecosystems. *Science* 305, 1926-1929
- Rillig, M.C., Caldwell, B.A., Wosten, H.A.B., Sollins, P., 2007. Role of proteins in soil carbon and nitrogen storage: controls on persistence. *Biogeochemistry* 85, 25-44.
- Rovira, P., Vallejo, V. R., 2002. Labile and recalcitrant pools of carbon and nitrogen in organic matter decomposing at different depths in soil: An acid hydrolysis approach. *Geoderma* 107, 109-141.
- Schimel, J.P., Bennett, J., 2004. Nitrogen mineralization: Challenges of a changing paradigm. *Ecology* 85, 591-602.
- Schnitzer M., 1991. Soil organic matter – the next 75 years. *Soil Science* 151(1), 41-58.
- Schoning, I., Morgentoth, G., Kogel-Knabner, I., 2005. O/N-alkyl and alkyl C are stabilised in fine particle size fractions of forest soils. *Biogeochemistry* 73, 475–497.
- Schulten, H.R., Schnitzer, M., 1998. The chemistry of soil organic nitrogen: a review. *Biology and Fertility of Soils* 26, 1-15.
- Shibu, M.E., Leffelaar, P.A., Van Keulen, H., Aggarwal, P.K., 2006. Quantitative description of soil organic matter dynamics – A review of approaches with reference to rice-based cropping systems. *Geoderma* 137, 1-18.
- Six, J., Elliott, E.T., Paustian, K., 1999. Aggregate and soil organic matter dynamics under conventional and no-tillage systems. *Soil Science Society of America Journal* 63, 1350-1358.
- Six, J., Elliott, E.T., Paustian, K., 2000. Soil macroaggregate turnover and microaggregate formation: a mechanism for carbon sequestration under no tillage agriculture. *Short Communication in Soil Biology and Biochemistry* 32, 2099-2103.

- Six, J., Conant, R.T., Paul E.A., and Paustian, K., 2002a. Stabilization mechanisms of soil organic matter: Implications for C-saturation of soils. *Plant and Soil* 241, 155–176.
- Six, J., Feller, C., Deneff, K., Ogle, S.M., de Moraes, J.C., Albrecht, A., 2002b. Soil organic matter, biota and aggregation in temperate and tropical soils – Effects of no-tillage. *Agronomie* 22, 755–775.
- Six, J., Bossuyt, H., Degryze, S., Deneff, K., 2004. A history of research on the link between (micro)aggregates, soil biota, and soil organic matter dynamics. *Soil and Tillage Research* 79, 7–31.
- Smith, P., Powlson, D.S., Smith, J.U., Elliott, E.T., 1997. Evaluation and comparison of soil organic matter models using datasets from seven long-term experiments. *Geoderma* 81, 1-225.
- Smith, P., Andren, O., Brussaard, L., Dangerfield, M., Ekschmitt, K., Lavelle, P., Tate, K. 1998. Soil biota and global change at the ecosystem level: describing soil biota in mathematical models. *Global Change Biology* 4, 773-784.
- Solberg, E.D., Nyborg, M., Izaurralde, R.C., Malhi, S.S., Janzen, H.H., Molina-Ayala, M., 1997. Carbon Storage in soils under continuous cereal grain cropping: N fertilizer and straw. In *Management of Carbon Sequestration in Soil*. Eds. R. Lal, J M Kimble, R F Follett and B A Stewart. pp 235–254. CRC Press, Boca Raton,
- Sollins P., Swanston C., Kramer M., 2007. Stabilization and destabilization of soil organic matter—a new focus. *Biogeochemistry* 85, 1–7.
- Susilo, F.X., Neutel, A.M., van Noordwijk, M., Hairiah, K., Brown, G., Swift, M.J., 2004. Soil biodiversity and food webs. Below-ground interactions in tropical agroecosystems: concepts and models with multiple plant components. Wallingford: CABI Publishing.
- Sutton R., Sposito G., 2005. Molecular Structure in Soil Humic Substances: The New View. *Environmental Science and Technology* 39(23), 9009-9015.
- Takeshi, I., and Moorcroft, P.R., 2006. The global-scale temperature and moisture dependencies of soil organic carbon decomposition: an analysis using a mechanistic decomposition model. *Biogeochemistry* 80, 217–231.
- Thevenot, M., Dignac, M., and Rumpel, C., 2010. Fate of lignins in soils: A review. *Soil Biology and Biochemistry* 42, 1200-1211.
- Thomas, D.E., 2007. A study of the mineral depletion of foods available to us as a nation over the period 1940 to 1991. *Nutrition and Health* 19, 21–25.
- Thornley, J.H.M., Verbene, E.L.J., 1989. A model of nitrogen flows in grassland. *Plant Cell Environment* 12, 863-886.
- Van-Camp., L., Bujarrabal, B., Gentile, A-R., Jones, R.J.A., Montanarella, L., Olazabal, C. and Selvaradjou, S.K., 2004. Reports of the Technical Working Groups Established under the Thematic Strategy for Soil Protection. EUR 21319 EN/1, 872 pp. Office for Official Publications of the European Communities, Luxembourg.
- Van Veen, J.A., and Paul, E.A., 1981. Organic carbon dynamics in grasslands and soils. 1. Background information and computer simulation. *Canadian Journal of Soil Science* 61, 185-201.
- Verbene, E.L.J., Hassink, J., de Willigen, P., Groot, J.J.R., van Veen, J.A., 1990. Modeling soil organic matter dynamics in different soils. *Netherlands Journal of Agricultural Science* 38, 221-238.
- Viaud, V., Angers, D.A., WALTER, C., 2010. Towards landscape-scale modeling of soil organic matter dynamics in agroecosystems. *Soil Science Society of America Journal* 74, 1-14.
- Virto, P., Barré, C., Chenu, 2008. Microaggregation and organic matter storage at the silt-size scale. *Geoderma* 146, 326–335.
- von Lützw M., Kögel-Knabner I., Ekschmitt K., Flessa H., Guggenberger G., Matzner E., Marschner B., 2007. SOM fractionation methods: Relevance to functional pools and to stabilization mechanisms. *Soil Biology and Biochemistry* 39, 2183-2207.
- Wagai, R., Mayer, L.M., Kitayama, K., Knicker, H., 2008. Climate and parent material controls on organic matter storage in surface soils: three-pool, density-separation approach. *Geoderma* 147, 23-33.
- Wershaw R.L., Llaguno E.C., Leenheer J.A., 1996. Mechanism of formation of humus coatings on mineral surfaces 3. Composition of adsorbed organic acids from compost leachate on alumina by solid-state <sup>13</sup>C NMR. *Coll Surf A: Physicochemical and Engineering Aspects*, 108, 213–223.

- Williams, R.J.B., 1970. Relationship between the composition of soils and physical measurements made on them. Rothamsted Experimental Station Report, Part 2. Harpenden, pp. 5–35
- Yang, X., Wang, M., Huang, Y., Wang, Y., 2002. A one-compartment model to study soil carbon decomposition rate at equilibrium situation. *Ecological Modeling* 151, 63–73.
- Yassoglou, N., Kosmas, C., Moustakas, N., 1997. The red soils, their origin, properties, use and management in Greece. *Catena* 28, 261–278.
- Zeng, N., 2003. Drought in teh Sahel. *Atmospheric Science* 302, 999-1000.
- Zimmermann, M., Leifeld, J., Schmidt, M.W.I., Smith, P., Fuhrer, J., 2007. Measured soil organic matter fractions can be related to pools in the RothC model. *European Journal of Soil Science* 58, 658–667.
- Zwarts, L., Bijlsma, R.G., van der Kamp, J., Wymenga, E., 2009. *Living on the edge: wetlands and birds in a changing Sahel*. Zeist: KNNV Publishing.



## 2. ROTH-C-CALIBRATION ISSUES AND UNCERTAINTY ANALYSIS

---

*Modeling topsoil carbon sequestration in two contrasting crop production to set-aside conversions with RothC – calibration issues and uncertainty analysis*

**Abstract:** Model simulations of soil organic carbon turnover in agricultural fields have inherent uncertainties due to input data, initial conditions, and model parameters. The RothC model was used in a Monte-Carlo based framework to assess the uniqueness of solution in carbon sequestration simulations. The model was applied to crop production to set-aside conversions in Iowa (sandy clay-loam soil, humid-continental climate) and Greece (clay-loam soil, Mediterranean). Fallow fields were left set-aside from crop production for 20 and 35 years in Iowa and Greece, respectively and native vegetation was developed (Grassland in Iowa and shrubland in Greece). The model was initialized and calibrated with particulate organic carbon data obtained by physical fractionation. The calibrated values for the Iowa grassland were 5.05 t C/ha, 0.34 1/y, and 0.27 1/y for plant litter input and decomposition rate constants for resistant plant material (RPM) and humus (HUM), respectively, while for the Greek shrubland these were 3.79 t C/ha, 0.21 1/y, and 0.0041 1/y, correspondingly. The calibrated RPM and HUM decomposition rate constants were significantly different compared to the default RothC values. Different clay content of the two sites affected differently 'apparent' sensitivity of decomposition to temperature and/or moisture. The model sensitivity analysis revealed that for both sites, the total plant litter input and the RPM rate constant showed the highest sensitivity in respect to the predicted soil organic carbon content. The Iowa soil was projected to sequester 17.5 t C/ha and the Greek soil 54 t C/ha over 100 years and the projected uncertainty was 65.6% and 70.8%, respectively. The implications of these uncertainties are important; hampering our ability to accurately predict carbon sequestration under set-aside conditions. The developed methodology can be used to assess the factors affecting carbon sequestration in agricultural soils and quantify the uncertainties.

## 2.1 INTRODUCTION

Conversion of native vegetated lands to croplands is known to induce soil organic carbon (SOC) losses due to ploughing. In medium to fine textured, structured soils, during ploughing, aggregates are partly destroyed and physically protected SOC is exposed, the bio-available fraction becomes then bio-accessible and can be microbially oxidized causing SOC decline and consequent CO<sub>2</sub> emissions (Balesdent et al., 1998). Most of the SOC loss, in structured soils, is attributed to the destruction of large macro-aggregates which consist primarily of labile SOC (Emadi et al., 2009). The free or occluded labile (light fraction with a density lower than 1.6-2 g cm<sup>-3</sup>) SOC, consisting primarily of particulate organic carbon (POC), is the fraction mostly affected by ploughing (Wagai et al., 2008), while the denser mineral fraction is mostly affected in the medium- to long-term time scale (Don et al., 2009). Particulate organic carbon, unprotected though, is also most affected due to ploughing in structureless sandy soils.

On the other hand, the conversion of cultivated fields to grasslands, shrublands or forests has been shown to sequester carbon in soils (Guo and Gifford, 2002), which is primarily attributable to POC changes in the topsoil (Potter and Derner, 2006). Soussana et al. (2004) have reported that it takes twice as long to restore the carbon content in restored grasslands compared to the time it takes to lose the carbon through cultivation (i.e. ploughing). The re-formation of soil aggregates after such landuse change indicates the 'soil resilience' potential (Lal, 1997). Particle aggregation provides structure to soils and has been related to soil fertility. An "agronomically valuable" soil is a soil where greater than 60% of the particle mass in the aggregated form is in the range between 0.25 and 10 mm (Banwart et al., 2011). The extent of soil degradation and restoration depends on management practices as well as the factors that determine soil structure and aggregation (Angers and Carter, 1996) which include SOC and total nitrogen (TN) content, soil mineralogy, and clay content, soil macrofauna (e.g. earthworms), and root, root hair and (vesicular-arbuscular) mycorrhizal hyphal densities, as well as the climate under which the soil was formed. Understanding the factors controlling landuse effects on soil particle aggregation is therefore very important in order to improve SOM modeling and soil restoration techniques (Angers and Carter, 1996; Rees et al., 2005). Physical fractionation schemes can be used to appraise the effect of landuse change on particle aggregation and estimate the fractions of carbon such as the humus and particulate fractions that can be used to calibrate the turnover of carbon with mathematical models.

The turnover of SOC is usually described with multi-compartment models. Many soil carbon models have been utilized in the scientific literature and comparison of their structure and modeling results can be found in review papers (e.g. Battle-Aguilar et al., 2010; Falloon and Smith, 2000; Manzoni and Porporato, 2009; Nikolaidis and Bidoglio 2012; Shibu et al., 2006; Smith et al., 1997). These models have been used to simulate SOC turnover of discrete soil organic carbon pools using either default or calibrated decomposition rate constants mostly without accounting for the uncertainty that arises from the initial conditions, model parameters, inputs as well as model structure with very few exceptions (Juston et al., 2010; Paul et al., 2003). However, models can be greatly constrained by using field measured carbon pools to initialize and calibrate the model. For example physical fractionation schemes like dispersing and sieving sieving (Skjemstad et al., 2004) as well as density fractionation (Zimmermann et al., 2007) have been used to measure modeled carbon pools in RothC carbon model. The complexity of the interrelationships among the carbon turnover model parameters and inputs require a modeling framework to assess the uniqueness of solution and the uncertainties due to model structure, initial conditions, model parameters and input data. In this study, the RothC carbon model which is one of the more widely used carbon models along with CENTURY and DNDC was selected for its simplicity and because physical fractionation data could be related with its carbon pools.

The objective of this study was twofold: a) develop a procedure for model parameter estimation applied to cases of cropland to fallow conversions (through initialization and calibration with field derived physical fractionation data) where the litter/manure input has not been measured and b) quantify the uncertainties in RothC modeling results.

## **2.2 METHODOLOGY**

A Microsoft Excel version of the Rothamsted Carbon Model-version RothC-26.3 (Coleman and Jenkinson, 1999) was developed (see paragraph 2.2.3 for details) and used in conjunction

with the statistical simulation package @RISK (PALISADES Corp.) in order to simulate the uncertainty in topsoil carbon turnover during cropland to set-aside from crop production (which was cultivated in the past and was left uncultivated with native vegetation) conversion in Iowa (grassland) and Greece (shrubland). A physical fractionation scheme was used to obtain the required data to initialize and calibrate the model.

### 2.2.1 Study sites

Two sites (Table 2.1) were chosen with paired plots of adjacent cropland and set-aside fields. The first site (indicated as IA) was in the outskirts of Iowa City, IA, USA (41°45'N, 91°44'W, 230 m), indicative of humid continental climate with soils with coarse texture-sandy loam. Mean annual temperature in the region is 10.3 °C (21.2±3.1 °C, May – Sep) and mean annual precipitation 923 mm (60%, May - Sep). The second site (indicated as GR) was in the northern part of Chania Prefecture, Crete, Greece (39°25'N, 51°41'E, 10 m), where typical semi-arid, Mediterranean climate dominates and soils have finer texture-clay loam. Mean annual temperature in the region is 18 °C (23.9±2.5 °C, May – Sep) and mean annual precipitation 652 mm (6.0%, May-Sep). In Iowa, the wet and warm cropping period lasts from May to September, while during the winter period soil is covered by snow. In Greece, most of the precipitation is taking place during the winter time, from November to March (77% of the annual precipitation) where the temperature is low (12.5±1.9 °C) and therefore warm cropping period is dry.

Soils in both sites were recent alluvial depositions. Iowan soils were very deep, poorly drained soils, formed in colluvium alluvial fans, and characterized as Udoolls (Udolls Mollisols or Phaeozems-FAO, 1998). Udolls are more or less freely drained Mollisols of humid climates that naturally were tall grass prairies and are used as croplands. Cretan alluvial depositions (Quaternary formations) are shallower than those at Iowa and characterized as calcaric Regosols-known also as para-rendzinas, or Entisols in the American System (FAO, 1998). Regosols are frequently associated with Leptosols and Arenosols and are soils with very limited soil development. Regosols and Phaeozems are used as arable lands and correspond to 7.1% and 9.7% of the total world area used for arable cultivation (which is 18 % of total world land cover) (The World Factbook, 2008).

The Iowa arable field was disk ploughed to about 30 cm soil depth and used for the production of corn and soybeans. Prior to being set-aside, about 20 years ago, the Iowa uncultivated field received the same management. Mollisols in the Midwest have been

cultivated for more than 150 years. However, most of the organic matter decline occurred by 1960 and has been at steady state under production practices in place since then (David et al., 2009). The Greek arable field was used for the production of green vegetables and tillage was lighter and shallower compared to Iowa. The Greek field had been set-aside from crop production about 35 years. For modeling purposes, the soils have been assumed to be at steady state in terms of carbon content; however this assumption is inherently uncertain.

**Table 2.1 Study sites location and characteristics.**

	<b>Iowa River Basin floodplain, IA, USA</b>	<b>Koiliaris River basin floodplain, Crete, GR</b>
<b>Coordinates</b>	41°45'N, 91°44'W	39°25'N, 51°41'E
<b>Elevation, m</b>	230	10
<b>Climate type</b>	Humid continental	Mediterranean
<b>PREC, mm/y</b>	923 (60% MAY - SEP)	652 (77% NOV-MAR)
<b>TEMP, °C</b>	10.3 (21.2±3.2 MAY – SEP)	18.1 (12.5±1.9 NOV – MAR)
<b>Bedrock type</b>	Loess and till glacial	Alluvial sediments (Quaternary)
<b>Soil type</b>	Udolls Mollisols or Phaeozems	Entisols or calcaric Regosols
<b>Texture</b>	Sandy loam	Clay Loam
<b>Tillage</b>	Intensive till/disk plow	Light and shallow plowing
<b>Crops</b>	Corn, bean	Vegetables
<b>Set-aside</b>	Grassland	Shrubland
<b>Set-aside, y</b>	20	35

Soil sampling was designed based on the objective to simulate the evolution of soil carbon from cultivation to set-aside conditions. As reported in previous studies (Potter and Derner, 2006) most of the changes in aggregation and SOC storage are known to take place in the topsoil down to plant rooting depth. Typical rooting depth of Mediterranean shrublands found in Greece was 10 cm (Beier et al., 2009). Organic carbon has been found to concentrate in the top 10 cm and a sharp decline has been observed in the subsoil of both tilled ( $2.1 \pm 0.5$  times) and no tilled ( $1.6 \pm 0.3$  times) fields of olive groves in the alluvial plain of Koiliaris River Basin (Figure 2.1, details about these data are given in chapter 5). On the other hand although the rooting depth in Iowa grassland is deeper, most of the root biomass is found in the topsoil. Studies have indicated that 73-87% of the total root biomass (0-125 cm) across different plants in Iowa was found in the 0-35 cm (Tufekcioglu et al., 2003), while 90% of prairie root biomass (0-50 cm) was found in the 0-25 cm and 60% in the upper 5-cm (Buyanovsky et al., 1987). In order to compare the results between Greece and Iowa, surface soil was sampled from 0-10 cm in both croplands and set-aside fields. Each disturbed sample

was a composite of five representative subsamples. A stainless steel shovel was used to turnover the soil to a pre-specified depth. Samples were taken from the middle of the pile paying attention not to break the aggregates and minimizing compression. The composite sample was the combination of five subsamples obtained from different locations within the same field. Bulk density was calculated using 100 cm<sup>3</sup> cores (undisturbed samples). The 10-30 cm soil depth was also sampled from the Iowa soils in order to account for the greater rooting depth and validate the changes in total SOC storage. Recent plant residues and very large stones were removed from the fresh soil samples by hand. Large stones comprised only a very small percent of soil composition in the Greek soils and were not present at all in Iowa soils. They were not taken into account in SOC stocks calculations. The samples were air dried and stored in a cool-dry place not more than 2-3 months until further analysis. Subsoil samples were measured for SOC and TN content and bulk density.

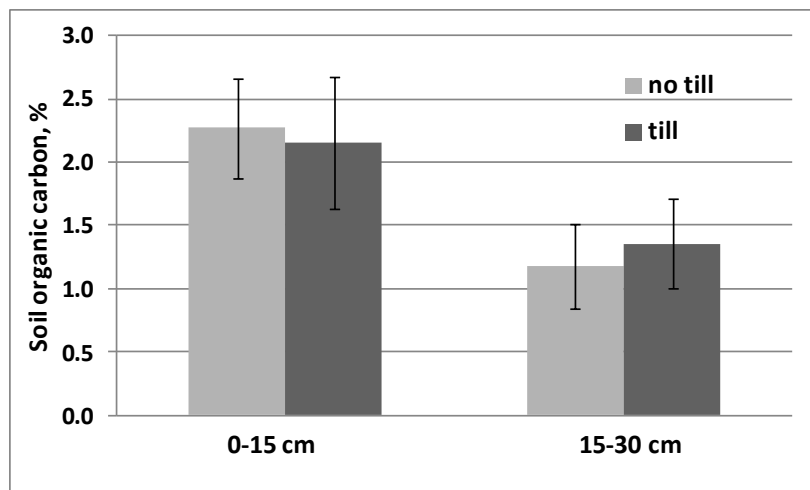


Figure 2.1 Soil organic carbon content in topsoil (0-15 cm) and subsoil (15-30 cm) of tilled and no-tilled olive grove fields (samples taken from the area between the trees) in the alluvial plain of Koiliaris River Basin (average and standard deviation derived by three spatial samples). (Details about these data are given in Chapter 5).

### 2.2.2 Physical fractionation

The methodological approach was based on the physical fractionation scheme given in Figure 2.2. Soils were separated in different water stable aggregate (WSA) fractions and the macro-aggregates were further separated in particulate organic matter (POM) (sand sized fractions

and POM) and smaller micro-aggregates. All fractions were measured for their content in total C and N. The FTIR spectra of the aggregate fractions were also obtained.

#### *Aggregate fractionation procedure*

Bulk soil was gently sieved to pass through an 8 mm sieve and residual litter was removed. Then the soil was separated into five water stable aggregate (slake resistant) fractions according to the procedure described by Elliott (1986): i) large macro-aggregates (>2000  $\mu\text{m}$ ), ii) medium macro-aggregates (1000-2000  $\mu\text{m}$ ), iii) small macro-aggregates (250-1000  $\mu\text{m}$ ), iv) micro-aggregates (53-250  $\mu\text{m}$ ), and v) silt-clay sized micro-aggregates and minerals (<53  $\mu\text{m}$ ). Aggregate fractions were determined on triplicates, where air-dried soil (40 g) was quickly submerged in deionized water on top of the 2000  $\mu\text{m}$  sieve (for 5 min), which was then moved up and down over 2 min with a stroke length of 3 cm for 50 strokes. The organic material floating on the water in the 2000  $\mu\text{m}$  sieve was removed after the 2 min cycle because it is not considered SOM. Sieving was repeated on the 1000  $\mu\text{m}$  (40 strokes), 250- $\mu\text{m}$  (30 strokes) and 53- $\mu\text{m}$  (10 strokes) sieves using the soil plus water that passed through the next larger sieve. Clay from the 53  $\mu\text{m}$  sieve was gently removed. Aggregates remaining on each sieve were oven-dried at (40°C), weighed and stored in glass jars at room temperature. Sand content was determined on aggregate fraction subsamples after dispersing soil in sodium hexametaphosphate (0.5%) for 18 h on a rotary shaker at 190 rpm. The samples were then passed through the sieve corresponding to the lower limit of each aggregate size (e.g. the 1000-2000  $\mu\text{m}$  sized aggregated with the 1000  $\mu\text{m}$  sieve) and the sand mass retained in the sieve was used for sand correction. Mean weight diameter (MWD) was calculated by summing the weighted proportion of each aggregate fraction and was used as an index of aggregate stability.

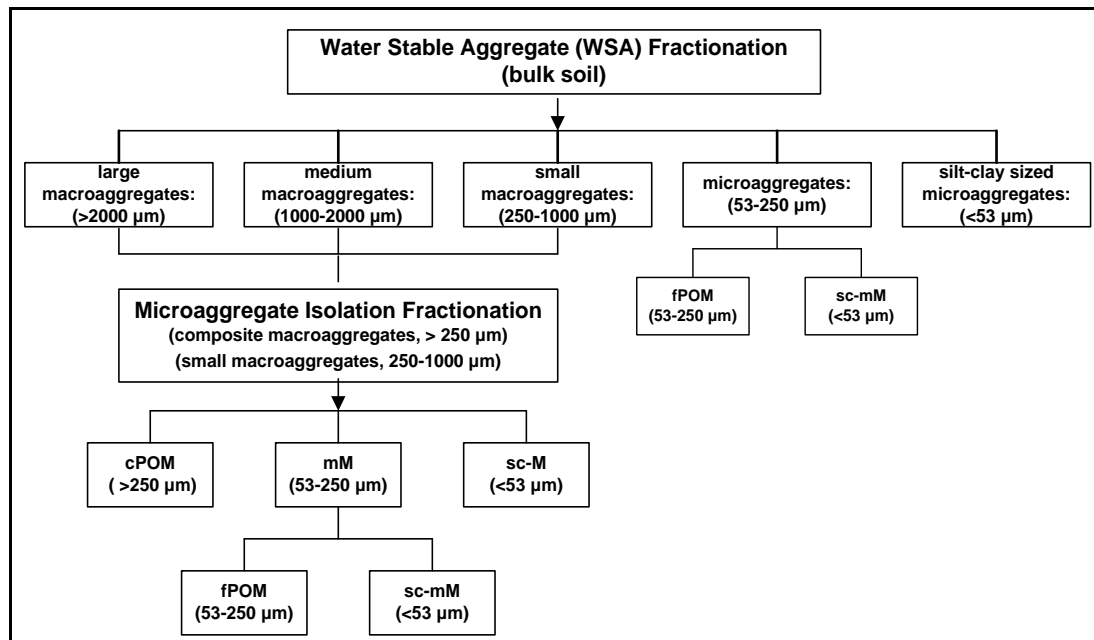


**Figure 2.2 Physical fractionation scheme used in the study. cPOM = coarse particulate organic matter, mM = micro-aggregates within macro-aggregates, sc-M = easily dispersed silt-clay fraction, fPOM = fine particulate organic matter, sc-mM = silt-clay fraction of the microaggregate. POM fractions correspond to sand sized fractions and free POM.**

*Micro-aggregate isolation procedure*

In order to reveal possible differences in the composition and turnover rates of the macro-aggregates of different sizes and the patterns of the decomposition sequence the micro-aggregate isolation procedure outlined in Lichter et al., (2008) was followed to both small macro-aggregates (250-1000 μm) and composite macro-aggregates (>250 μm) samples. A subsample (10 g) of small macro-aggregates (250-1000 μm) and of composite macro-aggregates (>250 μm) was further separated into the following fractions by the micro-aggregate isolation procedure outlined in Lichter et al., (2008): i) coarse particulate organic matter and sand (cPOM: >250 μm), ii) micro-aggregates (mM: 53-250 μm), and iii) easily dispersed silt-clay fractions (sc-M <53 μm). Briefly, the subsample of the aggregates was immersed in deionized water on top of a 250- mm mesh screen and gently shaken with 50 glass beads (4 mm in diameter) with continuous and steady water flow through the device to ensure that micro-aggregates were immediately flushed onto a 53-mm sieve and were not exposed to any further disruption by the beads (Six et al., 2000). After all macro-aggregates were broken up, the material on the 250 μm sieve was collected (cPOM) and sieved through the 53-μm sieve to ensure that the isolated micro-aggregates were water stable (mM). The fraction that passed through the 53 μm sieve (sc-M) was also collected. The three fractions

were oven-dried at (40°C), weighed and stored in glass jars at room temperature. The micro-aggregates within the macro-aggregates (mM) as well as the 53-250 µm sized aggregates (micro-aggregates) were similarly separated to fine particulate organic matter and sand (fPOM: 53-250 µm) and silt-clay fraction of the micro-aggregate (sc-mM <53 µm). Using Lichter et al., (2008) as a guide for this procedure, the free POM and intra POM were not separated, as it was observed that during the floatation procedure the macro-aggregates are collapsed and the separation cannot always be successful. Free POM which is also reported as occluded POM is negligible in terms of mass (1% and 2% for agricultural and forest soils respectively), but has the same C-to-N ratio as the free fraction (John et al., 2005).

#### *FTIR spectra*

Fourier transform infrared spectroscopy (FTIR) was used as an easy and quick estimation of the chemical composition of the soil organic matter for each aggregate fraction, and specifically the aromatic carbon as indicative of the plant derived material. Spectral characterization of soil aggregates was performed by diamond attenuated total reflectance (DATR) FTIR spectroscopy using a Nicolet Magna-IR 550 FTIR spectrometer (Thermo Electron, Warwick, UK) fitted with a potassium bromide beam splitter and a deutroglycine sulphate detector without the dilution with KBr (Artz et al., 2008). Dry and powdered samples were placed directly on the crystal and a tip powder press was used to achieve even distribution and contact. Spectra were acquired by averaging 20 scans at 4 1/cm resolution over the range 4000–350 1/cm. Baseline was obtained before every run. All spectra were corrected for attenuation by water vapor and CO<sub>2</sub>. The baseline and ATR correction were also applied (Omic software, version 8.0, Thermo Electron). In order to quantify the relative changes in the FTIR spectra and for spectral comparison, relative absorbance (rA) was calculated by dividing the corrected peak height of a distinct peak (e.g. 2920, 1630, 1440, 1030 1/cm) by the sum of the heights of all peaks and multiplying it by 100. The parameters for each peak were as follows: Base 1/peak/Base 2 (all in 1/cm) 3000/2920/2800; 1700/1630/1560; 1490/1440/1400; 1190/1050/900 (Gerzabek et al., 2006).

#### *Physico-chemical analysis*

Soils were measured for dry bulk density (gravimetric method), pH and soluble salts (conductivity)-measured in a 1:2 soil to water ratio (Methods of Soil Analysis, 1982), and texture (Bouyoucos, 1936). The KCl extraction (2 M KCl in a 1:5 soil-to-solution ratio) was used for the estimation of potential mineralizable N ( $PMN=NH_3-N+NO_3-N$ ) of soils using standard operating procedures (Hack 2010 spectrophotometer procedures manual, 1999) for  $NO_3-N$  (Cadmium Reduction Method, 8039) and  $NH_4-N$  (Salicylate Method, 10023). Potential soluble organic nitrogen (PSON) was also measured by the Kjeldahl digestion technique (Nessler method, 8075). The potential soluble organic carbon (PSOC) was also estimated by a TOC analyzer (Shimadzu 5050), after the removal of inorganic carbon by air sparging for 10 min (Instruction Manual TOC-5050A, Shimadzu Corporation). The extracted pools were also measured for their content in carbohydrates colorimetrically using the phenol-sulfuric acid procedure (Piccolo et al., 1996). Bulk soil, aggregates, and fractions from the microaggregate isolation procedure were measured for their content in C by a TOC analyzer-solid sample module SSM-5000 (corrected for their inorganic C content) and N by the Kjeldahl digestion technique with a Hach digestahl digestion apparatus (Nessler method, 8075). The total C and N content of the sc-mM fraction was not measured but estimated as the difference between the micro-aggregate (mM) and the fPOM.

### **2.2.3 Carbon turnover modeling**

Topsoil carbon turnover during cropland to set-aside conversion in Iowa (grassland) and Greece (shrubland) was simulated with the RothC carbon model and the uncertainty was estimated. A Microsoft Excel version of the Rothamsted Carbon Model-version RothC-26.3 (Coleman and Jenkinson, 1999) was developed. An initial excel version was provided by Todorovic et al. (2010). The calculation of RothC 'abc' parameters (described in the following paragraph) was added in the excel version that was developed. The model was cross verified with the original exe of RothC-26.3 with the default values of model parameters and gave identical results. No structural changes were made.

RothC is based on a monthly time step calculation and can simulate SOC turnover over a period ranging from a few years to a few centuries. Soil organic carbon is split into four active pools which decompose by a first-order process, each with its own characteristic rate and an amount of inert organic matter (IOM) resistant to decomposition (Figure 1.17). The four active compartments are Decomposable Plant Material (DPM), Resistant Plant Material

(RPM), Microbial Biomass (BIO) and Humified Organic Matter (HUM). The DPM and RPM carbon pools correspond to the carbon related with particulate organic matter and the BIO and HUM to the carbon related with the silt-clay fraction. The name of the HUM pool is only operational and does not correspond to humus of the old view (see the literature review presented in Chapter 1). The model default decomposition rate constants ( $k$ , 1/y) for each compartment are: DPM: 10.0, RPM: 0.3, BIO: 0.66, and HUM: 0.02. The decomposition rate constants are corrected by a rate modifying factor for temperature (a), the topsoil moisture deficit rate modifying factor (b), and the soil cover factor (c). The model apportions plant litter input between DPM and RPM depending upon the vegetation type (1.44 for grassland and 0.67 for shrubland). Both DPM and RPM decompose to form CO<sub>2</sub>, BIO and HUM. The proportion that goes to CO<sub>2</sub> and to BIO and HUM is determined by the clay content of the soil. The BIO and HUM is then split into 46% BIO and 54% HUM. BIO and HUM both decompose to form more CO<sub>2</sub>, BIO and HUM.

The meteorological data used in the modeling exercise (average monthly mean temperature, precipitation, and evapotranspiration) were obtained by the Local Climate Estimator (New LocClim 1.10, Grieser 2006) and are presented in Table 2.2. Soil thickness was set to 10 cm. The set-aside fields were covered the whole year by grass (IA) and shrubs (GR).

**Table 2.2 Mean monthly meteorological data used for the application of the RothC model in the two sites (taken from the Local Climate Estimator-New LocClim 1.10, Grieser, 2006).**

	IA (Iowa, USA)			GR (Crete, Greece)		
	TEMP	PREC	PET	TEMP	PREC	PET
January	-6	25	22	11	142	51
February	-4	24	27	11	112	57
March	3	60	55	13	81	80
April	11	94	96	16	32	112
May	17	103	133	20	13	159
June	22	115	160	24	5	203
July	25	125	165	26	1	222
August	23	112	143	26	2	199
September	19	99	108	23	19	142
October	13	72	82	19	80	94
November	5	54	45	16	73	64
December	-3	40	25	13	94	55
<b>Annual</b>	10	923	1060	18	652	1437

### *Initialization/Calibration*

The measured SOC and POC contents (Table 2.7), derived by the applied physical fractionation scheme were used to estimate initial carbon pools (croplands) and calibrate (set-aside fields) the model, since the particulate organic carbon (carbon content of the fraction >50  $\mu\text{m}$ ) has been associated with the RPM and DPM pool of RothC (Galdo et al., 2003; Krull et al., 2005; Gottschalk et al., 2010). Initial SOC was partitioned among the different carbon pools (RPM, DPM, BIO, IOM and HUM) using the following approach. The POC corresponds to the sum of RPM and DPM fractions and was apportioned by calibration. Following RothC model recommendations, BIO was assumed to be 3% of the total SOC and IOM was estimated by using the equation suggested by Falloon et al. (1998):  $\text{IOM} = 0.049 \cdot \text{SOC}^{1.139}$ . For the estimation of IOM content, the set-aside SOC content was used since the inert carbon it is not usually considered to change significantly because of cultivation in a few decades. However, due to the uncertainty of this assumption in the uncertainty analysis the range of the IOM pool is from zero to the value taken by Falloon's equation. Finally, the HUM pool was calculated by difference of the other pools from the total SOC.

The developed excel version of the RothC model was used in combination with @RISK (PALISADES Corp.) in order to simulate the uncertainty in carbon turnover during set-aside conditions due to initial conditions, model parameters, and inputs. First, RothC/@RISK was used in a Monte-Carlo fashion in order to identify the optimal/unique solution of model parameters and input that best simulates each soil. Plant litter input and six model parameters were considered simultaneously with uniform distributions (Table 2.8). Since the plant litter had not been measured, the appropriate range found in the literature for the specific climate and landuse was used to constrain the model. The carbon input of plant residues for the set-aside field in Iowa (grassland) was the sum of average values for the above and below-ground (0-15 cm) potential input for recently restored grasslands in south central Iowa as 5 to 10 t C/ha (Guzman et al., 2010); while within this range has been also found the maximum litter residue (7.59 t C/ha) in prairies in central Missouri (Buyanovsky et al., 1987).

Beier et al. (2009) found in six shrublands across Europe that plant litter ranged from 1.0 to 5.3 t C/ha for the 0-20 cm soil depth and above ground litter contributed 14.7% to 62.3% (0.33 to 1.43 t C/ha). If it is assumed that 80% of the belowground litter was found in the 0-10 cm, which was the main rooting depth in all six sites as it is indicated in the study, the

plant litter should range from 1 to 4.5 t C/ha. Similar values for litterfall in Mediterranean shrublands (0.65-1.45 t C/ha, assuming that carbon content of litterfall biomass is 50%, as it is indicated by the study) were reported by Fioretto et al. (2003). An initial range based on the values that have been reported in the literature was introduced for the RPM (0.1 to 0.8 1/y) and HUM (0.0001 to 0.3 1/y) decomposition rate constants. For the remaining model parameters (DPM and BIO decomposition rate constants, DPM-to-RPM ratio, and BIO%, the range was established as  $\pm 10\%$  of their default RothC values.

Monte-Carlo simulations with 5000 iterations were conducted using the distributions of the plant input and the six model parameters described above. The simulation run was for the 20 and 35 years in Iowa and Greece, respectively, since during these years the SOC content of the set-aside fields was measured and used for calibration. The solution producing the best fit between the measured (the measured values of the set-aside fields) and modeled SOC and POC data was considered as the optimum solution and the values of the parameters that generated the solution as the calibrated values. The ensemble of solutions falling within the  $\pm 5\%$  of the SOC and POC measured values was also examined in order to confirm the uniqueness of the optimum solution. The standard uncertainty of the mean SOC and POC measured value corresponds to the assumption of normal distribution with coefficient variation 7% (Zhang et al., 2011), where the 90% confidence interval would be 5.1% (considering  $n=5$  for soil samples). We acknowledge that due to limited data (one composite sample of five subsamples) in this study the 5% is set arbitrarily. However with this 5%, we aim to correspond to the 90% confidence interval of the mean, for the described assumptions. The initial range of plant input as well RPM and HUM decomposition rate constants was narrowed (Table 2.8), so as more iterations to pass the criterion and calculate better statistics. The low standard deviations of the plant input and six model parameters of the selected solutions suggest the uniqueness of the optimum solution.

### *Sensitivity Analysis*

Once the model was calibrated, sensitivity analysis was performed with respect to the change of the SOC content the 20<sup>th</sup> and 35<sup>th</sup> year after the conversion of croplands to set-aside fields in Iowa and Greece, respectively. The six model parameters (DPM, RPM, BIO, and HUM decomposition rate constants, DPM-to-RPM ratio, HUM%) and the plant litter input were varied  $\pm 10\%$  and  $\pm 50\%$  from the calibrated values.

### *Uncertainty Analysis*

Finally, the propagation of uncertainty in the simulated results due to initial conditions (SOC, DPM, RPM, BIO, HUM, and IOM carbon pools), plant litter input and soil clay content, as well the six model parameters used for calibration was conducted for each category separately and all together. The simulation run was for 100 years for both sites. The distribution for each parameter derived from the Monte-Carlo simulation for the iterations falling within the  $\pm 5\%$  of the SOC and POC field measured values was used in the uncertainty analysis. Field variability for initial conditions and clay content could not be estimated since soil samples were only one composite of five subsamples. To address this issue, the distribution was selected to be normal having as mean the measured value and a standard deviation of 5% of the mean. The uncertainty of the IOM pool was considered to be a uniform distribution ranging from zero to the value obtained by Falloon's equation. The HUM pool was calculated by difference.

## **2.3 RESULTS AND DISCUSSION**

### **2.3.1 Soil Characterization**

#### *Bulk soil physicochemical characteristics*

The basic physicochemical soil measurements are presented in Table 2.3. The pH of the set-aside IA soil was almost neutral (6.9), while the cropland soil pH was acidic due to fertilization (6.2). The pH of both Greek soils was basic (7.7-7.8) reflecting the calcareous composition of the soils. Potential mineralizable N (PMN), potential soluble organic N and C (PSON and PSOC), as well carbohydrate C increased in the set-aside soils by a factor of 4.9, 3.5, 2.9, and 2.7 for Iowa and only 1-1.5 times for Greece.

Set-aside from crop production in Iowa and Greek soils for 20 and 35 years, respectively, as it was indicated by the field measurements resulted in similar rates of C increase (0.777 and 0.648 t C/ha y) in topsoil (10 cm), while the N increase was doubled for Iowa as compared with Greece (0.048 and 0.019 t N/ha y). The measured increase of SOC was accompanied by 16% and 6% decrease of soil bulk density for IA and GR, respectively. Subsoil carbon density

in set-aside and cropland fields in the Iowa site (Table 2.3) was found to differ only by about 2%, verifying the assumption that most of the SOC gain found in the topsoil where the dense root system is found (Potter and Derner, 2006).

**Table 2.3 Chemical and physical properties of IA and GR soils.**

	IA (Iowa, USA)		GR (Crete, Greece)	
	Cropland IA	Set-aside IA	Cropland GR	Set-aside GR
<b>Bulk Density (kg/m<sup>3</sup>)</b>	1110/1217 <sup>a</sup>	930/1024 <sup>a</sup>	1180	1110
<b>pH</b>	6.2	6.9	7.8	7.7
<b>Sand (%)</b>	38	63	30.1	27.4
<b>Clay (%)</b>	7	7	30	30
<b>SOC<sup>b</sup> (%) – BS<sup>c</sup>/AF<sup>d</sup>/Subsoil</b>	1.70/1.68/1.59	3.70/3.55/1.85	2.94/2.90	5.17/5.27
<b>TN (%) - BS/AF/Subsoil</b>	0.14/0.14/0.11	0.27/0.26/0.17	0.24/0.22	0.32/0.31
<b>C-to-N - BS/AF</b>	11.7/11.7	13.6/13.8	12.3/12.9	16.4/16.9
<b>Recovery (%) - AF: OC/TKN</b>	98.5/98.5	95.9/94.3	98.6/93.5	102/99.3
<b>PMN (mg N/kg<sup>-1</sup>)</b>	15.8	78.3	31.2	43.9
<b>PSON (mg N/kg<sup>-1</sup>)</b>	21.4	74.4	23.5	36.0
<b>PSOC (mg C/kg<sup>-1</sup>)</b>	132.7	390.7	228.9	360.8
<b>Carbohydrates /mg C/kg<sup>-1</sup>)</b>	45.1	123.1	42.0	42.3

<sup>a</sup> For the 10-30 cm subsoil.

<sup>b</sup> The Set-aside and cropland GR exhibited 0.98% and 0.17% inorganic carbon content, respectively, while the rest lower than 0.03%.

<sup>c</sup> BS: Bulk Soil

<sup>d</sup> AF: Aggregate Fractionation.

Accounting also for the subsoil (0-30 cm), the increase for the Iowa soil was found to be similar for C (0.736 t C/ha y; 0-30 cm), being however double for nitrogen (0.088 t N/ha y; 0-30 cm). The rates were similar with values for arable to grasslands conversions reported for French sites (0.48±0.26 t C/ha y) (Soussana et al., 2004) as well sites in the UK (0.3 to 0.8 t C/ha y) (Ostle et al., 2009). The C-to-N ratio was lower in croplands compared to set-aside fields, likely indicating less stabilized organic matter. The increase of the C-to-N ratio in set-aside fields was found to be higher in Greece compared to Iowa, indicating the effect of the plant litter material quality (shrubland in Greece versus grassland in Iowa) and possibly less decomposed organic matter.

### *Water stable aggregates, C/N distribution, C/N fraction concentration, and FTIR spectra*

The distribution of the (sand-free) WSA for the four soils is given in Table 2a and Figure 2.3a. The procedure for the water stable aggregates (WSA) isolation yielded that aggregate recovery was higher than 90% for the four soils (Table 2.4). The total WSA were found to be higher in set-aside fields by 68% (IA) and 10% (GR) compared to croplands. The increase of WSA weight and stability in set-aside soils was primarily attributed to large and medium sized macro-aggregate. At the same time, decline was observed in the microaggregate and the silt-clay sized fraction. The shift in composition to larger aggregates was very significant in the Iowa set-aside soil, where macro-aggregates (>250  $\mu\text{m}$ ) increased by 110% comprising 82% of soil composition compared to cropland where they were 39%. In Greece, the increase was smaller (43%) and macro-aggregates (>250  $\mu\text{m}$ ) comprised 66% in the set-aside soil. At the same time, decline was observed in the micro-aggregate (53-250  $\mu\text{m}$ ) and the silt-clay sized fractions (<53  $\mu\text{m}$ ). The shift in composition to larger aggregates was very significant in the Iowa set-aside soil; macro-aggregates (>250  $\mu\text{m}$ ) increased from 39% to 82% of soil composition (Table 2.4). In Greece, the increase was smaller (43%) and macro-aggregates comprised 66% in the set-aside soil. The shift in composition to larger aggregates caused an increase in the MWD by 108% (IA) and 52.5% (GR) in Iowa and Greece, respectively. The C and N content in the various aggregate fractions is presented in Table 2.4 and Figures 2.3b and 2.3c. Soil C in IA cropland was 16.8 g/kg with 60% in macro-aggregate fraction, while in IA set-aside was 35.5 g/kg with 90% in macro-aggregate fraction. Similarly, soil C in GR cropland was 29.1 g/kg with 58% in macro-aggregate fraction, while in GR set-aside was 52.8 g/kg with 71% in macro-aggregate fraction. Similar patterns were also observed for N.

The C and N concentration increased up to 2 times in the aggregate fractions in the Greek set-aside soil compared to cropland (Figure 2.4). Similarly, Bongiovanni et al. (2006) found small macro-aggregates and micro-aggregates in croplands converted from forested lands to have 2 times lower C concentrations. The C and N and particularly the C content of the easily dispersed silt-clay sized fraction (sc-M) and the micro-aggregate related silt-clay fraction (sc-mM) in the Greek set-aside soil were found to be significantly higher compared to the respective concentrations of cropland (Figure 2.5). The increase of C and N concentration in macro-aggregates was attributed both to particulate organic matter and mineral related organic matter. The POC contribution in the carbon content of the composite macro-aggregate fraction was 44 and 51% in set-aside and cropland field and 38 and 34% in the 250-1000  $\mu\text{m}$  fraction (Figure 2.6).

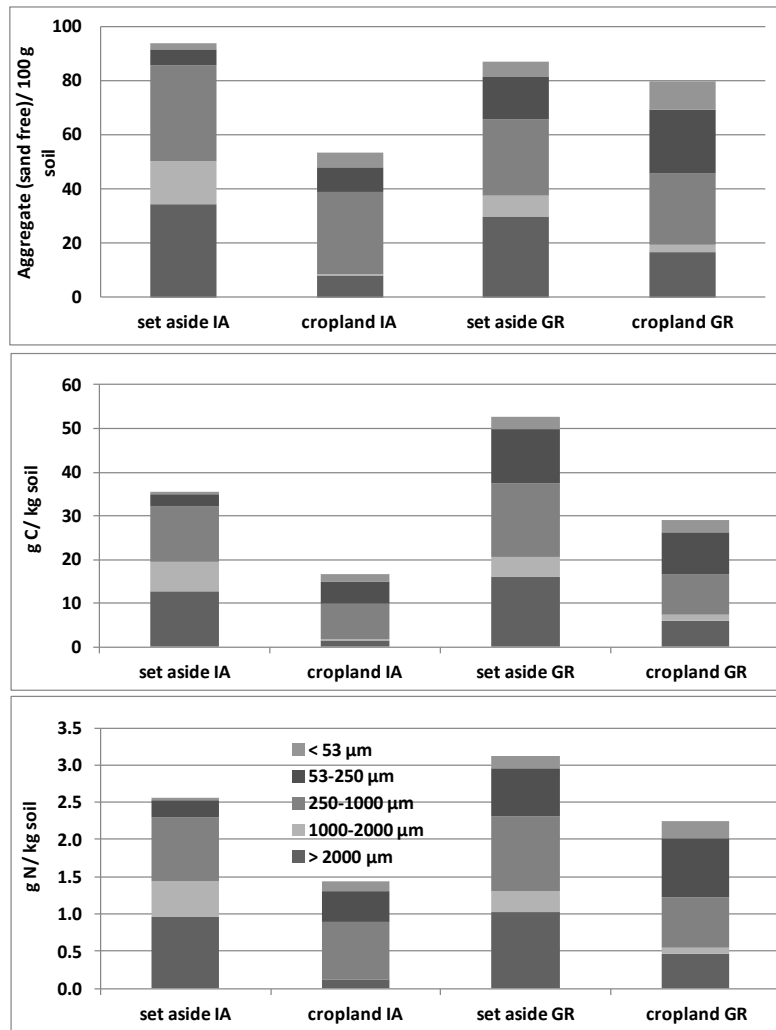


Figure 2.3 a) Soil water stable (sand free) aggregate distribution, b) C distribution among aggregates fractions, and c) N distribution among aggregates fractions.

Table 2.4 Soil water stable aggregate distribution (WSA, g sand-free aggregate/100 g soil), particle recovery, and mean weight diameter (MWD) as well C and N distribution among aggregates fractions (g/kg). Values are shown as means and standard deviation is given in brackets (n=3). Mean values followed by the same lowercase letter within the same column are not significantly different at P<0.05). Mean values followed by the same uppercase letter within the same row are not significantly different at P<0.05).

	Cropland IA			Set-aside IA			Cropland GR			Set-aside GR		
	WSA	C	N	WSA	C	N	WSA	C	N	WSA	C	N
> 2000 $\mu\text{m}$	8.2 (4.8)b, C	1.5	0.11	34.6 (3.3)a, A	12.8	0.96	16.6 (1.1)b, B	6.0	0.46	29.6 (5.8)a, A	16.1	1.03
1000-2000 $\mu\text{m}$	0.4 (0.04)c, D	0.2	0.01	15.7 (2.5)b, A	6.5	0.47	2.9 (0.5)d, C	1.4	0.09	8.1 (1.6)c, B	4.5	0.27
250-1000 $\mu\text{m}$	30.2 (4.4)a, AB	8.3	0.77	31.4 (2.4)a, A	12.7	0.87	26.5 (1.8)a, B	9.3	0.67	27.9 (2.4)a, AB	16.8	1.00
53-250 $\mu\text{m}$	9.4 (2.4)b, C	5.1	0.41	5.9 (0.4)c, C	3.0	0.22	23.7 (0.6)a, A	9.5	0.78	15.9 (2.8)b, B	12.6	0.65
< 53 $\mu\text{m}$	5.3 (1.1)b, B	1.7	0.13	2.2 (0.3)d, C	0.5	0.04	10.1 (0.7)c, A	2.9	0.24	5.6 (0.7)c, B	2.8	0.17
Recovery (%)	94.5 (1.0)			93.1 (1.6)			91.5 (1.5)			94.6 (3.6)		
WSA	53.4 (1.8) B			89.8 (0.19) A			79.6 (0.4) C			87.2 (2.0) A		
WSA (>250 $\mu\text{m}$ )	38.7 (4.0) B			81.7 (0.10) A			45.8 (1.5) D			65.5 (5.3) C		
MWD (mm)	1.16 (0.51) B			2.42 (0.24) A			1.36 (0.09) B			2.07 (0.38) A		

In Iowa set-aside soil increase of C and N concentration was observed only in macro-aggregates while in finer aggregates presented lower concentration (Figure 2.4). The latter has been also observed by Emadi et al. (2009). The micro-aggregate isolation confirmed that all the mineral fractions in Iowa set-aside field exhibited lower concentrations compared to the cropland (Figure 2.5). Don et al. (2009) also found that the conversion of cropland into grassland in a soil with very low clay content (5-7%) in contrast with a rich in clay soil (30%) did not result in the increase of the mineral-associated carbon fraction as it was limited by total clay surface area available for carbon stabilization. The increase of C and N concentration in macro-aggregates was attributed to POM. The C content of the composite and the 250-1000  $\mu\text{m}$  aggregate fraction attributed to POM in the Iowa cropland was 19% and 23%, respectively and changed to 63% and 50% in the set-aside field (Figure 2.6).

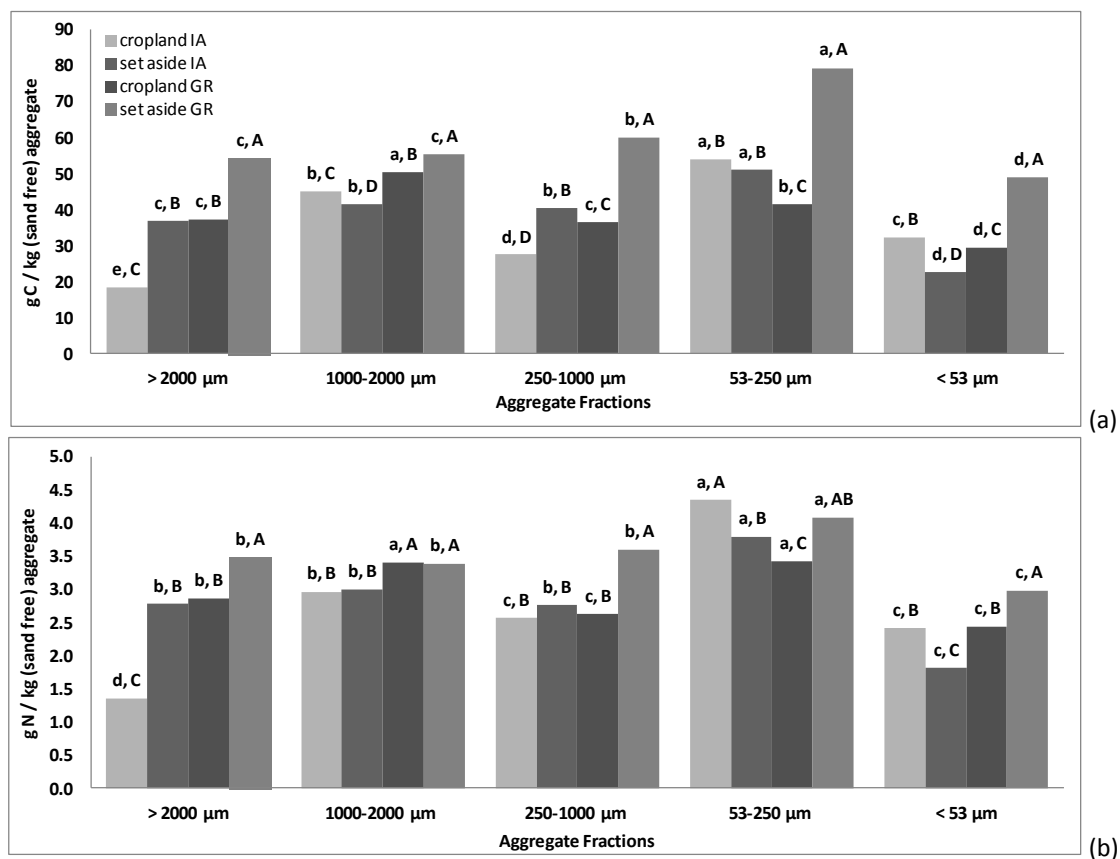


Figure 2.4 a) C and b) N concentration of the sand free aggregate fractions ( $\text{g kg}^{-1}$ ). Values are shown as means ( $n=3$ ). Standard deviation was lower than 1-3% for OC and 1-4% for N. Mean values followed by the same lowercase letter under the same series label are not significantly different ( $p<0.05$ ). Mean values followed by the same uppercase letter under the same x-axis legend are not significantly different ( $p<0.05$ ).

The C-to-N ratio increased in aggregate fractions of set-aside soils and the relative increase was found to be higher in Greece compared to Iowa, in accordance with the bulk soil measurements. More labile organic matter indicated by higher C-to-N ratio (Elliot, 1986) was found in macro-aggregates, attributed to the increase of C-to-N ratio of the particulate organic matter fractions in Iowa and both particulate and mineral associated carbon fractions in Greece.

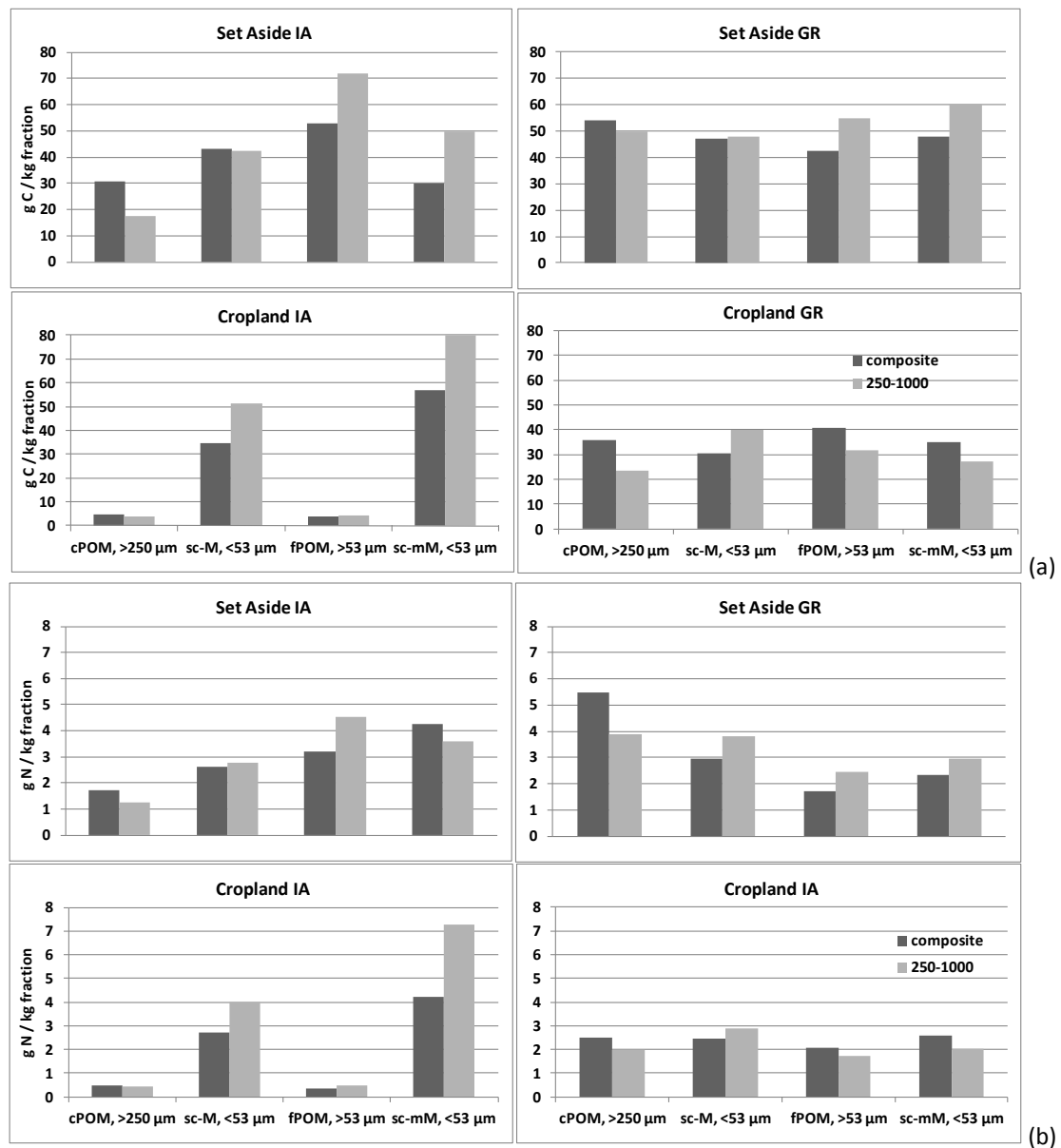
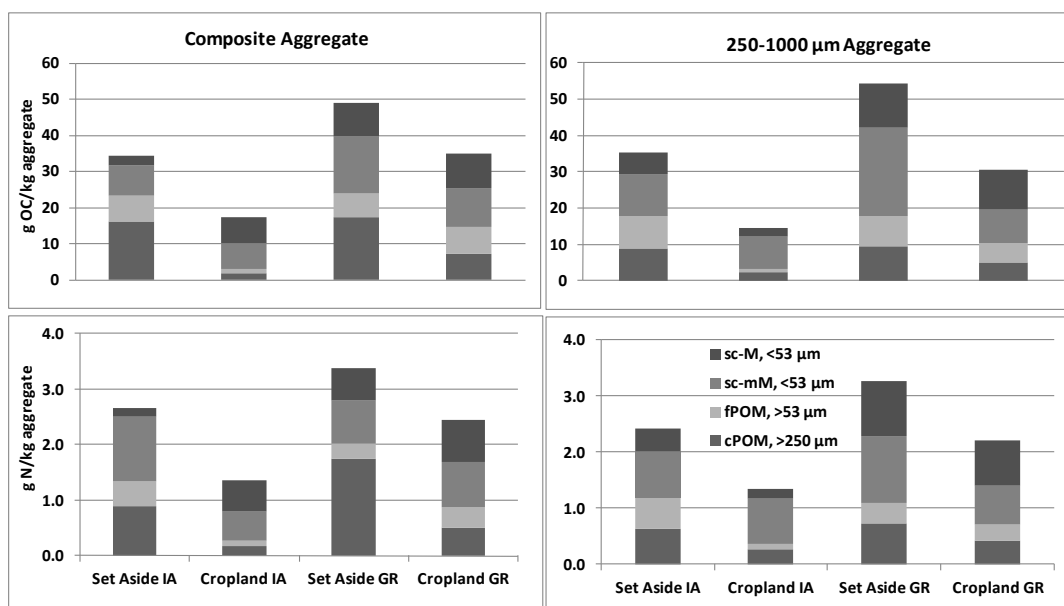


Figure 2.5 a) Carbon and b) Nitrogen concentration in fractions (related with particulate organic matter and the minerals) of composite microaggregates (>250 μm) and small macroaggregates (250-1000 μm).



**Figure 2.6 Carbon and Nitrogen distribution among the fractions of composite microaggregates (>250 μm) and small macroaggregates (250-1000 μm).**

FTIR spectra in accordance with the micro-aggregate isolation procedure revealed the changes of the C and N composition of macro-aggregates due to landuse changes. The FTIR spectra taken for the aggregate fractions indicated changes in the composition of the aggregates. The mean relative absorbance of FTIR spectra at 1630 1/cm (aromatic C=C structural vibrations, antisymmetrical stretching of C-O in COO<sup>-</sup> groups, conjugated carbonyl C=O of amide) could be indicative of plant derived material (Table 2.5). Therefore, POC seemed to increase in all aggregate fractions in GR set-aside field compared to cropland, but only in macro-aggregates in IA set-aside field. However, the relative increase was shown to be higher in the IA soil. The mean relative absorbance at 1630 1/cm was linear correlated with the aggregates C and N concentrations and the C-to-N ratio for Iowa soils ( $R^2 = 0.81, 0.80, \text{ and } 0.41,$ ), while for the Greek soils the correlation was very low. A possible explanation could be the different content of the Greek aggregate fractions in carbonates.

**Table 2.5 The relative absorbance of FTIR spectra at 1630 (1/cm).**

	cropland IA	set-aside IA	cropland GR	set-aside GR
>2000 μm	3.32 (0.04)	4.50 (0.06)	4.31 (0.23)	4.96 (0.25)
1000-2000 μm	ND	4.85 (0.16)	3.91 (0.09)	4.07 (0.07)
250-1000 μm	3.11 (0.10)	4.56 (0.08)	4.06 (0.33)	4.01 (0.06)
53-250 μm	3.92 (0.14)	3.76 (0.09)	4.10 (0.29)	4.12 (0.12)
<53 μm	4.31 (0.16)	4.21 (0.09)	4.08 (0.26)	4.28 (0.11)

ND: not determined due to sample shortage.

As the size and stability of water stable aggregates decreases, their turnover rate has been found to increase (Six et al., 2000). The ratio of the fPOC to cPOC has been suggested (Six et al., 2000) as an indication of turnover rate (the higher the ratio, the lower the turnover rate). The fPOC to cPOC ratio of the composite macro-aggregates (IA: 7.9, GR: 6.4) and the small macro-aggregates (IA: 9.5, GR: 7.5) in cropland soils is lower as compared with set-aside fields (composite macro-aggregates IA: 10, GR: 13.2 and small macro-aggregates IA: 23.4, GR: 10.2) (Table 2.6). Therefore the turnover rate is higher in croplands due to tillage and plant litter input quality (Sainju et al., 2003). In addition, the estimated turnover rates in Iowa are significantly lower for the small macro-aggregates compared with the composite macro-aggregates suggesting in accordance with the lower C-to-N ratio in the 250-1000  $\mu\text{m}$  fraction more decomposed and older particulate organic matter. On the contrary, this pattern was not observed in Greece, where C-to-N ratio was high even in micro-aggregates, indicating possible lower decomposition rates.

**Table 2.6 Ratio of fPOC-to-cPOC concentration.**

	<b>Cropland</b>	<b>Set-aside</b>	<b>Cropland</b>	<b>Set-aside</b>
	<i>Composite macro-aggregates</i>		<i>250-1000 <math>\mu\text{m}</math> macro-aggregates</i>	
<b>IA</b>	7.9	10.0	9.5	23.4
<b>GR</b>	6.4	13.2	7.5	10.2

### **2.3.2 Carbon turnover modeling**

The RothC model was initialized with the cropland soil data and calibrated with the soil data of the set-aside field to simulate the carbon turnover during cropland to set-aside from crop production conversion in Iowa (grassland) and Greece (shrubland). The clay content for the IA soil was 7% (Table 2.3), the initial SOC 18.6 t C/ha and the initial POC 2.6 t C/ha (Table 2.7). The initial carbon apportioning for the Iowa soil procedure was 1.94 t C/ha for RPM, 0.68 t C/ha for DPM, 0.56 t C/ha for BIO, 12.78 t C/ha for HUM, and 2.63 t C/ha for IOM. The simulation results were compared with the results presented in Table 2.7 for the set-aside field (SOC = 33 t C/ha, POC = 20 t C/ha). The clay content for the GR soil was 30% (Table 2.3), the initial SOC 34.3 t C/ha and the initial POC 14.3 t C/ha (Table 2.7) in the cropland. The initial carbon apportioning for the Greek soil procedure was 14 t C/ha for RPM, 0.3 t C/ha for DPM, 1.03 t C/ha for BIO, 13.89 t C/ha for HUM, and 5.05 t C/ha for IOM. The simulation

results were compared with the results presented in Table 2.7 for the set-aside field (SOC = 58.5 t C/ha, POC = 21.8 t C/ha).

**Table 2.7 Distribution of C and N in the particulate organic matter (POM) and in the silt-clay fractions.**

	Total	POM-fractions	Silt-clay fractions
<b>Carbon (t/ha)</b>			
Cropland IA	18.6 <sup>a</sup>	2.6 <sup>b</sup>	16.0
Set-aside IA	33.0 <sup>a</sup>	20.0 <sup>b</sup>	13.0
Cropland GR	34.3 <sup>a</sup>	14.3 <sup>b</sup>	20.6
Set-aside GR	58.5 <sup>a</sup>	21.8 <sup>b</sup>	36.8
<b>Nitrogen (t/ha)</b>			
Cropland IA	1.6	0.2	1.3
Set-aside IA	2.4	1.2	1.2
Cropland GR	2.6	0.8	1.9
Set-aside GR	3.5	1.7	1.8

<sup>a</sup>SOC values

<sup>b</sup>POC values

The results of the Monte-Carlo simulations are presented in Table 2.8. input distributions were used for the plant litter input and model parameters were. The optimum solution was used in order to obtain the calibrated model results (Table 2.8). The predicted SOC and POC values (Figure 2.7) were deviated from the field measured values lower than 0.7% and 0.3 % in Iowa and Greece respectively. The calibrated values for Iowa were 5.05 t C/ha for plant litter input and 0.34 1/y for RPM and 0.27 1/y for HUM, while for Greece were 3.79 t C/ha for plant litter input and 0.21 1/y for RPM and 0.0041 1/y for HUM.

The statistics of the ensemble of simulations that fall within  $\pm 5\%$  of both SOC and POC measurements are also presented in Table 2.8. The distribution type in most of the parameters was found to be triangular and some of them uniform and beta general. The standard deviation was found to be less than 10% of the mean value for all parameters apart from the RPM decomposition rate constant where it was 13.9%, in the case of Iowa. Similarly, in Greece, the standard deviation was found to be less than 10% of the mean value for all parameters except for the RPM and HUM decomposition rate constants for which it was 10.6% and 58.1%, respectively. The narrow values of the resulted standard deviations confirm the uniqueness of optimum solution since they represent a well constrained system that does not allow acceptable solutions with extreme parameter value combinations.

**Table 2.8 Parameter information about the input and output distributions for the Monte-Carlo simulation and the optimum solutions.**

Parameter	total plant input	DPM/RPM ratio	BIO% <sup>a</sup>	DPM <sup>b</sup>	RPM <sup>b</sup>	BIO <sup>b</sup>	HUM <sup>b</sup>
<b>RothC default values</b>	input	1.44 (grassland) 0.67 (shubland)	46	10	0.3	0.66	0.02
<b>IOWA</b>							
<b>Input of MonteCarlo simulation</b>							
<b>distribution type</b>	Uniform	Uniform	Uniform	Uniform	Uniform	Uniform	Uniform
<b>min</b>	5.00	1.30	41.40	9.00	0.30	0.59	0.10
<b>max</b>	10.00	1.58	50.60	11.00	0.80	0.73	0.30
<b>Statistics for the iterations passed the criterion<sup>c</sup></b>							
<b>distribution type</b>	Triang	BetaGeneral	Triang	Triang	Triang	Triang	Triang
<b>min</b>	5.01	1.32	41.47	8.66	0.32	0.59	0.22
<b>max</b>	6.47	1.58	49.84	10.99	0.56	0.72	0.30
<b>mean</b>	5.50	1.44	47.05	10.21	0.40	0.68	0.27
<b>std</b>	0.35	0.09	1.97	0.55	0.06	0.03	0.02
<b>Chi-sq</b>	0.43	6.24	2.43	0.90	1.29	1.29	2.43
<b>Optimum solution</b>	<b>5.05</b>	<b>1.51</b>	<b>48.90</b>	<b>10.37</b>	<b>0.34</b>	<b>0.69</b>	<b>0.27</b>
<b>GREECE</b>							
<b>Input of MonteCarlo simulation</b>							
<b>distribution type</b>	Uniform	Uniform	Uniform	Uniform	Uniform	Uniform	Uniform
<b>min</b>	2.00	0.60	41.40	9.00	0.10	0.59	0.0001
<b>max</b>	4.50	0.74	50.60	11.00	0.30	0.73	0.04
<b>Statistics for the iterations passed the criterion<sup>c</sup></b>							
<b>distribution type</b>	Triang	BetaGeneral	Triang	Uniform	BetaGeneral	Uniform	Triang
<b>min</b>	2.95	0.60	41.41	8.99	0.14	0.59	0.0000
<b>max</b>	4.49	0.73	50.64	10.97	0.26	0.72	0.0241
<b>mean</b>	3.98	0.67	46.03	9.98	0.22	0.66	0.0122
<b>std</b>	0.36	0.04	2.66	0.57	0.02	0.04	0.0071
<b>Chi-sq</b>	7.44	9.26	10.69	3.36	3.81	6.76	2.00
<b>Optimum solution</b>	<b>3.79</b>	<b>0.67</b>	<b>44.95</b>	<b>10.45</b>	<b>0.21</b>	<b>0.60</b>	<b>0.0041</b>

<sup>a</sup>The proportion that goes to BIO (100-BIO% is the proportion that goes to HUM)

<sup>b</sup>The respective decomposition rate constants

<sup>c</sup>Statistics for the iterations passing the criterion of SOC and POC falling within the  $\pm 5\%$  of the field measured values.

For Iowa, the ‘adjusted’ model was able to capture the increase of POC and SOC content very well, which was likely attributed to POC material (Figure 2.7). Monthly decomposition rates for RPM and HUM pools for both sites are presented in Table 2.9. The annual decomposition rate (decomposition rates constants multiplied by the rate modifying factor for temperature, topsoil moisture deficit, and soil cover) for RPM was found to be 0.093 1/y and 0.105 1/y for Iowa and Greece, respectively, while for HUM was 0.075 1/y and 0.002 1/y, likewise. The high decomposition rate of the HUM pool in Iowa could be attributed to the very low clay content in accordance with Balesdent et al. (1998) and Gottschalk et al. (2010). Balesdent et al. (1998) showed that SOC in the size fraction <50 µm is made up of the relatively rapidly decomposing pool of silt associated C, and a relatively slowly decomposing pool of clay associated C. The clay associated C had a decomposition rate of 0.03 1/y (Balesdent et al., 1998), while the silt associated C had a measured decomposition rate of 0.12 1/y, declining almost as rapidly as that in the POC fraction, especially under cultivation (Gottschalk et al., 2010). Nevertheless, the wet and warm summers in Iowa stimulated organic matter decomposition.

**Table 2.9 Monthly and annual decomposition rates<sup>a</sup> (1/y) for resistant plant material (RPM) and humus (HUM) soil organic pools of ROTHC model for the Greek and Iowa sites.**

	IA (Iowa, USA)		GR (Crete, Greece)	
	RPM	HUM	RPM	HUM
<b>January</b>	0.001	0.001	0.152	0.003
<b>February</b>	0.008	0.006	0.157	0.003
<b>March</b>	0.073	0.059	0.039	0.001
<b>April</b>	0.248	0.201	0.051	0.001
<b>May</b>	0.093	0.075	0.070	0.001
<b>June</b>	0.132	0.107	0.091	0.002
<b>July</b>	0.151	0.123	0.101	0.002
<b>August</b>	0.140	0.114	0.098	0.002
<b>September</b>	0.105	0.085	0.085	0.002
<b>October</b>	0.061	0.049	0.066	0.001
<b>November</b>	0.092	0.075	0.161	0.003
<b>December</b>	0.008	0.007	0.186	0.004
<b>Annual</b>	0.093	0.075	0.105	0.002

<sup>a</sup>Decomposition rates constant multiplied by the rate modifying factor for temperature (a), the topsoil moisture deficit rate modifying factor (b), and the soil cover factor (c).

Similarly, in Greece, the ‘adjusted’ model was able to capture the increase of POC, HUM and SOC content, and the results were consistent with the fractionation measurements where

the increase in carbon stock was attributed to both POC and HUM material (Figure 2.7). Lower HUM decomposition rate in Greece is attributed to dry climatic conditions and high clay content which result in higher protection. Slaking of the soil surface can result in fine soil particles moving into inter-aggregate pores in the surface area, which can reduce the infiltration rate of rainfall or irrigation water and reduce hydraulic conductivity (Hillel, 1998). In addition, residue quality (lignin/N ratio, C/N ratio and N concentration) of shrublands affects the rate of decomposition and the aggregation rate (Aerts, 1997; Sainju et al., 2003).

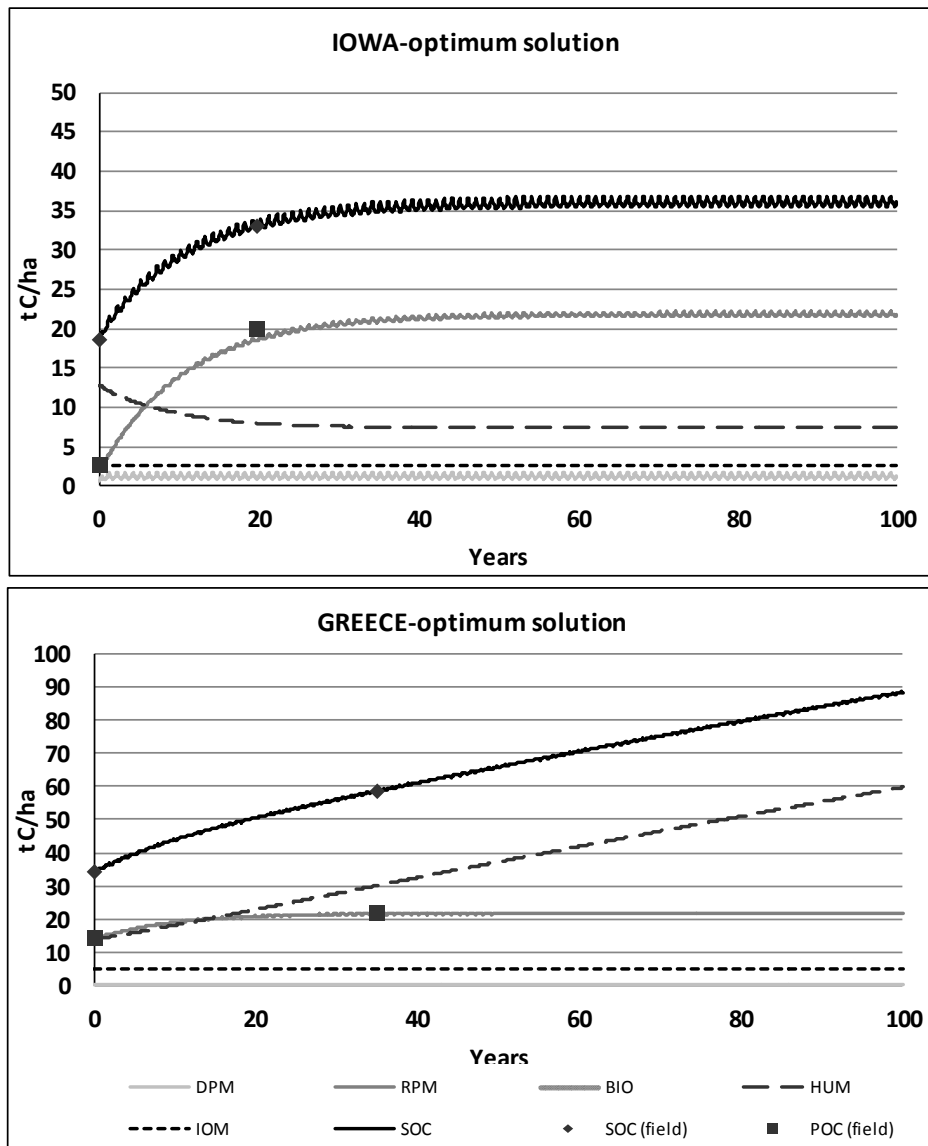


Figure 2.7 RothC simulation results under optimum solution for Iowa and Greece (carbon pools: RPM=resistant plant material, DPM=decomposable plant material, HUM=humus, BIO= biomass, IOM= inert organic matter, SOC= soil organic carbon, POC particulate organic carbon). DPM in both graphs is very low and coincides with the x-axis.

Sensitivity analysis with respect to the change of the SOC content in the field measured set-aside fields (the 20<sup>th</sup> and the 35<sup>th</sup> year of the simulation in Iowa and Greece, respectively) at the  $\pm 10\%$  and  $\pm 50\%$  ranges of the calibrated values for the six model parameters and the plant input was conducted. The tornado graphs are presented in Figure 2.8 and the sensitivity coefficients (the absolute value of the ratio:  $(\Delta Y/Y)/(\Delta x/x)$ , where Y is the SOC content and x the parameter value) in Table 2.10. In both sites the total plant litter input and the RPM decomposition rate constant had the highest sensitivity. In Iowa, the BIO% as well as the BIO and DPM decomposition rate constants presented the lowest sensitivity with coefficients lower than 0.1 and 0.07 for the 50% and 10% case, respectively. In Greece, the coefficients were found to be in general lower than 0.04 for HUM, BIO and DPM decomposition rate constants for both the 50% and 10%. The results emphasize the importance of measurement of plant litter input when conducting carbon sequestration studies as well as the necessity of developing a methodology to model carbon sequestration in soils in the absence of such measurements.

**Table 2.10 Sensitivity coefficients (the absolute value of the ratio:  $(\Delta Y/Y)/(\Delta x/x)$ , where Y is the SOC content and x the parameter value) at the  $\pm 10\%$  and  $\pm 50\%$  ranges of the RothC calibrated values for the six model parameters and plant input. Sensitivity analysis was conducted with respect to the change of the SOC content from the set-aside field measured values (the 20th and 35th years of the simulation in Iowa and Greece, respectively).**

parameter	IA (Iowa, USA)				GR (Crete, Greece)			
	(-50%)	(+50%)	(-10%)	(+10%)	(-50%)	(+50%)	(-10%)	(+10%)
total plant input	0.802	0.802	0.802	0.802	0.649	0.649	0.649	0.649
RPM <sup>a</sup>	0.460	0.272	0.365	0.329	0.504	0.207	0.329	0.276
DPM/RPM ratio <sup>b</sup>	0.425	0.228	0.316	0.280	0.154	0.102	0.128	0.118
HUM <sup>c</sup>	0.270	0.153	0.211	0.189	0.023	0.022	0.023	0.022
BIO% <sup>d</sup>	0.064	0.066	0.065	0.065	0.175	0.193	0.182	0.186
BIO <sup>e</sup>	0.099	0.045	0.069	0.059	0.042	0.014	0.024	0.019
DPM <sup>f</sup>	0.058	0.018	0.031	0.025	0.008	0.003	0.005	0.004

<sup>a</sup>Resistant plant material decomposition rate constant

<sup>b</sup>The apportionment ratio of Plant litter input between decomposable plant material (DPM) and RPM

<sup>c</sup>Humus decomposition rate constant

<sup>d</sup>The proportion that goes to BIO (100-BIO% is the proportion that goes to HUM)

<sup>e</sup>Biomass decomposition rate constant

<sup>f</sup>Decomposable plant material decomposition rate constant

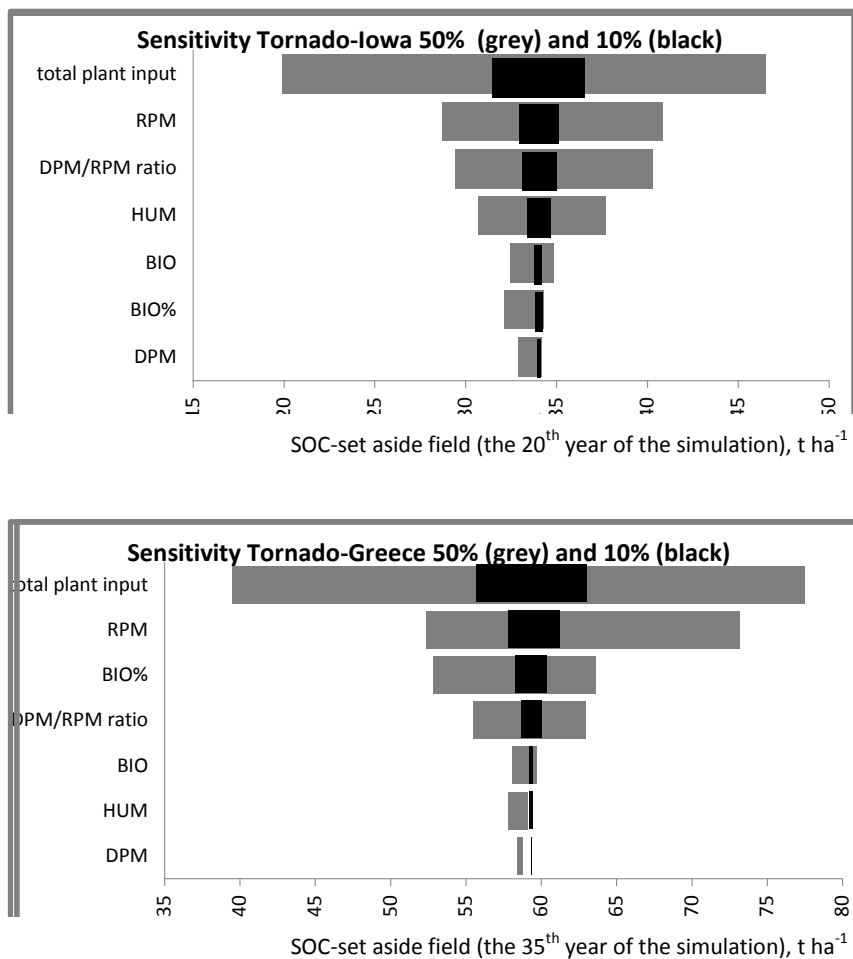


**Figure 2.8 Tornado Graphs for 10% (black indicated) and 50% (grey indicated) sensitivity analysis. RPM=resistant plant material decomposition rate constant, DPM=decomposable plant material decomposition rate constant, HUM=humus decomposition rate constant, BIO= biomass decomposition rate constant, DPM/RPM ratio=the apportionment ratio of plant litter input DPM and RPM carbon pools, BIO%=the proportion that goes to BIO (100-BIO% is the proportion that goes to HUM). The x-axis of the graphs corresponds to the model predicted SOC content (t C/ha) in the set-aside fields the 20<sup>th</sup> and 35<sup>th</sup> year of the simulation in Iowa and Greece respectively.**

Figure 2.9 presents a comparison of the optimum simulation for both SOC and POC and the uncertainties attributed to the initial conditions (SOC, DPM, RPM, BIO, HUM, and IOM carbon pools) the input data (plant litter input and clay content), and the six model parameters used for calibration parameters (DPM, RPM, BIO, and HUM decomposition rate constants, DPM-to-RPM ratio, HUM%), in terms of the mean of the ensemble of Monte Carlo simulations plus/minus one standard deviation. The model output distributions by the Monte-Carlo

simulations of SOC and POC content after 100 years of set-aside conditions due to total uncertainty are given in Figure 2.10. The simulated SOC and POC value by the optimum simulation is also indicated. The respective graphs corresponding to the uncertainty due to initial conditions, inputs and model parameter are given in Figure A2.1 in the appendix.

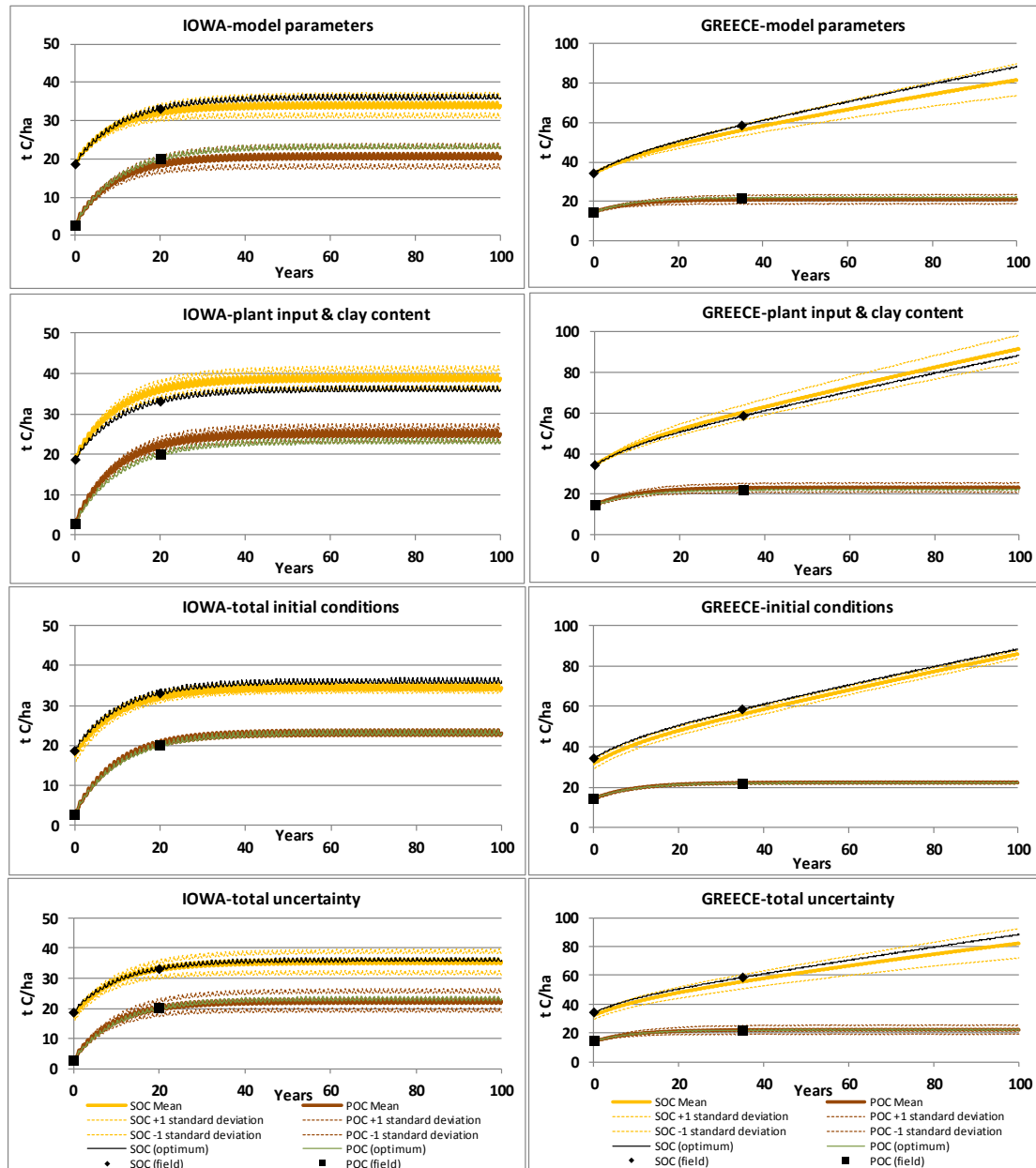


Figure 2.9 Uncertainty of soil organic carbon (SOC) and particulate organic carbon (POC) due to model parameters, input data, and initial conditions, as well as the total uncertainty, compared with the optimum solution (calibration).

In Iowa, the uncertainty of prediction (90% of the distribution, range between 5 and 95%) due to input data, model parameters, and initial conditions corresponded to 43.3%, 51%, and 14.3% of the total carbon sequestered in the 100 years, respectively and the probability of over predicting carbon sequestration was at the same order 0.94, 0.25, and 0, respectively. Similarly, the uncertainty of POC due to input data, model parameters, and initial conditions corresponded to 25.5%, 42.4%, and 0% of the total increase in POC in the 100 years, respectively and the probability of over predicting POC was 0.94, 0.21, and 1, respectively.

In Greece, the uncertainty of prediction due to input data, model parameters, and initial conditions corresponded to 42.1%, 49.5%, and 13% of the total carbon sequestered in the 100 years, respectively and the probability of over predicting carbon was 0.69, 0.24, and 0.12, respectively. Similarly, the uncertainty of POC due to input data, model parameters, and initial conditions corresponded to 90.5%, 102%, and 0% of the total increase in POC in the 100 years, respectively and the probability of over predicting POC was 0.7, 0.29, and 0. The Iowa soil was projected to sequester 17.5 t C/ha and the Greek soil 54 t C/ha in 100 years. Overall, the uncertainty of the model predictions for SOC and POC (65.6% and 140% of the total carbon sequestered and POC increase for Iowa and 70.8% and 51.6% of the total SOC and POC increase for Greece, respectively) were quite significant, while the probability of overpredicting SOC and POC (0.4 and 0.64 for Iowa and 0.31 and 0.46 for Greece) suggested that the mean of the Monte Carlo simulation distributions were close to the optimum simulation.

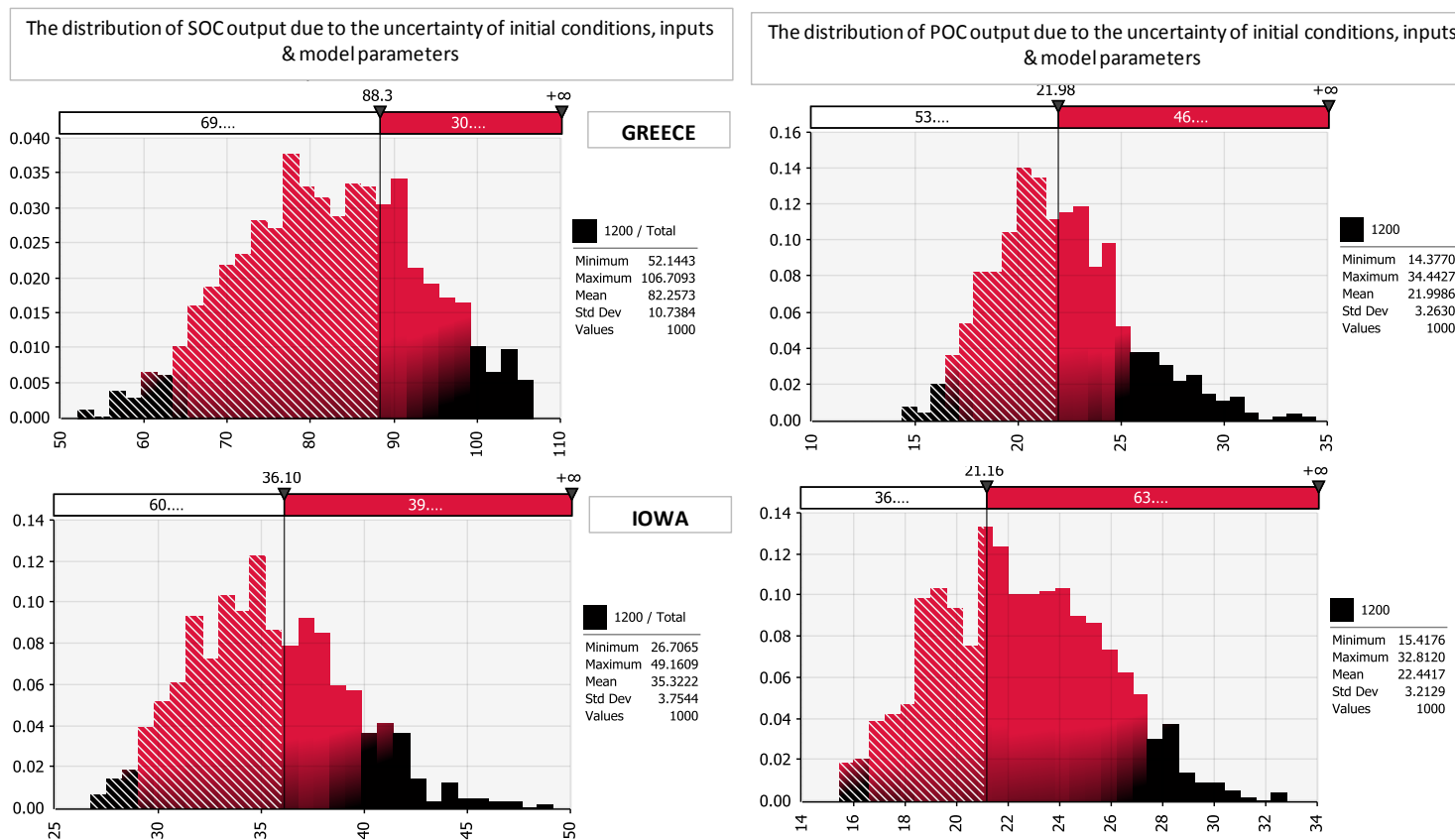


Figure 2.10 The output distributions by the Monte-Carlo simulations for the calculation of the total uncertainty for 100 y of simulation in Greece and Iowa for soil organic carbon (SOC) and Particulate organic carbon (POC). The x-axis indicates the SOC or POC content in t C/ha. The value of the optimum solution for SOC and POC is indicated in the top of the plot separating the distribution in two parts: the left part (light shaded histogram bars) indicates the area of the distribution below the value of the optimum solution and the right (dark shaded histogram bars) indicates the area of the distribution below the value of the optimum solution. The percentage covered in each area is given in the bars at the top of each plot.

## 2.4 CONCLUSIONS

A Monte Carlo based methodology was developed to assess the uniqueness of solution C sequestration modeling of cultivated to set-aside conditions and the uncertainties due to initial conditions, model parameters and time series of the RothC model. POC data obtained by soil physical fractionation were used successfully to initialize and calibrate the carbon model and provided boundary conditions to effectively constrain the solution of the model.

- The calibrated RPM decomposition rate constants in Iowa, similarly with the HUM decomposition rate constants, was higher (13.3%) and in Greece lower (31%) than the defaults rates suggesting that commonly used RothC model functions for decomposition rate correction due to temperature systematically underestimate and overestimate decomposition at low and at high temperatures, respectively.
- The calibrated HUM decomposition rate constants were significantly different than the defaults rates in both Iowa (13.5 times higher) and Greece (48.8 times lower). The significant difference between the two sites is attributed to significant differences in clay content. Finer texture in Greece resulted in higher protection of the HUM pool and presumably lower ‘apparent’ sensitivities (Davidson and Janssens, 2006, Kleber and Johnson, 2010) to temperature and/or moisture effect on decomposition in contrast with the coarser Iowa site where the opposite pattern was observed.
- Model sensitivity analysis revealed that predicted SOC exhibited the highest sensitivity to total plant litter input and the RPM decomposition rate constants and the lowest to BIO and DPM decomposition rate constants in both sites.
- Uncertainty analysis suggested that total uncertainty of C sequestration under set-aside from crop production conditions over 100 y can be as much as 70% of the total amount that was sequestered in both the Greek and Iowa soil. In both sites plant litter input was a major source of uncertainty. The uncertainty analysis results highlight the importance of obtaining accurate plant input data for landuses for the various climatic zones in order to minimize uncertainty in C sequestration estimates and determine more accurate the variability of C transformation rate constants as a function of climatic conditions.

The methodology developed in this study can be used to assess the factors affecting C sequestration in agricultural soils, quantify the uncertainties in predictions as well as assist in the design of field experiments and measurements to minimize the uncertainties and improve carbon sequestration estimates that relate directly to soil fertility.

## 2.5 LITERATURE CITED

- Aerts, R., 1997. Climate, Leaf Litter Chemistry and Leaf Litter Decomposition in Terrestrial Ecosystems: A Triangular Relationship. *Oikos* 79, 439-449.
- Angers D.A., Carter, M.R., 1996. Aggregation and organic matter storage in cool, humid agricultural soils. In: Carter M.R., Stewart B.A., eds. *Structure and organic matter storage in agricultural soils*. Boca Raton, FL: Lewis Publ, 193-211.
- Artz, R.R.E., Chapman, S.J., Robertson, A.H.J., Potts, J.M., Laggoun-Dedfage, F., Gogo, S., Comont, L., Disnar, J.R., Francez, A.J., 2008. FTIR spectroscopy can be used as a screening tool for organic matter quality in regenerating cutover peatlands. *Soil Biology and Biochemistry* 40, 515-527.
- Balesdent, J., Besnard, E., Arrouays D., Chenu, C., 1998. The dynamics of carbon in particle-size fractions of soil in a forest-cultivation sequence. *Plant and Soil* 201, 49-57.
- Banwart, S., Bernasconi, S.M., Bloem, J., Blum, W., Brandao, M., Brantley, S., Chabaux, F., Duffy, C., Kram, P., Lair, G., Lundin, L., Nikolaidis, N., Novak, M., Panagos, P., Ragnarsdottir, K.V., Reynolds, B., Rousseva, S., de Ruiter, P., van Gaans, P., van Riemsdijk, W., White, T., Zhang, B., 2011. Assessing Soil Processes and Function in Critical Zone Observatories: hypotheses and experimental design. *Vadose Zone Journal* 10, 974-987.
- Battle-Aguilar, J., Brovelli, A., Porporato, A., Barry, D.A., 2010. Modeling soil carbon and nitrogen cycles during landuse change: a review. *Agronomy for Sustainable Development* 31, 251-274.
- Beier, C., Emmett, B.A., Tietema, A., Schmidt, I.K., Penuelas, J., Lang, E.K., Duce, P., De Angelis, P., Gorissen, A., Estiarte, M., de Dato, G.D., Sowerby, A., Kröel-Dulay, G., Lellei-Kovács, E., Kull, O., Mand, P., Petersen, H., Gjelstrup, P., Spano, D., 2009. Carbon and nitrogen balances for six shrublands across Europe. *Global Biogeochemical Cycles*, 23 (GB4008), p. 13. ISSN 0886-6236.
- Bongiovanni, M.D., Lobartini, J.C., 2006. Particulate organic matter, carbohydrate, humic acid contents in soil macro- and micro-aggregates as affected by cultivation. *Geoderma* 136, 660-665.
- Bouyoucos, G.J., 1936. Directions for making mechanical analysis of soils by the hydrometer method. *Soil Science* 4, 225-228.
- Buyanovsky, G.A., Kucera, C.L., Wanger, G.H., 1987. Comparative analyses of carbon dynamics in native and cultivated ecosystems. *Ecology* 68, 2023-2031.
- Coleman, K., Jenkinson, D.S., 1999. RothC-26.3 - A Model for the turnover of carbon in soil: Model description and windows users guide: November 1999 issue. Lawes Agricultural Trust Harpenden. ISBN 0 951 4456 8 5.
- David, M.B., McIsaac, G.F., Darmody, R.G., Omonode, R.A., 2009. Long-Term Changes in Mollisol Organic Carbon and Nitrogen. *Journal of Environmental Quality*, 38, 200-211.
- Davidson, E.A., Janssens, I.A. 2006. Temperature sensitivity of soil carbon decomposition and feedbacks to climate change. *Nature* 440, 165-173.
- Don, A., Scholten, T., Schulze E.D., 2009. Conversion of cropland into grassland: Implications for soil organic-carbon stocks in two soils with different texture. *Journal of Plant Nutrition and Soil Science* 172, 53-62
- Elliott, E.T., 1986. Aggregate structure and carbon, nitrogen, and phosphorus in native and cultivated soils. *Soil Science Society of America Journal* 50, 627-633.
- Emadi, M., Baghernejad, M., Memarian, H.R., 2009. Effect of land-use change on soil fertility characteristics within water-stable aggregates of two cultivated soils in northern Iran. *Landuse Policy* 26, 452-457.
- Falloon, P.D., Smith, P., 2000. Modeling refractory soil organic matter. *Biology and Fertility of Soils* 30, 388-398.
- Falloon, P., Smith, P., Coleman, K., Marshall, S., 1998. Estimating the size of the inert organic matter pool from total soil organic carbon content for use in the Rothamsted Carbon model. *Soil Biology and Biochemistry* 30, 1207-1211.
- FAO 1998. World Reference Base for Soil Resources. (<http://www.fao.org/ag/agl/agll/wrb/>)
- Fioretto, A., Papa, S., Fuggi, A. 2003. Litter-fall and litter decomposition in a low Mediterranean shrubland. *Biology and Fertility of Soils* 39, 37-44

- Galdo, I.D., Six, J., Peressotti, A., Cotrufo, M.F., 2003. Assessing the impact of land-use change on soil C sequestration in agricultural soils by means of organic matter fractionation and stable C isotopes. *Global Change Biology* 9, 1204–1213.
- Gerzabek, M.H., Antil, R.S., Kogel-knabner, I., Knicker, H., Kirchmann, H., Haberhauer, G., 2006. How are soil use and management reflected by soil organic matter characteristics: a spectroscopic approach. *European Journal of Soil Science* 57, 485-494.
- Gottschalk, P., Bellarby, J., Chenu, C., Foereid, B., Smith, P., Wattenbach, M., Zingore, S., Smith, J., 2010. Simulation of soil organic carbon response at forest cultivation sequences using <sup>13</sup>C measurements. *Organic Geochemistry* 41, 41–54.
- Grieser, J, Gommel, R, Bernardi, M., 2006. New LocClim—the local climate estimator of FAO. *Geophysical Research Abstracts* 8:08305.
- Guo, L.B., Gifford, R.M., 2002. Soil carbon stocks and landuse change: a meta analysis. *Global Change Biology* 8, 345–360.
- Guzman, J.G., Al-Kaisi, M.M., 2010. Soil Carbon Dynamics and Carbon Budget of Newly Reconstructed Tall-grass Prairies in South Central Iowa. *Journal of Environmental Quality* 39, 136–146.
- HACH DR/2010 Spectrophotometer Procedures Manual; 7th edition 1999; HACH Company; Loveland, Co.
- Hillel, D. 1998. *Environmental Soil Physics*. Academic Press. San Diego, CA
- Instruction Manual Total Organic Carbon Analyzer Model TOC-5050A, Shimadzu Corporation, Environmental Instrumental Division.
- John, B., Yamashita, T., Ludwig, B., and Flessa, H., 2005. Storage of organic carbon in aggregate and density fractions of silty soils under different types of landuse. *Geoderma* 128, 63-79.
- Juston, J., Andr n, O., K tterer, T., Jansson, P.E., 2010. Uncertainty analyses for calibrating a soil carbon balance model to agricultural field trial data in Sweden and Kenya. *Ecological Modeling* 221, 1880-1888.
- Kleber, M., Johnson, K.J., 2010. Advances in Understanding the Molecular Structure of Soil Organic Matter: Implications for Interactions in the Environment. *Advances in Agronomy* 106, 77-142.
- Krull, E.S., Skjemstad, J.O., Burrows, W.H., Bray, S.G., Wynn, J.G., Bol, R. et al. 2005. Recent vegetation changes in central Queensland, Australia: Evidence from  $\delta^{13}C$  and  $^{14}C$  analyses of soil organic matter. *Geoderma* 12, 241–259.
- Lal R. 1997. Residue management, conservation tillage and soil restoration for mitigating greenhouse effect by CO<sub>2</sub>-enrichment. *Soil and Tillage Research*, 43, 81-107.
- Lichter, K., Govaerts, B., Six, J., Sayre, K.D., Deckers, J., Dendooven, L., 2008. Aggregation and C and N contents of soil organic matter fractions in a permanent raised-bed planting system in the highlands of Central Mexico. *Plant and Soil*, 305, 237-252.
- Manzoni, S., Porporato, A., 2009. Soil carbon and nitrogen mineralization: Theory and models across scales, *Soil Biology and Biochemistry* 41, 1355-1379.
- Methods of Soil Analysis, Part 3- Chemical Methods, 2nd Ed. Rev. Soil Science Society of America, Black, C.A et al., 1982.
- Nikolaidis, N.P., Bidoglio, G., 2012. Soil organic matter dynamics and structure. *Sustainable Agriculture Reviews* (In Press).
- Ostle, N.J., Levy, P.E., Evans, C.D., Smith, P., 2009. UK landuse and soil carbon sequestration-Review. *Landuse Policy* 26S, S274–S283.
- Paul, K.I., Polglase, P.J., Richards, G.P., 2003. Predicted change in soil carbon following afforestation or reforestation, and analysis of controlling factors by linking a C accounting model (CAMFor) to models of forest growth (3PG), litter decomposition (GENDEC) and soil C turnover (RothC). *Forest Ecology and Management* 177, 485-501.
- Piccolo, A., Zena, A., Conte, P., 1996. A comparison of acid hydrolyses for the determination of carbohydrate content in soils. *Communication in Soil Science and Plant analysis* 27, 2909-2915.
- Potter, K.N., Derner, J.D., 2006. Soil carbon pools in central Texas: Prairies, restored grasslands, and croplands. *Journal of Soil and Water Conservation* 61, 124-128.

- Rees, R.M., Bingham, I.J., Baddeley, J.A., Watson, C.A., 2005. The role of plants and land management in sequestering soil carbon in temperate arable and grassland. *Geoderma* 128, 130-154.
- Sainju, U.M., Whitehead, W.F., Singh, B.P., 2003. Cover crops and nitrogen fertilization effects on soil aggregation and carbon and nitrogen pools. *Canadian Journal of Soil Science* 83, 155–165.
- Six, J., Elliott, E.T., Paustian, K., 2000. Soil macroaggregate turnover and microaggregate formation: a mechanism for carbon sequestration under no tillage agriculture. *Short Communication in Soil Biology and Biochemistry* 32, 2099-2103.
- Shibu, M.E., Leffelaar, P.A., Van Keulen, H., Aggarwal, P.K., 2006. Quantitative description of soil organic matter dynamics – A review of approaches with reference to rice-based cropping systems. *Geoderma*, 137, 1-18.
- Skjemstad, J., Spouncer, L., Cowie, B., Swift, R., 2004. Calibration of the Rothamsted organic carbon turnover model (RothC ver. 26.3), using measurable soil organic carbon pools. *Australian Journal of Soil Research* 42, 79-88.
- Smith, P., Powlson, D.S., Smith, J.U., Elliott, E.T., 1997. Evaluation and comparison of soil organic matter models using datasets from seven long-term experiments. *Geoderma* 81, 1-225.
- Soussana, J.F., Loiseau, P., Vuichard, N., Ceschia, E., Balesdent, J., Chevallier, T., Arrouays, D., 2004. Carbon cycling and sequestration opportunities in temperate grasslands. *Soil Use and Management* 20, 219-230.
- The World Factbook, 2008 (<https://www.cia.gov/library/publications/the-world-factbook/>)
- Todorovic, G.R., Stemmer, M., Tatzber, M., Katzlberger, C., Spiegel, H., Zehetner, F., Gerzabek, M.H., 2010. Soil-carbon turnover under different crop management: Evaluation of RothC-model predictions under Pannonian climate conditions. *Journal of Plant Nutrition and Soil Science* 173, 662–670.
- Tufekcioglu, A., Raich, J.W., Isenhardt, T.M., Schultz R.C., 2003. Biomass, carbon and nitrogen dynamics of multi-species riparian buffers within an agricultural watershed in Iowa, USA. *Agroforestry Systems* 57, 187-198.
- Wagai, R., Mayer, L.M., Kitayama, K., Knicker, H., 2008. Climate and parent material controls on organic matter storage in surface soils: three-pool, density-separation approach. *Geoderma* 147, 23-33.
- Zimmermann, M., Leifeld, J., Schmidt, M.W.I., Smith, P., Fuhrer, J., 2007. Measured soil organic matter fractions can be related to pools in the RothC model. *European Journal of Soil Science* 58, 658–667.
- Zhang, W., Weindorf, D.C., Zhu, Y., 2011. Soil Organic Carbon Variability in Croplands: Implications for Sampling Design. *Soil Science* 176, 367-371.

### 3. CARBON LOSS DUE TO LANDUSE CHANGE ALONG A CLIMATIC GRADIENT

---

---

*Modeling with RothC C turnover and predicting the effectiveness of carbon addition after the conversion of native lands to croplands along a climatic gradient: uncertainty analysis*

**Abstract:** The change of soil organic carbon (SOC) stock after the conversion of a native land to cropland depends on landuse type and decomposition regime (determined by climatic conditions, size of the carbon litter input, texture and other factors). Field data and modeling exercises were used for the assessment of the turnover of different carbon pools in order to optimize organic input strategies for carbon sequestration in stable forms so as to maintain soil structure and fertility. In this work, native land to cropland conversions along a climatic gradient from Desert to Forest (Budyco's Radiational Index of Dryness ranging from 3.94 to 0.96) were modeled with RothC. Chronosequence data from six sites obtained from recently published studies were modeled. The methodological approach for model calibration and estimation of uncertainty presented in the previous chapter was followed. The sensitivity analysis suggested that parameter sensitivity greatly depends on the available data for calibration. The most sensitive parameters were the HUM and RPM decomposition rate constants as well as the plant litter input and the RPM initial pool for the sites it was not measured. The uncertainty of the simulated carbon loss after 100 years cultivation was 26.9% -Tibet, 122.5% -Dakota, 21.9% -China, 48.9% -Turkey, 108% -Ethiopia, and 31.6% -Madagascar of the total amount of C decline due to the landuse conversion. The uncertainty was smaller in the sites with available field measured particulate organic carbon (POC) data and information about the plant input. These results emphasize the necessity of obtaining accurate plant input data and other physical soil parameters as well as quantifying the variability of initial conditions in order to reduce the uncertainty of carbon turnover projections. The average rate of carbon decline after the conversion to cropland as an average percentage of the initial SOC (% of the initial SOC/y) as well as amount of carbon (t/ha y) greatly varied among the study sites and followed a logarithmic pattern with time (e.g. decline relative to the initial SOC 1% to 10% after 1 year cultivation and 0.32%/y to 0.77%/y after 100 years. The POC to SOC ratio of the native land greatly determines the % loss in the long term. The time it takes the soil to reach a new stable carbon content varied greatly with the climatic gradient from more than 100 years (Tibet, Desert) to 20-30

(Ethiopia, Forest). Scenarios of carbon addition of materials of different quality were also conducted to assess their effectiveness under different climatic conditions and soil types. The study sites with the lower HUM decomposition rate also presented higher effectiveness in carbon addition and carbon stabilization in the silt-clay fraction. In all cases the Net C to C amended ratio (Net C: the extra carbon sequestered compared to the soil under no amendment, C amended: the cumulative load of the carbon added to soil as amendment) significantly decline with time over a logarithmic pattern. Such long term model simulations are important for the design of sustainable agricultural practices (carbon sequestration, e.g. HUM increase) under different climatic regimes and soil textures. The 'apparent' temperature sensitivity of the RPM and HUM RothC carbon pools was estimated with the calculation of the Q10 factor. It was verified that RothC underestimates decomposition at low temperatures and overestimates it at high temperatures.

### 3.1 INTRODUCTION

Conversion of native vegetated lands to croplands induces SOM losses due to gradual changes in land management like plowing and less litter input. On a global basis biological oxidation is considered to be the dominant pathway of carbon loss (Rees, et al., 2005; Rasmussen et al., 1998), while leaching of dissolved organic carbon cannot explain more than 10% of the soil organic carbon (SOC) loss (Schulze and Freibauer, 2005). On the other hand, erosion can be viewed as a transport process that influences the location of the environment in which oxidation takes place (Lal, 2008). Under plowing, macro-aggregates are partly rapidly destroyed, while physically protected bio-available SOM becomes bio-accessible and can be microbially oxidized (Balesdent et al., 1998). Particulate organic carbon (POC) is the fraction mostly affected by plowing in the short term (Wagai et al., 2008). In addition, incoming OM is re-exposed faster than it is occluded due to the higher macro-aggregate turnover. Therefore more OM is mineralized and less stabilized in micro-aggregates and silt-clay sized soil fractions (Six et al., 2000) in the medium- to long-term time scale (Don et al., 2009).

The average rate of SOC stock decline (t C/ha y) after the conversion of a native land to cropland has been found to decrease in time (see Figure 1.4). Variations depend on the initial SOC content and apportionment to its pools, which is highly depended on previous landuse type, the size and litter quality and the decomposition regime which is primarily determined

by the climatic conditions and the texture among other factors (Mann, 1986). Conversion of natural to agricultural ecosystems can deplete the soil organic carbon (SOC) pool by 50% in about 5 years in the tropics and 50 years in temperate ecoregions (Lal, 2001).

Decline of SOM stocks is related to poor soil fertility and structural stability (particle aggregation) in several agricultural areas of the world, making soils more susceptible to erosion and desertification with global consequences for food security, climate change, biodiversity, water quality, and agricultural economy (Lal, 2004; Mafongoya et al., 2006). An “agronomically valuable” soil is the soil where greater than 60% of the aggregated particle mass is in the range between 0.25 and 10 mm (Banwart et al., 2011). An appropriate management of organic matter additions like composts to soils would increase aggregate stability and thus reduce crusting and erosion problems (Abiven et al., 2008).

Carbon simulations can be used as a tool for the estimation of the quantity/quality of organic matter amendment necessary to ensure sustainable production with the optimization of other objectives (minimum land degradation, maximum biodiversity conservation) and can serve as a management decision tool. RothC has been extensively used worldwide. However, as it was shown by the study presented in the previous chapter, as well as by other studies, the default decomposition rate constants in RothC do not always correspond well under different climatic types. Having reliable model simulations is very essential and therefore RothC combination with physical fractionation data (POC, carbon content of fraction with particle sizes  $>50 \mu\text{m}$ ) which has been associated with the RPM pool of RothC (Galdo et al., 2003; Gottschalk et al., 2010;) for initialization and calibration can be used for this purpose (Gottschalk et al., 2010; study presented in Chapter 2).

Moreover, in most cases models have been used without accounting for the uncertainty that arises from the initial conditions, model parameters, inputs and model structure with very few exceptions (Juston et al., 2010; Paul et al., 2003; study presented in the previous chapter). The study presented in Chapter 2 indicated that as much as 70% uncertainty of the total amount that was sequestered in 100 years in set-aside from crop production fields in both humid continental climate (Iowa, USA) and Mediterranean (Crete, Greece), underlying also the importance of obtaining accurate plant input data for the various climates in the world in order to minimize carbon sequestration estimates and determine more accurately the variability of carbon transformation rate constants as a function of climatic conditions. Nevertheless, a five to ten year period is the minimum timescale to monitor changes in

carbon pools, otherwise in certain cases a clear pattern cannot be drawn due to uncertainties.

In this work the Microsoft Excel version of the Rothamsted Carbon Model-version RothC-26.3 (Coleman and Jenkinson, 1999) modified in the work presented in the previous chapter was used in conjunction with a statistical simulation package @RISK (PALISADES Corp.) with the methodology developed and presented in Chapter 2 in order to calibrate, assess the sensitivity and simulate the uncertainty, due to initial conditions and model parameters and inputs, in carbon turnover during native land to cropland conversion along a climatic gradient with data obtained by relative published studies. Scenarios of carbon addition of materials of different quality were also simulated to assess their effectiveness under different climatic conditions and soil types.

## **3.2 METHODOLOGY**

### **3.2.1 Study sites**

Landuse conversions of six sites with data obtained from six published studies were modeled (Table 3.1): Tibet (Li et al., 2009), North Dakota-USA (Frank et al., 2006), China (Wu et al., 2004), Turkey (Evrendilek et al., 2004), Ethiopia (Ashagrie et al., 2007), Madagascar (Vagen et al., 2006). Three of the studies had available physical fractionation data for the POC fraction Tibet (Li et al., 2009), China (Wu et al., 2004), and Ethiopia (Ashagrie et al., 2007). The used studies were strictly selected to correspond to landuse conversions from native land to cropland with known the length of the conversion and moreover carefully selected to provide site coordinates, bulk density, and sufficient information about the previous landuse, crops grown and crop management (Table A3.1 in the Appendix)

The climatic gradient was characterized by the climatic classes defined by ranges of Budyco's Radiational Index of Dryness (RID): Desert ( $>3.4$ ), Semiarid (2.3-3.4), Steppe (1.1-2.3), Forest (0.35-1.1), Tundra ( $<0.35$ ). RID is the ratio of the local radiation balance ( $R_o$ =mean annual net radiation for a wet surface) and the energy needed to evaporate all precipitation ( $L$ =latent heat of vaporization multiplied by  $P$ =mean annual precipitation). The lower the RID value the higher is the annual precipitation compared to the radiation energy available for evaporation and the wetter is the area. The RID of the eight sites ranged from 3.94 (Desert, Tibet) to 0.96 (Forest, Madagascar). The mean annual temperature (TEMP) of the sites ranged from 4.9°C

to 17.9°C and the mean annual precipitation (PREC) from 279 mm to 1529 mm, while the amount of annual rain missing to fully compensate potential evapotranspiration (PET), the precipitation deficit, from 843 mm (water deficit) to -483 mm (water surplus), along the Desert (Tibet) to Forest (Madagascar) gradient. The values for the climatic gradient for other aridity indices are presented in Table 1. Aridity Index (AI) is the ratio of PREC to PET, the higher the less arid. Moisture Index (MI) is calculated by 'AI' as  $100*(AI-1)$ . The higher the value of the index the wetter the climate is characterized (Thornthwaite and Mather, 1962). De Martonne Index is the ratio of PREC to TEMP plus 10°C (De Martonne, 1926). This index is a way to measure humidity; values larger than 20 are usually considered to characterize humid climates.

The climatic Net Primary Productivity (NPP) potential has been estimated based on the 'Miami' model (minimum of NPP taken by a monotonic function of temperature and precipitation) first introduced by Lieth (1972) and ranged from 508 g DM/m<sup>2</sup> y (Desert, Tibet) to 1913 g DM/m<sup>2</sup> y (Forest, Madagascar). The length of growing season (humid period) and dry period for each site are presented also in Table 3.1. The moist period of the growing season is when PREC is higher than PET and the humid period when the PREC to PET ratio higher than 0.5.

Soil types and soil characteristics for both native lands and croplands of the eight sites are presented in Table 3.1. Soil depth in two sites was 30 cm and in the rest of the sites 20 cm. Total soil carbon stock ranged from 56.8 t C/ha (20 cm) to 115 t/ha (30 cm soil depth), while clay content from 18.3% to 70%. The length of the landuse conversion ranged from 12 to 42 years. The average rate of SOC decline (t C/ha y) ranged from (years, Madagascar, Forest) to 0.48 (30 years, North Dakota-USA, Semiarid).

Table 3.1 Study sites location and characteristics.

Reference	Li et al. (2009)	Frank et al. (2006)	Wu et al. (2004)	Evrendilek et al. (2004)	Ashagrie et al. (2007)	Vagen et al. (2006)
Site Location/ Climate Class	Tibet-Desert	North Dakota-Semiarid	China-Steppe	Turkey-Steppe	Ethiopia-Steppe	Madagascar-Forest
Latitude	38o20oN	46o46oN	36o11 56'N	37o11'N	7o34oN	20o30oS
Longitude	101o30oE	100o55oW	112o55o31E	34o 38'E	38o53oE	47o25oE
Elevation, m	2650	518	900	1400	2400	1360
Koepfen Climate Class	Bsk	Dfb	Dwa	Bsk	Cwb	Bsh
Radiational Index of Dryness	3.94	2.56	1.93	1.76	1.20	0.96
Mean Annual TEMP, oC	4.9	5.4	9.8	13.9	12.6	17.9
Mean Annual PREC, mm	279.3	397.0	586.0	752.0	1333.0	1529.0
Mean Annual PET, mm	1122.4	984.5	943.9	1112.4	1130.7	1045.5
Precipitation deficit	843	588	358	360	-202	-483
Aridity index	0.25	0.4	0.62	0.68	1.18	1.46
Moisture Index	-75	-60	-38	-32	18	46
De Martonne Index	19	26	30	31	59	55
Growing season humid period	-	1/1 to 18/2	11/7 to 2/9	29/10 to 31/3	10/3 to 15/10	29/10 to 19/4
Dry period	1/1 to 31/12	8/2 to 27/11	24/10 to 9/6	14/5 to 28/10	1/11 to 21/1	2/7 to 9/10
NPP, g(DM)/m <sup>2</sup> y	508	695	967	1078	1635	1913
NPP limited by	Prec	Prec	Prec	Prec	Temp	Prec
Soil type	Mollisol	Pachic Haplustoll	Haplic Greyxems	Typic Haploxeroll	Rhodic Nitisols	Oxisol
Soil depth, cm	30	30	20	20	20	20
pH	8.3	6.6	8.3	7.4	5.6	4.5
CaCO <sub>3</sub> (g/kg)	75.5	-	99.4	210	-	-
Silt/Clay Content, %	72/18.3	54/25	63.4/25.4	41.5/38.5	30/49	/70
Years after the conversion	30	30	0,4,10,20,42	12	26	1,3,>50, approx75
Initial SOC, t C/ha	115.3	84.4	56.8	57.3	124	110.3
Initial POC, t C/ha	37.2	-	14.7	-	78	-
Final SOC, t C/ha	79.1	70	16.7	32.6	67	28.5
Final POC, t C/ha	17.1	-	1.4	-	12.1	-

### 3.2.2 RothC modeling-methodological approach

#### *Initialization/ Calibration*

The meteorological data used in the modeling exercise (average monthly mean temperature, precipitation, and potential evapotranspiration) were obtained by the Local Climate Estimator (New LocClim 1.10, 2006) according to site coordinates by the closest meteorological station (Table A3.2 in the Appendix). Soil thickness was set to 20 or 30 cm according to the field measurements of each site (Table 3.1). Clay content was also obtained by field measurements (Table 3.1). The fields were covered by crops during the cropping period (Table A3.1 in the appendix). Field measured SOC and POC content (Table 3.1) in the cropland were used as calibration criteria. The C of POC (particle sizes >50  $\mu\text{m}$ ) has been associated with the RPM pool of RothC (Galdo et al., 2003; Gottschalk et al., 2010, study presented in chapter 2). Initial SOC was partitioned among the different carbon pools (RPM, DPM, BIO, IOM and HUM) using the following approach. The POC content is the sum of RPM and DPM fractions apportioned by calibration. Following Roth-C-26.3-model recommendations, BIO was assumed to be 3% of the total SOC and IOM using the equation suggested by Falloon et al. (1998):  $\text{IOM} = 0.049 * \text{SOC}^{1.139}$ . For the estimation of the IOM content, we used the native land SOC content since the inert carbon is not usually considered to change significantly because of cultivation during a few decades. However, due to the uncertainty of this assumption in the uncertainty analysis the range of the IOM pool is from zero to the value taken by the Falloon's equation. Finally, the HUM pool was calculated by difference of the other pools from the total SOC.

First, RothC/@RISK was used in a Monte-Carlo fashion in order to identify the optimal/unique solution of model parameters and input that best simulates each soil. Plant litter input and six model parameters were considered simultaneously with uniform distributions (Table 3.2). Since the plant litter was not measured, the appropriate range found in the literature for the specific climate and landuse was used. In addition any information given in the manuscripts was used. In specific the input uniform distribution of plant input was for the six sites: 0.1-1.2 t C/ha (Tibet), 0.5-1.1 t C/ha (Dakota), 0.3 to 1.0 t C/ha (China), 0.5-3.5 t C/ha (Turkey), 1.5 to 7 t C/ha (Ethiopia), 1.0-4.0 t C/ha (Madagascar). Regarding the range of the RPM and HUM decomposition rate constants it was expanded if needed by preliminary simulations (in general RPM: 0.1 to 0.8 or 1.0 1/y and HUM: 0.009 to 0.1 or 0.3 1/y). For the remaining model parameters (DPM and BIO decomposition rate constants, DPM-to-RPM ratio, and

BIO%), the range was established as  $\pm 10\%$  of the default model values. In the three cases where POC measurements were not available, POC was also included in the calibration procedure. The range ( $\pm 20\%$  of the predicted value) of POC to SOC ratio found by preliminary simulation for the native land conditions was used to initialize the model and it was also optimized. The input ranges of the POC to SOC ratio introduced to the model were: 45-65% (Dakota), 25-40% (Turkey), 20-40% (Madagascar).

Monte-Carlo simulation with 5000 iterations was conducted using the distributions of the plant input and the six model parameters described above. The simulation period was 100 years. The solution with the lowest deviation ( $< \pm 1\%$ ) from both SOC and POC field measurements was considered as the optimum solution and the values of the parameters that generated the solution as the calibrated values. The ensemble of solutions falling within the  $\pm 5\%$  of the SOC and POC field measured values was also examined in order to confirm the uniqueness of the optimum solution. For the China site where chronosequence data for both SOC and POC were available, the ensemble of solutions falling within the least percentage of the SOC and POC field measured values that covers all the chronosequence data was used instead of the 5%. The standard deviations of the selected solutions of the plant input and the six model parameters were calculated and their values were compared with the initial distributions. Low standard deviations suggest the uniqueness of the optimum solution since the system is inherently constrained and does not allow solutions with extreme combinations of parameter values.

### *Sensitivity analysis*

Once the model was calibrated, sensitivity analysis was performed with respect to the change of the SOC and POC (sum of DPM and RPM) content in the year used for calibration. In the China site the last year of the available chronosequence data was used. The six model parameters (DPM, RPM, BIO, and HUM decomposition rate constants, DPM-to-RPM ratio, HUM%) and the plant litter input were varied by  $\pm 10\%$  and  $\pm 50\%$  from the calibrated values. The sensitivity coefficients (the absolute value of the ratio:  $(\Delta Y/Y)/(\Delta x/x)$ ) were calculated for SOC and POC content; Y is the SOC or POC content and x the parameter value).

### *Uncertainty analysis*

Finally, the propagation of uncertainty in the simulated results due to initial conditions (SOC, DPM, RPM, BIO, HUM, and IOM carbon pools), plant litter input and soil clay content, as well as the six model parameters used for calibration was conducted for each category separately and all together. The simulation run was for 100 years for both sites. The distribution for each parameter derived from the Monte-Carlo simulation for the iterations falling within the  $\pm 5\%$  of the SOC and POC field measured values was used in the uncertainty analysis. Field variability for initial conditions and clay content was considered as normal distribution with mean the measured value and a standard deviation of 5% of the mean. The uncertainty of the IOM pool was considered to be a uniform distribution ranging from zero to the value obtained by Falloon's equation. The HUM pool was calculated by difference.

### *Carbon addition scenarios*

The effectiveness of carbon addition of various qualities was assessed. Three types of exogenous organic matter with gradual increase in RPM and HUM content were added in the landuse conversions at the same rate of 2.5 t C/ha just before the cropping period at one dose. Amendments like manure are usually used to fulfill the agronomic needs of the plants at doses 1-1.5 kg/m<sup>2</sup>, considering that their carbon content would be at least 25%, then the carbon added to the system would be higher than 2.5 t C/ha (Stamati et al., 2011). Other composts of lower nutrient quality are added in higher doses, but they usually contain lower carbon content. The composition of the amendments tested in terms of DPM/RPM/HUM content was as follows: 49/49/2, 30/60/10, and 10/70/20. The first type is representative of manure, following the suggestion of RothC manual, while the other two correspond to green waste and sludge and sludge or peat, respectively, according to Peltre et al. (2010) (they optimized these percentages for several exogenous organic materials applied to soils). The simulation period was 100 years. The Net C to C amended ratio of effectiveness was calculated for every year of the simulation period. The carbon amended is the cumulative load of the exogenous organic matter added to the soil (2.5 t C/ha multiplied by the years of the application). The Net C refers to the extra carbon that is sequestered as compared with the soil where no amended was applied.

### 3.3 RESULTS AND DISCUSSION

#### *Model calibration*

The statistics of the ensemble of the Monte-Carlo simulations that fall within  $\pm 5\%$  of SOC and POC measurements are presented in Table 3.2. In three cases (Dakota, Turkey, and Madagascar) POC was not measured in the field, as already mentioned before. Moreover, in the case of China the ensemble of solutions falling within the percentage of the SOC and POC field measured values that covers all the chronosequence data was used instead of the 5%; this percentage was found to be 30%. The standard deviation was found to be more than 10% of the mean values of the RPM and HUM decomposition rate constants and the plant input and the RPM initial pool, almost in all cases, indicating that the system was not well constrained with the available data for calibration and may be allow acceptable solutions with extreme parameter value combinations. Nevertheless, in the three cases where the POC pool was field measured and used for calibration this uncertainty was reduced (Tibet, China, Ethiopia). In China where chronosequence data were also available it was observed the least variability. In Ethiopia, however, the fact that it was introduced a high range of plant input for calibration due to the limited information resulted in less constrained ensemble of solutions that fall within the  $\pm 5\%$  of SOC and POC measurements. It is clear that measurement of POC to initialize and calibrate the model can greatly reduce uncertainty in calibrated parameters. The mean as well as the optimum RPM and HUM decomposition rate constants were found to be significantly different than the default values used in RothC. The optimum value for HUM rate was found to be higher than RothC in all sites apart from Ethiopia. The optimum value for RPM rate was found to be higher than RothC in China, Turkey, and Madagascar.

**Table 3.2 Statistics of the parameter distributions for the solutions fell within the  $\pm 5\%$  of the SOC and POC field measured stocks as well as the optimum solutions derived by the Monte-Carlo simulation.**

Parameter	total plant input	DPM/RP M ratio	POC fraction initial	BIO%	DPM	RPM	BIO	HUM
<b>Li et al. (2009), Tibet-Desert</b>								
distribution type	uniform	triang	-	uniform	triang	betaGeneral	uniform	uniform
min	0.10	1.26	-	41.30	8.92	0.23	0.59	0.0821
max	1.18	1.60	-	50.74	11.28	0.30	0.73	0.1496
mean	0.74	1.45	-	46.02	9.89	0.27	0.66	0.1159
std	0.25	0.07	-	2.72	0.50	0.02	0.04	0.0195
Chi-sq	2.76	7.98	-	4.71	3.73	3.41	4.06	4.7142
Optimum	<b>0.73</b>	<b>1.49</b>	-	<b>46.12</b>	<b>10.88</b>	<b>0.26</b>	<b>0.64</b>	<b>0.1150</b>
<b>Frank et al. (2006), North Dakota-Semiarid</b>								
distribution type	betaGeneral	Uniform	betaGeneral	betaGeneral	Uniform	betaGeneral	Uniform	betaGeneral
min	0.50	1.29	0.45	41.50	8.99	0.10	0.59	0.0022
max	1.10	1.58	0.64	50.60	11.08	0.30	0.73	0.1044
mean	0.86	1.44	0.539	45.68	10.00	0.14	0.66	0.0348
std	0.17	0.08	0.0582	2.79	0.59	0.03	0.04	0.024
Chi-sq	2.62	5.22	16.027	11.00	7.38	4.78	13.00	18.4054
Optimum	<b>0.94</b>	<b>1.50</b>	<b>0.54</b>	<b>46.16</b>	<b>9.91</b>	<b>0.13</b>	<b>0.68</b>	<b>0.0370</b>
<b>Wu et al. (2004), China-Stepp</b>								
distribution type	triang	triang	-	uniform	betaGeneral	triang	triang	triang
min	0.30	1.26	-	40.98	9.03	0.29	0.60	0.0866
max	0.97	1.60	-	51.05	10.76	0.51	0.72	0.1453
mean	0.61	1.46	-	46.01	9.91	0.38	0.68	0.1257
std	0.14	0.07	-	2.91	0.64	0.05	0.03	0.0138
Chi-sq	1.67	2.81	-	0.90	1.19	2.05	1.67	1.6667
Optimum	<b>0.73</b>	<b>1.53</b>	-	<b>44.24</b>	<b>9.89</b>	<b>0.41</b>	<b>0.68</b>	<b>0.1347</b>
<b>Evrendilek et al. (2004), Turkey-Steppe</b>								
distribution type	betaGeneral	betaGeneral	betaGeneral	betaGeneral	Uniform	betaGeneral	betaGeneral	betaGeneral
min	0.50	1.30	0.25	41.40	9.00	0.20	0.59	0.0620
max	3.50	1.58	0.40	50.60	11.00	0.80	0.73	0.2000
mean	1.69	1.44	0.3282	46.19	10.00	0.54	0.66	0.146
std	0.80	0.08	0.0445	2.67	0.58	0.16	0.04	0.0341
Chi-sq	26.71	27.85	26.9205	14.74	19.23	18.37	11.53	17.1616
Optimum	<b>2.00</b>	<b>1.48</b>	<b>0.32</b>	<b>45.90</b>	<b>10.22</b>	<b>0.55</b>	<b>0.64</b>	<b>0.1580</b>
<b>Ashagrie et al. (2007), Ethiopia-Steppe</b>								
distribution type	triang	uniform	-	triang	betaGeneral	uniform	triang	triang
min	1.63	1.29	-	41.44	9.07	0.19	0.57	0.0111
max	6.96	1.59	-	51.49	10.98	0.51	0.73	0.0726
mean	5.18	1.44	-	44.79	9.93	0.35	0.67	0.0409
std	1.26	0.09	-	2.37	0.62	0.09	0.04	0.0126
Chi-sq	3.20	3.60	-	5.40	8.20	5.60	3.20	4.4
Optimum	<b>2.67</b>	<b>1.38</b>	-	<b>44.17</b>	<b>10.67</b>	<b>0.22</b>	<b>0.72</b>	<b>0.0170</b>
<b>Vagen et al. (2006), Madagascar-Forest</b>								
distribution type	betaGeneral	uniform	uniform	betaGeneral	triang	betaGeneral	betaGeneral	triang
min	1.00	1.30	0.20	41.49	8.83	0.20	0.59	0.0217
max	3.99	1.59	0.40	50.53	11.14	0.78	0.72	0.0692
mean	2.85	1.44	0.2999	46.12	10.08	0.49	0.66	0.0424
std	0.90	0.08	0.0583	2.80	0.48	0.18	0.04	0.0093
Chi-sq	6.79	7.32	5.1973	8.35	6.97	5.20	10.68	9.7959
Optimum	<b>2.46</b>	<b>1.40</b>	<b>0.27</b>	<b>49.98</b>	<b>10.67</b>	<b>0.40</b>	<b>0.71</b>	<b>0.0357</b>

### *Sensitivity analysis*

Sensitivity analysis with respect to the change of the SOC and POC content in the field measured croplands (the year used for calibration) at the  $\pm 10\%$  and  $\pm 50\%$  ranges of the calibrated values (Table 3.2) for the six model parameters and the plant input as well the RPM initial carbon pool when applicable (the three cases not measured in the field) was conducted. The tornado graphs are presented in Figure 3.1 and the sensitivity coefficients (the absolute value of the ratio:  $(\Delta Y/Y)/(\Delta x/x)$ ) in Table A3.3 in the Appendix. In all sites regarding the sensitivity of the parameters on the simulated POC (the sum of the DPM and RPM pools), the most sensitive parameters were the RPM decomposition rate constant and the plant litter input and secondary the DPM to RPM ratio and the DPM decomposition rate constant (see Table A3.3). In the cases where the RPM initial pool was not known its sensitivity was found to be negligible to very low. The sensitivity of the DPM and BIO decomposition rate constants on the simulated SOC in all cases was very low.

Highest sensitivity (in terms of sensitivity coefficient at 10% indicated in the parenthesis) was presented by the HUM decomposition rate constant in China (10%: 0.899, 50%: 1.415), followed by the HUM in Madagascar (10%: 0.836, 50%: 1.362), the HUM in Turkey (10%: 0.368, 50%: 0.419), the plant litter input in Ethiopia (10%: 0.265, 50%: 0.470 for the RPM decomposition rate constant), the RPM decomposition rate constant in Dakota (10%: 0.230, 50%: 0.263), and finally the HUM in Tibet (10%: 0.202, 50%: 0.216). Sensitivity coefficients were found higher than the value 0.100 for the parameters HUM (all sites apart from Dakota), RPM (all, but for Madagascar only for the -50%), plant litter input (all apart from Tibet), BIO% (for Ethiopia, Madagascar, and China), and RPM initial pool (for Turkey and Dakota). The results emphasize that depending on the climatic region, the available data for the calibration of the parameters, they respond differently to the sensitivity. Moreover the fact that the year after the conversion varies between the sites from 12 to 75 years also influences the sensitivity patterns observed.

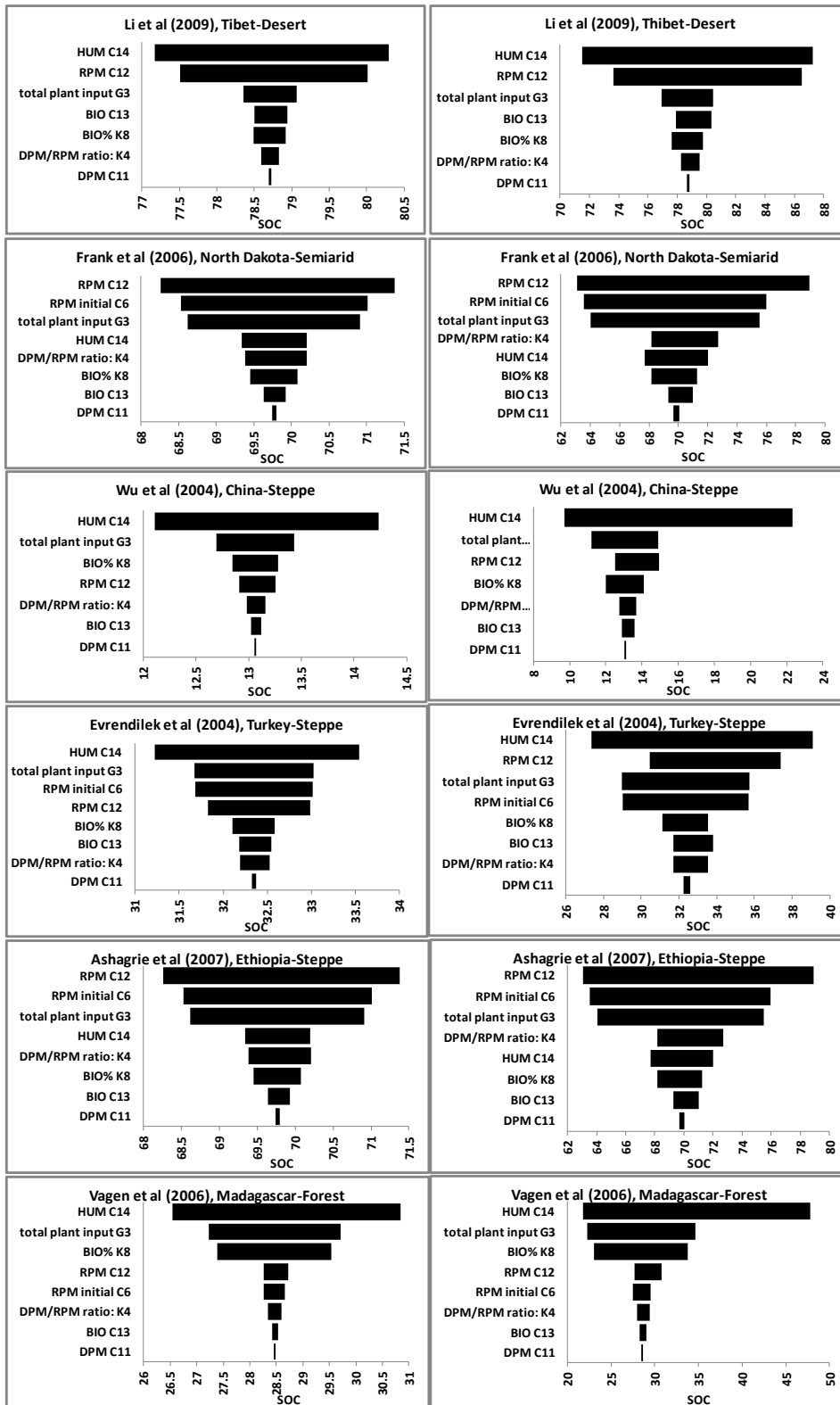


Figure 3.1 Tornado Graphs for 10% (left) and 50% (right) sensitivity analysis. Decomposition rate constants for RPM=resistant plant material, DPM=decomposable plant material, HUM=humus, and BIO=biomass, DPM/RPM ratio=the apportionment ratio of plant litter input DPM and RPM carbon pools, BIO%=the proportion that goes to BIO (100-BIO% is the proportion that goes to HUM), and RPM initial=the initial RPM carbon pool.

### *Uncertainty Analysis*

A comparison of the optimum simulation for both SOC and POC and the uncertainties attributed to the initial conditions (SOC, DPM, RPM, BIO, HUM, and IOM carbon pools) the input data (plant litter input and clay content), and the six model parameters used for calibration parameters (DPM, RPM, BIO, and HUM decomposition rate constants, DPM-to-RPM ratio, HUM%), in terms of the mean of the ensemble of Monte Carlo simulations plus one standard deviation are presented in Figure A3.1 in the Appendix. The total uncertainty for the six sites is presented in Figure 3.2. The uncertainty is smaller in the sites with available field measured POC data (the three sites on the left column of Figure 3.2) and higher in the sites where the calibration was conducted only with the SOC data (the three sites on the right column of Figure 3.2). However, the Ethiopia constitutes an exception since information about the plant input was scarce and therefore presented higher uncertainty as compared with the other two sites with available POC data, actually as high as the sites with no POC data. Similar patterns were found regarding the total uncertainty of the POC predictions.

The average SOC loss (t/ha y) by the optimum solution and the statistics derived by the total uncertainty are presented in Table 3.3. Moreover, the two last columns of the table give the total uncertainty (90% of the distribution range between 5 and 95%) of the prediction of the optimum solution. Specifically the 5% and 95% value of the SOC distribution describing the total uncertainty for the 100<sup>th</sup> year of the landuse conversion corresponds to 22.2% lower and 4.8% higher of the optimum value for Tibet, 49.7% lower and 72.8% higher for Dakota, 5.0% lower and 16.9% higher for China, 20.9% lower and 28.0% higher for Turkey, 46.0% higher and 62.0% lower for Ethiopia, and finally 9.9% higher and 21.7% lower for Madagascar. Totally, the uncertainty of the simulated carbon loss after 100 years cultivation was 26.9% -Tibet, 122.5% -Dakota, 21.9% -China, 48.9% -Turkey, 108% -Ethiopia, and 31.6% -Madagascar of the total amount of C decline due to the landuse conversion.

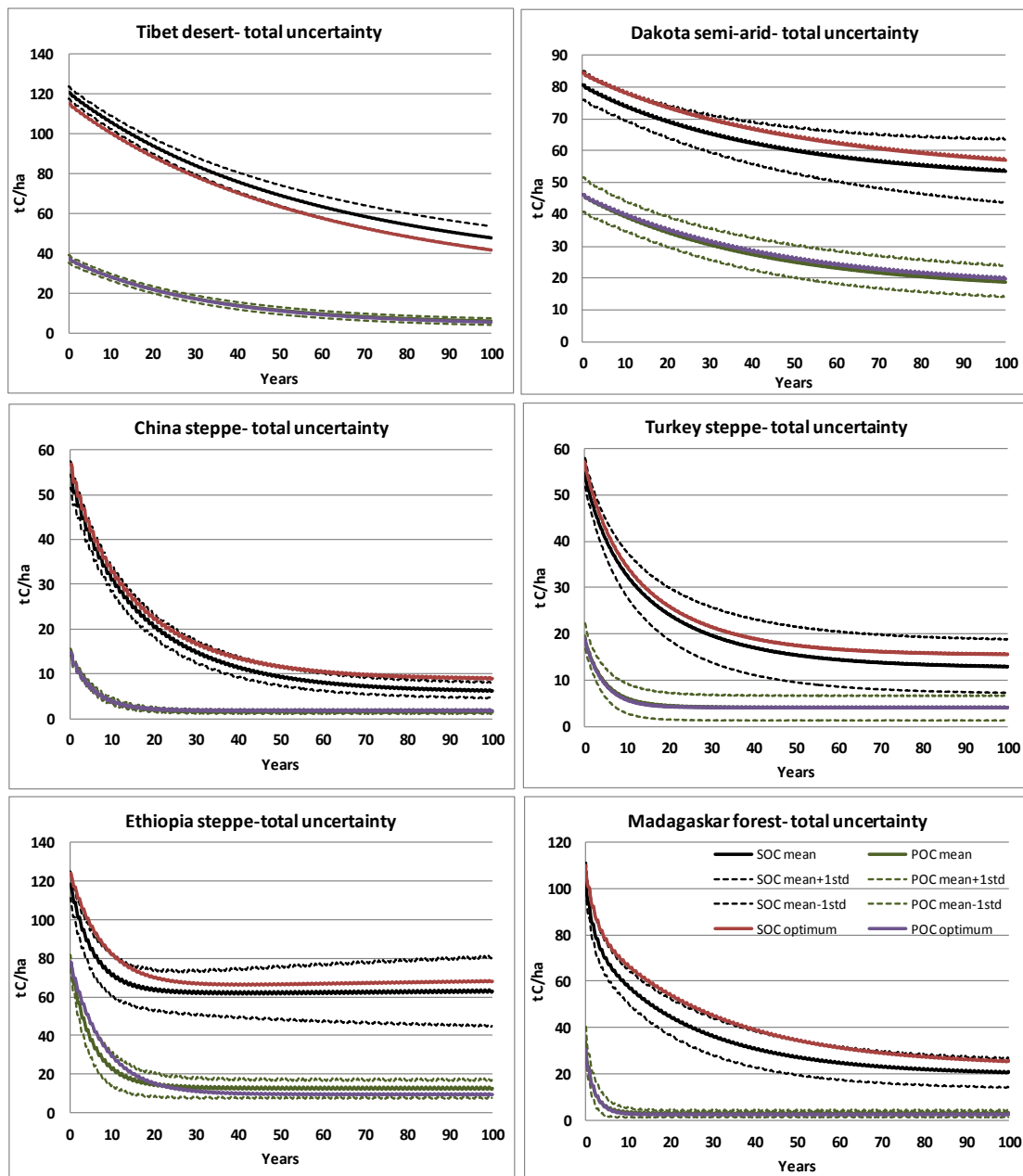


Figure 3.2 Total uncertainty of total organic carbon (SOC) and particulate organic carbon (POC) due to model parameters, input data, and initial conditions compared with the optimum solution (calibration) for the six sites.

**Table 3.3 The average SOC loss (t C/ha y) by the optimum solution and the statistics derived by the total uncertainty. In the last two columns it is presented the percentage variation of the 5% and 95% from the optimum solution.**

	optimum	Min	Mean	Max	Median	Std dev	5%	95%	% from optimum	
									5%	95%
<b>Tibet</b>										
<b>1</b>	1.87	-9.17	-3.60	2.11	-3.62	3.16	-8.59	1.34	-560.0	-28.1
<b>5</b>	1.60	-0.77	0.52	1.83	0.51	0.65	-0.48	1.51	-130.3	-5.1
<b>10</b>	1.48	0.19	0.95	1.70	0.94	0.35	0.41	1.50	-72.7	1.2
<b>20</b>	1.34	0.60	1.07	1.53	1.07	0.20	0.75	1.39	-43.7	4.3
<b>50</b>	1.03	0.66	0.92	1.17	0.93	0.11	0.75	1.09	-27.7	5.9
<b>75</b>	0.86	0.59	0.79	0.96	0.79	0.08	0.65	0.91	-24.5	5.6
<b>100</b>	0.73	0.52	0.68	0.81	0.68	0.06	0.57	0.77	<b>-22.2</b>	<b>4.8</b>
<b>Dakota</b>										
<b>1</b>	0.96	0.79	4.85	9.75	4.79	2.24	1.45	8.48	51.1	785.5
<b>5</b>	0.70	0.37	1.52	3.02	1.50	0.49	0.72	2.32	3.1	230.9
<b>10</b>	0.63	0.28	1.05	2.14	1.04	0.30	0.56	1.56	-10.3	148.4
<b>20</b>	0.55	0.19	0.77	1.57	0.75	0.22	0.43	1.14	-21.9	108.2
<b>50</b>	0.40	0.10	0.49	0.97	0.48	0.14	0.26	0.74	-36.6	82.6
<b>75</b>	0.33	0.06	0.38	0.73	0.38	0.12	0.18	0.57	-44.2	75.0
<b>100</b>	0.27	0.03	0.31	0.58	0.31	0.10	0.14	0.47	<b>-49.7</b>	<b>72.8</b>
<b>China</b>										
<b>1</b>	3.89	3.16	6.20	9.51	6.15	1.49	3.92	8.58	0.8	120.2
<b>5</b>	2.97	2.36	3.35	4.40	3.35	0.39	2.73	3.99	-8.1	34.1
<b>10</b>	2.40	1.95	2.57	3.24	2.57	0.24	2.18	2.97	-9.2	23.9
<b>20</b>	1.72	1.41	1.81	2.22	1.81	0.15	1.57	2.05	-8.8	19.0
<b>50</b>	0.90	0.76	0.95	1.15	0.95	0.06	0.85	1.06	-6.5	17.0
<b>75</b>	0.63	0.53	0.66	0.80	0.66	0.04	0.60	0.74	-5.4	16.9
<b>100</b>	0.48	0.40	0.50	0.60	0.50	0.03	0.45	0.56	<b>-5.0</b>	<b>16.9</b>
<b>Turkey</b>										
<b>1</b>	3.86	1.54	6.35	11.05	6.33	1.82	3.26	9.23	-15.5	139.2
<b>5</b>	2.91	1.25	3.35	5.21	3.39	0.74	2.08	4.50	-28.5	55.0
<b>10</b>	2.27	0.92	2.46	3.68	2.51	0.49	1.63	3.22	-27.9	42.0
<b>20</b>	1.57	0.61	1.65	2.38	1.69	0.30	1.13	2.10	-27.9	33.8
<b>50</b>	0.80	0.34	0.84	1.15	0.85	0.13	0.60	1.03	-24.6	29.0
<b>75</b>	0.55	0.25	0.58	0.79	0.59	0.09	0.43	0.71	-22.5	28.1
<b>100</b>	0.42	0.20	0.44	0.59	0.45	0.06	0.33	0.53	<b>-20.9</b>	<b>28.0</b>
<b>Ethiopia</b>										
<b>1</b>	7.00	4.40	15.24	26.46	15.14	4.37	8.07	22.41	15.3	220.2
<b>5</b>	5.46	3.62	7.91	12.07	7.96	1.68	5.04	10.44	-7.7	91.1
<b>10</b>	4.20	2.74	5.29	7.70	5.34	0.93	3.68	6.70	-12.3	59.6
<b>20</b>	2.69	1.60	3.03	4.49	3.02	0.49	2.23	3.81	-17.0	41.8
<b>50</b>	1.15	0.41	1.24	2.09	1.24	0.28	0.81	1.70	-29.6	48.8
<b>75</b>	0.75	0.15	0.82	1.48	0.82	0.22	0.46	1.18	-38.7	56.6
<b>100</b>	0.56	0.01	0.61	1.14	0.62	0.18	0.30	0.90	<b>-46.0</b>	<b>62.0</b>
<b>Madagascar</b>										
<b>1</b>	11.07	7.47	18.82	32.47	18.61	4.85	11.23	27.54	1.4	148.8
<b>5</b>	6.46	4.92	8.23	12.40	8.19	1.35	6.00	10.55	-7.1	63.4
<b>10</b>	4.29	3.25	5.23	7.55	5.20	0.74	4.08	6.49	-5.0	51.3
<b>20</b>	2.79	1.94	3.28	4.55	3.25	0.43	2.58	4.02	-7.3	44.2
<b>50</b>	1.51	0.98	1.66	2.21	1.67	0.18	1.36	1.95	-9.6	29.6
<b>75</b>	1.09	0.71	1.17	1.52	1.18	0.11	0.98	1.36	-9.9	24.3
<b>100</b>	0.85	0.56	0.90	1.15	0.90	0.08	0.76	1.03	<b>-9.9</b>	<b>21.7</b>

### *Patterns of carbon loss*

An important observation is that the time soil needs to reach a new stable carbon content varies greatly with the climatic gradient (Figure 3.2). While in the driest and coldest Tibet desert it seems that after 100 years the soil has not reached a new stable carbon content and its carbon content continues to decline, the Dakota site needs more than 70-80, the China site 50-60 years, the Turkey site 40-50 years, the Ethiopia site 20-30 and the Madagascar site 40 -50 years (the sequence of the sites was given according to the climatic index RID). However, apart from the climatic conditions, other soil properties as well as crop type and management play a crucial role. For example, the soil in the Madagascar contains 70% clay and this might explain why it requires more extended period of time to reach a new stable carbon content as compared to the soil in Ethiopia.

In order to compare the pattern of carbon loss in the climatic gradient constituted by the six sites the average SOC loss (t C/ha y) with time is given in Figure 3.3a. The cumulative decline of SOC, proportional to the initial stocks is also presented in Figure 3.3b. The carbon decline in the 1<sup>st</sup> year after the landuse conversion to cropland was found to vary in the study sites from 1% to 10% of the initial SOC and the amount of carbon lost was found to be 1 to 11 t/ha. After 100 year cultivation the average carbon loss varied from 0.32% to 0.77% of the initial SOC (respectively cumulative loss from 32%/y to 77%/y of the initial SOC, Figure 3.3b) and as amount of carbon lost was found to be 0.27 to 0.85 t/ha y. Figure 3.3c presents the ratio of the POC loss to SOC loss. The values higher to 1 indicate that in the specific site the carbon related to the silt-clay fraction increases. This pattern was observed in Ethiopia, while a very slight decline was also observed in Dakota. Apart from these two sites the ratio of POC decline to SOC decline decreased in time.

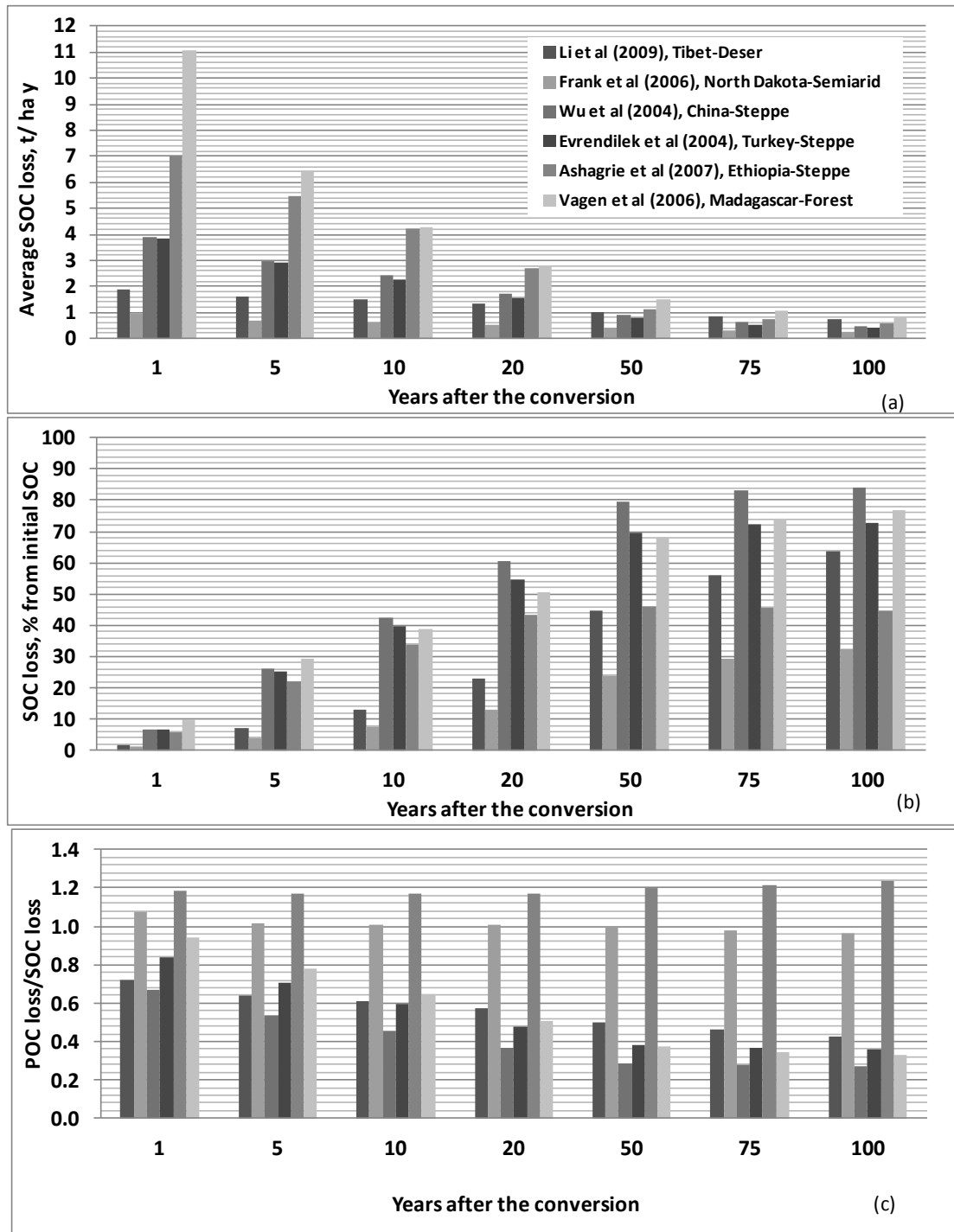


Figure 3.3 a) Carbon loss in terms of average SOC loss, b) The cumulative loss of SOC proportional to the initial stocks, c) the ratio of the POC loss to the SOC loss.

In all sites the average rate of carbon decline (t C/ha y) as well as average proportional to the initial SOC amount carbon loss (% of the initial SOC/y) follows a logarithmic pattern, as it is depicted in Figure 3.4a and 3.4b, respectively. For comparison, the data taken from Mann (1986) are also drawn as inserts within these two figures. Mann's compilation of data refers to studies published between the years 1914-1983. The upper limit of the y axis of the small figures was higher (see Figure 1.4) but for comparison reasons it is given the same with the large figures. The data set used describes the carbon loss in an extended climatic gradient and it seems that it covers a larger area (upper limit-see carbon loss after the 20<sup>th</sup> year of the conversion, as well lower limit-see carbon loss the early years after the conversion) than the area covered by the data taken by Mann (1986). A higher carbon decline was observed by Mann (1986) for the very early years after the conversion (1-3 years). However, while the sites correspond to lower limit of this study refer to 30 cm soil depth like Mann's (1986) data, the soil depth of the sites found in the upper limit is 20 cm, and may be a loss referred to 30 cm would be higher. Nevertheless, seasonal influences may be also responsible for the observed high rates of carbon loss in the first years.

The stepwise regression (Table 3.4) of the average % from the initial SOC per year carbon loss with the POC to SOC ratio and the temperature (TEMP) as well with the POC to SOC ratio and the Radiational Index of Dryness (RID) indicated that the first 20 years TEMP or RID could better explain the variation of the sites and their effect gradually decreased and afterwards (see the column with the 50<sup>th</sup> year in the table) the POC to SOC ratio explained better the observed variation and its effect gradually increased.

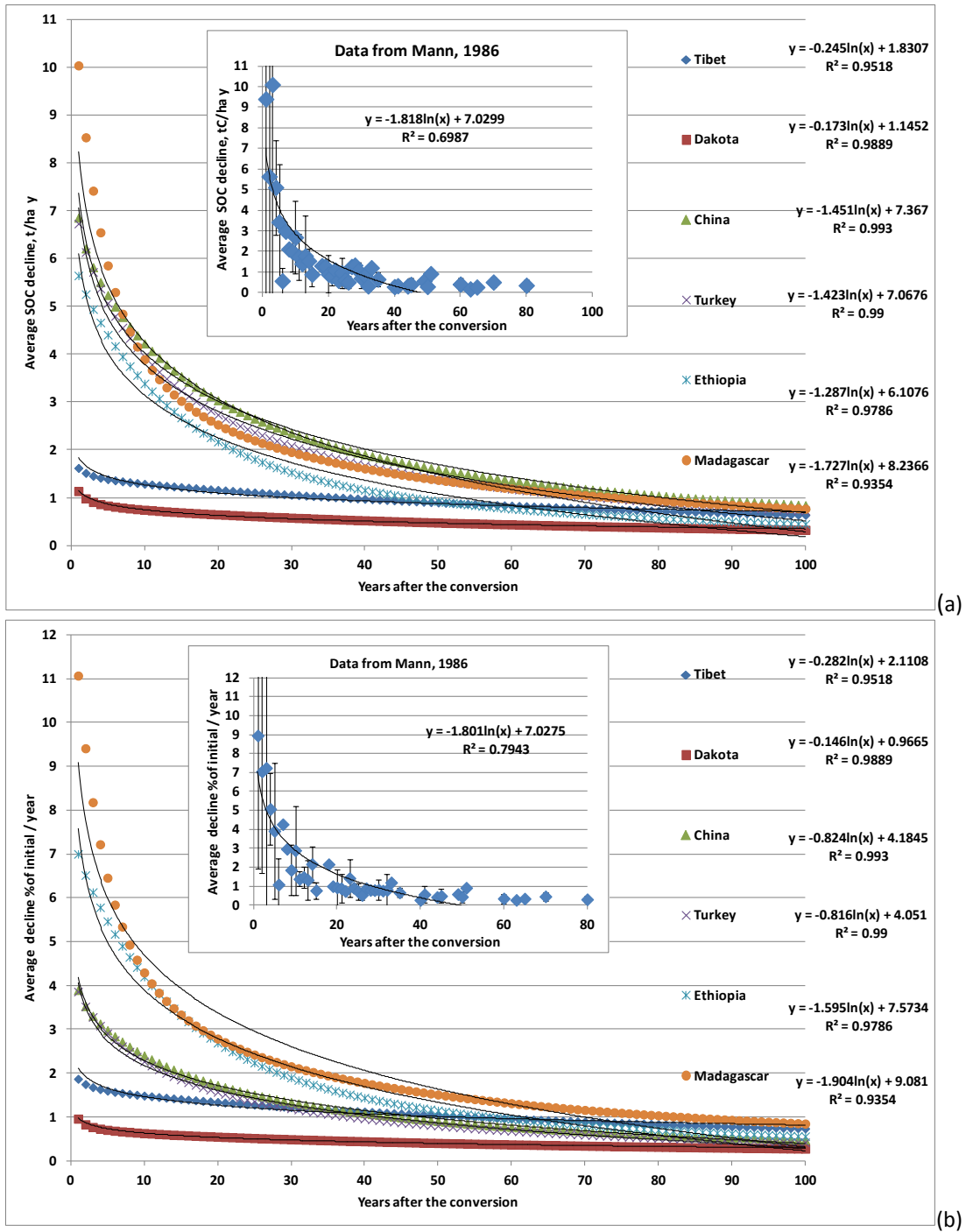


Figure 3.4 Carbon loss in terms of a) average rate of SOC loss, b) and as proportional to initial SOC amount. The data of Mann (1986) are also drawn in the inserts within the figures, soil depth 30 cm.

Table 3.4 Stepwise regression of the average % from the initial SOC/ y loss (for the 1<sup>st</sup>, 5<sup>th</sup>, 10<sup>th</sup>, 20<sup>th</sup>, 50<sup>th</sup>, 75<sup>th</sup>, and the 100<sup>th</sup> year after the conversion) with the POC to SOC ratio and the temperature (TEMP) and the POC to SOC ratio and the Radiational Index of Dryness (RID).

Year after the conversion	1		5		10		20		50		75		100	
<b>constant</b>	1.303	-1.137	5.7021	-0.608	13.37	3.694	30.45	11.77	67.3	94.62	83.84	104.31	93.95	108.84
<b>POC/SOC</b>	-0.05		-0.13		-0.21		-0.4		-0.84	-0.99	-1	-1.12	-1.09	-1.17
<b>T-Value</b>	-1.22		-0.78		-0.66		-0.94		-2.24	-2.2	-3.42	-3.23	-4.5	-4.35
<b>P-Value</b>	0.31		0.495		0.554		0.416		0.111	0.093	0.042	0.032	0.02	0.012
<b>TEMP</b>	0.55	0.58	1.68	1.77	2.16	2.3	2.4	2.6	1.9		1.43		1.04	
<b>T-Value</b>	4.48	4.62	3.37	3.85	2.42	2.85	1.94	2.26	1.78		1.7		1.5	
<b>P-Value</b>	0.021	0.01	0.043	0.018	0.094	0.046	0.147	0.087	0.173		0.188		0.23	
<b>S</b>	1.4	1.5	5.8	5.5	10.4	9.7	14.2	14.0	12.5	15.6	9.9	11.9	8.1	9.3
<b>R-Sq</b>	<b>89.5</b>	<b>84.2</b>	<b>82.3</b>	<b>78.7</b>	<b>71.3</b>	<b>67.1</b>	<b>66.0</b>	<b>56.0</b>	<b>78.0</b>	<b>54.7</b>	<b>85.9</b>	<b>72.3</b>	<b>90.1</b>	<b>82.6</b>
<b>R-Sq(adj)</b>	82.4	80.3	70.5	73.4	52.2	58.9	43.4	45.0	63.3	43.4	76.5	65.4	83.4	78.2
Year after the conversion	1		5		10		20		50		75		100	
<b>constant</b>	15.8	10.64	50.23	35.48	71.06	50.59	94.25	64.32	119.2	94.62	122.4	104.3	121.5	108.8
<b>POC/SOC</b>	-0.12		-0.34		-0.48		-0.7		-1.08	-0.99	-1.18	-1.12	-1.22	-1.17
<b>T-Value</b>	-4.78		-2.63		-1.85		-1.93		-3.36	-2.2	-4.51	-3.23	-5.34	-4.35
<b>P-Value</b>	0.017		0.078		0.162		0.149		0.044	0.093	0.02	0.032	0.013	0.012
<b>RID</b>	-2.79	-2.58	-8.6	-8	-11.2	-10.4	-12.6	-11.4	-10.3		-7.5		-5.3	
<b>T-Value</b>	-7.81	-2.87	-4.63	-2.76	-3.06	-2.26	-2.44	-1.72	-2.24		-2.02		-1.63	
<b>P-Value</b>	0.004	0.046	0.019	0.051	0.055	0.087	0.092	0.161	0.111		0.137		0.201	
<b>S</b>	0.9	2.2	4.5	7.0	8.8	11.2	12.3	16.0	11.0	15.6	9.0	11.9	7.8	9.3
<b>R-Sq</b>	<b>96.2</b>	<b>67.3</b>	<b>89.6</b>	<b>65.6</b>	<b>79.4</b>	<b>56.0</b>	<b>74.3</b>	<b>42.5</b>	<b>83.0</b>	<b>54.7</b>	<b>88.2</b>	<b>72.3</b>	<b>90.8</b>	<b>82.6</b>
<b>R-Sq(adj)</b>	93.7	59.1	82.6	57.0	65.7	45.1	57.2	28.2	71.7	43.4	80.4	65.4	84.6	78.2

### *Carbon addition scenarios*

The effectiveness of carbon addition by the application of amendments of different quality at an annually rate of 2.5 t C/ha, was expressed by the ratio of the Net C to carbon amended presented in Figure 3.5a. Net C refers to the extra carbon sequestered as compared with the soil where no amended was applied and carbon amended refers to the cumulative load of the carbon amended to soil. The Net C to C amended ratio was found in all sites to be higher for the 10/70/20 compost, followed by the 30/60/10 and the 49/49/2. In all cases the ratio significantly decline with time over a logarithmic pattern, indicating the importance of such simulation in the design of long-term agricultural management plans. The long term effectiveness is higher in Tibet, Dakota, and Ethiopia. Specifically, the effectiveness of the 49/49/2, 30/60/10, and 10/70/20 was in Dakota 0.30, 0.39, and 0.49, respectively; in Tibet 0.25, 0.32, and 0.40, correspondingly and in Ethiopia 0.15, 0.21, and 0.27. In the rest three sites and for the three amendment types was lower and ranged from 0.06 to 0.11. In the three sites presenting the highest effectiveness, the average annual decomposition rate of the RPM (0.023 to 0.125 1/y) and particularly the HUM pool (0.006 to 0.013 1/y) was very low compared to the other three sites (RPM: 0.183 to 0.446 1/y, HUM: 0.039 to 0.063 1/y). Worth noting is the low decomposition rates observed in Ethiopia which could be probably related to high clay content of the soil (49%).

The proportion of the carbon sequestered due to the application of the amendment that is stabilized in the silt-clay fraction (the BIO and HUM RothC modeled pools) is presented in Figure 3.5b. The proportion increases with time and it is higher (2% to 4.5%) in the amendments contain more RPM and HUM carbon pools. More significant was the difference in the Tibet and Dakota sites, due to the extremely low HUM decomposition rates. After 100 years of application for example for the 30/60/10 amendment the carbon stabilized in the silt-clay fraction from the totally carbon sequestred was 40.8% in Tibet, 39.8% in Dakota, 60.6% in China, 64.2% in Turkey, 78% in Ethiopia and 83.1% in Madagascar.

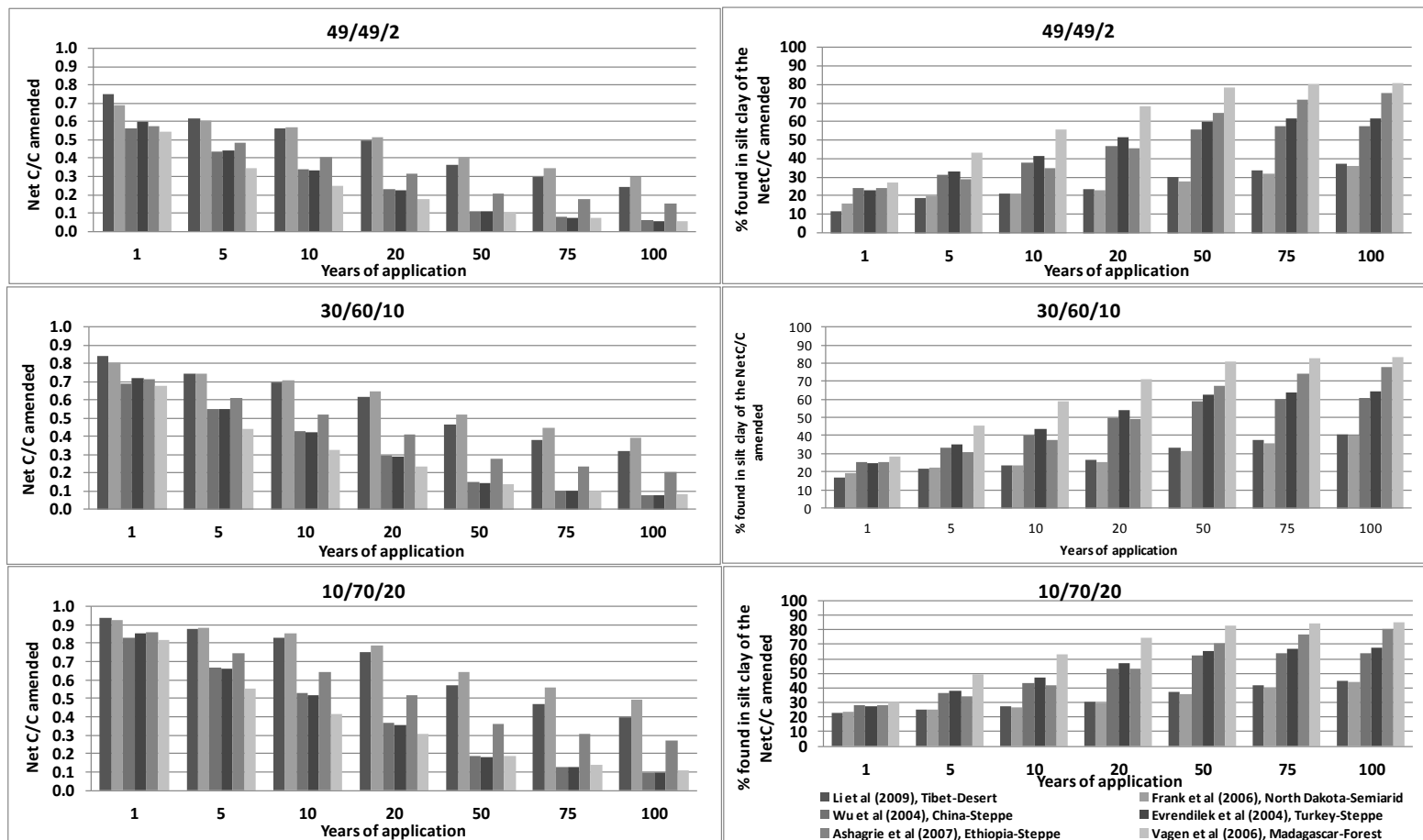


Figure 3.5 a) The effectiveness of carbon addition by the application of amendments of different quality at annually doses of 2.5 t C/ha (carbon amended: the cumulative load of the carbon amended to soil, Net C: the extra carbon sequestered as compared with the soil where no amended was applied), b) the proportion of the carbon sequestered that is stabilized in the silt-clay fraction.

### *Decomposition rates and the Q10 factor*

The linear correlation of the annual RPM and HUM decomposition rate constants with climatic indexes, soil clay content and the size of the initial POC pool is presented in Figure 3.6. The RPM constant correlates better with the climatic indices as compared with the HUM constant. Other soil properties like the clay content should affect significantly the rates. The HUM rate was found to be negatively correlated with the POC initial pool. Temperature (TEMP) gave the best correlation for both RPM and HUM as compared with the Aridity Index and the Radiational Index of Dryness. The stepwise regression (Person correlation) conducted for the HUM with POC initial, TEMP, and clay (Table 3.5) indicated R-Sq for POC initial 64.43%, for POC initial and TEMP, 84.53% and POC initial, TEMP and clay 94.44%. The HUM rate increases for higher TEMP and lower initial POC and clay. The stepwise regression of the RPM with POC initial and TEMP (Table 3.5) indicated R-Sq for TEMP 79.42% and for TEMP and POC initial 84%. The RPM rate increases for higher TEMP and lower initial POC. The strong linear relation of RPM with the clay is responsible for that. However this effect is an artifact, since clay content increases in sites with lower RID and TEMP. Multiple tests of stepwise regressions (not presented here) were conducted to examine if there are other possible combinations to describe the results.

The Q10 temperature factor, which indicates the measure of the change of the decomposition rate as a consequence of increasing the temperature by 10 °C given by the equation  $Q_{10}=(R_2/R_1)^{10/(T_2-T_1)}$ , was calculated for both the RPM and HUM pools (Table 3.6). The decomposition rate as given by multiplying the RothC 'a' temperature correction with the calibrated decomposition rate constant was linear correlated with temperature and the Q10 was calculated for the 5-15 °C and 15-30 °C temperature range ( $R^2$  higher than 0.9 with few exceptions higher than 0.8). The HUM rate did not have significant correlation with TEMP and therefore the two sites with clay content 49 and 70% were excluded (Ethiopia and Madagascar) to obtain a good correlation. The Q10 was re-calculated for RPM again.

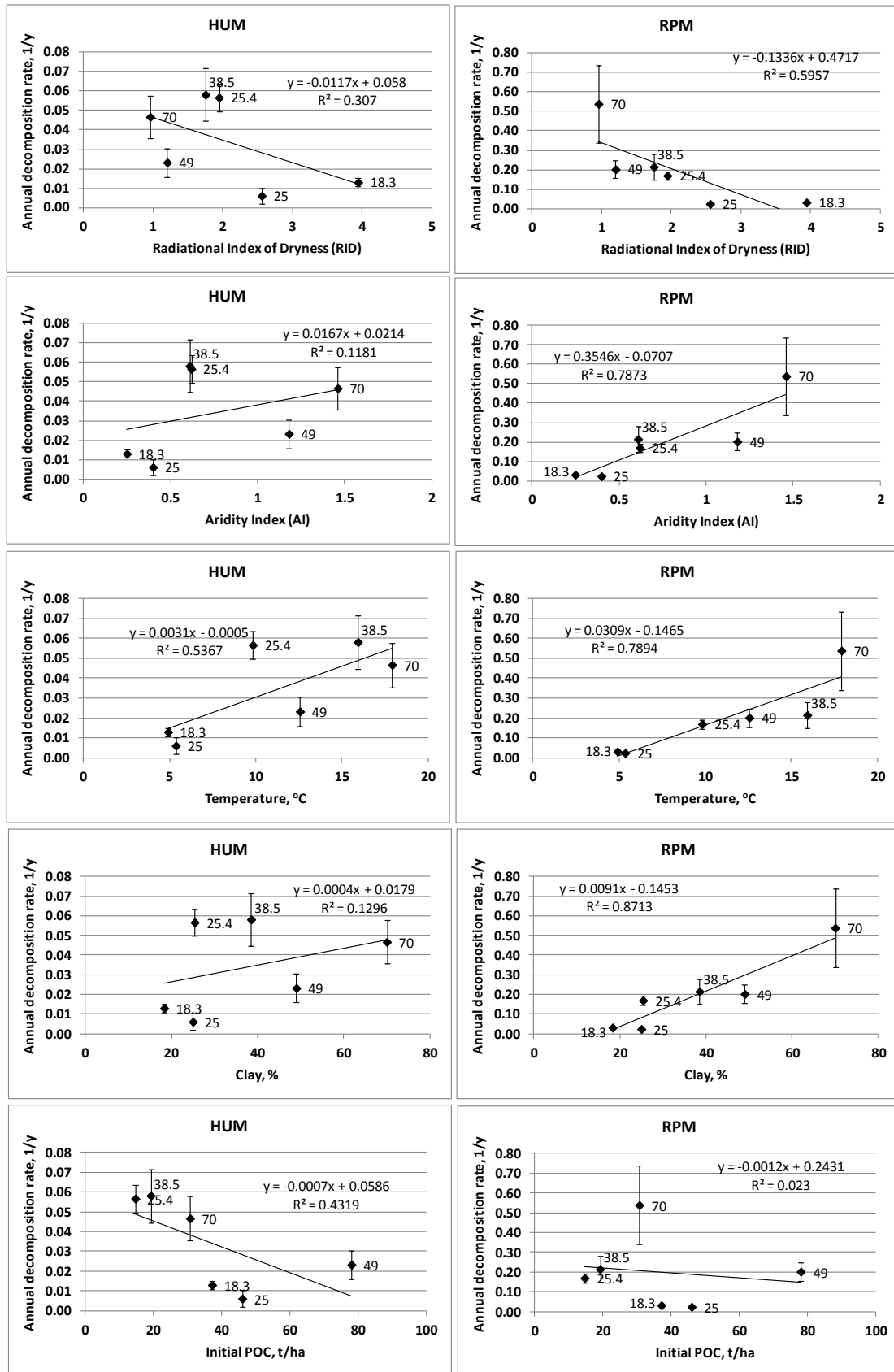


Figure 3.6 Linear correlations of the annual RPM and HUM decomposition rates with climatic indexes, the soil clay content and the Particulate Organic Carbon (POC) initial pool.

**Table 3.5 Stepwise regression (Pearson correlation) of the RPM and HUM annual decomposition rates with the clay (only in the case of HUM) content, the temperature (TEMP) and the particulate organic carbon (POC) initial pool.**

	HUM			RPM	
	3	2	1	2	1
<b>constant</b>	0.02959	0.03912	0.06628	-0.0504	-0.11627
<b>clay</b>	-0.00109				
<b>T-Value</b>	-1.89				
<b>P-Value</b>	0.2				
<b>TEMP</b>	0.0058	0.0022		0.025	0.0259
<b>T-Value</b>	2.79	1.97		3.68	3.93
<b>P-Value</b>	0.108	0.143		0.035	0.017
<b>POC initial</b>	-0.00054	-0.00083	-0.00091	-0.0015	
<b>T-Value</b>	-2.21	-3.2	-2.69	-0.93	
<b>P-Value</b>	0.158	0.049	0.055	0.423	
<b>S</b>	0.00968	0.0132	0.0173	0.0807	0.0792
<b>R-Sq, %</b>	<b>94.44</b>	<b>84.53</b>	<b>64.43</b>	<b>84.00</b>	<b>79.42</b>
<b>R-Sq(adj), %</b>	86.1	74.21	55.53	73.34	74.28

Finally, one more correction was conducted; since the soil depth for Tibet and Dakota was 30 cm and for the other four sites was 20 cm, the decomposition rate in the sites with 30 cm soil depth was increased by 30%, according to the suggestions of the RothC manual and the Q10 was re-calculated. This analysis aimed to examine what would be the Q10 in the study sites with the use of the specific corrections for soil moisture cover ('b' correction factor) and soil cover ('c' correction factor) used by RothC. The calculations were also conducted apart from the calibrated values of the optimum simulation for the rates derived by the mean, min and max of the distributions of the parameters that calculated by the sensitivity analysis. For the range of the 15-25 °C the Q10 for RPM was estimated to be 1.66 to 1.88 (4 sites and soil depth correction-optimum, 1.75) and for HUM 1.63 to 1.74 (4 sites and soil depth correction-optimum, 1.66). The Q10 for the HUM pool was found to be lower than the Q10 for the RPM by 5% (4 sites and soil depth correction-optimum); 0.7% to 9.2% was addressed by the uncertainty analysis. The default RothC Q10 factor (15-25 °C) deriving by the equation used for the temperature correction ( $a=47.9/(1+\exp(106/T+18.3))$ ) is 2.0, verifying that RothC overestimate decomposition at high temperatures. On the other hand in the lower temperature range of 5-15 °C the Q10 for RPM was estimated to be as high 2.96 to 8.17 (4 sites and soil depth correction-optimum, 4.04) and for HUM 2.71 to 3.78 (4 sites and soil depth correction-optimum, 2.98). The Q10 for the HUM pool was found to be lower than the Q10 for the RPM by 26.1% (4 sites and soil depth correction-optimum); 4.8% to 45.5% was addressed by the uncertainty analysis. The default RothC Q10 factor (5-15 °C)

deriving by the equation used for the temperature correction is 3.8 verifying the reported indications that RothC underestimates decomposition at low temperatures, in the case of the RPM pool. However regarding the HUM pool it seems that the Q10 temperature factor is lower than the default RothC Q10 factor in this dataset. In both temperature ranges and particularly in the lower range (5-15 °C) it is clear that Q10 should be significantly lower in the HUM pool. These results verify the indications that have been reported that temperature sensitivity of decomposition varies between different carbon pools, while typically most soil carbon models consider that soil SOM pools are equally sensitive to temperature (Takeshi et al., 2006). The apparent sensitivity estimated by this study includes also the textural gradient (clay content) of the sites. Sites with low temperature and dry conditions had low clay content (<20) which gradually increased with temperature and the moisture regime. Therefore, in the former sites, if clay content was higher, the ‘apparent’ temperature sensitivity would be lower and in the latter sites, if clay content was lower, the sensitivity would be higher.

**Table 3.6 The Q10 temperature factor (‘apparent’ sensitivity) for the RPM and HUM RothC model pools as calculated by the calibrated values of this study.**

	6 sites	6sites	4 sites <sup>2</sup>		4 sites <sup>2</sup>	
		soil depth correction <sup>1</sup>			soil depth correction <sup>1</sup>	
	RPM	RPM	RPM	HUM	RPM	HUM
<b>5-15°C</b>						
<b>mean</b>	5.76	4.40	5.06	2.75	3.93	2.79
<b>mean-1std</b>	3.68	2.96	3.84	3.65	3.05	2.94
<b>mean+1std</b>	8.17	5.93	6.18	3.48	4.71	2.71
<b>optimum</b>	4.82	3.77	5.15	3.78	<b>4.04</b>	<b>2.98</b>
<b>15-25°C</b>						
<b>mean</b>	1.83	1.77	1.80	1.64	1.75	1.64
<b>mean-1std</b>	1.73	1.66	1.74	1.73	1.67	1.66
<b>mean+1std</b>	1.88	1.83	1.84	1.71	1.79	1.63
<b>optimum</b>	1.79	1.73	1.81	1.74	1.75	1.66

<sup>1</sup>the decomposition rate in sites with 30 cm soil depth was increased by 30% to correspond to 20 cm.

<sup>2</sup>Excluded Ethiopia (49% clay) and Madagascar (70% clay)

### 3.4 CONCLUSIONS

In this work the methodology developed and presented in chapter 2 was used in order to calibrate, assess the sensitivity and simulate the uncertainty in carbon turnover (RothC model) during native land to cropland conversion along a climatic gradient from Desert to Forest (Budyco's Radiational Index of Dryness from 3.94 to 0.96) with data obtained by relative published studies. Scenarios of carbon addition of materials of different quality were also conducted to assess their effectiveness under the different climatic conditions and soil types. The 'apparent' temperature sensitivity of the RPM and HUM RothC carbon pools was estimated with the calculation of the Q10 factor.

- The sensitivity analysis suggested that the most sensitive parameters were the HUM and RPM decomposition rate constants, as well as the plant litter input and the RPM initial pools in the sites where it was not field measured with physical fractionations. Sensitivity greatly depended on the available data for the calibration of the parameters.
- The uncertainty of the simulated carbon loss after 100 years cultivation was 26.9% -Tibet, 122.5% -Dakota, 21.9% -China, 48.9% -Turkey, 108% -Ethiopia, and 31.6% -Madagascar of the total amount of C decline due to the landuse conversion. The uncertainty was smaller in the sites with available field measured POC data and information about the plant input. The analysis showed that the resulting uncertainties are significant emphasizing the necessity of obtaining accurate plant input data and other physical soil parameters as well as quantifying the variability of initial conditions in order to reduce the uncertainty of carbon turnover projections, in accordance with the results of the previous chapter.
- The average carbon loss per year-as a percentage of the initial SOC- after the conversion to cropland varied in the study sites from 1% to 10% the 1<sup>st</sup> year after the conversion and from 0.32%/y to 0.77%/y the 100<sup>th</sup> year. The average amount of carbon lost varied from 1 to 11 t C/ha the 1<sup>st</sup> year and 0.27 to 0.85 t C/ha y the 100<sup>th</sup> year. The decline of the rates follows a logarithmic pattern. POC losses were more significant in the early years after the conversion and losses of the carbon related to the silt-clay fraction, basically the BIO and HUM RothC modeled pool in the later years. The POC to SOC ratio of the soil before the conversion greatly determines the % loss in the long term. The time to reach the soil a new stable carbon content varies greatly with the climatic gradient varying from more than 100 years (Tibet, Desert) to 20-30 (Ethiopia, Forest)
- The Net C to C amended ratio as an index of the effectiveness of carbon addition varied greatly between sites. For example after 100 years of application (2.5 t C/ha y) of an

amendment with composition 30/60/10 (DPM/RPM/HUM) the Net C to C amended ratio was found to be in Dakota 0.39, in Tibet 0.32, in Ethiopia 0.21, in China and Madagascar 0.08, and in Turkey 0.07. The carbon stabilized in the silt-clay fraction from the totally carbon sequestered was 40.8% in Tibet, 39.8 in Dakota, 60.6 in China, 64.2 in Turkey, 78% in Ethiopia and 83.1 in Madagascar. The study sites presented the lower HUM decomposition rate presented also more effectiveness in carbon addition and more carbon was stabilized in the silt-clay fraction. In all cases the Net C to C amended ratio significantly decline with time over a logarithmic pattern. Reliable long term model simulations are important for the design of long-term sustainable agricultural practices (carbon sequestration, e.g. HUM increase) like the appropriate carbon addition under different climatic regimes and soil textures.

- The Q10 factor for the RPM pool (1.75, range 1.66-1.88) was found to be lower than the default RothC Q10 factor (2.00) in the 15-25 °C and higher in the range 5-15 °C (4.04, range 2.96-8.7 versus 3.88 in RothC). The Q10 factor for the HUM pool was found to be lower than the Q10 for the RPM by 5% (0.7% to 9.2%) in the 15-25 °C range and 26.1% (4.8% to 45.5%) in 15-25 °C range, indicating that temperature sensitivity of decomposition varies between different carbon pools and this should be included in carbon models. It was verified that RothC underestimates decomposition at low temperatures and overestimate at high temperatures. However, regarding the HUM pool at low temperatures in this dataset it seems that the Q10 factor is lower than the default RothC Q10 factor.

### 3.5 LITERATURE CITED

- Abiven, S., Menasseri, S., Chenu, C., 2009. The effects of organic input over time on soil aggregate stability – a literature analysis. *Soil Biology and Biochemistry* 41, 1-12.
- Ashagrie, Y., Zech, W., Guggenberger, G., Mamo T., 2007. Soil aggregation, and total and particulate organic matter following conversion of native forests to continuous cultivation in Ethiopia. *Soil and Tillage Research* 94, 101–108.
- Balesdent, J., Besnard, E., Arrouays D., Chenu, C., 1998. The dynamics of carbon in particle-size fractions of soil in a forest-cultivation sequence. *Plant Soil* 201, 49–57.
- Banwart, S., Bernasconi, S.M., Bloem, J., Blum, W., Brandao, M., Brantley, S., Chabaux, F., Duffy, C., Kram, P., Lair, G., Lundin, L., Nikolaidis, N., Novak, M., Panagos, P., Ragnarsdottir, K.V., Reynolds, B., Rousseva, S., de Ruyter, P., van Gaans, P., van Riemsdijk, W., White, T., Zhang, B., 2011. Assessing Soil Processes and Function in Critical Zone Observatories: hypotheses and experimental design. *Vadose Zone Journal* 10, 974-987.
- Coleman, K., Jenkinson, D.S., 1999. RothC-26.3 - A Model for the turnover of carbon in soil: Model description and windows users guide: November 1999 issue. Lawes Agricultural Trust Harpenden. ISBN 0 951 4456 8 5.
- Don, A., Scholten, T., Schulze E.D., 2009. Conversion of cropland into grassland: Implications for soil organic-carbon stocks in two soils with different texture. *Journal of Plant Nutrition and Soil Science* 172, 53–62.
- Evrendilek, F., Celik, I., Kilic, S., 2004. Changes in soil organic carbon and other physical soil properties along adjacent Mediterranean forest, grassland, and cropland ecosystems in Turkey. *Journal of Arid Environments*. 59, 743-752.
- Falloon, P., Smith, P., Coleman, K., Marshall, S., 1998. Estimating the size of the inert organic matter pool from total soil organic carbon content for use in the Rothamsted Carbon model. *Soil Biology and Biochemistry* 30, 1207–1211.
- Frank, A.B., Liebig, M.A., Tanaka, D.L., 2006. Management effects on soil CO<sub>2</sub> efflux in northern semiarid grassland and cropland. *Soil and Tillage Research* 89, 78-85.
- Galdo, I.D., Six, J., Peressotti, A., Cotrufo, M.F., 2003. Assessing the impact of land-use change on soil C sequestration in agricultural soils by means of organic matter fractionation and stable C isotopes. *Global Change Biology* 9, 1204–1213.
- Gottschalk, P., Bellarby, J., Chenu, C., Foereid, B., Smith, P., Wattenbach, M., Zingore, S., Smith, J., 2010. Simulation of soil organic carbon response at forest cultivation sequences using <sup>13</sup>C measurements. *Organic Geochemistry* 41, 41–54.
- Gottschalk, P., Bellarby, J., Chenu, C., Foereid, B., Smith, P., Wattenbach, M., Zingore, S., Smith, J., 2010. Simulation of soil organic carbon response at forest cultivation sequences using <sup>13</sup>C measurements. *Organic Geochemistry* 41, 41–54.
- Juston, J., Andr n, O., K tterer, T., Jansson, P.E., 2010. Uncertainty analyses for calibrating a soil carbon balance model to agricultural field trial data in Sweden and Kenya. *Ecological Modeling* 221, 1880-1888.
- Lal, R., 2001. World cropland soils as a source or sink for atmospheric carbon. *Advances in Agronomy* 71, 145–191.
- Lal R., 2004b. Soil Carbon Sequestration Impacts on Global Climate Change and Food Security. *Science* 304, 1623–1627.
- Lal, R., 2008. Carbon sequestration. *Philosophical Transactions of the Royal Society* 363, 815-830.
- Li, X.G., Zhang, P.L., Yin, P., Li, Y.K., Ma, Q.F., Long, R.J., Li, F.M., 2009. Soil organic carbon and nitrogen fractions and water-stable aggregation as affected by cropping and grassland reclamation in an arid sub-alpine soil. *Land Degradation and Development* 20, 176-186.
- Mafongoya, P.L., Bationo, A., Kihara, J., Wasw, B.S., 2006. Appropriate technologies to replenish soil fertility in southern Africa. *Nutrient Cycling in Agroecosystems* 76, 137–151.
- Mann, L.K., 1986. Changes in soil carbon storage after cultivation. *Soil Science* 142, 279-288.

- Martínez-Blanco, J., Muñoz, P., Antón A., and Rieradevall, J., 2009. Life cycle assessment of the use of compost from municipal organic waste for fertilization of tomato crops. *Resources, Conservation and Recycling* 53, 340–351.
- Paul, K.I., Polglase, P.J., Richards, G.P., 2003. Predicted change in soil carbon following afforestation or reforestation, and analysis of controlling factors by linking a C accounting model (CAMFor) to models of forest growth (3PG), litter decomposition (GENDEC) and soil C turnover (RothC). *Forest Ecology and Management* 177, 485-501.
- Peltre C., Christensen B.T., Dragon S., Icard C., Kätterer T., Houot S., 2010. Optimisation of the RothC model pools to simulate C dynamics after application of exogenous organic matters in soils. 14th Ramiran International Conference, Lisboa (PRT), 13-15/09/2010, (oral communication, abstract).
- Rasmussen, P.E., Goulding, K.W.T., Brown, J.R., Grace, P.R. Janzen, H.H., M., Körschens, 1998. Long-Term Agroecosystem Experiments: Assessing Agricultural Sustainability and Global Change. 282, 893-896.
- Rees, R.M., Bingham, I.J., Baddeley, J.A., Watson, C.A., 2005. The role of plants and land management in sequestering soil carbon in temperate arable and grassland. *Geoderma* 128, 130-154.
- Schulze, E.D., Freibauer, A., 2005. Carbon unlocked from soils. *Nature* 437, 205-206.
- Six, J., Elliott, E.T., Paustian, K., 2000. Soil macroaggregate turnover and microaggregate formation: a mechanism for carbon sequestration under no tillage agriculture. *Short Comm. Soil Biology and Biochemistry* 32, 2099-2103.
- Stamati, F.E., Kotronakis, M., Fragia, T., Paranychianakis, N., Kalogerakis, N., Nikolaidis, N.P. Modeling carbon sequestration potential in Cretan soils. 5th Bioremediation, July 4-7, 2011 in Chania, Crete, Greece
- Takeshi, I., and Moorcroft, P.R., 2006. The global-scale temperature and moisture dependencies of soil organic carbon decomposition: an analysis using a mechanistic decomposition model. *Biogeochemistry* 80, 217–231.
- Thornthwaite, C. W. and J. R. Mather. 1962. Average climatic water balance data of the continents. Part 1, Africa. Centerton, NJ: 15(2) 172pp C. W. Thornthwaite Associates.
- Vagen, T.G., Andrianorofanomezana, M.A.A., Andrianorofanomezana, S., 2006. Deforestation and cultivation effects on characteristics of oxisols in the highlands of Madagascar. *Geoderma* 131, 190-200.
- Wagai, R., Mayer, L.M., Kitayama, K., Knicker, H., 2008. Climate and parent material controls on organic matter storage in surface soils: three-pool, density-separation approach. *Geoderma* 147, 23-33.
- Wu, T., et al. 2004. Influence of cultivation and fertilization on total organic carbon and carbon fractions in soils from the Loess Plateau of China. *Soil and Tillage Research* 77, 59-68.



#### 4. DEVELOPMENT OF A COUPLED CARBON, AGGREGATION AND STRUCTURE TURNOVER (CAST) MODEL FOR TOPSOILS

---

*Validation with field data of two contrasting crop production to set-aside conversions*

---

**Abstract:** The current multi-pool soil organic carbon (SOC) models, although a major improvement over single-pool ones, are not always able to capture soil saturation capacity and give reliable predictions for climate change effects, since they do not account for environmental constraints, like physical protection. In this work, a soil carbon, aggregation, and structure turnover (CAST) model was developed based on the concept suggested by many authors in the scientific literature that macro-aggregates are formed around particulate organic matter, followed by the release of micro-aggregates. A simplified mechanistic Nitrogen model was also developed. The CAST model was evaluated by field data of cropland to set-aside conversions of Critical Zones Observatories in Greece (fine textured Mediterranean) and Iowa (coarse textured humid continental). The model was able to capture the carbon content and the C-to-N ratio content of the pools comprising the three aggregate types (macro-aggregates: >250  $\mu\text{m}$ , micro-aggregates: 53-250  $\mu\text{m}$ , silt-clay sized aggregates: <53  $\mu\text{m}$ ) in both sites. The soil system reached maximum macro-aggregation/porosity and minimum bulk density after 7 and 14 years in Greece and Iowa, respectively. From then onward, macro-aggregate disruption presented a constant seasonal pattern and any further SOC increase was due to micro-aggregation resulting in the increase of bulk density and decrease of porosity towards a stable value. The CAST model can assist in revealing the primary factors determining organic matter, aggregation, and structure turnover in different ecosystems and in describing the response of the soil system to management practices, landuse changes, and climate change in order to design and optimize the appropriate measures/practices.

## 4.1 INTRODUCTION

The current multi-pool soil carbon models have been a major improvement over the single pool ones (Davidson and Janssens, 2006). However, they are not always able to capture the soil saturation capacity to bind carbon (Powlson et al., 2011) and give reliable predictions for landuse changes, management practices, and climate change effects, since they do not account for environmental constraints, like physical protection (Davidson and Janssens, 2006, Kleber and Johnson, 2010, see also paragraph 1.3.2). Six et al. (2002a) acknowledged that one of the major knowledge gaps and a research priority is the mechanistic explanation of the saturation capacity level. Van Veen and Paul (1981), have recognized long ago that the equilibrium level of soil organic carbon (SOC) is more dependent on the extent of protection than on the decomposition rate of the plant residues added to soil.

Most models were designed based on the assumption that biochemically protected carbon contributing to humus, inert or passive, organic carbon pools was the product of the humification process resulting in a very stable highly aromatic material (Kleber and Johnson, 2010). Aromatic structures found in stable materials are the products of incomplete combustion (biochar) and are not the result of the natural decomposition process (Knicker, 2007; Baldock, 2007; Kleber and Johnson, 2010). The combination of physical fractionations (aggregate, particle size, and density fractions) with various chemical and spectroscopic methods for the chemical characterization of these fractions, have offered evidence and insight for the formulation of a more mechanistic conceptualization of soil organic matter (SOM) turnover, composition and stabilization (see reviews of Lützow et al., 2007 and Grandy and Neff, 2008, see also paragraph 1.2.2). An updated concept of the dynamic nature of SOM is the realization that inaccessibility and sorption interactions with mineral surfaces may provide powerful protection against decomposition, explicitly including carbohydrates, proteins and other 'labile' materials (Kleber and Johnson, 2010). Stabilization of SOM is thought to be due to (see also paragraph 1.2.4): 1) stabilization by organo-mineral interactions-association with silt and clay (OM that is absorbed to minerals or entrapped in very small micro-aggregates) and 2) physical protection within macro-aggregate and micro-aggregate structures (Six et al., 2002a; Six et al., 2002b).

Physical protection in SOM turnover has been included in models using simplified parameterization such as reduced life-time, protection coefficient or periodically transferred to a more labile pool during cultivation events (Van Veen and Paul, 1981; Molina et al.,

1983). Hassink and Whitmore (1997) developed a model where the rate at which organic matter became protected depended on the degree to which the protective capacity was filled, incorporating the processes of desorption and adsorption in order to model silt and clay protection of SOM. Most of the current models of SOM dynamics simply affect the decay rates of SOM pools by an empirical parameter corresponding to landuse. Recently, Malamoud et al. (2008) made the assumption that the primary interactions occur between clay particles and SOC components to form organo-mineral associations, which were then bound together to form aggregates (STRUC-C model). Even though STRUC-C has significant limitations, as outlined by the authors, it is the most comprehensive attempt to model soil aggregate stability and turnover as well as soil structure in the scientific literature thus far (Nikolaidis and Bidoglio, 2011; Adams et al., 2011). The STRUC-C model considered each aggregate type as being a single carbon pool and did not account for particulate organic matter (POM) in the aggregation process; the DPM (Decomposable Plant Material) and RPM (Resistant Plant Material) RothC carbon pools. In addition, the formation of macro-aggregates (>250  $\mu\text{m}$ ) was considered as the aggregation product of micro-aggregates (>53-250  $\mu\text{m}$ ), although macro-aggregates are known to consist of both micro-aggregates and silt-clay sized aggregates (<53  $\mu\text{m}$ ) as well as POM.

Adams et al. (2011) argued that it is essential to model SOM dynamics more deterministically in order to reproduce the processes of physical protection. The conceptual model suggested by many authors in the scientific literature, that macro-aggregates are formed around particulate organic matter (POM), followed by the release of micro-aggregates as the occluded organic materials are decomposed (Golchin 1994; Balesdent et al., 2000; Puget et al., 2000; Plante and McGill, 2002; Six et al., 2002a; Six et al., 2002b; Six et al., 2004; Bronick and Lal, 2005, Helfrich et al., 2008; Nikolaidis and Bidoglio, 2011) has not been modeled yet. Significant improvement of carbon modeling will entail a deterministic explanation of the saturation capacity of the different carbon pools, estimation of the rates of occlusion or release of labile organic materials and therefore their availability for mineralization or stabilization (Plante and McGill, 2002), evaluation of soil structure (related with soil hydraulics and fertility) and optimization of the appropriate measures/practices to manage landuse changes, and climate change (Bronick and Lal, 2005; Rees et al., 2005).

In this work a soil carbon, aggregation, and structure turnover (CAST) model and a simplified mechanistic N model were developed, based on current knowledge of the proposed mechanism in the relevant scientific literature that suggests that macro-aggregates are

formed around POM, followed by the release of micro-aggregates. The model was evaluated using field data of cropland to set-aside conversions in a fine textured Mediterranean site in Greece and a coarse textured humid continental site in Iowa.

## **4.2 METHODOLOGY**

### **4.2.1 Model conceptualization and description**

A schematic overview of current knowledge on macro-aggregate formation and disruption is provided in Figure 4.1. Plant residue is incorporated in the soil system and is colonized by microbial decomposers. Fungal hyphae, microbial metabolites and root exudates provide the binding for soil particles and smaller aggregates to cells of bacteria or fungi and form macro-aggregates around POM. Macro-aggregated POM is further decomposed and fragmented into smaller particles. Some of this finely fragmented POM becomes encrusted with mineral particles (silt-clay sized micro-aggregates) and microbial byproducts, leading to the formation of micro-aggregates within macro-aggregates. Biodegradation of the easily decomposable incorporated OM, results in the decrease of the microbial growth/activity and the supply of microbial biopolymers and macro-aggregates become less stable. Then if slaking occurs with rapid contact of aggregates with water, these macro-aggregates would release stabilized micro-aggregates and silt –clay sized aggregates and highly decomposed residual POM would become unprotected. These materials may subsequently be reincorporated into new aggregates if fresh plant residue enters the system.

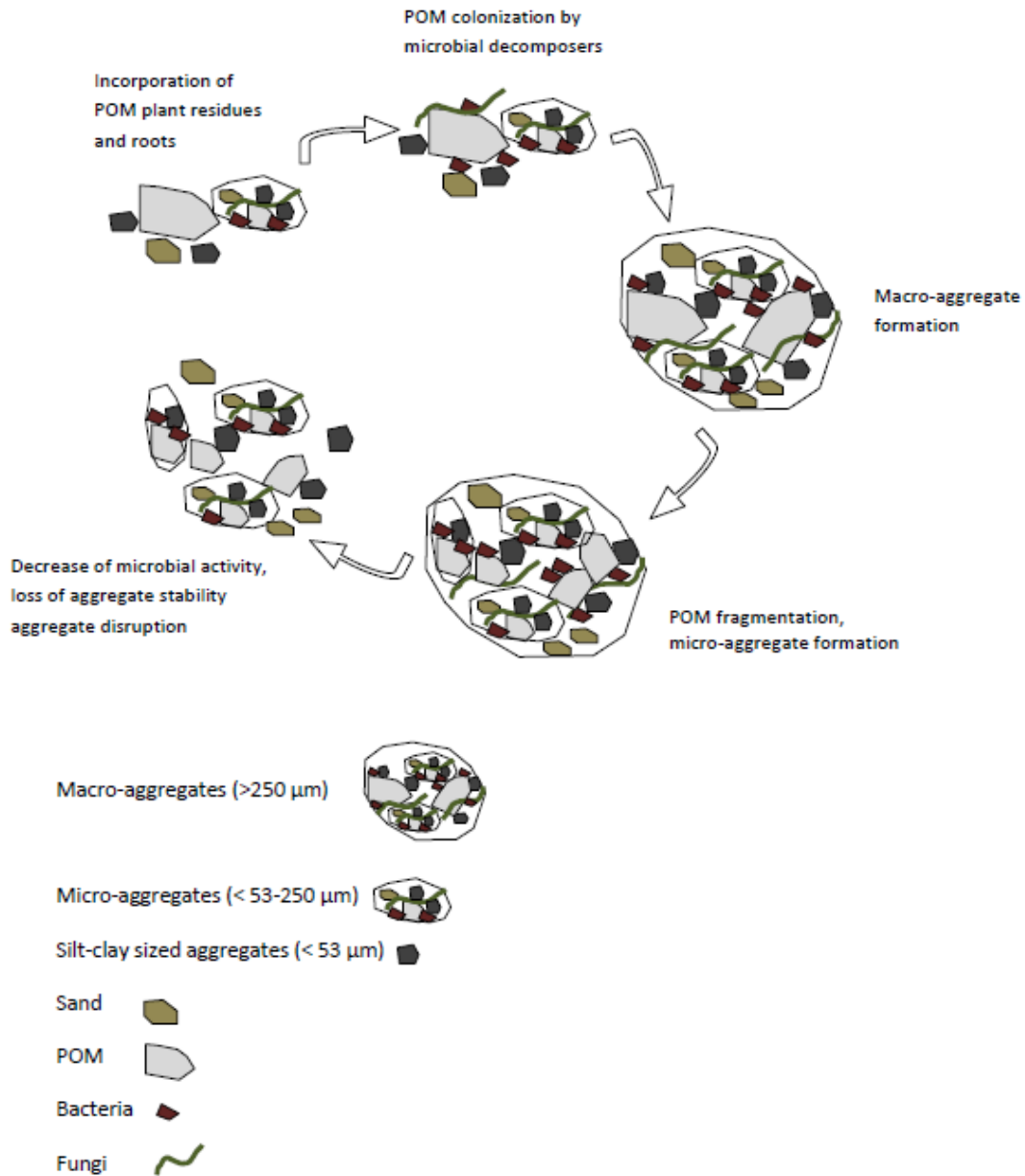


**Figure 4.1 Schematic overview of macro-aggregation.**

The structure of the developed soil carbon, aggregation, and structure turnover (CAST) model is depicted in Figure 4.2. The model was developed in MATLAB (Version 7.10.0499 (R2010a)). Three aggregate types are considered consisting of the relative RothC carbon pools with distinct turnover rates (Figure 4.2): Decomposable Plant Material (DPM), Resistant Plant Material (RPM), Microbial Biomass (BIO), Humified Organic Matter (HUM) and Inert Organic Matter (IOM). AC1, AC2, and AC3 are the three types of aggregate sizes incorporated in the model. The AC1 aggregate type corresponds to silt-clay sized aggregates (<53  $\mu\text{m}$ ), consisting

of BIO, HUM, and IOM. The AC2 aggregate type corresponds to micro-aggregates (53–250  $\mu\text{m}$ ) consisting of BIO, HUM, IOM, and fine DPM and RPM pools. The AC3 aggregate type corresponds to macro-aggregates (>250  $\mu\text{m}$ ) consisting of BIO, HUM, IOM, and fine and coarse deriving DPM and RPM pools. Each carbon pool of the aggregate types decomposes by a first-order process with its own characteristic rate, in the same way as in RothC producing  $\text{CO}_2$ , BIO and HUM, apart from the IOM pool which corresponds to biochar and is resistant to decomposition. The decomposition rate constant ( $k$ ) is corrected by the product ( $abc$ ) of three correction factors for the major factors determine microbial activity (' $a$ ' for temperature, ' $b$ ' for water deficit and ' $c$ ' for soil cover) as in RothC. The proportion that goes to  $\text{CO}_2$  and to BIO and HUM is determined by the clay content of the soil (Coleman and Jenkinson, 1999). The remaining C that is not lost is split into 46% BIO and 54% HUM, which are the default values for microbial efficiency used in RothC. In each time step, each organic compound is considered to decompose once; i.e. decomposition of each pool will follow fragmentation and aggregation after the updating of the pool mass.

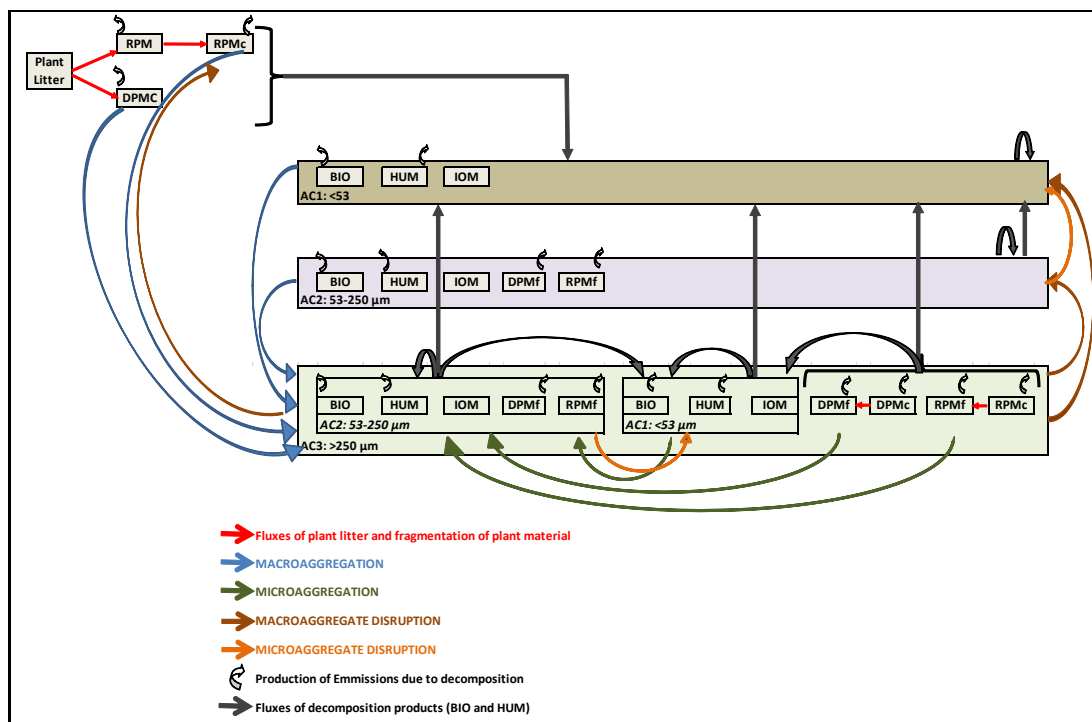


Figure 4.2 Schematic representation of the carbon and aggregate turnover in the CAST model.

The calculations of the processes represented in Figure 4.2 are presented in the following descriptive mass balance equations followed by detailed justification of the conceptual and model description.

$$\begin{aligned}
 D(\text{Plant litter})/Dt &= \text{Plant litter input}_{RPM} - \text{fragmentation}(RPM \text{ to } cRPM) \\
 &\quad - \text{decomposition}(\text{Plant litter}_{RPM} \text{ to } AC1)
 \end{aligned}$$

$$\begin{aligned}
 D(cPOM - \text{litter})/Dt &= \text{fragmentation}(RPM \text{ to } cRPM) + \text{Plant litter input}_{DPM} \\
 &\quad - \text{macroaggregation}(cPOM \text{ to } cPOM_{i n_{AC3}}) \\
 &\quad - \text{decomposition}(cPOM \text{ to } AC1) \\
 &\quad + \text{macroaggregate destruction}(cPOM_{i n_{AC3}} \text{ to } cPOM)
 \end{aligned}$$

$$\begin{aligned}
 D(AC1)/Dt &= \text{decomposition}(\text{plant litter to } AC1) - \text{macroaggregation}(AC2 \text{ to } AC3) \\
 &\quad + \text{decomposition}(AC1 \text{ to } AC1) + \text{decomposition}(AC2 \text{ to } AC1) \\
 &\quad + \text{decomposition}(AC3 \text{ to } AC1) \\
 &\quad + \text{macroaggregate destruction}(AC3 \text{ to } AC1) \\
 &\quad + \text{microaggregate destruction}(AC2 \text{ to } AC1)
 \end{aligned}$$

$$\begin{aligned}
 D(AC2)/Dt &= -\text{macroaggregation}(AC2 \text{ to } AC3) + \text{decomposition}(AC2 \text{ to } AC2) \\
 &\quad - \text{decomposition}(AC2 \text{ to } AC1) \\
 &\quad + \text{macroaggregate destruction}(AC3 \text{ to } AC2) \\
 &\quad - \text{microaggregate destruction}(AC2 \text{ to } AC1)
 \end{aligned}$$

$$\begin{aligned}
 D(cPOM_{i n_{AC3}})/Dt &= \text{macroaggregation}(cPOM \text{ to } cPOM_{i n_{AC3}}) \\
 &\quad - \text{fragmentation}(cPOM_{i n_{AC3}} \text{ to } fPOM_{i n_{AC3}}) \\
 &\quad - \text{decomposition}(cPOM_{i n_{AC3}} \text{ to } AC1) \\
 &\quad - \text{decomposition}(cPOM_{i n_{AC3}} \text{ to } AC1_{i n_{AC3}}) \\
 &\quad - \text{macroaggregate destruction}(cPOM_{i n_{AC3}} \text{ to } cPOM)
 \end{aligned}$$

$$\begin{aligned}
 D(fPOM_{i n_{AC3}})/Dt &= \text{fragmentation}(cPOM_{i n_{AC3}} \text{ to } fPOM_{i n_{AC3}}) \\
 &\quad - \text{microaggregation} - \text{decomposition}(fPOM_{i n_{AC3}} \text{ to } AC1) \\
 &\quad - \text{decomposition}(fPOM_{i n_{AC3}} \text{ to } AC1_{i n_{AC3}}) \\
 &\quad - \text{macroaggregate destruction}(fPOM_{i n_{AC3}} \text{ to } fPOM)
 \end{aligned}$$

$$\begin{aligned}
 D(AC1_{i n_{AC3}})/Dt &= \text{macroaggregation}(AC1 \text{ to } AC1_{i n_{AC3}}) - \text{microaggregation}(AC1_{i n_{AC3}} \text{ to } AC2_{i n_{AC3}}) \\
 &\quad - \text{decomposition}(AC1_{i n_{AC3}} \text{ to } AC1) + \text{decomposition}(AC1_{i n_{AC3}} \text{ to } AC1_{i n_{AC3}}) \\
 &\quad + \text{decomposition}(POM_{i n_{AC3}} \text{ to } AC1_{i n_{AC3}}) + \text{decomposition}(AC2_{i n_{AC3}} \text{ to } AC1_{i n_{AC3}}) \\
 &\quad - \text{macroaggregate destruction}(AC1_{i n_{AC3}} \text{ to } AC1) \\
 &\quad + \text{microaggregate destruction}(AC2_{i n_{AC3}} \text{ to } AC1_{i n_{AC3}})
 \end{aligned}$$

$$\begin{aligned}
 D(AC2_{i n_{AC3}})/Dt &= \text{macroaggregation}(AC2 \text{ to } AC2_{i n_{AC3}}) \\
 &\quad + \text{microaggregation}(AC1_{i n_{AC3}} \text{ to } AC2_{i n_{AC3}}) \\
 &\quad - \text{decomposition}(AC2_{i n_{AC3}} \text{ to } AC1) \\
 &\quad - \text{decomposition}(AC2_{i n_{AC3}} \text{ to } AC1_{i n_{AC3}}) \\
 &\quad + \text{decomposition}(AC2_{i n_{AC3}} \text{ to } AC2_{i n_{AC3}}) \\
 &\quad - \text{macroaggregate destruction}(AC2_{i n_{AC3}} \text{ to } AC2) \\
 &\quad - \text{microaggregate destruction}(AC2_{i n_{AC3}} \text{ to } AC1_{i n_{AC3}})
 \end{aligned}$$

### *Plant litter input apportionment and fragmentation*

Plant material is considered to consist of the organic materials with different resistance to decomposition; progressively resistant carbohydrates and proteins, cellulose, hemicelluloses, and lignin (Van Veen and Paul, 1981). The model apportions plant litter input between Decomposable Plant Material (DPM), i.e. easily decomposable carbohydrates (i.e. O-alkyl C) and Resistant Plant Material (RPM), like recalcitrant long chained C (i.e. alkyl C) (Golchin et al., 1994) using the factors reported by Coleman and Jenkinson (1999); i.e. 1.44 for grassland and 0.67 for shrubland. The DPM pool is assumed to consist of coarse POM (53-250  $\mu\text{m}$ ), due to its very small turnover time. The RPM pool is fragmented due to earthworms, nematodes and other small fauna to coarse POM (>250  $\mu\text{m}$ ) (RPMc). The fragmentation is described by first order kinetics. The two rate constants of fragmentation are corrected with the same 'abc' correction factors used for decomposition assuming that fragmentation will follow the same pattern. The RPM pool is the only pool of the fresh plant material that is not aggregated.

### *Macro-aggregate formation*

Fresh plant material is rapidly colonized by microbial decomposers when it enters the soil matrix. Fungal hyphae mechanically bind the soil particles that surround the organic resource (Helfrich et al., 2008). Root mucilages as well as microbial mucilages released, like extracellular polysaccharides provide the glueing that bind them to cells of bacteria or fungi and form macro-aggregates around POM. Enough young POM is considered to have been incorporated for stable aggregates to be created (Puget et al., 2000). Macro-aggregation is therefore induced by the plant input and especially the DPM. It was considered that aggregation will take place when available plant material exists with favorable conditions for microbial activity (soil moisture and temperature), following first order kinetics at the same manner as decomposition (Equations 1-2). No aggregates will be formed if there is no DPM material. Coarse DPM and RPM is aggregated with AC1 and AC2 aggregates. It was assumed that aggregates of constant composition (coarse plant material, AC1, and AC2) will be created depending on the rate of aggregation, the availability of plant material and the availability of AC1 and AC2. If neither AC1 nor AC2 is the limiting factor equations 3-6 are used for the calculations. As there is no evidence if macro-aggregation can take place even if

AC1 or AC2 is not available it was assumed that both of them are limiting factors. Therefore, for example if AC2 is the limiting factor, Equations 7-9 are used ("carbon-limited" conditions).

$$DPMc_{aggr} = DPMc - DPMc e^{-k_{aggr} DPMc \Delta t} \quad \text{Equations 1}$$

$$RPMc_{aggr} = RPMc - RPMc e^{-k_{aggr} RPMc \Delta t} \quad \text{Equations 2}$$

$$POMc_{aggr} = DPMc_{aggr} + RPMc_{aggr} \quad \text{Equations 3}$$

$$AC3_{formed} = \frac{POMc_{aggr}}{\text{Percent composition of formed AC3 in POMc}} \quad \text{Equations 4}$$

$$AC1_{aggr} = AC3_{formed} * \text{Percent composition of formed AC3 in AC1}_{aggr} \quad \text{Equations 5}$$

$$AC2_{aggr} = AC3_{formed} * \text{Percent composition of formed AC3 in AC2}_{aggr} \quad \text{Equations 6}$$

$$AC3_{formed} = \frac{AC2_{aggr}}{\text{Percent composition of formed AC3 in AC2}} \quad \text{Equations 7}$$

$$AC1_{aggr} = AC3_{formed} * \text{Percent composition of formed AC3 in AC1}_{aggr} \quad \text{Equations 8}$$

$$POM_{aggr} = AC3_{formed} * \text{Percent composition of formed AC3 in POM}_{aggr} \quad \text{Equations 9}$$

The relative contribution of the pools within AC1 (BIO and HUM) and AC2 (BIO, HUM, fDPM, and fRPM) which are aggregated is determined proportional to the composition of the aggregates in these pools at this time step. For example in the case of AC1 Equations 10 and 11 are used.

$$BIO_{AC1(aggr)} = AC1_{aggr} * \text{Percent composition of AC1 in BIO}_{AC1} \quad \text{Equations 10}$$

$$HUM_{AC1(aggr)} = AC1_{aggr} * \text{Percent composition of AC1 in HUM}_{AC1} \quad \text{Equations 11}$$

The free coarse POM and AC1 and AC2 carbon pools are updated due to macro-aggregation. *Fragmentation of coarse POM in AC3:* As the intra-aggregate coarse DPM and RPM POM decomposed are further fragmented with first order kinetics into smaller particles, finely fragmented POM (fPOM), and the microbial exudates are released, the macro-aggregates become more stable.

### *Micro-aggregate formation*

Some of this fine plant material becomes encrusted with mineral particles and microbial byproducts (AC1 silt-clay sized micro-aggregates within AC3), leading to the formation of micro-aggregates within macro-aggregates (AC2 in AC3) and consequently an increased physical protection of the POM (Six et al., 2002a, Six et al., 2004). It was assumed that micro-aggregation also follows first order kinetics and that micro-aggregates of constant composition (fine plant material and AC1) will be created depending on the rate of aggregation, the availability of plant material and the availability of AC1, which is also a limiting factor. The existence of labile POM material (DPM) is not considered a limiting factor for micro-aggregation, since turnover times of micro-aggregates is order of magnitudes higher than the turnover time of decomposable plant materials. The composition of AC1 (BIO and HUM) aggregated is determined proportional to the composition of the pools at this time step (similarly with equations 10 and 11). The fine POM as well as AC1 in AC3 carbon pools are updated due to micro-aggregation.

### *Decomposition of carbon pools*

The physical protection exerted by macro- and/or micro-aggregates is attributed to (Six et al., 2002a): (1) the compartmentalization of substrate and microbial biomass, (2) the reduced diffusion of oxygen into macro-aggregates and especially micro-aggregates which leads to a reduced activity within the aggregates, and (3) the compartmentalization of microbial biomass and microbial grazers. Grazing pressure on bacteria by bacterivorous nematodes for example is greater in sandy soils than in loams and clays resulting in a higher N mineralization rate per bacterium (Hassink et al., 1993). The compartmentalization between substrate and microbes by macro- and micro-aggregates is indicated by the highest abundance of microbes on the outer part of the aggregates and a substantial part of SOM being at the center of the aggregates (Golchin et al., 1994). The inaccessibility of substrate for microbes within aggregates is due to pore size exclusion and related to the water-filled porosity. The reduced diffusion of oxygen into macro-aggregates has been verified by increasing N<sub>2</sub>O fluxes observed with increasing water stable aggregate sizes, due to the existence of hot spots of anaerobiosis (Six et al., 2002a). Most of the decomposition products (BIO and HUM) of each pool in the AC3 and AC2 aggregates are assumed to contribute to the aggregate in which it is contained and only a small percent is leaked out in the free AC1 pool,

since microorganisms and their immediate products of decay are considered to form a tightly closed system (Van Veen and Kuikman, 1990) (Figure 4.2, notice grey arrows indicating respective fluxes). Specifically, it was assumed that 95% of the products produced by the decomposition of the coarse and fine DPM and RPM in the AC3 aggregate remain in the aggregate and are added in the AC1 within the AC3, while 5% is transferred in the free AC1 aggregate. Similarly, 95% of the products produced by the decomposition of the pools (BIO, HUM, fDPM, and fRPM) contained in the micro-aggregates within the macro-aggregates (AC2 in AC3) remain in the micro-aggregates and half of the rest are added in the AC1 within the AC3, while the other half is transferred in the free AC3 aggregate. Likewise, 95% of the products produced by the decomposition of the free macro-aggregates (AC2) remain in the micro-aggregates and the rest 5% is transferred in the free AC1 aggregate. The decomposition products of the free AC1 as well the AC1 aggregate inside the macro-aggregates remain in the same pool. The carbon pools of the fresh organic matter (DPM, RPM and RPMc) decompose and the decomposition products (BIO and HUM) are transferred in the free AC1 aggregate.

#### *Macro-aggregate/ Micro-aggregate disruption*

Conceptually, further decomposition of the incorporated OM (utilization of the more labile pool, like the more easily decomposable carbohydrates), results in the decrease of the microbial growth/activity and the supply of microbial biopolymers and macro-aggregates become less stable. Then if slaking occurs with rapid contact of aggregates with water these macro-aggregates would release stabilized micro-aggregates and silt –clay sized aggregates and highly decomposed residual POM would become unprotected. It was assumed that the consumption of the glue (microbial metabolites) which cause the macro-aggregate disruption would be positively correlated with the availability of the DPM pools. New aggregates will be formed in a system where permanent flow of decomposable material is introduced if there is availability of free AC1 and AC2. However, older aggregates will be deteriorated and eventually destroyed. Therefore, a pseudo percent value was introduced for the fine and coarse DPM pools content of the AC3 aggregate, below which macro-aggregates are considered unstable and therefore ‘potentially’ destroyed. Macro-aggregate disruption is determined by the concentration of the labile pool of the particulate organic matter (DPM pools). In the field, water unstable macro-aggregates will be destroyed if

slaking occurs in relation to the precipitation and irrigation events. Aggregate disruption due to tillage has not been introduced at this point in the model. The pools of the free plant material and the free AC1 and AC2 are updated after the disruption of the macro-aggregates and the final calculations are made. These materials may subsequently be reincorporated into new aggregates if fresh plant residue is introduced in the system. Similarly, micro-aggregates, both the free and the micro-aggregates within macroaggregates were destroyed when their fPOM was under a limited value.

#### *Checking of saturation capacity of the silt-clay fraction*

At the end of each step the saturation capacity (SC) of the silt-clay fraction to stabilize carbon is checked. The user has the option either to introduce in the model a calibrated value or to let it use the Hassink equation (Hassink, 1997):  $SC=4.09+0.37*\text{silt-clay}$ , where silt-clay is the fraction, % and SC is the g C/kg soil under saturation. If the saturation capacity has been exceeded in a silt-clay fraction (BIO and HUM pools of AC1, AC2, AC1 with in AC3, and AC2 within AC3) an amount of Carbon is leached out of the soil. The mass and the concentration of the silt-clay fraction is calculated as described in the following paragraph.

#### *Soil bulk density and porosity sub-model*

Porosity was calculated according to the equation:  $\text{porosity (\%)} = (D_s - D_b) / D_s$ , where  $D_s$  is the soil particle density, and  $D_b$  the soil bulk density.  $D_s$  is calculated according to Adams (1973):  $D_s = 100 / (\text{OM\%} / D_{om} + (100 - \text{OM\%}) / D_m)$ , where  $D_{om}$  is the organic matter particle density and  $D_m$ , the particle density of the mineral phase.  $D_{om}$  and  $D_m$  were calibrated so as to obtain the field measurements of bulk density and porosity. OM% is the soil organic matter content in g/100 g soil which is calculated by multiplying the SOC content by the factor 1.724. Soil bulk density is calculated by dividing the soil mass with the apparent volume of the aggregates. In order to estimate the apparent volume of the aggregates, the bulk density of the aggregates is calculated first. It was considered in accordance with Malamoud et al. (2008) that aggregates are regarded as spheres with different packing systems to explain the differences in bulk density (Equations 12-14). Aggregate type 1 is the less porous whereas the type 3 is the less dense.

Aggregate type 1: pyramidal system,  $BD_1 = \frac{\pi}{3\sqrt{2}} D_{s1}$  Equation 12

Aggregate type 2: tetragonal sphenoidal,  $BD_2 = \frac{2\pi}{9} D_{s2}$  Equation 13

Aggregate type 3: simple cubic,  $BD_3 = \frac{\pi}{6} D_{s3}$  Equation 14

$D_s$  of each aggregate is calculated again according to Adams (1973). The OM% of each aggregate is taken by the equation  $OM_x = AC_x * 1.724 * 100 / mass\_AC_x$ . However, the bulk density of the mineral phase for each aggregate is assumed to be the same in this modeling exercise, although it would be by definition vary, being higher in smaller aggregates. Then the apparent volume of each aggregate type is calculated via:  $V_x = mass\_AC_x / BD_x$ . Soil mass changes as OM content changes. In order to estimate the mass of the three aggregate types, it was assumed that carbon transfer related with aggregation and disruption can be related with silt-clay mass transfers, whereas only clay mass was assumed from Malamoud et al., (2008) under a different conceptualization, where mass transfers were not calculated. Silt-clay mass transfer is determined by its concentration in Carbon and the carbon transfer calculated by macro-aggregation, micro-aggregation, and disruption in every time step (equation 15, an example of Silt-clay mass transfer for macro-aggregation). A correction factor (cf) to adjust for non linearities is introduced in each aggregate. Silt-clay related carbon is considered the BIO and HUM pools (equation 16). The mass of the aggregates is then calculated according to equations 17-19. The fractions that determine the distribution of sand mass in each aggregate type (f1 and f2) are estimated by the field measurements.

$$mass_{SILT-CLAY_{AC1}(Aggr)} = \frac{cf1 * AC1_{aggr}(SILT-CLAY)}{Conc_{AC1}(SILT-CLAY)} \quad \text{Equation 15}$$

$$AC1_{aggr}(SILT-CLAY) = BIO_{AC1}(aggr) + HUM_{AC1}(aggr) \quad \text{Equation 16}$$

$$mass_{AC1} = mass_{SILT-CLAY_{AC1}} + AC1 * 1.724 \quad \text{Equation 17}$$

$$mass_{AC2} = mass_{SILT-CLAY_{AC2}} + AC2 * 1.724 + f1 * mass_{SAND} \quad \text{Equation 18}$$

$$mass_{AC3} = mass_{SILT-CLAY_{AC3}} + AC3 * 1.724 + f2 * mass_{SAND} \quad \text{Equation 19}$$

#### *Mechanistic estimation of N stocks*

Finally, a simplified mechanistic model was developed for the estimation of the N stocks of the organic matter pools of the CAST model. N stocks for each 'x' pool were calculated

according to the equation:  $N_x = C_x / (C/N)_x$ , where  $C_x$  is the respective calibrated value derived by the CAST model. The C-to-N ratio of each pool is then calibrated to meet the field measured N stocks. The optimization was constrained by the following conditions:  $4 < (C/N)_x < 50$ ,  $4 < (C/N)_{\text{BIOx}} < 14$ , and  $(C/N)_{\text{RPM}} \& \text{RPMC} > (C/N)_{\text{DPMC}}$ , for the free POM pools. An optimization routine in excel, the 'solver' (Microsoft Office Excel, 2007) was used for the optimization procedure.

#### 4.2.2 Field data used for model evaluation

Data from Koiliaris River Basin and Clear Creek Basin, Critical Zone Observatories ([www.soiltrec.eu](http://www.soiltrec.eu)) were used to evaluate the model. The two modeled sites are described in detail in paragraph 2.21. The first site (indicated as IA) was Iowa City, IA, USA (41°45'N, 91°44'W, 230 m), indicative of humid continental climate with soils of coarse texture-sandy loam (clay=7%). The second site (indicated as GR) was in the northern part of Chania Prefecture, Crete, Greece (39°25'N, 51°41'E, 10 m), where typical semi-arid, Mediterranean climate dominates with soils of finer texture-clay loam (clay=30%). Topsoil (10 cm) samples were analyzed for water stable aggregates (Elliott 1986); macro-aggregates (>250  $\mu\text{m}$ ), ii) micro-aggregates (53-250  $\mu\text{m}$ ), and iii) silt-clay sized micro-aggregates and minerals (<53  $\mu\text{m}$ ). Macro-aggregates were separated, according to the procedure described by Lichter et al., (2008) into the following fractions: i) coarse particulate organic matter and sand (cPOM: >250  $\mu\text{m}$ ), ii) easily dispersed silt-clay fractions (sc-M <53  $\mu\text{m}$ ), and iii) micro-aggregates (mM: 53-250  $\mu\text{m}$ ). The mM fraction was further separated to fine particulate organic matter and sand (fPOM: 53-250  $\mu\text{m}$ ) and silt-clay fraction of the micro-aggregate (sc-mM <53  $\mu\text{m}$ ). Similarly, micro-aggregates (53-250  $\mu\text{m}$ ) were separated to fine particulate organic matter (fPOM: 53-250  $\mu\text{m}$ ) and the silt-clay fraction (sc-mM <53  $\mu\text{m}$ ) they contained. The C and N distributions in the isolated carbon pools as well the silt-clay mass of the aggregate fractions and its concentration in carbon (Table 4.1a and 4.1b) were used for the initialization and calibration of the model.

### 4.2.3 Methodological approach for initialization and calibration of the model

The following assumptions were made in order to initialize the model. Litter carbon pools (DPM, RPM, RPMc) were assumed to be zero. The fine POM contained in free micro-aggregates and micro-aggregates within the macro-aggregates were equally apportioned to DPM and RPM. The fine POM, both DPM and RPM, in the macro-aggregates not occluded in micro-aggregates, was considered zero. The coarse POM contained in the macro-aggregates was primarily attributed to RPM and a small fraction to DPM. Biomass was considered to be 5% of the related silt-clay sized carbon pool. The biochar (IOM), since there were no available field measurements in the modeling exercise, was considered to be zero. The percent of the decomposition products (BIO and HUM) of each pool which contribute to the aggregate within which the pool is contained, and the percent that is leaked out in the free AC1 pool were estimated as discussed above. Since the two sites had been calibrated before with the RothC model (see Chapter 2), the calibrated plant litter input (3.79 t C/ha and 5.05 t C/ha in Greece and Iowa, respectively) was introduced in the model and the estimated decomposition rate constants were used as initial values for the calibration procedure. The decomposition rate constants were calibrated by testing proportionally higher values for the unprotected and less protected pools and proportionally lower for the most protected pools, assuming that decomposition occurs at a slower rate within macro-aggregates as compared with non-aggregate-associated POM due to diffusion limitation of O<sub>2</sub>(g).

Table 4.1a Field measured water stable aggregates (WSA) as well as sand corrected WSA and Carbon and Nitrogen content of the field measured pools for the Greek and the Iowa cropland and set-aside fields, used for the initialization and calibration of the model, respectively.

	Aggregate fraction	WSA g/100 g soil	WSA (sand free) g/100 g soil	Carbon/Nitrogen Content									
				Aggregate		cPOM		AC1		AC2		fPOM in AC2	
				t C/ha	t N/ha	t C/ha	t N/ha	t C/ha	t N/ha	t C/ha	t N/ha	t C/ha	t N/ha
Set-aside IA	AC3 (>250 $\mu\text{m}$ )	86.2	81.7	29.77	2.14	12.98	0.72	2.19	0.13	14.59	1.29	5.80	0.35
	AC2 (53-250 $\mu\text{m}$ )	11.5	5.9	2.78	0.21							1.22	0.08
	AC1 (< 53 $\mu\text{m}$ )	2.2	2.2	0.46	0.04								
Cropland IA	AC3 (>250 $\mu\text{m}$ )	65.8	38.7	11.08	1.00	1.35	0.12	5.25	0.41	4.48	0.46	0.81	0.08
	AC2 (53-250 $\mu\text{m}$ )	28.9	9.4	5.62	0.45							0.47	0.05
	AC1 (< 53 $\mu\text{m}$ )	5.3	5.3	1.89	0.14								
Set-aside GR	AC3 (>250 $\mu\text{m}$ )	68.5	65.6	41.45	2.56	13.19	1.33	6.99	0.44	21.27	0.79	4.97	0.20
	AC2 (53-250 $\mu\text{m}$ )	25.9	15.9	14.02	0.72							3.61	0.17
	AC1 (< 53 $\mu\text{m}$ )	5.7	5.7	3.08	0.19								
Cropland GR	AC3 (>250 $\mu\text{m}$ )	51.7	45.8	19.68	1.44	5.80	0.30	5.72	0.46	8.82	0.73	4.49	0.23
	AC2 (53-250 $\mu\text{m}$ )	38.3	23.7	11.19	0.93							4.00	0.27
	AC1 (< 53 $\mu\text{m}$ )	10.1	10.1	3.39	0.28								

Table 4.1b Field measured silt-clay (SC) mass (t) in bulk soil and different aggregate fractions and its concentration in carbon (t C/100 t SC mass, %), used for the initialization and calibration of the model, respectively.

	soil	AC1		AC2		AC1 within AC3		AC2 within AC3	
	SC mass, t	SC mass, t	Conc, %	SC mass, t	Conc, %	SC mass, t	Conc, %	SC mass, t	Conc, %
Set-aside IA	410.7	15.0	2.7	35.8	2.5	67.7	3.8	292.1	1.0
Cropland IA	410.7	70.0	3.0	118.6	3.2	138.8	4.4	83.3	3.1
Set-aside GR	790.6	62.9	4.9	169.8	6.1	207.7	3.4	350.2	4.7
Cropland GR	790.6	118.6	2.9	267.9	2.7	199.0	2.9	205.0	2.1

### 4.3 RESULTS AND DISCUSSION

The CAST model was able to capture the SOC content as well the carbon content of the three aggregate types in both Greek and Iowa sites (Figure 4.3Aa and 4.3Ba). The carbon content of the aggregate type 3 (AC3) plus the coarse particulate organic matter of the non aggregated pools (cPOM) is compared with the field measured carbon content of the macro-aggregates (Figure 4.3Ab and 4.3Bb). Similarly, the composition of the AC3 in silt-clay sized aggregates (AC1 in AC3) and micro-aggregates (AC2 in AC3) was calibrated. The fine particulate organic matter of the micro-aggregates (fPOM AC2inAC3) plus the intra macro-aggregated fPOM (fPOM inAC3) was compared with the respective field measured fPOM.

The calibrated values of the rate constants and turnover times of the carbon, aggregate and structure turnover model for the Greek and the Iowa cropland to set-aside conversion are presented in Table 4.2. The monthly correction factors 'abc' for rate constants are presented in Table 4.3. Litter fragmentation to coarse POM exhibited turnover times of 0.12 and 0.18 years in Greece and Iowa respectively. Litter fragmentation due to earthworms, nematodes and other small fauna seem to be facilitated in the coarser texture of the Iowa site. The turnover time of fragmentation of the coarse macro-aggregated POM was similar in both sites for the DPM pool 3.5 years (Greece) and 3.6 years (Iowa). On the contrary, the RPM pool turnover time (fragmentation) was almost 4 times higher in Greece (17.7 years) as compared with Iowa (4.6 years). This pattern could be attributed to different quality composition of the RPM material (shrubland in Greece versus grassland in Iowa), while the composition of the DPM materials seem to be similar in both sites.

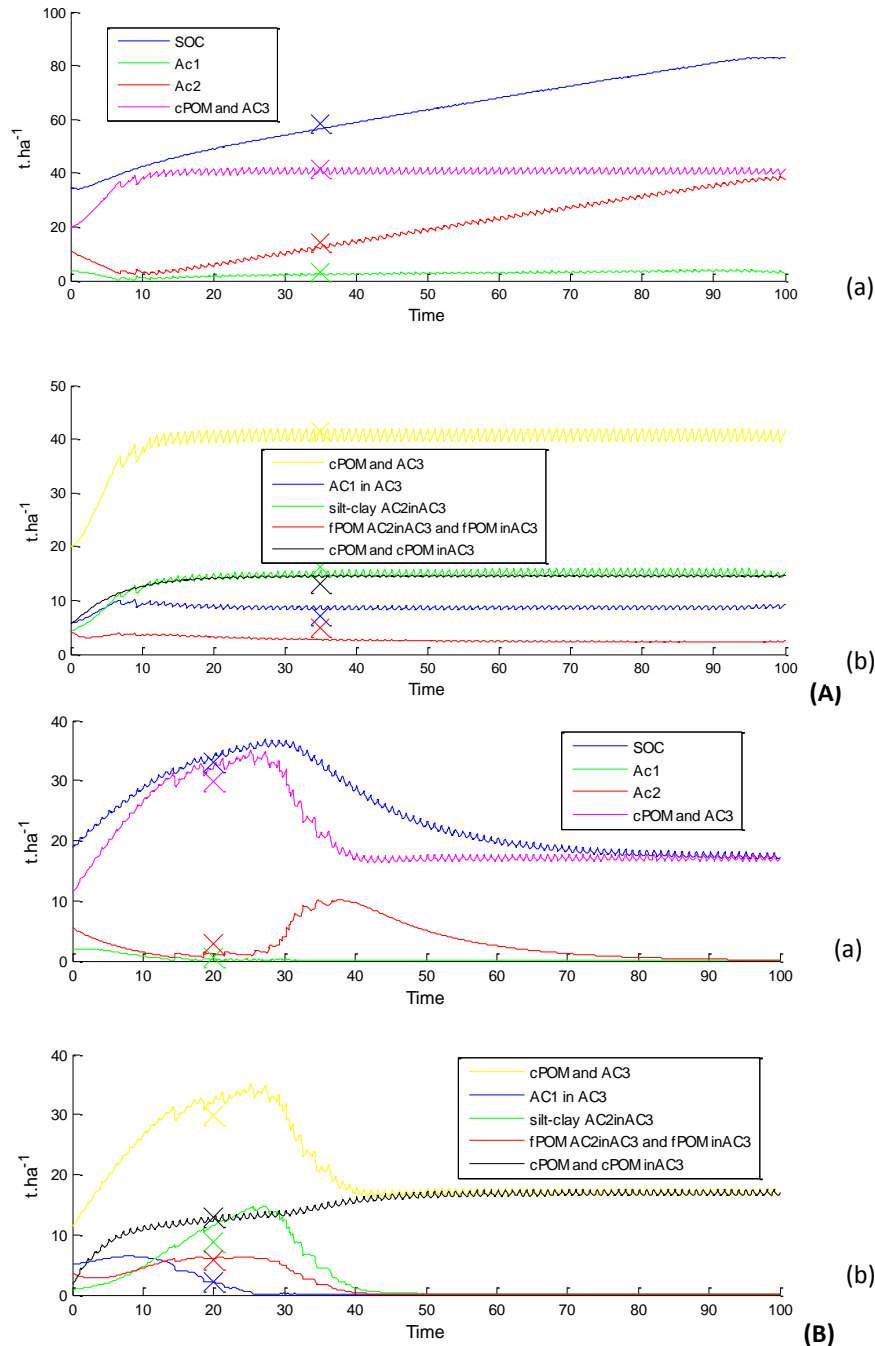


**Figure 4.3** Simulated evolution of carbon content of modeled pools in the A) Greek and the B) Iowa cropland (initial conditions) to set-aside conversion (data used for calibration), a) soil (SOC), aggregate type 1 (AC1), type 2 (AC2), and type 3 (AC3) plus the coarse POM of the non aggregated pools (cPOM), b) the different pools contained in the aggregate type 3: silt-clay sized aggregates (AC1 in AC3), silt-clay related carbon of the micro-aggregates (silt-clay AC2inAC3), fine POM of the micro-aggregates (fPOM AC2inAC3) plus the intra macro-aggregated fPOM (fPOM inAC3), macro-aggregated cPOM (cPOM inAC3) plus the cPOM of the non aggregated pools. Points indicate the field measurements of the same colored line.

The turnover time in years (1/annual decomposition rate) was estimated to be for the litter and non-aggregated resistant to decomposition POM 5.8 and 7.3 years for the Greek and Iowa site respectively, while macro-aggregation resulted in doubling the protection (11.8 years) in Greece while it was 1.4 times higher in Iowa (10.4 years). The coarse POM has been found to be the primary source of mineral N in topsoil (Zeller and Dambrine, 2011). Its C/N ratio is negatively related with mineralization due to immobilization. Potential mineralizable N, potential soluble organic N and C, as well carbohydrate C increased in the set-aside soils by a factor of 4.9, 3.5, 2.9, and 2.7 for Iowa and only 1-1.5 times for Greece (see results of Chapter 2 Table 2.1). The more increase observed in the case of Iowa may be related with the quality of the litter (grassland versus shrubland). Moreover, the seasonal pattern of decomposition due to climatic conditions may also play a role (Figure 4.4).

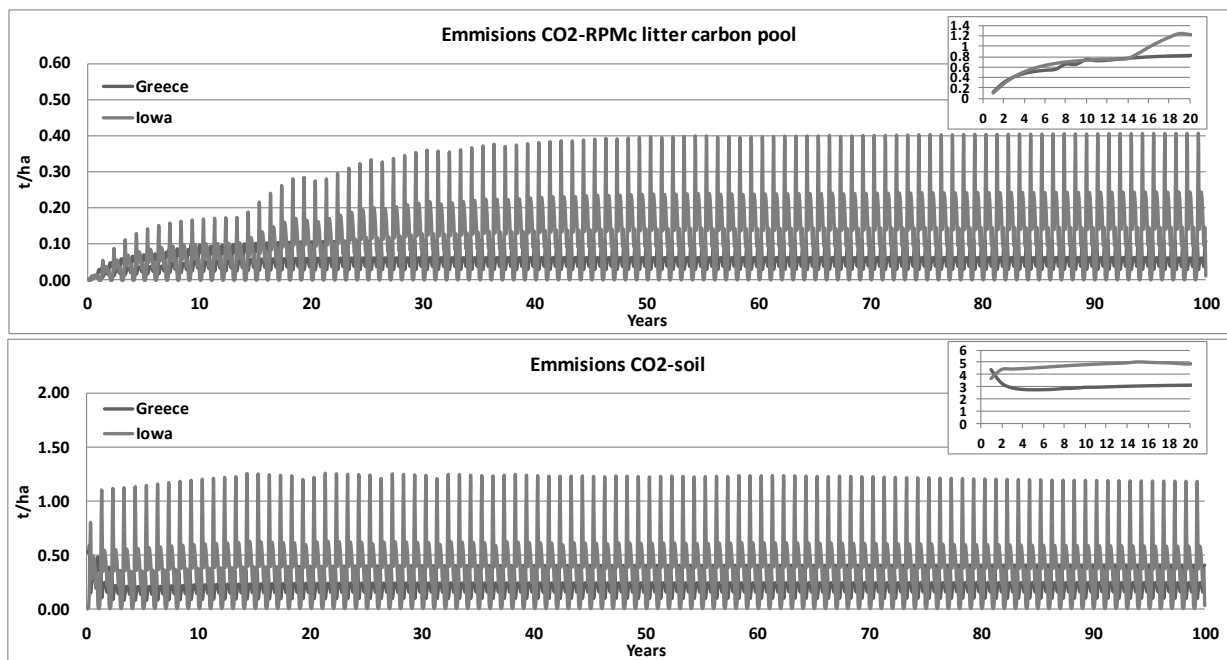


**Figure 4.4** Seasonal pattern of emissions of a) the coarse RPM litter pool and b) the soil (in the right up corner the small figure indicates the annual emissions for 20 years).

More protected was the respective fine POM in micro-aggregates within the macro-aggregates; a 40% more protection as compared with the macro-aggregated cPOM was estimated (16.5 and 14.6 years, for the Greek and Iowa site, respectively). The fine RPM of the free micro-aggregates

presented turnover times (8.5 and 9.4 years, for the Greek and Iowa site, respectively) lower than both the fine and coarse RPM related with macro-aggregates, but higher than the non-aggregated RPM carbon pools. On the other hand the coarse decomposable plant material presented more than 3 times higher turnover due to macro-aggregation (0.6 and 1.2 years, for the Greek and Iowa site, respectively) as compared with the non-aggregated coarse DPM (0.2 and 0.4 years, for the Greek and Iowa site, respectively). The fine DPM of both macro and micro aggregates (1.2 and 2.4 years, for the Greek and Iowa site, respectively) exhibited 2 times higher turnover compared to the relative coarse macro-aggregated POM. The turnover time of the silt-clay related carbon (humus) of the micro-aggregates within macro-aggregates (841.8 and 72.9 years, for the Greek and Iowa site, respectively) was 1.5 and 3.8 times, for the Greek and Iowa site, higher than the silt-clay sized aggregates within macro-aggregates (570.3 and 19.2 years, for the Greek and Iowa site, respectively). Whereas, the turnover time of the micro-aggregates (AC2) and silt-clay sized aggregates (AC1) was lower (346.6 for the Greek and 12.2 and 8.1 years for the Iowa site, respectively). Finally, the calibrated turnover of the biomass carbon pools was the same in all fractions and estimated to be 2.9 years in the Greek site and 5.5 years in the Iowa site.

Overall, the decomposition rates were found to be significantly higher in the Iowa site as compared to the Greek, which can be attributed primarily to the climatic conditions and the soil texture of the two sites. The high decay constant of the HUM pools (silt-clay associated carbon) in the Iowa site as it was suggested by the results of chapter 2 is attributed to the very low clay content in accordance with Balesdent et al. (1998) and Gottschalk et al. (2010). They showed that SOC in the size fraction  $<50 \mu\text{m}$  is made up of the relatively rapidly decomposing pool of silt associated C (decomposition rate of  $0.12 \text{ 1/y}$ ), and a relatively slowly decomposing pool of clay associated C (decomposition rate of  $0.03 \text{ 1/y}$ ). Nevertheless, the wet and warm summers in Iowa hasten organic matter decomposition. On the other hand, the significantly low HUM decomposition rates in Greece have been attributed to slaking of the soil surface due to high clay content which can result in fine soil particles moving into inter-aggregate pores in the surface area, which can reduce the infiltration rate of rainfall or irrigation water and reduce hydraulic conductivity. Presence of biochar could be another possible explanation.

Table 4.2 Calibrated values of the rate constants and turnover time (1/rate constant -corrected with the 'abc' factors, see Table 4.3) of the model for the Greek and the Iowa cropland to set-aside conversion.

		Rate Constants, 1/y		Turnover time, y			
		GR	IA	GR	IA		
Fragmentation		RPM	15	20	0.1	0.2	
		RPMc	0	0			
		RPMc(AC3)	0.1	0.8	17.7	4.6	
		DPMc(AC3)	0.5	1	3.5	3.6	
		DPM	10.45	10	0.2	0.4	
Decomposition	plant litter pools	RPM	0.305	0.5	5.8	7.3	
		RPMc	0.305	0.5	5.8	7.3	
		RPMf	0.305	0.5	5.8	7.3	
		RPMc(AC3)	0.15	0.35	11.8	10.4	
	AC3 Aggregate type	RPMf(AC3)	0.15	0.35	11.8	10.4	
		DPMc(AC3)	3	3	0.6	1.2	
		DPMf(AC3)	1.5	1.5	1.2	2.4	
		BIO(AC1 within AC3)	0.6	0.66	2.9	5.5	
		HUM(AC1 within AC3)	0.0031	0.19	570.3	19.2	
		BIO(AC2 within AC3)	0.6	0.66	2.9	5.5	
		HUM(AC2 within AC3)	0.0021	0.05	841.8	72.9	
		RPMf(AC2 within AC3)	0.1069	0.25	16.5	14.6	
	AC2 Aggregate type	DPMf(AC2 within AC3)	1.5	1.5	1.2	2.4	
		BIO(AC2)	0.6	0.66	2.9	5.5	
		HUM(AC2)	0.0051	0.3	346.6	12.2	
		RPMf(AC2)	0.2069	0.39	8.5	9.4	
	AC1 Aggregate type	DPMf(AC2)	1.5	1.5	1.2	2.4	
		BIO(AC1)	0.6	0.66	2.9	5.5	
	Macro-aggregation		HUM(AC1)	0.0051	0.45	346.6	8.1
			RPMc(AC3)	0.6	0.65	2.9	5.6
Micro-aggregation		DPMc(AC3)	0.47	0.65	3.8	5.6	
		RPMf(AC2 within AC3)	0.2	0.3	8.8	12.2	
Percentages of macro-aggregation (AC3), %		DPMf(AC2 within AC3)	0.2	0.3	8.8	12.2	
		RPMc	20	30			
		DPMc	20	30			
		AC1	30	35			
Percentages of micro-aggregation in AC3, %		AC2	30	5			
		RPMf(AC2 within AC3)	23.4	18			
		DPMf(AC2 within AC3)	0	0			
		AC1 within AC3	76.6	82			
Criterion for macro-aggregate (AC3) disruption (DPM within AC3), %			0.15	1			
Criterion for micro-aggregate (AC2 within AC3) disruption (DPM+RPM in AC2 within AC3), %			0.15	1			
Criterion for micro-aggregate disruption (AC3) (DPM+RPM in AC2), %			0.15	1			
The maximum concentration of the silt clay fraction in carbon (g C/g soil)			55	15000			
Correction factor to adjust for silt-clay flow, cf		AC1	0.8	0.8			
		AC2	2.2	2			
		AC1 within AC3	0.16	0.4			
Distribution of sand mass in aggregates, %		f1 (AC2)	0.46	0.29			
		f2 (AC3)	0.54	0.71			
Particle density of the mineral phase, Dm			2.2	1.9			
Organic matter particle density, Dom			0.7	0.5			

**Table 4.3 Monthly correction factor for rate constants; the product of the rate modifying factor for temperature (a), the topsoil moisture deficit rate modifying factor (b), and the soil cover factor (c).**

	<b>GR (Crete, Greece)</b>	<b>IA (Iowa, USA)</b>
<b>January</b>	0.733	0.004
<b>February</b>	0.760	0.022
<b>March</b>	0.901	0.216
<b>April</b>	0.246	0.733
<b>May</b>	0.340	0.274
<b>June</b>	0.441	0.391
<b>July</b>	0.488	0.448
<b>August</b>	0.474	0.415
<b>September</b>	0.410	0.310
<b>October</b>	0.317	0.180
<b>November</b>	0.776	0.272
<b>December</b>	0.901	0.025

The turnover time for macro-aggregation under no limiting factor was found to be a few years (Puget et al., 2000), 2.9 years in Greece and 5.6 years in Iowa. Similarly the micro-aggregation inside the macro-aggregates exhibited turnover time of 8.8 and 12.2 years respectively. The formed macro-aggregates contained 30% carbon related with the AC1 and 30% carbon related with the AC2, in the case of the Greek site. In Iowa, the formed macro-aggregates contained 35% carbon related with the AC1 and 5% carbon related with the AC2. The formed micro-aggregates inside the macro-aggregates exhibited 23.4 and 18% fine POM content, in Greece and Iowa, respectively. The soil system reaches a maximum macro-aggregation after about 7 years in the Greek site and 14 years in the Iowa site (Figure 4.3). Jastrow et al. (1996) also found that macro-aggregation reached a maximum after 10.5 complete growing seasons since cultivation (prairie restorations). In both sites, the limiting factor for macro-aggregation is the availability of AC1. The sum of the carbon related with the AC3 and the free cPOM is stabilized to a stable C content.

Macro-aggregate disruption is taking place after this period from January to April in Greece and from June to November in Iowa, presenting a relative constant seasonal pattern, in accordance with Plante et al. (2002) and Six et al. (2004) who suggested that, macro-aggregation in agroecosystems shows seasonal dynamic. Total SOC after this period increases due to the increase of micro-aggregates (AC2), indicating that maximum physical protection capacity for SOM is determined by the maximum micro-aggregation, which is in turn, determined by clay

content and type, in accordance with the suggestions by Six et al., (2002a). Macro-aggregate disruption takes place when macro-aggregates contain lower than 0.15% DPM in both sites. However with the same limit micro-aggregation did not take place in the 100 year simulation indicating that under set-aside conditions this process is not important. Totally from the soil in Greece in the 100 years of the simulation 2.3 tC/ha were leached out of the soil due to the oversaturation of silt-clay fractions, which corresponds to the 0.6% of the total plant litter input in 100 years (3.79 tC/ha y). However most of the leach out happens during the years 94 to 100, when the respective percentage was 8.1%. In Iowa, the pattern of leach out was similar throughout the period of the 100 years and the percentage of the carbon leached out was 12.6% of the total total plant litter input during this (5.6 tC/ha y).

The simulated evolution of silt-clay mass and carbon content (%) of the silt-clay fraction, related to aggregate type 1 (AC1), type 2 (AC2), silt-clay sized aggregates within the type 3 (AC1 in AC3), and micro-aggregates within the type 3 (AC2 in AC3) are presented in Figure 4.5. The calibrated values of the particle density of the organic matter ( $D_{om}$ ) and the mineral phase were found to be 2.2 and 0.7 g/cm<sup>3</sup> in Greece and 1.9 and 0.5 g/cm<sup>3</sup> in Iowa. Lower density of the mineral phase in Iowa is in accordance with the coarser texture. The lower density of the organic matter can be possibly explained by the different litter quality and would be expected to be lower in grassland (Iowa) compared to shrubland (Greece) due to lower lignin content. The 46% of the sand mass in the Greek site was found to be in the free micro-aggregates (AC2) and the rest 54% in the macro-aggregates (AC3). Coarser sand was found in the Iowa site, where 29% was related with the micro-aggregates (AC2) and 71% with the macro-aggregates (AC3). The correction factors to adjust for non linearities for silt-clay flow related with macro-aggregation and micro-aggregation inside the macro-aggregates were found to be in the Greek site 0.8, 2.2 and 0.16 for the AC1, AC2 and AC1 in AC3, respectively. Similarly, for the Iowa site they were 0.8, 2.0, and 0.4. A value close to 1 means that silt-clay mass flow is linearly related to OC flow. The significantly higher than 1 value supports the recent imaging and X-ray spectroscopic work (see Review of Kleber and Johnson, 2010) which suggest that substantial parts of mineral surfaces are not covered by organic matter and differentiate from the mineral sorbent—organic sorbate idea. Finally, the significantly lower than 1 values, possibly indicate hot-spots of high OC concentration, where the micro-aggregation is induced.

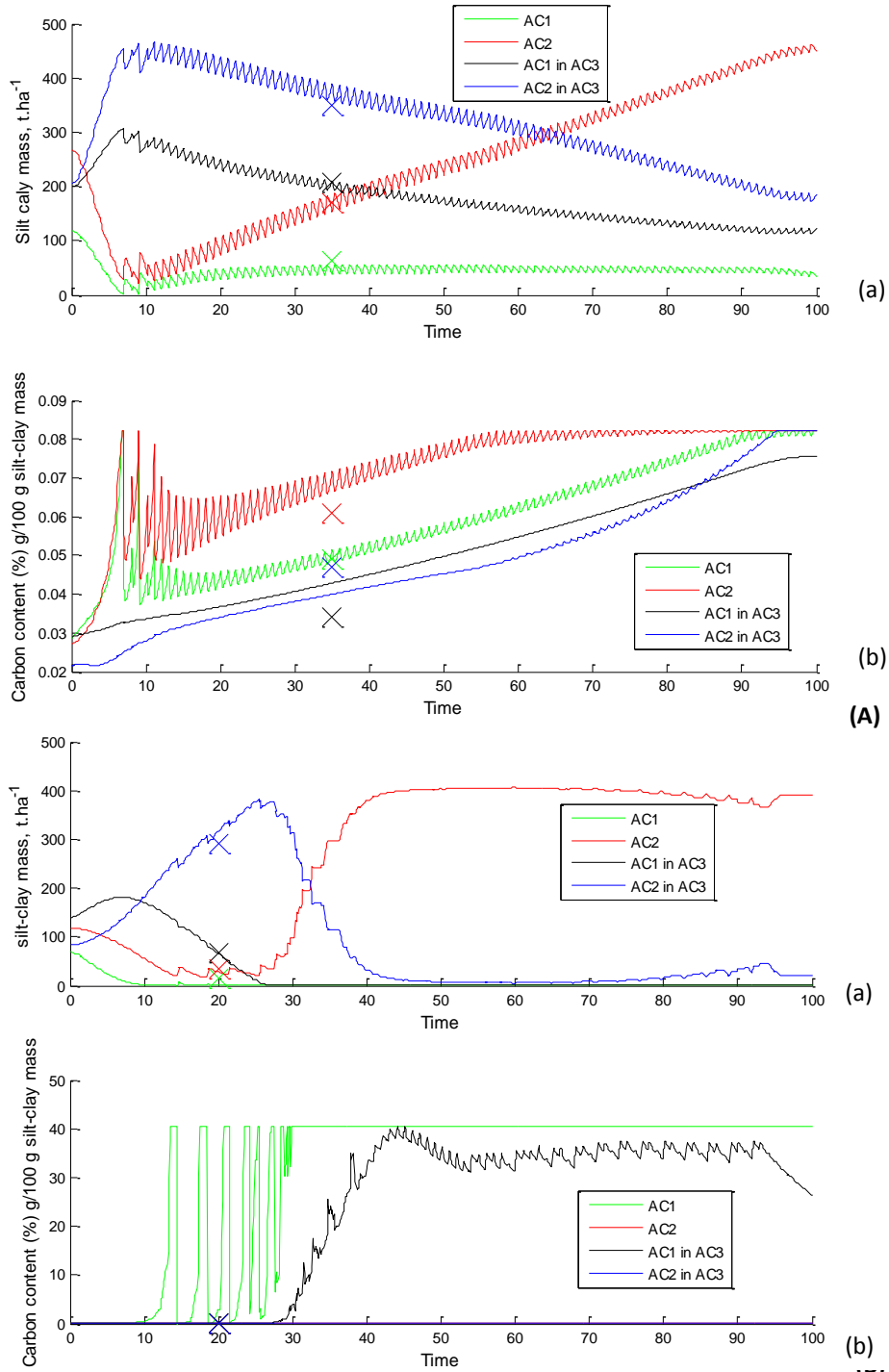


**Figure 4.5 Simulated evolution in the A) Greek and the B) Iowa cropland to set-aside conversion of a) silt-clay mass and b) carbon content (%) of the silt-clay fraction, related to aggregate type 1 (AC1), type 2 (AC2), silt-clay sized aggregates within the type 3 (AC1 in AC3), and micro-aggregates within the type 3 (AC2 in AC3).**

With this approach the prediction of the OC (%) content of the different silt-clay fractions was achieved. When the soil system is at maximum macro-aggregation in both sites (7<sup>th</sup> year, Greece, 14<sup>th</sup> year Iowa), the silt-clay mass of the AC1 and AC2 is at minimum and the OC (%) content of these pools reaches a maximum. In both sites, the limiting factor for macro-aggregation is the availability of AC1. In both sites porosity and bulk density reach a maximum and minimum, respectively, when the soil system is at the maximum macro-aggregation and then due to the increase of micro-aggregates bulk density increases and porosity decreases towards to a stable value, both presenting however an inter-annual variability (Figure 4.6).

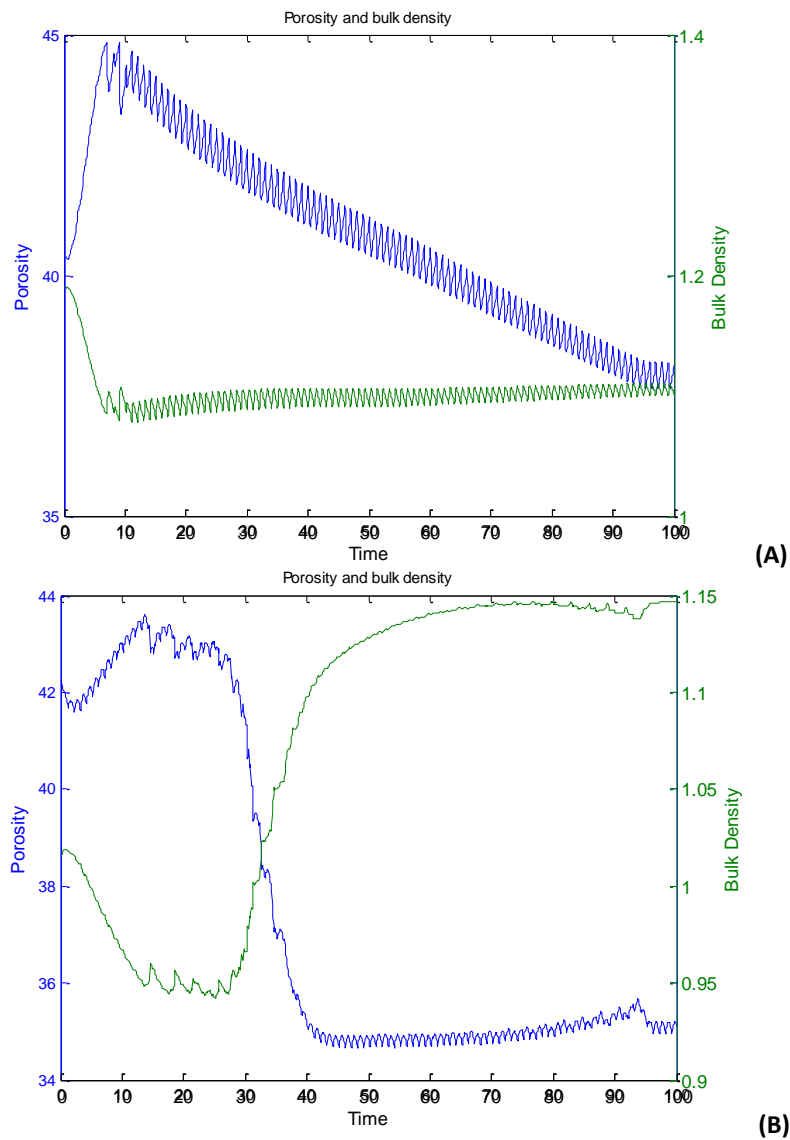


**Figure 4.6 Simulated evolution in the A) Greek and the B) Iowa cropland to set-aside conversion of porosity (%) and bulk density (g/cm<sup>3</sup>). Points indicate the field measurements of the same colored line.**

The C-to-N ratio of the OM pools after the calibration of the mechanistic N model for the Greek and the Iowa cropland to set-aside conversion are given in Table 4.4. The simulated evolution of the C-to-N ratio of soil, AC1, AC2, and AC3 plus the non-aggregated cPOM are presented in Figure 4.7. In the Iowa site the model was able to capture the variation of C-to-N ratio in all aggregate pools. The C-to-N ratio in soil, AC2, and AC3 plus the non-aggregated cPOM increased to a maximum value similarly with macro-aggregation and porosity maximum and bulk density minimum, and then decrease to a stable value. On the contrary, the C-to-N ratio of the AC1 aggregate type decreased to a stable value. In the Greek site, the optimum solution could not represent the field variation of the C-to-N ratio of the AC1 aggregate. The C-to-N ratio of soil, AC2, and AC3 plus the non-aggregated cPOM seem to increase towards a stable value. The C-to-N ratio of the biomass pools was found to be, in general higher in the Iowa site (11.2 to 14) as compared with Greek site (4.3 to 14), indicating possible more abundance of fungi populations. The biomass found in the macro-aggregates exhibited higher C-to-N ratio compared to the biomass related to the AC1 and AC2 aggregates in Iowa, indicating in this way a possible relation of fungi presence with macro-aggregation in the coarse textured Iowa site. Conversely, in the Greek site higher C-to-N ratio was observed in the biomass pools related to AC1 and AC1 in AC3, in comparison with the biomass pools related to AC2 and AC2 in AC3, where values which indicate bacteria predominance were found (6.7 and 4.3 respectively). The C-to-N ratio of the HUM pools in the Iowa site was lower than in the Greek site. In the Iowa site the ratio ranged from 10 to 13.5 being lowest in the HUM pool of the AC2 in AC3. In the Greek site the respective ratio ranged from 7.3 to 30.1, being highest in the HUM pool of the AC2 in AC3. The C-to-N ratio of the litter and non aggregated POM pools was higher in the Iowa site compared to the Greek site, whereas the aggregated POM pools exhibited higher C-to-N ratio in the Greek site as compared with the Iowa site, apart from two exceptions (DPM fine POM in AC2 and DPM fine POM in AC3). In general, the DPM pools showed higher C-to-N ratio compared to the RPM pools in both sites, apart from the DPM and POM pools of (AC2 in AC3).

Table 4.4 Calibrated values of the C-to-N ratio of the mechanistic N model for the Greek and the Iowa cropland to set-aside conversion.

OC pool	Calibrated C-to-N ratio: GR	Calibrated C-to-N ratio: IA
RPM	42.4	41.6
DPMc	30.4	41.6
RPMc	30.4	41.6
RPMf	50.0	50.0
BIO(AC1)	14.0	11.5
HUM(AC1)	14.1	13.5
BIO(AC2)	6.7	11.2
HUM(AC2)	19.5	13.2
RPMf(AC2)	21.8	14.5
DPMf(AC2)	4.3	8.1
RPMc(AC3)	30.5	7.7
RPMf(AC3)	50.0	50.0
DPMc(AC3)	30.5	15.7
DPMf(AC3)	9.8	11.7
BIO(AC1_in_AC3)	14.0	14.0
HUM(AC1_within AC3)	7.2	14.0
BIO(AC2_within AC3)	4.3	14.0
HUM(AC2_within AC3)	30.0	9.4
RPMf(AC2_within AC3)	10.3	9.0
DPMf(AC2_within AC3)	18.7	12.6

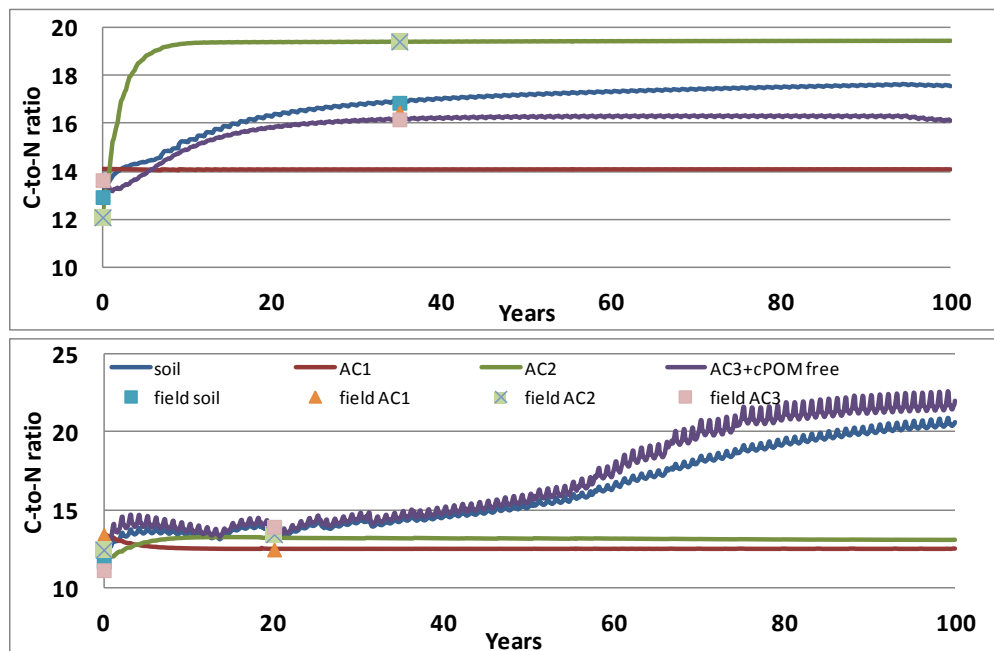


Figure 4.7 Simulated evolution of C-to-N ratio in the A) Greek and B) Iowa cropland to set-aside conversion, of soil, aggregate type 1 (AC1), type 2 (AC2), and type 3 (AC3) plus the coarse particulate organic matter of the non aggregated pools (cPOM). Points indicate the field measurements.

SOM stabilization efficiency was reduced after the soil system reached maximum aggregation (Figure 4.3 and 4.4). Plante and McGill (2002) and Six et al. (2004) have also suggested that in native systems, at the maximum aggregate level lower amount newly incoming fresh residue is stabilized in accordance with the results presented in Figure 4.3a. An intermediate aggregate turnover is optimum in order to have aggregate formation and occlusion and subsequent protection of C (highest sequestration rate). This conceptualization is in accordance with Kimetu et al. (2009) findings, which indicate that SOM stabilization efficiency was highest with intermediate cultivation history of about 20 years as compared with both degraded soils and high C-containing soils. They suggested that depending on the C saturation limit of a soil, soils with high soil organic C have high rates of labile C mineralization possibly due to limited protection of organic matter by minerals. Silt and clay content and type apart from the surface area for adsorption exert also an indirect influence on the protection of POM by affecting aggregate dynamics (Six et al., 2002a; Six et al., 2002b). The reduced efficiency was less pronounced in the Greek site which contained higher amounts of clay.

#### **4.4 CONCLUSIONS**

This work constitutes the first attempt to model the conceptual macro-aggregate formation around particulate organic matter and subsequent release of micro-aggregates due to macro-aggregate turnover. Soil carbon pools as described by the RothC model were coupled with aggregate and structure turnover modules and validated with field data from two sites. The developed CAST model was successfully used for the simulation of carbon, aggregate, and structure turnover in cropland to set-aside conversions of Critical Zones Observatories in Greece (fine textured Mediterranean) and Iowa (coarse textured humid continental).

- The model was able to capture the carbon content and the C-to-N ratio content of the pools comprising the three aggregate types (macro-aggregates: >250  $\mu\text{m}$ , micro-aggregates: 53-250  $\mu\text{m}$ , silt-clay sized aggregates: <53  $\mu\text{m}$ ) in both sites in the year used for calibration (set-aside field).
- A more deterministic explanation of the saturation level of the different carbon pools and soil structure (porosity and bulk density) was obtained. The soil system reached maximum

macro-aggregation/porosity and minimum bulk density after 7 and 14 years in Greece and Iowa, respectively. Afterwards, macro-aggregate disruption presented a constant seasonal pattern and any further SOC increase was due to micro-aggregation resulting in the increase of bulk density and decrease of porosity towards to a stable value. Micro-aggregate disruption did not take place over the 100 years simulation.

- The module for the calculation of the silt-clay fractions mass flow between the aggregates and their carbon concentration supported the recent scientific findings suggesting that substantial parts of mineral surfaces are not covered by organic matter and differentiate from the mineral sorbent—organic sorbate idea (Kleber and Johnson, 2010), indicating however, also the existence of hot-spots of high OC concentration in the silt-clay sized aggregates, which probably induce micro-aggregation.
- The developed simple mechanistic Nitrogen model was a useful contribution, indicating plausible differences between the two sites. For example the C-to-N ratio of the biomass pools indicated possible more abundance of fungi populations in the coarser textured Iowa site, relating also the fungi presence to the macro-aggregation.

The CAST model can assist in revealing primary factors determine organic matter, aggregation, and structure turnover in different ecosystems. This capability should allow better prediction of the response of the soil system to management practices, landuse changes, and climate change in order to design and optimize the appropriate measures/practices (Bronick and Lal, 2005; Rees et al., 2005).

#### 4.5 LITERATURE CITED

- Baldock, J.A., 2007. Composition and cycling of organic carbon in soils. P. Marschner, and et al (eds), *Nutrient Cycling in Terrestrial Ecosystems, Soil Biology* 10, 1-35.
- Balesdent, J., Besnard, E., Arrouays D., Chenu, C., 1998. The dynamics of carbon in particle-size fractions of soil in a forest-cultivation sequence. *Plant Soil* 201, 49–57.
- Balesdent, J., Chenu, C., and Balabane, M., 2000. Relationship of soil organic matter dynamics to physical protection and tillage. *Soil and Tillage Research* 53, 215–230.
- Bechtold, J.S., Naiman, R.J., 2009. A Quantitative Model of Soil Organic Matter Accumulation During Floodplain Primary Succession. *Ecosystems* 12, 1352–1368.
- Bronick, C.J., Lal, R., 2005. Soil structure and management: a review. *Geoderma* 124, 3 –22.
- Davidson, E.A., Janssens, I.A. 2006. Temperature sensitivity of soil carbon decomposition and feedbacks to climate change. *Nature* 440, 165–173.
- Falloon, P., Smith, P., 2002. Simulating SOC changes in long term experiments with RothC and Century: model evaluation for a regional scale application. *Soil Use and Management* 18, 101-111.
- Gleixner, G., Poirier, N., Bol, R., Balesdent, J., 2002. Molecular dynamics of organic matter in a cultivated soil. *Organic Geochemistry* 33, 357–366
- Golchin, A., Oades, J.M., Skjemstad, J.O., Clarke, P., 1994 Study of free and occluded particulate organic matter in soils by solid state <sup>13</sup>C CP/MAS NMR spectroscopy and scanning electron microscopy. *Australian Journal of Soil Research* 32, 285–309.
- Golchin, A., Clarke, P., Oades, J.M., Skjemstad, J.O., 1995. The effects of cultivation on the composition of organic matter and structural stability of soils. *Australian Journal of Soil Research* 33, 975–993.
- Gottschalk, P., Bellarby, J., Chenu, C., Foereid, B., Smith, P., Wattenbach, M., Zingore, S., Smith, J., 2010. Simulation of soil organic carbon response at forest cultivation sequences using <sup>13</sup>C measurements. *Organic Geochemistry* 41, 41–54.
- Grandy A.S., Neff J.C., 2008. Molecular C dynamics downstream: The biochemical decomposition sequence and its impact on soil organic matter structure and function. *Science of the Total Environment* 404, 297-307.
- Hassink, J., Bouwman, L.A., Zwart, K.B., Bloem, J., Brussaard, L., 1993. Relationships between soil texture, physical protection of organic matter, soil biota, and C and N mineralization in grassland soils. *Geoderma* 57, 105-128.
- Hassink, J., 1997. The capacity of soils to preserve organic C and N by their association with clay and silt particles. *Plant Soil* 191, 77–87.
- Hassink, J., Whitmore, A.P., 1997. A model of the physical protection of organic matter in soils. *Soil Science Society of America Journal* 61, 131–139.
- Helfrich, M., Ludwig, B., Potthoff, M., Flessa, H., 2008. Effect of litter quality and soil fungi on macroaggregate dynamics and associated partitioning of litter carbon and nitrogen. *Soil Biology and Biochemistry* 40, 1823–1835.
- Jastrow, J.D. 1996. Soil aggregate formation and the accrual of particulate and mineral-associated organic matter. *Soil Biology and Biochemistry* 28, 665-676.
- Kleber, M., Johnson, K.J., 2010. Advances in Understanding the Molecular Structure of Soil Organic Matter: Implications for Interactions in the Environment. *Advances in Agronomy* 106, 77-142.
- Kleber M., Sollins P., Sutton R., 2007. A conceptual model of organo-mineral interactions in soils: self-assembly of organic molecular fragments into zonal structures on mineral surfaces. *Biogeochemistry* 85, 9–24.
- Kimetu, J.M., Lehmann, J., Kinyangi, J.M., Cheng, C.H., Thies, J., Mugendi, D.N., Pell, A., 2009. Soil organic C stabilization and thresholds in C saturation. *Soil Biology and Biochemistry* 41, 2100–2104.

- Knicker, H., 2007. How does fire affect the nature and stability of soil organic nitrogen and carbon? A review. *Biogeochemistry*, 85, 91–118.
- Malamoud, K., McBratney, A.B., Minasny, B., Field, D.J., 2009. Modeling how carbon affects soil structure. *Geoderma* 149, 19-26.
- Molina, J.A.E., Clapp, C.E., Shaffer, M.J., Chichester, F.W., Larson, W.E., 1983. NCSOIL, a model of nitrogen and carbon transformation in soil: description, calibration and behaviour. *Soil Science Society of America Journal* 47, 85-91.
- Nikolaidis, N.P. Bidoglio G., Modeling of Soil Organic Matter and Structure Dynamics: A Synthesis Review. *Geoderma* (submitted revisions).
- Plante, A.F., McGill, W.B., 2002. Soil aggregate dynamics and the retention of organic matter in laboratory-incubated soil with differing simulated tillage frequencies. *Soil and Tillage Research* 66, 79–92.
- Plante, A.F., Feng, Y., McGill, W.B., 2002. A modeling approach to quantifying soil macroaggregate dynamics. *Canadian Journal of Soil Science* 82, 181–190.
- Porter, C.H., Jones, J.W., Adiku, S., Gijsman, A.J., Gargiulo, O., Naab J.B. Modeling organic carbon and carbon mediated soil processes in DSSAT v4.5, *Operational Research*, 10(3), 247-278.
- Powlson, D.S., Whitmore, A.P., Goulding, K.W.T., 2011. Soil carbon sequestration to mitigate climate change: a critical re-examination to identify the true and the false. *European Journal of Soil Science* 62, 42-55.
- Puget, P., Chenu, C., Balesdent, J., 2000. Dynamics of soil organic matter associated with particle-size fractions of water-stable aggregates. *European Journal of Soil Science*, 51, 595-605.
- Schoning, I., Morgentoth, G., Kogel-Knabner, I., 2005. O/N-alkyl and alkyl C are stabilised in fine particle size fractions of forest soils. *Biogeochemistry* 73, 475–497.
- Six, J., Conant, R.T., Paul E.A., Paustian, K., 2002a. Stabilization mechanisms of soil organic matter: Implications for C-saturation of soils. *Plant and Soil* 241, 155–176.
- Six, J., Feller, C., Denef, K., Ogle, S.M., de Moraes, J.C., Alberecht, A., 2002b. Soil organic matter, biota and aggregation in temperate and tropical soils – Effects of no-tillage. *Agronomie* 22, 755–775.
- Six, J., Bossuyt, H., De Gryze, S., Denef, K., 2004. A history of research on the link between (micro)aggregates, soil biota, and soil organic matter dynamics. *Soil and Tillage Research* 79, 7–31.
- Takeshi, I., Moorcroft, P.R., 2006. The global-scale temperature and moisture dependencies of soil organic carbon decomposition: an analysis using a mechanistic decomposition model. *Biogeochemistry* 80, 217–231.
- Van Veen, J.A., Paul, E.A., 1981. Organic carbon dynamics in grasslands and soils. 1. Background information and computer simulation. *Canadian Journal of Soil Science* 61, 185-201.
- Van Veen, J.A., Kuikman, P.J., 1990. Soil structural aspects of decomposition of organic matter by micro-organisms *Biogeochemistry* 11, 213-233, 1990.
- Virto, P., Barré, C., Chenu, 2008. Microaggregation and organic matter storage at the silt-size scale. *Geoderma* 146, 326–335.
- von Lützw M., Kögel-Knabner I., Ekschmitt K., Flessa H., Guggenberger G., Matzner E., Marschner B., 2007. SOM fractionation methods: Relevance to functional pools and to stabilization mechanisms. *Soil Biology and Biochemistry* 39, 2183-2207.
- Yang, X., Wang, M., Huang, Y., Wang, Y., 2002. A one-compartment model to study soil carbon decomposition rate at equilibrium situation. *Ecological Modeling* 151, 63–73.
- Zeller, B., Dambrine, E., 2011. Coarse particulate organic matter is the primary source of mineral N in the topsoil of three beech forests. *Soil Biology and Biochemistry* 43, 542-550.

## 5. SYNTHESIS: SOIL DEGRADATION IN KOILIARIS RIVER BASIN CRITICAL ZONE OBSERVATORY

---

**Abstract:** This chapter presents the study conducted to assess the soil status of Koiliaris River Basin Critical Zone Observatory by assessing the primary factors of soil aggregation in the soils of the basin, quantifying the effects of landuse and climate changes and evaluating the effects of over-grazing to soil biochemical quality and water quality. A soil survey was conducted based on a soil mapping typology approach in order to assess primary control factors of soil aggregation in the basin. Principal component analysis revealed that there are two major soil groups which can be described by 13 soil parameters. Group-1 was distinguished from Group-2 by its lower content in macro-aggregates which was found to be related to the lower Ca extracted by BaCl<sub>2</sub> and the sandier texture (more coarse sand, less silt-clay). The content of the soils in macro-aggregates was described by a multi regression analysis by 6 parameters for Group-1 and 9 parameters for Group-2. Climate change (IPCC scenario A1B, 2010-2050) was found to result in less carbon sequestered (simulation of shrublands to croplands conversions) and correspond to 1.7% to 4.1% of the initial SOC stock of the modeled sites, while the carbon stock change due to landuse change under the present scenario (1990-2010) was 12% to 28% of the initial SOC. On the other hand, the climate change effects in 50 year old olive grove fields were estimated to be 2-3% of the initial SOC, while the change of stock due to cultivation for 20 years under the present scenario was estimated to be 1.7% to 8.9%. The results emphasize that management effects and particularly landuse change effects are so high that may be hinder our ability to detect climate change effects. Finally, this study provided evidence linking the DON export from river basins to livestock grazing intensity. A linear relationship between DON export and livestock N load was obtained for five Greek basins suggesting a mechanism that operate at regional scales. The de-vegetation of grazing lands in Koiliaris River highland calcaric leptosols was shown to be a primary factor causing the decline of soil biochemical quality and DON can be used as a reliable indicator for livestock grazing impacts to soil biochemical quality.

## 5.1 INTRODUCTION- KOILIARIS RIVER BASIN DESCRIPTION

The Koiliaris River Basin (KRB), Critical Zone Observatory (CZO) (Moraetis et al., 2010; Banwart et al., 2011) is located 25 km east from the city of Chania (005-12-489E, 039-22-112N), Crete, Greece and has a total area of 130 km<sup>2</sup>. The climate of the region is temperate (semi-arid) Mediterranean, characterized by precipitation and snowfall (at high altitudes) in winters and hot-dry summers in which evaporation exceeds precipitation and results in significant water deficit. The semi-arid in conjunction with the topography -elevation gradient which range from 0 to 2120 m MSL- create climatic gradients (ranging from typical Mediterranean to Alpine climate) that favor above-ground biodiversity (Nikolaidis, 2011). Figure 5.1 presents the three zones of elevation: 0-200 m (lowland), 200-800 m (mid altitude, semi-mountainous), and >800 m (high altitude, mountainous). The mean annual precipitation in the northern part of the catchment is 705 (447-1032) mm (low elevations and semi-mountainous zone), while in the southern part is 2125 mm (mountainous zone). The highest catchment's slope is 43% at the White Mountains, while gentle slopes (1-2%) are present in the valley and the estuary of Koiliaris.

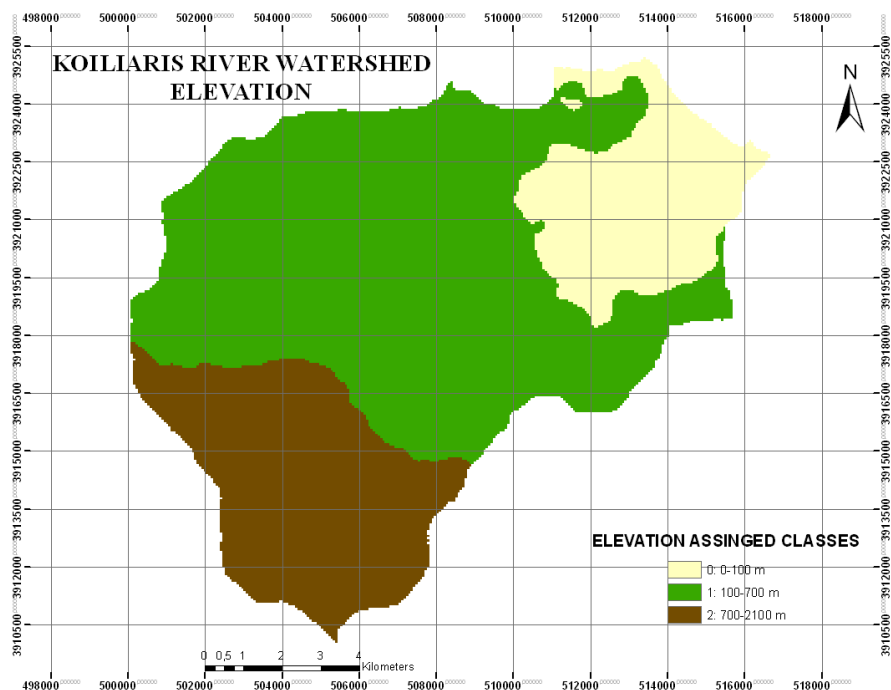


**Figure 5.1 Classification of elevation-contour mapping (digital data sets were obtained from the data base of the Region of Crete. The respective data derive from the topographic diagrams (1:50000 scale) of the Geographic Service of the Army).**

The main geologic and geomorphologic feature of Koiliaris River Basin is karstic formations of limestone and dolomites (Nikolaidis, 2011). In specific, the geology of the region (Figure 5.2) consists of 23.8% Plattenkalk (dolomites, marbles, limestones, and re-crystallized limestones with cherts), 31% Trypali units (recrystallized calcaric breccias), 9.4% limestones with Marls in Neogene formations, 13% Marls in Neogene formations, 12.8% Schists, and 10% Quaternary Alluvial deposits (Banwart et al., 2011). The class assignment is presented in Table 5.1.

**Table 5.1 Class assignments for geologic substrate types.**

Description	Symbol	Hydro-class	Assigned Class Code
Alluvial	Pt.t	P1	2
Neogene formations (mainly Marls)	M.m	P3	1
Neogene formations (Marly Limestones)	M.k	P2	3
Phyllites-quartzites (Schists)	ph	A2	0
Limestones - Trypali Units	Ts-Ji.mr.d	K1	5
Limestones and Dolomites - Plattenkalk	Jm-E.K	K2	4

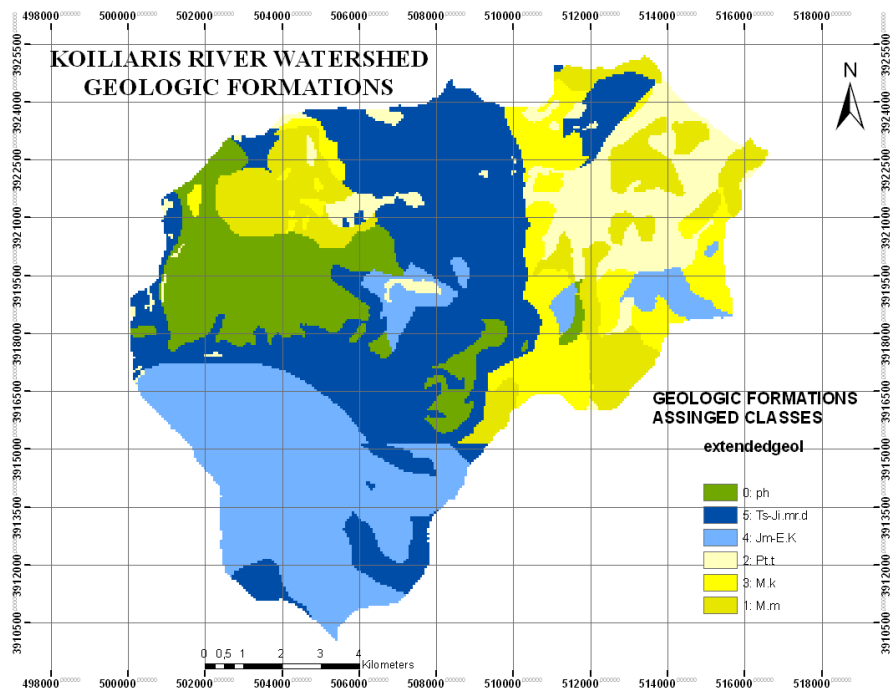


**Figure 5.2 Classification of geologic formations classes (Digital data sets were obtained from the data base of the Region of Crete. The respective data derive from the maps (1:50000 scale) of the Institute of Geology and Mineral Exploration (IGME)).**

Soils are thin poorly developed and follow the lithology of the region (Figure 5.3a and 5.3b). Soils in limestones correspond to alpine humic Ranker type and Podzols mixed with forest acid red soil, in high altitude are sparse and they are mainly developed in limestone cavities and/or around patches of shrubs (calcaric Lithosols, FAO). Thicker soil profiles of calcareous rendzines soil and mediterranean brown soil are developed in Neocene and Alluvial formations in low altitudes (calcaric regosols, FAO). The soils have been formed primarily by the weathering of limestone with high clay and iron oxide content which are the main ingredients of soil aggregate formation (Nikolaidis, 2011). Thin horizons of soils are also developed in schists with mainly coarse texture (eutric lithosols, FAO).

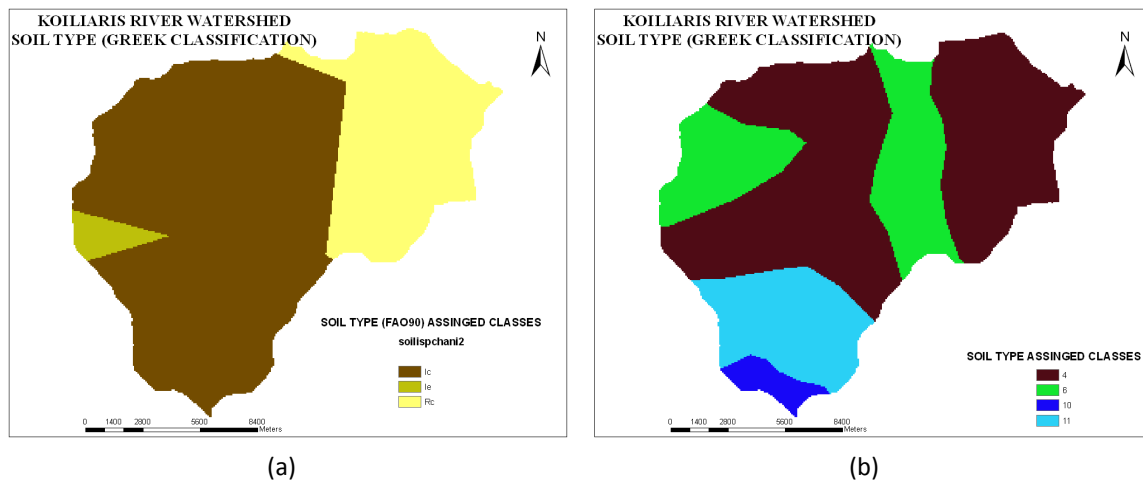


**Figure 5.3 a) Classification of soil types according to FAO - Calcaric Lithosols (Ic), Eutric Lithosols (Ie), and Calcaric Regosols (Rc), b) Greek classification for soil types - 4) Calcareous rendzines soil and mediterranean brown soil, 6) Brown and red-brown alkaline mediterranean soil, 10) Alpine humic Ranker type, 11) Podzols mixed with forest acid red soil.**

Landuse comprises olive groves, fruit trees (mainly orange, lemon), vines, and vegetables (29.4 %). Scrubland, which is intensively grazed by livestock, covers large areas (58%). Approximately  $50 \cdot 10^3$  goat-sheep exist in the area. Table 5.2 presents in detail the different level of information (Corine 2000). Similar land cover classes were combined to level 2 or 1. The classified map of land cover is shown in Figure 5.4.

**Table 5.2 Description of Land cover levels according to the CLC 2000 database and Class assignments for land cover types.**

Code Level3	Label Level1	Label Level2	Label Level3	Assigned Class Code	
112	Artificial surfaces	Urban fabric	Discontinuous urban fabric	0	
211	Agricultural areas	Arable land	Non-irrigated arable land	1	
222		Permanent crops	Fruit trees and berry plantations	2	
223			Olive groves	3	
242		Heterogeneous agricultural areas		Complex cultivation patterns	4
243				Land principally occupied by agriculture, with significant areas of natural vegetation	
311	Forest and semi natural areas	Forests	Broad-leaved forest	5	
321		Scrub and/or herbaceous vegetation associations		Natural grasslands	6
322				Moors and heathland	
323				Sclerophyllous vegetation	
324				Transitional woodland-shrub	
332		Open spaces with little or no vegetation		Bare rocks	0
333				Sparsely vegetated areas	6
334				Burnt areas	0

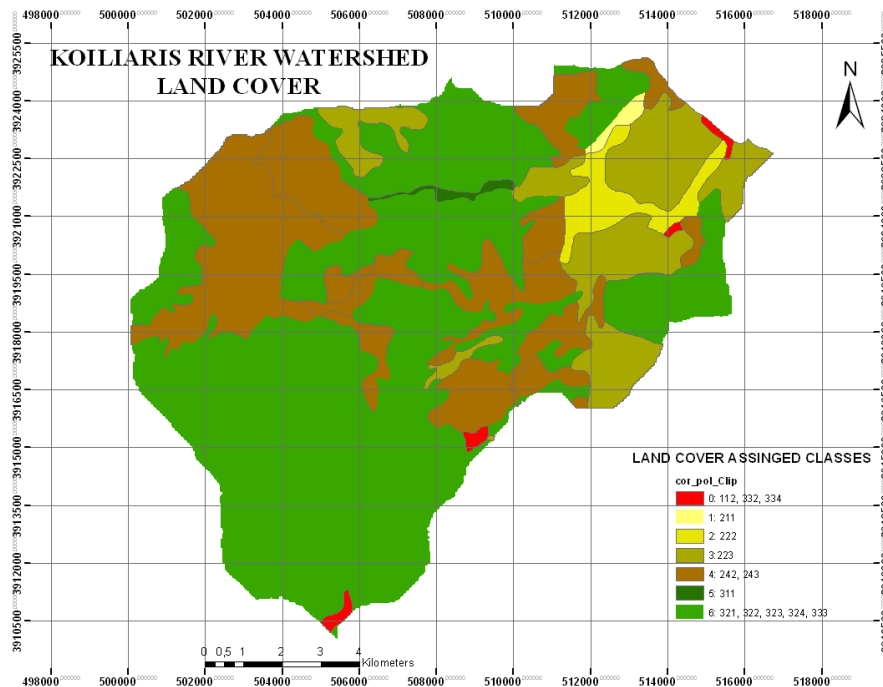


**Figure 5.4 Classification of land cover classes (digital data sets were obtained from the CLC 2000 (Corine Land Cover 2000) database which is available by the European Environment Agency).**

Within the watershed, there are 58 different ecosystem types according to classes of land cover (Fruit trees, Olive Groves, heterogeneous agriculture and scrub/herbaceous vegetation), geologic formations (Alluvial, Marls, Calcaric Marls, Trypalis Limestones and Plattenkalk Limestones), and elevation classes (0-100 m, 100-700 m, and 700-2100 m). The 16 types presenting covered the 87.5% of the whole watershed area are presented in Table 5.3 and Figure 5.5. Heterogeneous agriculture in the semi mountainous region is mainly covered by olive groves trees and secondary by vineyards.

**Table 5.3 The major types of soil mapping typology for the Koiliaris River Watershed (90% cover of the area) and the sampling design.**

ID	Geology	Land Cover	Elevation, m	Cover, %	Slope, mean	Slope, std
26	Alluvial	Fruit trees	0-100	2.40	2.43	2.55
12	Alluvial	Olive groves	0-100	4.14	3.43	2.76
20	Marls	Olive groves	0-100	3.63	5.8	3.77
5	Calcaric Marls	Heterogeneous agricultural	0-100	1.06	7.25	4.5
49	Marls	Olive groves	100-700	1.82	5.5	3.94
6	Marls	Heterogeneous agricultural	100-700	5.11	6.84	4.37
9	Calcaric Marls	Heterogeneous agricultural	100-700	3.60	8.12	4.59
16	Calcaric Marls	Scrub and herbaceous	100-700	3.13	7.9	4.21
25	Schists	Heterogeneous agricultural	100-700	7.95	11.8	5.9
37	Schists	Scrub and herbaceous	100-700	4.46	15.06	6.64
15	Trypalis	Olive groves	100-700	1.44	6.24	3.69
10	Trypalis	Heterogeneous agricultural	100-700	4.53	10.59	6.32
4	Trypalis	Scrub and herbaceous	100-700	20.09	11.99	6.61
41	Plattenkalk	Scrub and herbaceous	100-700	2.52	9.99	5.52
51	Trypalis	Scrub and herbaceous	700-2100	17.30	20.35	8.08
52	Plattenkalk	Scrub and herbaceous	700-2100	4.31	18.58	8.28

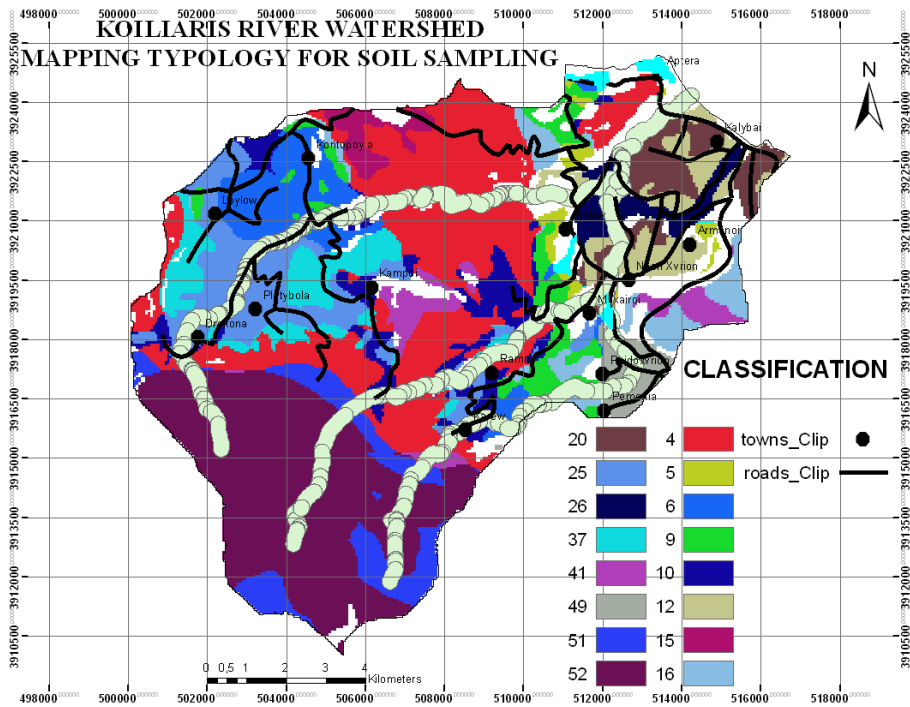


**Figure 5.5 Soil mapping typology for the Koiliaris River Watershed (excluded areas in white color), towns, roads, and riparian buffer.**

The main supply of water in Koiliaris River originates in the Karstic system of White Mountains and discharges through karstic springs throughout the year (Stilos-the main discharge, Zourbos and Armenoi and other minor or ephemeral springs) (Figure 5.6). Small aquifers are also present in Neocene formations where irrigation water is pumped through shallow wells. The Keramianos stream is the main temporary stream which joins two other smaller streams which get constant flow from the Stilos karstic springs (Figure 5.6). Keramianos River drains a small sub-catchment that generates surface runoff due to the predominant of schist geologic formation. The tributary then passes through Diktamos karstic gorge-a karstic gorge, aligned with a fault line- where the transmission losses are significant. The Koiliaris River Basin has been monitored for its hydrologic and geochemical characteristics 2004 (Kourgialas et al., 2010; Moraetis et al., 2010; Moraetis et al., 2011). A continuous telemetric monitoring network (pH, nitrate ( $\text{NO}_3^-$ -N), water temperature ( $^{\circ}\text{C}$ ), dissolved oxygen (mg/L), river stage (m), and water level and temperature in a deep well in the karst, as well two meteorological stations) has been established. Moreover, monthly field campaigns are conducted for both surface and ground water quality measurements.

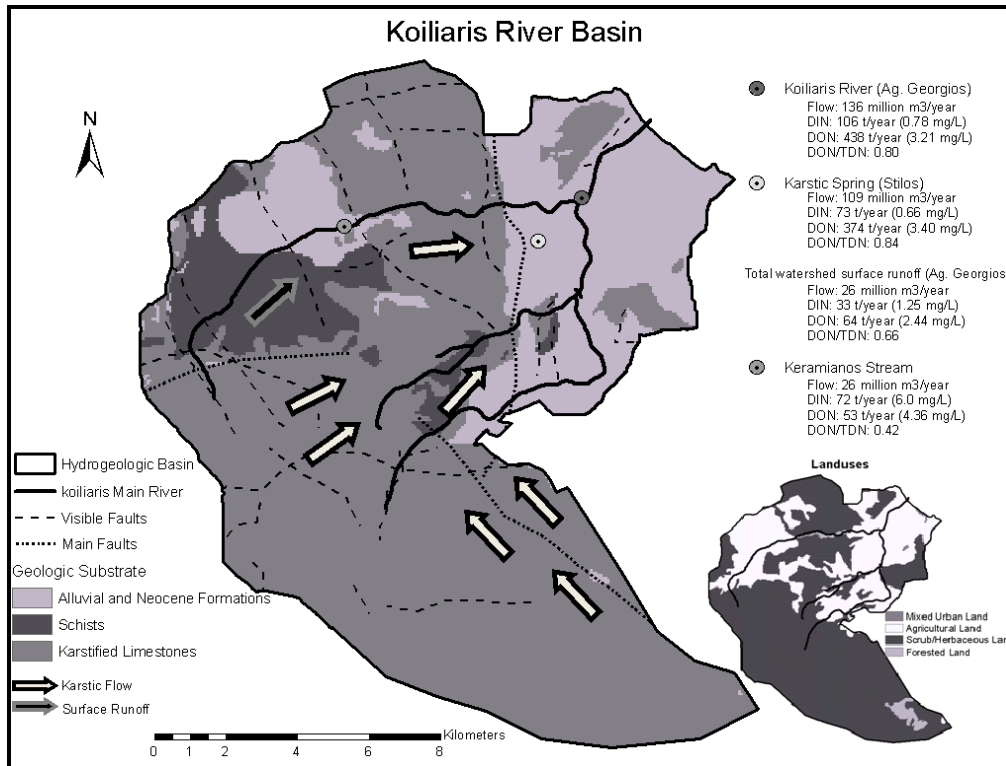


**Figure 5.6 Geologic formations, landuses and hydrologic and nutrient fluxes in Koiliaris River Basin. Note: Runoff from Keramianos stream is higher than the total watershed surface runoff as water is lost through a karstic gorge and only peak flows contribute to Koiliaris River (taken from Stamati et al., 2011).**

The River hydrograph as it has been simulated by a modified SWAT model is presented in Figure 5.7 (Nikolaidis et al., HESSD, under revision). There is a critical precipitation event of 152 mm, above which a flood event is produced by Keramianos River (11 flash flood events took place in 4 years) with recession rate constant of 0.034/hr and characteristic response time of 29 hrs (Moraetis et al. 2010). Flash floods contribute about 20% of the total runoff, altering the hydrologic and geochemical features of the River (Moraetis et al. 2010). It has been found that there is also an extended area of the karst outside the watershed of Koiliaris River which contributes to spring discharges and which has been estimated to be 50 km<sup>2</sup> (Stamati et al., 2006; Moraetis et al., 2010; Kourgialas et al., 2010). Within the karstic system there are “two reservoirs”; the upper reservoir with a faster response and the lower reservoir with a slower response. This is consistent with the fact that the springs are supplied by two geologic formations with different hydraulic characteristics: the Limestones of the Trypalis zone (Triassic

to Cretaceous period) and the autochthonous karstic group of Metamorphic Crystalline Limestones (Plattenkalk - Mesozoic period). A 'two part Maillet' model has been developed representing the upper and lower reservoirs (Stamati et al., 2006) and the recession coefficient for the upper reservoir was found to be 0.0996/d and for the lower reservoir measures 0.0261/d. The annual flow at the exit point of the basin outlet was estimated to be 136 million m<sup>3</sup>/year. The karstic flow contribution was 109 Mm<sup>3</sup>/year (80%) and the watershed flow was 31.5 Mm<sup>3</sup>/year. After evapotranspiration losses (4.20 Mm<sup>3</sup>/year), the net contribution of watershed flow to the river was 27.3 Mm<sup>3</sup>/year (20%) (Kourgialas et al., 2010). The total rainfall entering the extended karstic system was estimated to be 269 Mm<sup>3</sup>/year and the snow melt was 30.2 Mm<sup>3</sup>/year (Kourgialas et al., 2010). Water quality (nutrients) is discussed in the next section and can be found also in Moraetis et al (2011).

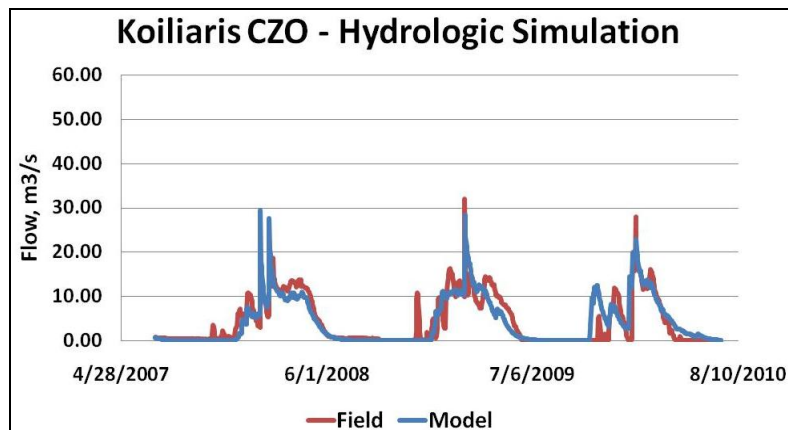


**Figure 5.7 Comparison of simulated flows with field data at the basin outlet (taken from Nikolaidis et al., HESSD, under revision)**

## 5.2 SOIL THREATS AND SOIL DEGRADATION IN KOILIARIS RIVER BASIN

The landscape in Koiliaris River Basin (KRB) and in general the Cretan landscape has been transformed during the past 50 years from a low intensity agrarian landscape with low impact agricultural practices, small size properties and high bio-diversity to mechanized, high intensity agriculture and larger size properties with monocultures (56% of the cultivated area are olive

and citrus plantations). Agricultural practices have been the primary cause of land degradation illustrated (tilling, no organic matter addition to soil, high pesticide and herbicide use). Fertilizer use in Greece from 1960 (159.000 t/yr) to 1985 (710.000 t/yr) increased 4.5 fold and then it declined by 43% (405.000 t/yr) while agricultural production has leveled off (Nikolaidis, 2011). Tourism and urban growth has extended soil sealing and compaction in valleys (high productivity land). Agricultural subsidies have made profitable the extension of farming to marginal, high slope, low productivity land. The sheep and goat population in Greece increased from 9 million to 11 million animals between 1960 and the present, while in Crete it increased from 0.4 to 1.8 million animals (Nikolaidis, 2011). Crete raises 16% of the total livestock population in Greece on only 6% of the Greek land area. The average stocking density in Crete ranges from 110 to 390 animals/km<sup>2</sup>, with an average of 227 animals/km<sup>2</sup>. The stocking density in Crete increased by a phenomenal 460% in 40 years (from 70 thousand in 1961 to 390 thousand in 1991 in the Prefecture of Rethymnon).

In Koiliaris River Basin, primarily drivers for soil degradation are agriculture and livestock grazing (Figure 5.8). Intensive cultivation and inappropriate management in the alluvial and Neocene formations of the lowlands have affected soil quality and fertility. Moreover, cultivation of olive groves has been extended also in areas of higher altitude and steeper slopes which increases the erosion. Grazing lands have been intensively extended in high altitudes and animal stock has been spread uncontrollable to forestry land on Limestones. Moreover, intentionally caused fires in grazing lands threaten soil quality and abandoned traditional agricultural practices, like terraces increases soil deterioration.

In these effects it should be superimposed also the effects of climate change (Figure 5.8). Climate change in semi-arid areas such as the Mediterranean region is expected to cause increases in temperature, CO<sub>2</sub> concentration, water vapor evaporation and declines in rainfall. Increases in temperature and CO<sub>2</sub> and decreases in soil moisture affect significantly soil ecosystem functions and can cause ecosystem shifts (Nikolaidis, 2011). This will impact freshwater quality and quantity due to increasing irrigation demands. Crete, located within 400 km of the Sahara desert, is projected to be at the center of climate change impacts according to the IPCC (2007) scenarios. Nikolaidis and Bidoglio (2011) suggested that in 2030-2050 compared to 2010-2020 it would have taken place a 17% decrease in precipitation, 8% decrease in evapotranspiration and 22% decrease in flow in Koiliaris River Basin. Warmer and drier

conditions are expected to intensify water shortages and droughts, forcing species migration at rates exceeding natural migration rates (leading to species loss), significant changes to vegetation structure resulting in loss of biodiversity and ecosystem services. Kazakis et al. (2007) studied the vascular plant diversity changes along an altitudinal gradient (1664-2339 m) and mean temperature gradient of 5° C as an indication to climate change impacts. The study recorded 70 species (20 endemic) belonging to 23 families. Cretan endemic species dominate the high altitude (the percent endemism varied between 31 and 36% at the four elevations) and species richness and turnover decreased with altitude (58 species at the 1664m elevation and decreased to 32 at 1965m and 18 and 14 species at the 2160 and 2339 m elevations). The plant cover density was 14% at the 1664m elevation and decreased to 4% at 1965m and 1% at both the 2160 and 2339 m elevations.

The aim of this work was to assess the soil status of Koiliaris River Basin Critical Zone Observatory by selecting with sophisticated statistics the appropriate soil parameters and quantify the effects of livestock grazing, landuse changes and climate change on soil biochemical quality and water quality. The soils of the basin were characterized in order to identify by statistical analysis the primary control factors of aggregation and soil organic carbon stabilization and assess the status of the soils. The effects of landuse change- native lands to croplands as well the climate change effects were assessed by modeling with RothC. Finally, the effects of over-grazing and the resulting de-vegetation (in the highlands of the basin) on soil biochemical quality and water quality were estimated.

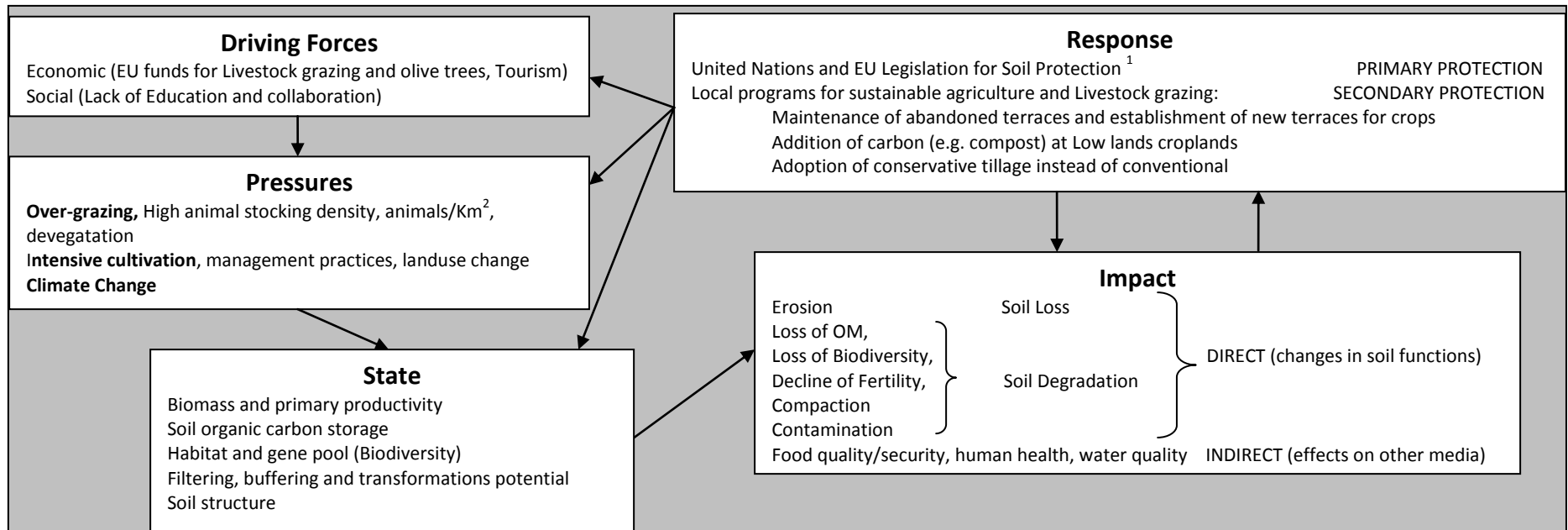


**Figure 5.8 The DPSIR Framework for soils in Koiliaris CZO.**

<sup>1</sup> EU Legislation for Soil Protection:

1. Soil Thematic Strategy (COM(2006) 231) and a proposal for a Soil Framework Directive (COM(2006) 232)
2. Commission Communication of 22 September 2006 entitled "Thematic strategy for soil protection" [COM(2006) 231 final - Not published in the Official Journal].
3. Proposal for a European Parliament and Council Directive of 22 September 2006 setting out a framework for soil protection and amending Council Directive 2004/35/EC.
4. Communication from the Commission of 5 September 2006 entitled: "Establishing an environment strategy for the Mediterranean" [COM(2006) 475 final - Not published in the Official Journal]
5. Communication of 16 April 2002 from the Commission to the Council, the European Parliament, the Economic and Social Committee and the Committee of the Regions - Towards a Thematic Strategy for Soil Protection [COM (2002) 179 final - Not published in the Official Journal].
6. Communication from the Commission to the Council, the European Parliament, the Economic and Social Committee and the Committee of the Regions of 27 January 1999: Approaches to sustainable agriculture [COM(1999) 22 final - Official Journal C 173 of 19.06.1999].
7. Proposal for a Directive of the European Parliament and of the Council of 23 January 2008 on the geological storage of carbon dioxide and amending Council Directives 85/337/EEC, 96/61/EC, Directives 2000/60/EC, 2001/80/EC, 2004/35/EC, 2006/12/EC and Regulation (EC) No 1013/2006
8. Council Directive 92/43/EEC of 21 May 1992 on the conservation of natural habitats and of wild fauna and flora
9. Desertification Convention The United Nations Convention to Combat Desertification

### 5.3 PRIMARY FACTORS CONTROLLING AGGREGATION OF KOILIARIS SOILS

The relation of aggregate stability to soil properties has been found to differ with climatic zones and soils (Idowu, 2011). There is, therefore, a need to study these relationships in different regions in order to isolate which properties to manage for improving soil aggregate stability in a given location. A soil survey (29 samples) was conducted based on the soil mapping typology approach presented in Figure 5.5 with objective to physico-chemically characterize the soils of the different geo-environments found in the basin and assess the relationship between physical and biochemical soil properties and soil aggregation in the Mediterranean geo-environment of Koiliaris River Basin. Sampling was conducted to the 0-15 cm and 15-30 cm soil depths. Part of the dataset obtained by this survey has been presented by Moraetis et al. (2011). Topsoil samples were measured for parameters known to affect aggregation (see section 1.2.5 in Chapter 1): dry Bulk Density (BD), pH, conductivity (COND), Soil organic carbon (SOC) (Walkley-Black acid dichromate digestion technique, Santi et al., 2006), Total Kjeldahl Nitrogen (TKN) (Hach digestion apparatus; Nessler method, 8075), Carbonates-CaCO<sub>3</sub> (Bernard volumetric Method), Water Stable Aggregates (WSA) (Elliott, 1986). Mean Weight Diameter (MWD) was calculated, and particle distribution was determined (the percentage of the soil particles <2 µm-clay, <20 µm-fine silt and clay, < 53 µm-silt and clay and <1000 µm-coarse sand). Potential Mineralizable N (PMN) was calculated by the 2 M KCl extraction (N-1week (40°C) minus N-1hour (20°C) (Nikolaidis et al., 1999; Burton et al., 2007); the extracted filtered-through a 0.45 µm Nylon filter – pools was analyzed for NH<sub>4</sub>-N by the Nessler method (8075). Measurements also included effective Cation Exchange Capacity (eCEC) and exchangeable cations (Na, Mg, K, Ca, Mn) by the BaCl<sub>2</sub> method (Hendershot and Duquette, 1986). The proportional contribution of the cations (Na, Mg, K, Ca) to the eCEC indicative of base saturation was calculated. Finally, extractable Al, Fe, and Mn were measured by the Acid Ammonium Oxalate Method (Mackeague and Day 1966) and by the Dithionite-Citrate Method (Soil Conservation Service, U.S. Department of Agriculture, 1972). The Fe-ox/Fe-d ratio was calculated and used in the analysis as a gross index of mineral weathering. These standard methods can be found in Soil Sampling and Methods of Analysis (2008). The measured soil parameters (31 parameters given in Table 5.4a) were correlated (Pearson correlation) with the indices of aggregate stability (WSA, WSA macro-aggregates >250 µm, WSA large and medium macro-aggregates >1000 µm, and the MWD). The WSA macro-aggregates >250 µm (WSA-250) were found to be the best index and mostly

correlated with soil parameters. The Pearson correlation results and the P-value are presented in Table 5.4. The inter-correlated parameters are also indicated. Correlations were conducted with the MINITAB statistical program.

**Table 5.4 Pearson Correlation results and P-Value in parenthesis of WSA-250 with measured soil properties; inter-correlated parameters are also indicated.**

	WSA-250	Inter-correlated with parameters	
<b>&gt;1000<math>\mu\text{m}</math></b>	<b>-0.828 (0)</b>		R-Sq
<b>eCEC</b>	<b>0.813 (0)</b>		
Ca-BaCl <sub>2</sub>	0.805 (0)	eCEC	0.992
<b>&lt;53<math>\mu\text{m}</math><sup>1</sup></b>	<b>0.744 (0)</b>	>1000 $\mu\text{m}$	-0.874
<b>BS_Na-BaCl<sub>2</sub></b>	<b>-0.723 (0)</b>		
<20 $\mu\text{m}$	0.663 (0)	<53 $\mu\text{m}$ , >1000 $\mu\text{m}$	0.941, -0.836
<b>TKN</b>	<b>0.636 (0)</b>		
<b>Al-ox</b>	<b>0.605 (0.001)</b>		
<b>K-BaCl<sub>2</sub></b>	<b>0.598 (0.001)</b>		
<b>&lt;2 <math>\mu\text{m}</math><sup>2</sup></b>	<b>0.594 (0.001)</b>	<20 $\mu\text{m}$ , <53 $\mu\text{m}$	0.816, 0.768
Mn-ox	0.586 (0.001)	Al-ox	0.846
<b>BD</b>	<b>-0.569 (0.001)</b>		
N-1week	0.558 (0.002)	PMN	0.996
<b>pH</b>	<b>0.54 (0.002)</b>		
<b>PMN</b>	<b>0.539 (0.003)</b>		
Mn-d	0.538 (0.003)	Mn-ox, Al-ox	0.965, 0.798
<b>N-1hour</b>	<b>0.534 (0.003)</b>		
<b>Fe-ox</b>	<b>0.523 (0.004)</b>		
<b>Fe-ox/F-d</b>	<b>0.495 (0.006)</b>		
TOC	0.473 (0.01)	TKN	0.916
Mn-BaCl <sub>2</sub>	-0.417 (0.024)		
C/N	-0.413 (0.026)		
COND	0.375 (0.045)		
Al-d	-0.318 (0.093)		
Mg-BaCl <sub>2</sub>	0.3 (0.114)		
Fe-d	-0.256 (0.18)		
BS_K-BaCl <sub>2</sub>	-0.213 (0.267)		
Na-BaCl <sub>2</sub>	-0.043 (0.826)		
BS_Ca-BaCl <sub>2</sub>	0.15 (0.437)		
BS_Mg-BaCl <sub>2</sub>	0.122 (0.527)		
CaCO <sub>3</sub>	0.065 (0.739)		

<sup>1</sup>Although it was significantly inter-correlated with the >1000  $\mu\text{m}$  fraction it was decided to keep this parameter, since it is soil type specific.

<sup>2</sup>The parameter is significantly inter-correlated with the <20  $\mu\text{m}$  fraction which has been removed, although it is correlated with the <53  $\mu\text{m}$  fraction (pearson correlation 0.768) it was decided to keep this parameter, since it is soil type specific.

The parameters presenting correlation (Pearson) with WSA-250 higher than 0.5 included in the Principal Component Analysis (PCA), in order to reveal similarities and differences between the soil samples, and the relationships between the different variables. The number of parameters used was reduced by removing those that are significantly inter-correlated (Table 5.4). Finally, a total of 15 parameters were used: WSA-250, BD, pH, TKN, particles < 53 µm, particles < 2 µm as well > 1000 µm, K-BaCl<sub>2</sub>, eCEC, BS-Na-BaCl<sub>2</sub>, Al-ox, Fe-ox, N-1hour, and PMN, Fe-ox/Fe-d (detailed data for each soil sample can be found in Table A5.1 in the Appendix). The intercorrelation of the 15 parameters is given in Table 5.5.

**Table 5.5 Pearson correlation results (R-Sq) of the 15 soil properties used in the PCA.**

	BD	pH	TKN	<2 µm	<53µm	>1000µm	K-BaCl <sub>2</sub>	eCEC	BS_Na-BaCl <sub>2</sub>	Al-ox	Fe-ox	Fe-ox/F-d	N-1hour	PMN
WSA-250	-0.569	0.54	0.636	0.594	0.744	-0.828	0.598	0.813	-0.723	0.605	0.523	0.495	0.534	0.539
BD		-0.459	-0.637	-0.067	-0.256	0.386	-0.033	-0.46	0.497	-0.619	-0.38	-0.133	-0.515	-0.593
pH			0.474	0.395	0.446	-0.557	0.385	0.728	-0.689	0.245	0.161	0.389	-0.029	0.43
TKN				0.175	0.555	-0.558	0.29	0.715	-0.371	0.736	0.53	0.363	0.626	0.703
<2 µm					0.768	-0.667	0.724	0.599	-0.459	0.192	0.207	0.224	0.136	-0.067
<53µm						-0.874	0.605	0.687	-0.474	0.476	0.33	0.43	0.388	0.258
>1000µm							-0.626	-0.683	0.556	-0.468	-0.438	-0.526	-0.422	-0.332
K-BaCl <sub>2</sub>								0.711	-0.478	0.181	0.408	0.538	0.328	0.187
eCEC									-0.76	0.564	0.508	0.602	0.443	0.587
BS_Na-BaCl <sub>2</sub>										-0.396	-0.331	-0.547	-0.279	-0.486
Al-ox											0.751	0.276	0.661	0.557
Fe-ox												0.486	0.748	0.596
Fe-ox/F-d													0.454	0.491
N-1hour														0.649

Yellow highlighted cells correspond to R-Sq higher than 0.5 and red highlighted cells correspond to R-Sq higher than 0.7.

The Eigenvalue was found to be higher than 1 for three PC components (Table 5.6). The loadings of the three most significant components are presented in Table 5.7 and Figures 5.8 and 5.10. In loading plots, positively and negatively correlated variables are positioned close to each other, or opposite each other, respectively. In the score plots (Figure 5.9 and 5.11) samples that are high in a specific variable are pulled towards the area of the score plot where the variable in the corresponding loading plot is located.

**Table 5.6 Eigenvalue, and proportionally and cumulative explanation of the variation of soil samples.**

	Eigenvalue	Proportion	Cumulative
<b>1</b>	<b>7.9166</b>	<b>0.528</b>	<b>0.528</b>
<b>2</b>	<b>2.3497</b>	<b>0.157</b>	<b>0.684</b>
<b>3</b>	<b>1.3384</b>	<b>0.089</b>	<b>0.774</b>
4	1.0369	0.069	0.843
5	0.5544	0.037	0.88
6	0.4642	0.031	0.911
7	0.3948	0.026	0.937
8	0.2759	0.018	0.955
9	0.2258	0.015	0.97
10	0.179	0.012	0.982
11	0.096	0.006	0.989
12	0.0802	0.005	0.994
13	0.0403	0.003	0.997
14	0.0286	0.002	0.999
15	0.0192	0.001	1

**Table 5.7 The three major components of the principal component analysis.**

Variable	PC1		PC2		PC3
<b>eCEC</b>	<b>0.325</b>	<b>PMN</b>	<b>0.348</b>	<b>N-1hour</b>	<b>0.381</b>
<b>WSA-250</b>	<b>0.323</b>	<b>N-1hour</b>	<b>0.328</b>	<b>Fe-ox</b>	<b>0.354</b>
<b>TKN</b>	<b>0.277</b>	<b>Al-ox</b>	<b>0.303</b>	<b>BD</b>	<b>0.344</b>
<b>&lt;53µm</b>	<b>0.275</b>	Fe-ox	0.258	<b>BS_Na-BaCl2</b>	<b>0.328</b>
Al-ox	0.254	TKN	0.238	K-BaCl2	0.261
Fe-ox	0.241	>1000µm	0.201	<2 µm	0.17
PMN	0.24	BS_Na-BaCl2	0.116	<53µm	0.159
K-BaCl2	0.233	Fe-ox/F-d	-0.044	Al-ox	0.115
N-1hour	0.233	WSA-250	-0.067	Fe-ox/F-d	0.111
Fe-ox/F-d	0.228	eCEC	-0.105	WSA-250	-0.021
pH	0.227	pH	-0.169	TKN	-0.073
<2 µm	0.203	<53µm	-0.247	>1000µm	-0.08
BD	-0.216	<b>BD</b>	<b>-0.299</b>	eCEC	-0.121
BS_Na-BaCl2	-0.265	<b>K-BaCl2</b>	<b>-0.329</b>	PMN	-0.158
<b>&gt;1000µm</b>	<b>-0.296</b>	<b>&lt;2 µm</b>	<b>-0.445</b>	<b>pH</b>	<b>-0.552</b>

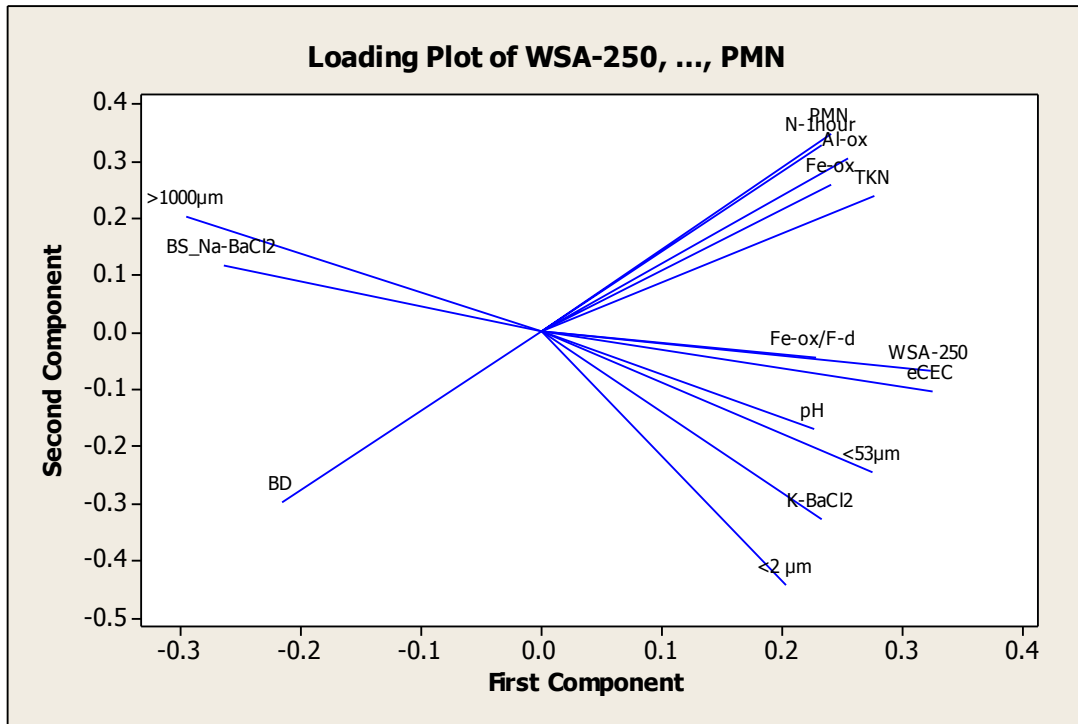


Figure 5.8 Loading plot of first versus second component of PCA analysis.

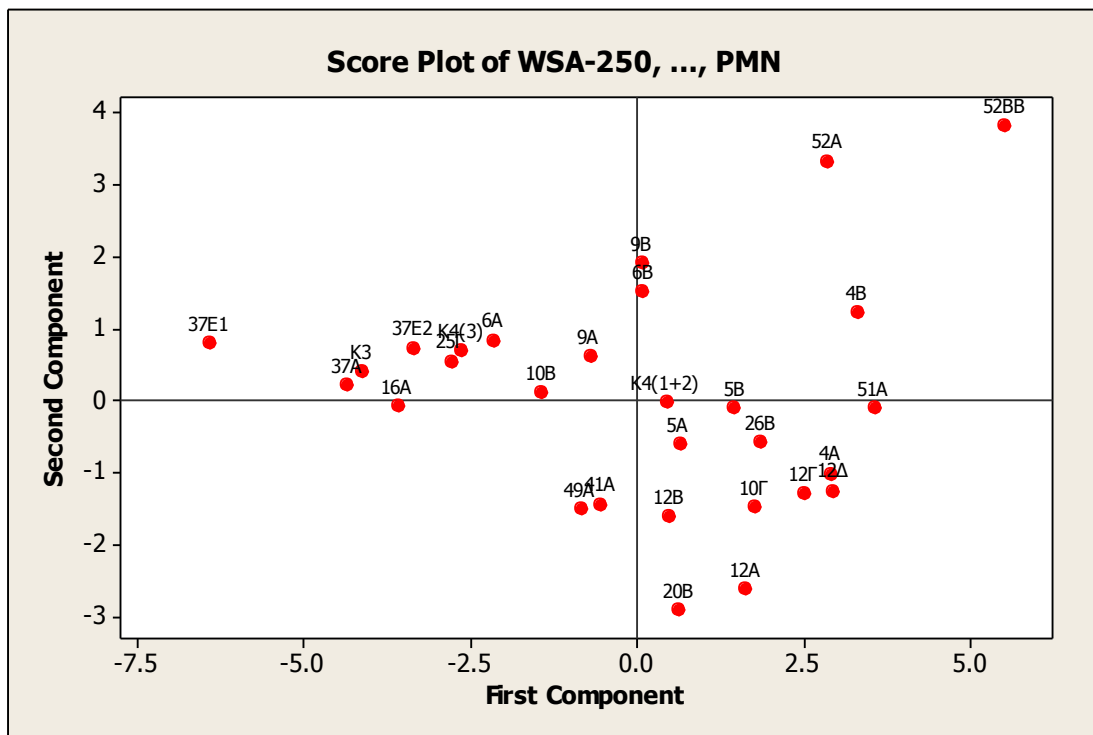


Figure 5.9 Score plot of first versus second component of PCA analysis.

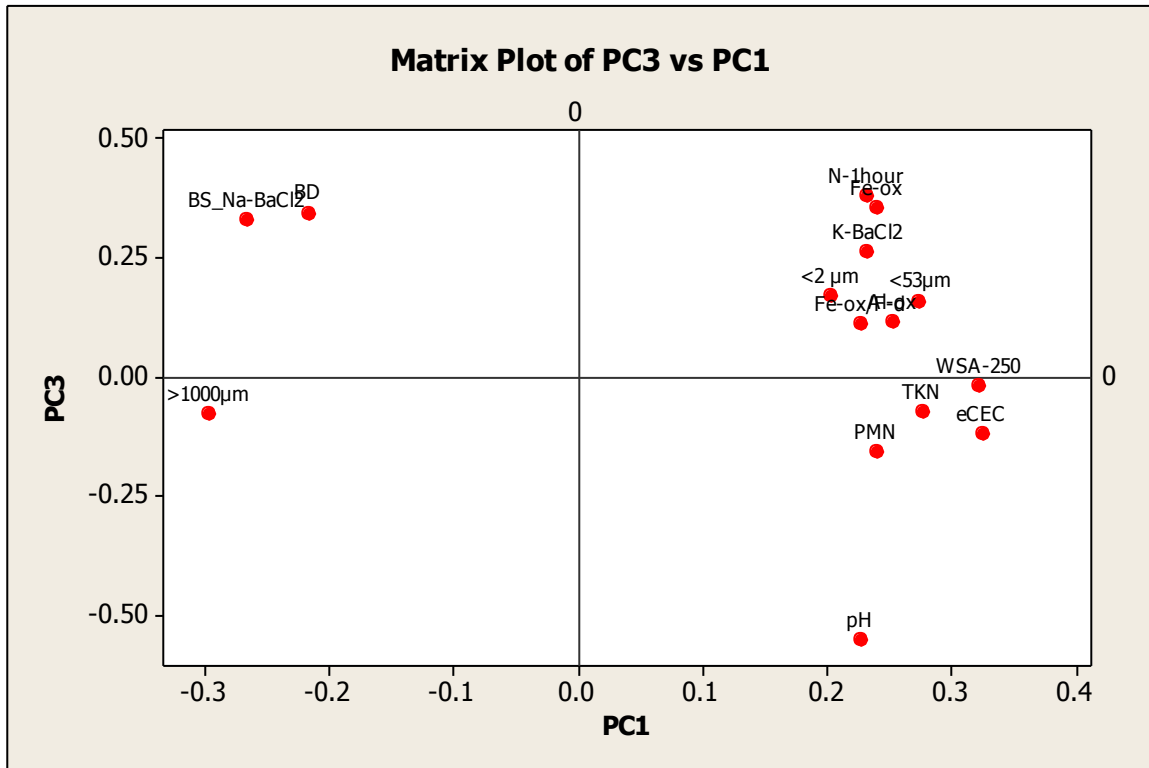


Figure 5.10 Loading plot of first versus third component of PCA analysis.

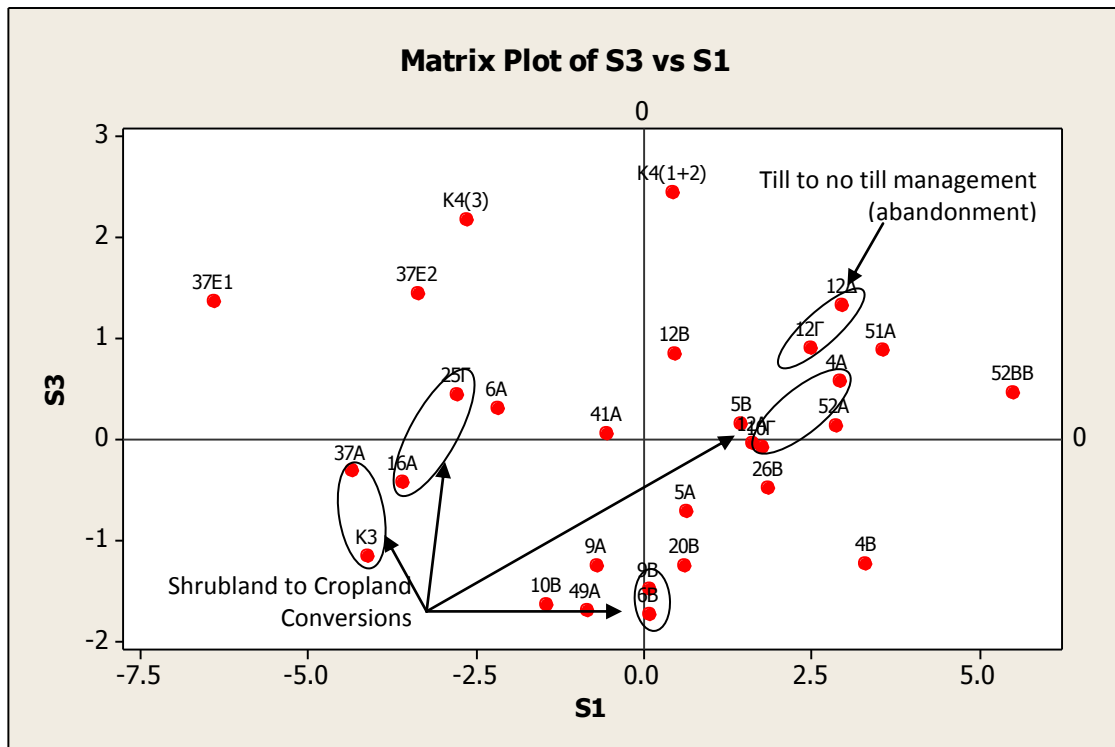


Figure 5.11 Score plot of first versus third component of PCA analysis.

The first component described 53% of the variation (Table 5.6) and clearly separated the two soil Groups. Out of the 29 samples, one was considered as outlier of Group-2 (52BB) 12 and 16 soil samples were grouped in soil group 1 and 2 respectively (mean values and statistics of soil parameters of the two groups resented in Table 5.8). Soils of Group-1 were characterized in comparison with Group-2 by sandier texture - coarser sand ( $22.5 \pm 10.9$  % versus  $8.5 \pm 8.3$ ) and lower silt-clay content ( $48.6 \pm 13.2$  % versus  $66.9 \pm 12.3$  %) as well as lower clay content ( $13.8 \pm 4.9$  % versus  $25.7 \pm 9.4$  %), in accordance with higher bulk density ( $1.18 \pm 0.09$  g/cm<sup>3</sup> versus  $1.11 \pm 0.08$  g/cm<sup>3</sup>), lower WSA macro-aggregates ( $33.8 \pm 14.0$  % versus  $64.4 \pm 11.6$ ), lower TKN content ( $0.16 \pm 0.06$  % versus  $0.30 \pm 0.09$ ), lower pH ( $6.45 \pm 1.10$  versus  $7.43 \pm 0.81$ ). In addition, they exhibited lower eCEC ( $2.55 \pm 1.84$  versus  $8.61 \pm 1.57$  cmol/kg) and K ( $0.15 \pm 0.09$  versus  $0.58 \pm 0.32$  cmol/kg) extracted by BaCl<sub>2</sub> and higher well base saturation regarding sodium ( $1.55 \pm 1.22$  versus  $0.31 \pm 0.12$  %). KCl-extracted NH<sub>3</sub>-N after 1-hour incubation at 20°C ( $5.9 \pm 3.1$  mgN/kg versus  $10.2 \pm 3.6$  mgN/kg) and potential mineralizable nitrogen ( $54.2 \pm 21.1$  mgN/kg versus  $89.8 \pm 27.9$  mgN/kg) was found to be lower in soil Group-1 comparing to Group-2. Finally, there were indications of lower Al and Fe extracted with the acid ammonium oxalate method and higher mineral weathering as depicted by the Fe-ox/Fe-d lower ratio. The range value for soil parameters characterizing the two soil Groups is presented in Table 5.9.

**Table 5.8 Mean value, standard deviation, minimum and maximum soil parameters used in PCA analysis of the two groups indicated by first component.**

Parameter	Units	GROUP-1				GROUP-2			
		mean	std	min	max	mean	std	min	max
WSA-250	%	33.8	14.0	12.7	54.8	64.4	11.6	44.2	90.5
BD	g/cm <sup>3</sup>	1.18	0.09	0.96	1.34	1.11	0.08	0.92	1.21
pH	-	6.45	1.10	4.70	8.13	7.43	0.81	4.72	8.10
TKN	%	0.16	0.06	0.08	0.30	0.30	0.09	0.14	0.49
<2 μm	%	13.8	4.9	7.1	22.7	25.7	9.4	9.5	38.4
<53 μm	%	48.6	13.2	31.0	72.5	66.9	12.3	43.1	83.4
>1000 μm	%	22.5	10.9	1.4	42.6	8.5	8.3	1.0	27.9
K-BaCl <sub>2</sub>	cmol/kg	0.15	0.09	0.01	0.30	0.58	0.32	0.11	1.05
eCEC	cmol/kg	2.55	1.84	0.53	6.01	8.61	1.57	5.97	10.75
BS_Na-BaCl <sub>2</sub>	%	1.55	1.22	0.33	3.91	0.31	0.12	0.18	0.64
Al-ox	%	0.23	0.15	0.09	0.61	0.57	0.37	0.06	1.26
Fe-ox	%	0.26	0.09	0.10	0.38	0.40	0.13	0.10	0.60
Fe-ox/F-d	-	0.46	0.29	0.16	0.95	0.71	0.21	0.29	1.06
N-1hour	mgN/kg	5.9	3.1	2.3	12.2	10.2	3.6	4.0	17.1
PMN	mgN/kg	54.2	21.1	20.3	93.1	89.8	27.9	37.1	143.0

**Table 5.9 The values for soil parameters characterizing the two soil Groups.**

Parameter	Units	Group-2	Group-1	Parameter needed for the Regression equations (Table 5.8) with No of parameters <sup>2</sup>
WSA-250	%	>54.8	<44.2	
BD	g/cm <sup>3</sup>	complex	complex	5
pH	%	complex	complex	5
TKN	%	>0.30	<0.14	5
>1000 μm	%	complex	>27.9	5
eCEC	cmol/kg	>6	<6	5
BS_Na-BaCl2	%	<0.33	>0.64	6
PMN	mgN/kg	>93.1	<37.1	6,7
<2 μm	%	>22.7	<9.5	8
N-1hour <sup>1</sup>	mgN/kg	>12.2	complex	9
<53 μm	%	>72.5	<43.1	11
K-BaCl2	cmol/kg	>0.30	<0.11	11
Fe-ox	%	>0.41	complex	12
Al-ox	%	>0.61	complex	14
Fe-ox/F-d		complex	complex	14

<sup>1</sup>It is not recommended to use this parameter to group the soils due to the low range of the differences between the two soil groups which creates uncertainties.

Soils in **Group-1** were from regions where Schist was the parent material as well as from Marls with sandy texture and acidic pH. Weathered Schists are known to have influenced soils of the basin in specific regions. However, this group includes also some soils with alkaline pH or significantly higher TKN content as compared to the average of the group; the main factors characterizing Group-1 were the low eCEC and the sandy texture and low clay content. All soils in Group-1 were found in elevation lower than 550 m where Schists and Marls can be found. The soil samples grouped in Group-1 are found in the area identified in the Greek soil classification: Brown and red-brown alkaline Mediterranean soils; soils on Schists according to FAO are eutric Lithosols (Figure 5.3b). Soils in **Group-2** were mostly derived from the alluvial plain and some alkaline (calcaric) Marls and from the semi-mountainous region where the Limestones of the Trypalis units are found. Most soils were croplands, cultivated with olive groves or orange trees (elevation 9-465 m) included also in the soil group shrublands on limestones (582-1098 m). The soils are characterized as calcaric Regosols and calcaric Lithosols, respectively, according to the FAO classification of soils and combined as Calcareous rendzines soil and Mediterranean brown soil according to the Greek classification (Figure 5.3b). All the soils in Group-1 and six out of the

sixteen soils in Group-2 exhibited WSA-250 lower than the limit value of 60% which indicates agronomically valuable soils (Banwart et al., 2011).

Multi Regression Analysis was used for the development of equations for the prediction of WSA macro-aggregates by soil parameters. The multi Regression Analysis with all the parameters for all the soil samples exhibited lower fitness as compared to the regression with the soil groups alone even when reduced parameters were used (Table 5.10). The equations developed are presented in Table 5.11. Detailed statistics for selected cases are presented in Figures 5.12-14. R-Sq was found to be higher than 90% with equal or more than 9 and 6 parameters in the cases of combined groups as well Group-2 and Group-1, respectively. The content of the soils in macro-aggregates, as revealed by the multi regression analysis, was adequately (R-Sq > 95%) described by 7 parameters for Group-1: BD, pH, TKN, particles >1000 $\mu$ m, eCEC, BS\_Na-BaCl<sub>2</sub>, and PMN and 11 parameters for Group-2: BD, pH, TKN, particles >1000  $\mu$ m, particles <53  $\mu$ m, particles <2  $\mu$ m, eCEC, BS\_Na-BaCl<sub>2</sub>, PMN, N-1hour (KCl extracted), and K-BaCl<sub>2</sub>. The equation with the 11 parameters developed for the combined groups yielded in a R-Sq of 90%. The 11 parameters require the same calculation effort with the 6 parameters.

Most studies aiming to predict aggregate stability have correlated it only to SOC content (see Krull et al., 2004), while few studies that have used more soil parameters have not yield to high predictability (e.g. Chappell et al., 1999 and Idohu, 2011 both for tropical soils). Dimoyiannis et al., (2008) correlated soil aggregate stability with soil parameters for 10 soil samples from Central Greece (Thessaly), however their work did not resulted in a predicted equation.

**Table 5.10 Statistics of the multi-regression analysis of all samples together and each group separately.**

<b>Combined Group-1 &amp; Group-2 (28 soil samples)</b>		S	R-Sq,%	R-Sq(adj),%
14	BD, pH, TKN, >1000µm, eCEC, BS_Na-BaCl2, PMN, <2 µm, N-1hour, <53 µm, K-BaCl2, Fe-ox, Al-ox, Fe-ox/F-d	8.676	90.8	80.8
12	BD, pH, TKN, >1000µm, eCEC, BS_Na-BaCl2, PMN, <2 µm, N-1hour, <53 µm, K-BaCl2, Fe-ox	8.221	90.4	82.8
<b>11</b>	<b>BD, pH, TKN, &gt;1000µm, eCEC, BS_Na-BaCl2, PMN, &lt;2 µm, N-1hour, &lt;53 µm, K-BaCl2</b>	<b>7.975</b>	<b>90.4</b>	<b>83.8</b>
9	BD, pH, TKN, >1000µm, eCEC, BS_Na-BaCl2, PMN, <2 µm, N-1hour	7.542	90.3	85.5
8	BD, pH, TKN, >1000µm, eCEC, BS_Na-BaCl2, PMN, <2 µm	7.809	89.1	84.5
7	BD, pH, TKN, >1000µm, eCEC, BS_Na-BaCl2, PMN	7.622	89.0	85.2
6	BD, pH, TKN, >1000µm, eCEC, PMN	7.482	88.9	85.7
6	BD, pH, TKN, >1000µm, eCEC, BS_Na-BaCl2	7.888	87.7	84.1
5	BD, pH, TKN, >1000µm, eCEC	7.933	86.9	84.0
<b>Group-2 (16 soil samples)</b>				
14	BD, pH, TKN, >1000µm, eCEC, BS_Na-BaCl2, PMN, <2 µm, N-1hour, <53 µm, K-BaCl2, Fe-ox, Al-ox, Fe-ox/F-d	4.014	99.2	88.0
12	BD, pH, TKN, >1000µm, eCEC, BS_Na-BaCl2, PMN, <2 µm, N-1hour, <53 µm, K-BaCl2, Fe-ox	4.401	97.1	85.5
<b>11</b>	<b>BD, pH, TKN, &gt;1000µm, eCEC, BS_Na-BaCl2, PMN, &lt;2 µm, N-1hour, &lt;53 µm, K-BaCl2</b>	<b>4.934</b>	<b>95.2</b>	<b>81.8</b>
9	BD, pH, TKN, >1000µm, eCEC, BS_Na-BaCl2, PMN, <2 µm, N-1hour	4.707	93.4	83.5
8	BD, pH, TKN, >1000µm, eCEC, BS_Na-BaCl2, PMN, <2 µm	6.232	86.5	71.0
7	BD, pH, TKN, >1000µm, eCEC, BS_Na-BaCl2, PMN	7.461	77.9	58.5
6	BD, pH, TKN, >1000µm, eCEC, PMN	7.984	71.5	52.4
5	BD, pH, TKN, >1000µm, eCEC	7.612	71.2	56.8
<b>Group-1 (12 soil samples)</b>				
8	BD, pH, TKN, >1000µm, eCEC, BS_Na-BaCl2, , PMN <2 µm	5.048	96.5	87.0
<b>7</b>	<b>BD, pH, TKN, &gt;1000µm, eCEC, BS_Na-BaCl2, PMN</b>	<b>4.566</b>	<b>96.1</b>	<b>89.4</b>
6	BD, pH, TKN, >1000µm, eCEC, BS_Na-BaCl2	5.524	92.9	84.4
5	BD, pH, TKN, >1000µm, eCEC	6.197	89.3	80.4

\*52BB was excluded as outlier from all calculations

**Table 5.11 Statistics of the multi-regression analysis of all samples and groups separately.**

<b>Combined Group-1 &amp; Group-2</b>	
14	WSA-250 = 195 - 64.0 BD - 10.0 pH - 50.5 TKN - 0.092 <2 μm + 0.079 <53μm - 1.12 >1000μm - 1.9 K-BaCl2 + 3.98 eCEC - 1.73 BS_Na-BaCl2 + 0.6 Al-ox + 3.8 Fe-ox - 7.7 Fe-ox/F-d - 0.88 N-1hour + 0.180 PMN
12	WSA-250 = 204 - 73.6 BD - 10.7 pH - 38.8 TKN + 0.081 <2 μm + 0.058 <53μm - 1.04 >1000μm - 2.6 K-BaCl2 + 3.57 eCEC - 1.46 BS_Na-BaCl2 + 4.5 Fe-ox - 1.15 N-1hour + 0.186 PMN
11	WSA-250 = 205 - 71.7 BD - 10.7 pH - 38.1 TKN + 0.105 <2 μm + 0.023 <53μm - 1.08 >1000μm - 2.9 K-BaCl2 + 3.63 eCEC - 1.43 BS_Na-BaCl2 - 1.06 N-1hour + 0.187 PMN
9	WSA-250 = 207 - 72.5 BD - 10.7 pH - 31.4 TKN + 0.117 <2 μm - 1.07 >1000μm + 3.31 eCEC - 1.76 BS_Na-BaCl2 - 1.14 N-1hour + 0.190 PMN
8	WSA-250 = 159 - 58.7 BD - 6.40 pH - 36.1 TKN + 0.076 <2 μm - 0.937 >1000μm + 2.82 eCEC - 1.69 BS_Na-BaCl2 + 0.124 PMN
7	WSA-250 = 163 - 59.5 BD - 6.52 pH - 39.5 TKN - 0.969 >1000μm + 3.04 eCEC - 1.56 BS_Na-BaCl2 + 0.116 PMN
6	WSA-250 = 167 - 65.4 BD - 6.42 pH - 49.8 TKN - 0.990 >1000μm + 3.39 eCEC + 0.129 PMN
6	WSA-250 = 159 - 55.2 BD - 6.19 pH - 13.4 TKN - 0.872 >1000μm + 2.89 eCEC - 3.43 BS_Na-BaCl2
5	WSA-250 = 169 - 69.0 BD - 5.85 pH - 32.2 TKN - 0.896 >1000μm + 3.74 eCEC
<b>Group-2</b>	
14	WSA-250 = 258 - 122 BD - 18.9 pH - 70.3 TKN - 0.040 <2 μm + 0.684 <53μm - 2.02 >1000μm - 20.7 K-BaCl2 + 6.15 eCEC - 6.1 BS_Na-BaCl2 - 18.4 Al-ox + 83.0 Fe-ox + 7.5 Fe-ox/F-d - 4.38 N-1hour + 0.608 PMN
12	WSA-250 = 267 - 75.0 BD - 20.7 pH - 53.4 TKN - 2.21 >1000μm + 6.99 eCEC - 25.1 BS_Na-BaCl2 + 0.600 PMN - 0.192 <53μm + 0.672 <2 μm - 4.12 N-1hour - 20.4 K-BaCl2 + 30.4 Fe-ox
11	WSA-250 = 258 - 70.5 BD - 20.4 pH - 15.7 TKN - 2.14 >1000μm + 6.98 eCEC - 22.2 BS_Na-BaCl2 + 0.600 PMN - 0.574 <53μm + 1.34 <2 μm - 3.20 N-1hour - 19.9 K-BaCl2
9	WSA-250 = 190 - 81.7 BD - 13.4 pH + 2.8 TKN + 0.880 <2 μm - 1.43 >1000μm + 3.12 eCEC + 2.9 BS_Na-BaCl2 + 0.508 PMN - 1.91 N-1hour
8	WSA-250 = 94.2 - 46.9 BD - 6.26 pH + 25.5 TKN + 0.845 <2 μm - 1.10 >1000μm + 1.64 eCEC + 13.4 BS_Na-BaCl2 + 0.344 PMN
7	WSA-250 = 104 - 22.0 BD - 6.28 pH + 6.0 TKN - 1.35 >1000μm + 2.47 eCEC + 7.6 BS_Na-BaCl2 + 0.201 PMN
6	WSA-250 = 91.7 + 2.5 BD - 6.62 pH + 57.5 TKN - 0.895 >1000μm + 1.34 eCEC - 6.0 BS_Na-BaCl2
5	WSA-250 = 91.4 + 0.1 BD - 6.69 pH + 57.7 TKN - 0.903 >1000μm + 1.54 eCEC
<b>Group-1</b>	
8	WSA-250 = 324 - 122 BD - 18.0 pH - 221 TKN - 1.51 >1000μm + 11.1 eCEC + 6.38 BS_Na-BaCl2 + 0.123 PMN - 0.355 <2 μm
7	WSA-250 = 307 - 112 BD - 18.5 pH - 1.44 >1000μm + 10.9 eCEC + 0.190 PMN - 232 TKN + 6.49 BS_Na-BaCl2
6	WSA-250 = 301 - 112 BD - 16.4 pH - 200 TKN + 5.60 BS_Na-BaCl2 - 1.46 >1000μm + 10.5 eCEC
5	WSA-250 = 241 - 82.0 BD - 11.9 pH - 134 TKN - 1.25 >1000μm + 6.12 eCEC

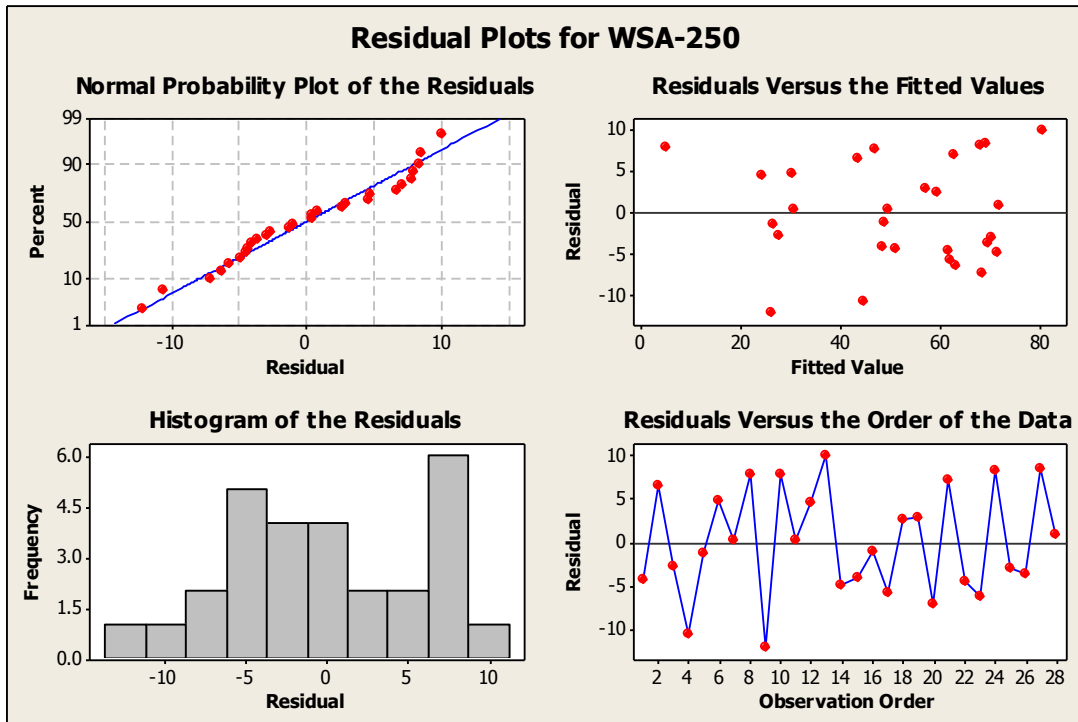


Figure 5.12 Multi-regression analysis for combined Group-1 and Group-2 with 11 parameters used.

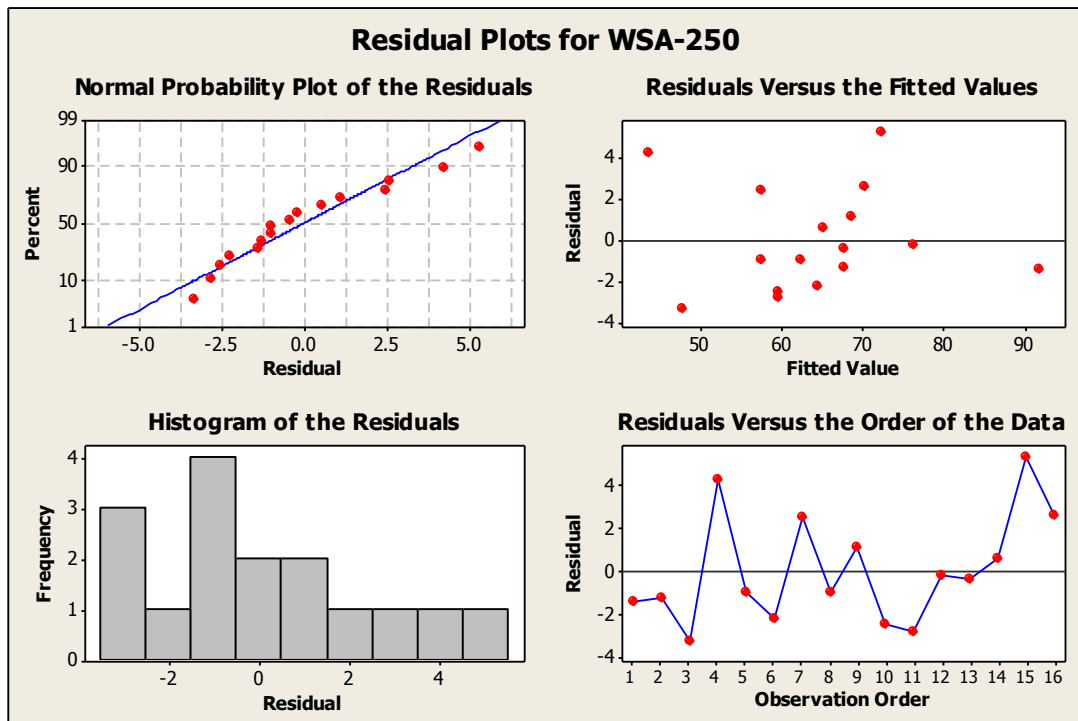


Figure 5.13 Multi-regression analysis for Group-2 with 11 parameters used.

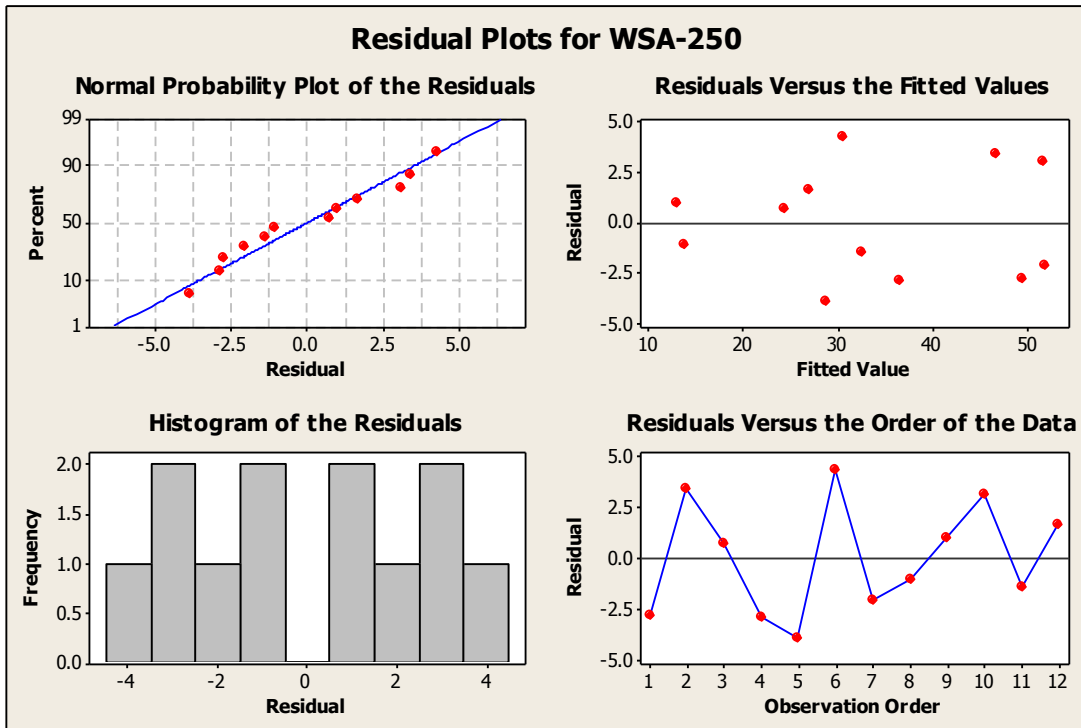


Figure 5.14 Multi-regression analysis for Group-1 with 7 parameters used.

## 5.4 LANDUSE AND CLIMATE CHANGE IMPACTS: MODELING OF SOC CHANGE IN SHRUBLAND TO CROPLAND CONVERSIONS

Landuse change from native land (shubland) to cropland (olive groves) under three lithologies and similar elevation were modeled to assess the effect on SOC turnover, make climate change scenarios and evaluate also the alternatives of carbon addition on major soil types of the basin. The soil samples used are indicated in Figure 5.11 and the values of the soil parameters for the shrublands and olive grove fields for the three lithologies are presented in Table 5.12. The methodological approach followed, for the initialization/calibration, as well as sensitivity/uncertainty analysis with the use of RothC carbon model, was presented in detail in Chapters 2 and 3.

**Table 5.12 Soil parameters for the shrublands and olive grove fields under different lithology in the Koiliaris River Basin CZO used for the simulation with RothC.**

Geologic formation		Schists		Marls		Trypalis	
Land cover		Cropland	Shrubland	Cropland	Shrubland	Cropland	Shrubland
Sample ID		25G	16A	6B	9B	10G	4A
Altitude		290	219	383	383	375	308
BD	g/cm <sup>3</sup>	1.20	1.19	1.08	1.09	1.19	1.10
pH	-	6.53	5.99	7.86	7.68	7.59	7.67
COND	μS/cm	24.5	23.0	106.0	96.5	79.5	86.5
TOC (0-15 cm)	%	1.47	1.63	2.77	3.78	2.62	3.03
POC/TOC (0-15 cm)	%	32.07	37.11	56.98	43.44	43.71	52.25
TOC (15-30 cm)	%	1.67	0.67	1.72	3.10	1.62	2.67
POC/TOC (15-30 cm)	%	29.92	12.17	8.19	13.54	9.13	7.54
TKN, 0-15	%	0.13	0.10	0.31	0.34	0.36	0.29
TOC (0-30 cm)	t/ha	<b>56.7</b>	<b>40.1</b>	<b>72.8</b>	<b>112.8</b>	<b>76.5</b>	<b>101.1</b>
POC (0-30 cm)	t/ha	<b>17.5</b>	<b>12.2</b>	<b>27.9</b>	<b>33.8</b>	<b>23.0</b>	<b>29.5</b>
POC/TOC (0-30 cm)	%	<b>30.9</b>	<b>30.2</b>	<b>38.3</b>	<b>30.0</b>	<b>30.2</b>	<b>29.7</b>
Clay (<2 μm)	%	<b>13.1</b>	<b>17.7</b>	<b>16.5</b>	<b>12.4</b>	<b>28.8</b>	<b>32.7</b>
Silt -Clay (<53 μm)	%	39.8	40.8	51.6	43.1	76.9	73.5
Coarse sand (>1000 μm)	%	24.3	32.0	25.1	27.9	1.4	3.1
WSA (> 250 μm)	%	28.6	34.8	44.2	47.6	69.7	77.7
MWD	mm	1.6	2.1	2.5	2.3	2.5	3.0

In all sites olive groves were about 50 year old and therefore the duration of the landuse conversion was estimated to be 50 years. The soil depth of the simulation was 30 cm. The

climatic data used for the simulation are presented in Table A5.2 in the Appendix. The soil organic carbon content and the particulate organic carbon content (POC) given in Table 5.12 were measured according to the methods describe in Chapter 2 and used for the initialization and calibration of the model. Table 5.13 presents the statistics of the parameter distributions for the ensemble of the Monte-Carlo simulations fell within the  $\pm 5\%$  of the SOC and POC field measured stocks as well as the optimum solutions derived by the Monte-Carlo simulation for the three shrubland to cropland conversions

**Table 5.13 Statistics of the parameter distributions for the solutions fell within the  $\pm 5\%$  of the SOC and POC field measured stocks as well as the optimum solutions derived by the Monte-Carlo simulation for the three shrubland to cropland conversions simulated in the Koiliaris River Basin CZO.**

Parameter	total plant input	DPM/RPM ratio	BIO%	DPM	RPM	BIO	HUM
<b>Schists</b>							
distribution type	BetaGeneral	BetaGeneral	Uniform	Uniform	Triang	BetaGeneral	Triang
min	4.41	1.30	41.41	8.99	0.10	0.59	0.0155
max	5.99	1.58	50.63	10.97	0.14	0.73	0.0655
mean	5.37	1.43	46.04	9.98	0.11	0.66	0.0435
std	0.39	0.09	2.67	0.57	0.01	0.04	0.0104
Chi-sq	9.49	10.32	7.82	12.62	12.20	2.39	9.4870
Optimum	<b>5.25</b>	<b>1.34</b>	<b>44.84</b>	<b>10.25</b>	<b>0.11</b>	<b>0.62</b>	<b>0.0427</b>
<b>Marls</b>							
distribution type	Uniform	Uniform	Uniform	Triang	BetaGeneral	BetaGeneral	BetaGeneral
min	4.00	1.29	41.57	8.69	0.10	0.60	0.0409
max	6.04	1.57	50.60	10.97	0.16	0.72	0.0603
mean	5.02	1.43	46.09	10.21	0.12	0.65	0.0521
std	0.59	0.08	2.61	0.54	0.01	0.04	0.0055
Chi-sq	9.09	2.55	2.18	5.45	3.64	4.00	4.0000
Optimum	<b>5.03</b>	<b>1.40</b>	<b>46.28</b>	<b>9.99</b>	<b>0.12</b>	<b>0.68</b>	<b>0.0495</b>
<b>Trypalis</b>							
distribution type	BetaGeneral	BetaGeneral	Uniform	Uniform	Triang	Uniform	Triang
min	3.60	1.30	41.28	9.02	0.09	0.60	0.0248
max	5.97	1.58	50.68	11.02	0.18	0.73	0.0487
mean	4.97	1.43	45.98	10.02	0.14	0.66	0.0377
std	0.76	0.09	2.71	0.58	0.02	0.04	0.0049
Chi-sq	8.86	5.71	9.43	2.86	7.14	5.71	6.2857
Optimum	<b>4.68</b>	<b>1.47</b>	<b>46.19</b>	<b>9.98</b>	<b>0.13</b>	<b>0.67</b>	<b>0.0351</b>

No significant differences were found between three lithologies regarding the calibrated value and the uncertainty of the plant input and the model parameters. The plant litter input in three sites was found to be 4.68 to 5.25 t C/ha. The RPM decomposition rate constant was 0.11 to 0.13 1/y and the HUM decomposition constant was 0.0351 to 0.0495 1/y. The monthly and average annual decomposition rates are presented in Table A3.3 in the appendix. The average annual rate for the RPM pool was estimated to be 0.073 to 0.080 1/y and for the HUM pool 0.022 to 0.032 1/y. Worth noting is that the soil found on the Trypalis lithology seems to exhibit lower decomposition rate as compared with the other two, in accordance with the fact that exhibited higher clay content (28.8 to 32.7%) as compared with the soils on Schists (13.1 to 17.7%) and Calcaric Marls (12.4 to 16.5%); silt clay content was also higher.

Sensitivity analysis at the  $\pm 10\%$  and  $\pm 50\%$  ranges of the calibrated values (optimum solution Table 5.13) for the six model parameters and the plant input was conducted. The tornado graphs are presented in Figure 5.15 and the sensitivity coefficients (the absolute value of the ratio:  $(\Delta Y/Y)/(\Delta x/x)$ ) in Table A5.4 in the Appendix. In all sites, regarding the sensitivity of the parameters on the simulated POC (the sum of the DPM and RPM pools), the most sensitive parameters were the RPM decomposition rate constant and the plant litter input (value sensitivity close to the value 1) and secondarily the DPM to RPM ratio (value sensitivity close to the value 0.5) (see Table A5.4). The most sensitive parameter for the SOC was the plant litter input and the DPM and BIO decomposition rate constants exhibited negligible sensitivity.

Figure A5.1 in the Appendix presents a comparison of the optimum simulation for both SOC and POC and the uncertainties attributed to the initial conditions (SOC, DPM, RPM, BIO, HUM, and IOM carbon pools) the input data (plant litter input and clay content), and the six model parameters used for calibration parameters (DPM, RPM, BIO, and HUM decomposition rate constants, DPM-to-RPM ratio, HUM%), in terms of the mean of the ensemble of Monte Carlo simulations plus one standard deviation. The total uncertainty for the six sites is presented in Figure 5.16. The uncertainty of the simulated carbon change after 100 years cultivation was 40.3% -Schists, 32.7% -Marls, and 72.8% -Trypalis of the total amount of C change due to the landuse conversion.

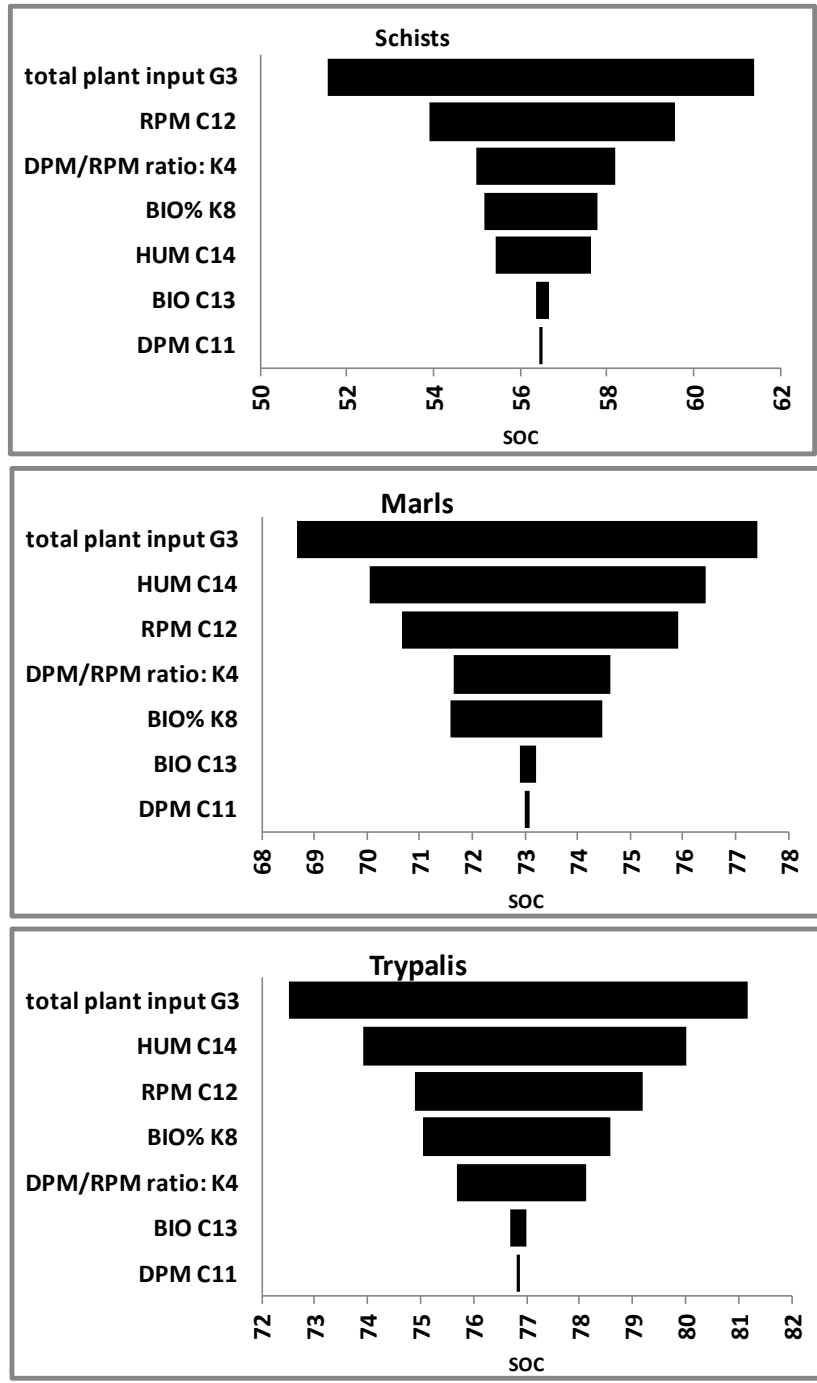


Figure 5.15 Tornado Graphs for 10% (left) and 50% (right) sensitivity analysis for the three shrubland to cropland conversions simulated in the Koiliaris Reiver Basin CZO. RPM=resistant plant material decomposition rate constant, DPM=decomposable plant material decomposition rate constant, HUM=humus decomposition rate constant, BIO= biomass decomposition rate constant, DPM/RPM ratio=the apportionment ratio of plant litter input DPM and RPM carbon pools, BIO%=the proportion that goes to BIO (100-BIO% is the proportion that goes to HUM).

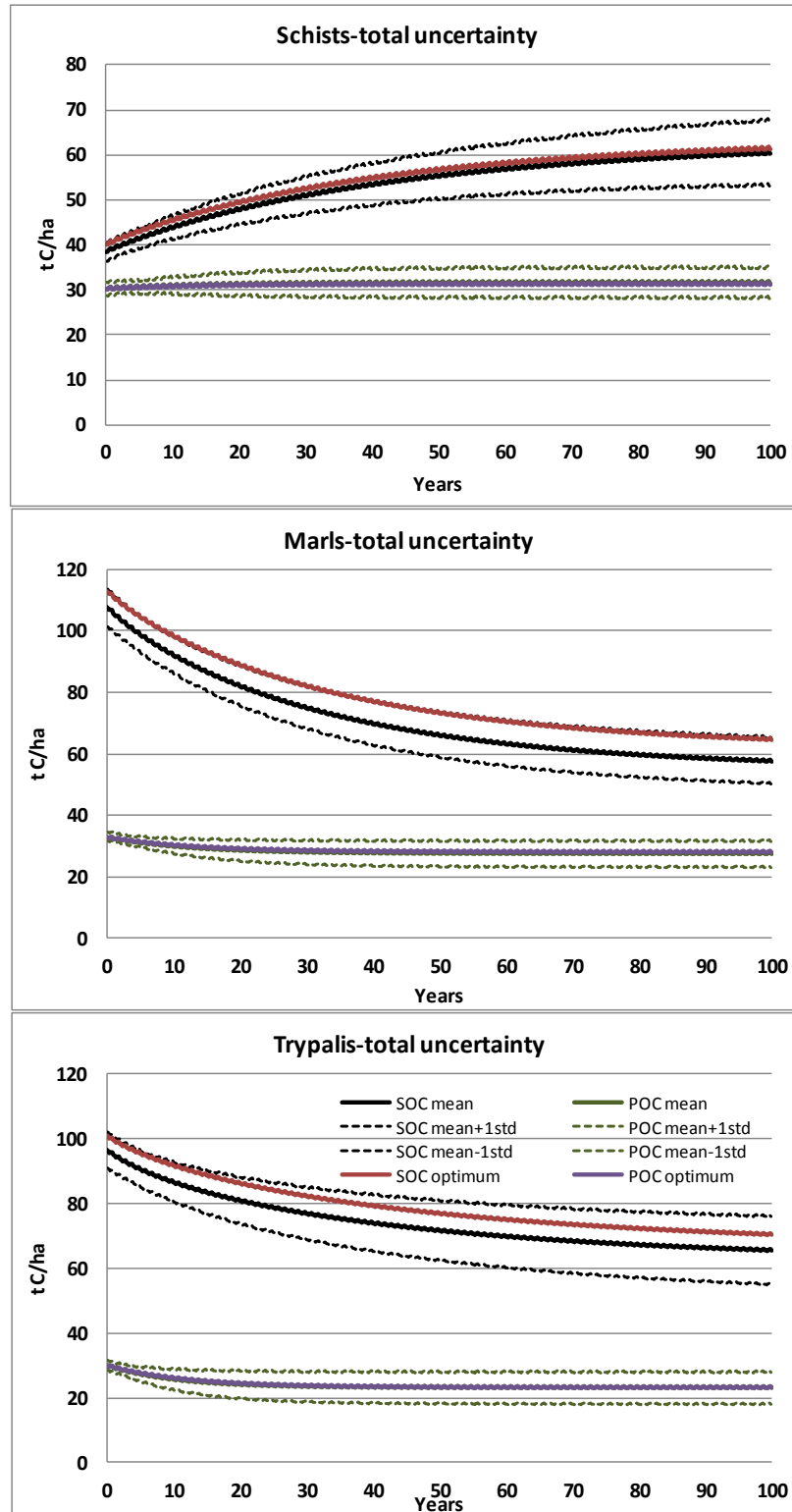
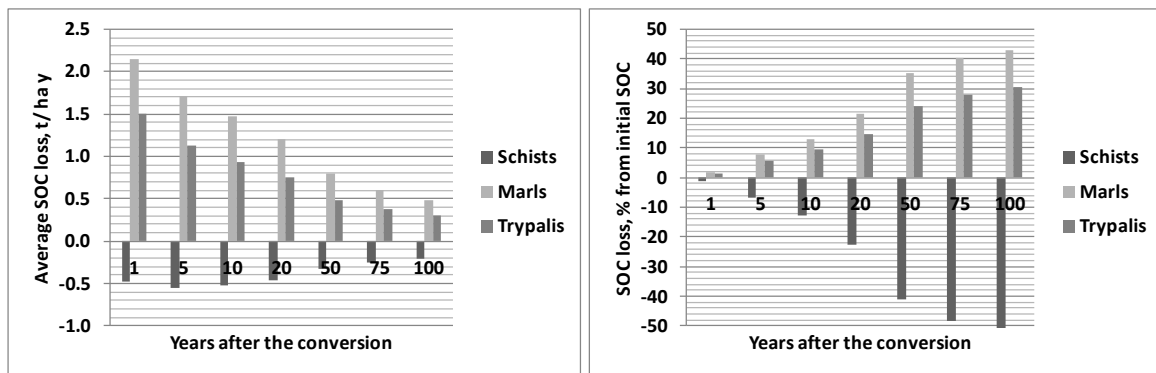


Figure 5.16 Total uncertainty of total organic carbon (SOC) and particulate organic carbon (POC) due to model parameters, input data, and initial conditions compared with the optimum solution (calibration) for the six sites.

The average rate of the change of carbon stock and the cumulative change of carbon stock change proportional to the initial stocks are given in the Figure 5.17. The conversion of shrublands to olive grove fields, after 100 years of cultivation was predicted to result in the increase of carbon stock by 50% in the Schists, and a decline in the Marls and Trypalis by about 40% and 30% respectively. The increase of SOC stock observed in the already degraded soils on schists is presumably attributed to the increase of plant litter input under the cultivated soil as compared with the shrubland. The shrublands grow on Schists present apparently lower biomass productivity as compared to shublands grow on Marls and Trypalis.



**Figure 5.17** The average rate of the change of carbon stock and the cumulative change of carbon stock change proportional to the initial stocks.

The effect of climate change on SOC stocks was also assessed with data obtained by Nikolaidis et al., (HESSD under revision) and which have been used to estimate the effect of climate change on the Koiliaris River basin water balance with the use of SWAT model. The combination of General Circulation Models (GCM) [ECHAM5 (Roeckner, 2003); BCA (Déqué et al., 1994)] and three Regional Circulation Models (RCM) [RACMO2 (van Meijgaard et al., 2008); RCA (Kjellstrom et al., 2005); REMO (Jacob, 2001)] were selected for climate change scenarios. They are based on the A1B storyline. The A1 family of scenarios is based on rapid economic growth, an increase in population until the mid-century and a decrease thereafter and the introduction of new and more efficient technologies. Scenario A1B puts a balanced emphasis on all energy sources (IPCC, 2000). The three combinations used were ECHAM-RACMO, BCA-RCA and ECHAM-REMO. All time series covered the time period 1990-2050. All climate change time series were corrected

for bias as detailed by Rojas et al. (2011). The climatic data of the climate change scenarios used for the simulation are presented in Table A5.2 in the Appendix.

In order to quantify the changes due to climate, given the local decadal climatic variability, the simulation was conducted for 20 years and specifically for the decades 2010-2030 and 2030-2050. The calculated 20-year average (and standard deviation) from the three climate change scenarios was compared with the average of the 'present' scenario the decades 1990-2010. Two sets of simulation were conducted: the effect of landuse change along with the landuse conversion of a shrubland to cropland and the effect of climate change on a 50 year old olive grove field. The summarized results of the simulations are presented in Tables 5.14a and 5.14b. The average annual decomposition increased in the years 2010-2030 by -0.4%, 9.8% and 5.1% according to the scenarios BCA-RCA, ECHAM-RACMO and ECHAM-REMO, while at the same order in the years 2030-2050 the increase was found to be 0.4%, 8.0% and 6.9%. The mean value of the increase for the three scenarios was 4.8% and 5.1% for 2010-2030 and 2030-2050, respectively. The latter two scenarios presented higher temperature increase.

The conversion of a shrubland to cropland on schists results in a 27.9% (11.2 t/ha) increase of SOC (1990-2010). Due to climate change in the decades 2010-2030 and 2030-2050 1.92 t/ha and 1.82 t/ha less carbon will be sequestered. This amount corresponds to the 4.1% and 3.8% of the initial carbon stock. Similarly in Marls and Trypalis conversions the climate change will result in more carbon loss and the less carbon sequestered will correspond to the 2.6% and 1.7-1.8% of the initial SOC stock, respectively, while the carbon loss due to landuse change under the present scenario (1990-2010) is 18% and 12% of the initial SOC. On the other hand, the climate change effects in 50 year old olive grove fields were estimated to be 2-3% of the initial SOC, while the change of stock due to the landuse and management was estimated for Schists, Marls and Trypalis, 8.9% increase, 3.1% decline and 1.7% decline. As amount of carbon (t/ha) that was not sequestered due to climate change was higher in Schists and lower in Marls and Trypalis as compared with the shrubland to cropland conversion, because of the higher SOC content of croplands in Schists and lower in Marls and Trypalis as compared with the shrublands. The results emphasize that management effects and particularly landuse change affects are such high that may be hinder our ability to detect climate change effects. RothC has been used similarly with other carbon models to predict climate change effects on soils mostly without being calibrated (rate constants) and being initialized with field data (e.g. Wam et al., 2011).

Table 5.14a The effect of climate change on SOC stocks after the conversion of a shrubland to olive grove field.

	Schists		Marls		Trypalis	
Initial SOC, t C/ha	40.08		112.80		101.10	
SOC change-20 years cultivation, t C/ha	11.20		-20.58		-12.32	
SOC change-20 years cultivation, % of initial SOC	27.94		-18.24		-12.18	
Climate effect on change, % (less sequestration)	mean	mean+std	mean	mean+std	mean	mean+std
2010-2030	14.61	30.62	14.14	29.24	14.19	29.21
2030-2050	13.78	26.21	14.45	26.63	15.36	27.20
Less sequestration (20 years) due to climate change, t/ha						
2010-2030	1.64	3.43	2.91	6.02	1.75	3.60
2030-2050	1.54	2.94	2.97	5.48	1.89	3.35
Less sequestration (20 years) due to climate change, % of initial SOC						
2010-2030	4.08	8.55	2.58	5.33	1.73	3.56
2030-2050	3.85	7.32	2.64	4.86	1.87	3.31

Table 5.14b The effect of climate change on SOC stocks in a 50 year old olive grove field.

	Schists		Marls		Trypalis	
Initial SOC, t C/ha	56.49		73.05		76.84	
SOC change-20 years cultivation, t C/ha	5.00		-2.25		-1.30	
SOC change-20 years cultivation, % of initial SOC	8.85		-3.09		-1.69	
Climate effect on change, % (less sequestration)	mean	mean+std	mean	mean+std	mean	mean+std
2010-2030	38.69	42.45	95.28	101.73	111.54	118.12
2030-2050	36.37	33.12	97.66	81.40	121.29	92.69
Less sequestration (20 years) due to climate change, t/ha						
2010-2030	1.93	4.06	2.15	4.44	1.45	2.99
2030-2050	1.82	3.47	2.20	4.04	1.58	2.79
Less sequestration (20 years) due to climate change, % of initial SOC						
2010-2030	3.42	7.18	2.94	6.08	1.89	3.89
2030-2050	3.22	6.15	3.01	5.52	2.05	3.62

The effectiveness of carbon addition by the application of amendments of different quality at an annually rate of 2.5 t C/ha, as expressed by the ratio of the Net C sequestered as compared with the soil where no amended was applied to the cumulative carbon amended it is presented in Figures 5.18-5.20. The Net C to C amended ratio as it was expected it was found in all sites to be higher for the 10/70/20 compost, followed by the 30/60/10 and the 49/49/2 being in the first two 1.6 and 1.3 times higher as compared with the last. In all cases the ratio significantly decline with time over a logarithmic pattern, indicating the importance of such simulation in the design of long-term agricultural management plans. The long term effectiveness was higher in the Trypali soil followed by the Marls and Schists due to the lower decomposition rate of the HUM pool of the Trypali soil which is related with the higher clay content. The values were higher than the Mediterranean site in Turkey and lower than the site in Ethiopia (see Figure 3.5).

The effect of climate change on Net C to C amended ratio is presented in Table 5.15. It was found that instead of 18 t/ha (49/49/2), 23 t/ha (30/60/10), and 29 t/ha (10/70/20) that can be sequestered after 20 years of 2.5 t/ha y application of the amendementt under the present scenario, 0.35 to 0.8 t/ha less carbon will be sequestered (0.67 to 1.61 with the uncertainty of the one standard deviation).

**Table 5.15 The effect of climate change on carbon addition effectiveness in shrubaland to cropland conversions of different lithologies (% change of the Net C to C amended ratio, negative values indicate decline).**

	Schists		Marls		Trypali		Amendement type		
	mean	stdev	mean	stdev	mean	stdev	RPM	RPM	HUM
<b>2010-2030</b>	<b>-2.69</b>	3.02	<b>-2.93</b>	3.16	<b>-1.97</b>	2.27	49	49	2
	<b>-2.57</b>	2.88	<b>-2.80</b>	3.02	<b>-1.88</b>	2.16	30	60	10
	<b>-2.46</b>	2.75	<b>-2.69</b>	2.90	<b>-1.79</b>	2.05	10	70	20
<b>2030-2050</b>	<b>-2.53</b>	2.15	<b>-3.01</b>	2.31	<b>-2.16</b>	1.58	49	49	2
	<b>-2.41</b>	2.06	<b>-2.87</b>	2.22	<b>-2.05</b>	1.51	30	60	10
	<b>-2.30</b>	1.98	<b>-2.75</b>	2.14	<b>-1.95</b>	1.45	10	70	20

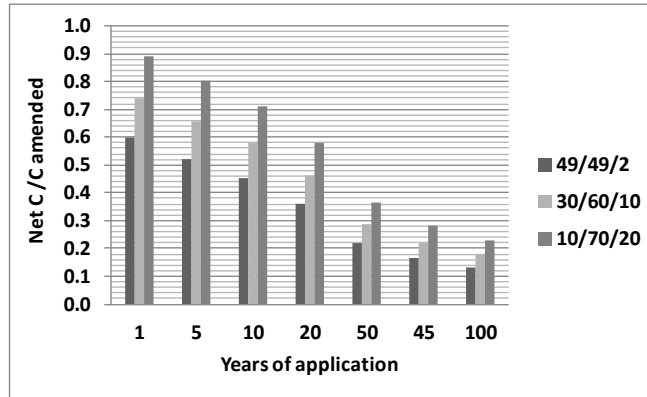


Figure 5.18 The effectiveness of carbon addition by the application of amendments of different quality at annually doses of 2.5 tC/ha on Trypalis soils (carbon amended: the cumulative load of the carbon amended to soil, Net C: the extra carbon sequestered as compared with the soil where no amended was applied).

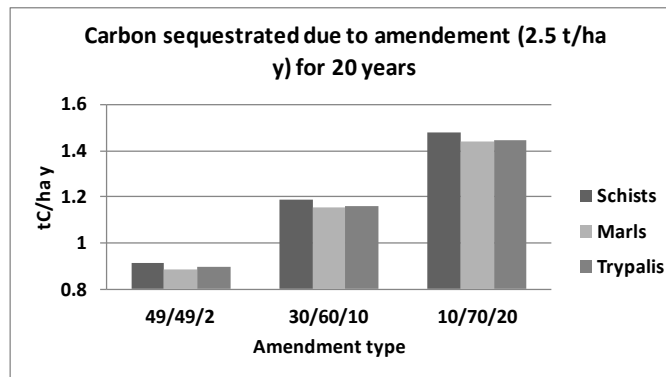


Figure 5.19 The average rate of carbon sequestered due to the application of amendments of different quality at annually doses of 2.5 tC/ha for 20 years on Schists, Marls and Trypalis soils.

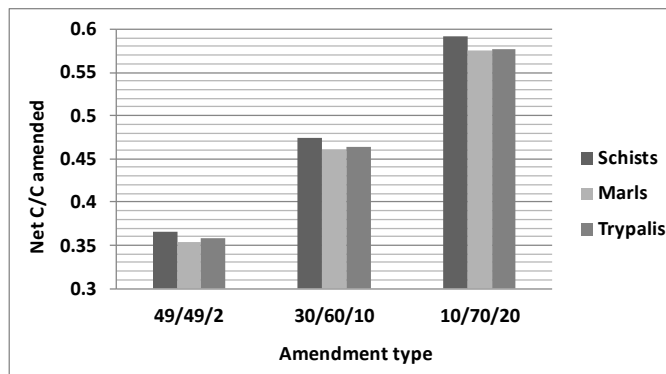


Figure 5.20 The effectiveness of carbon addition by the application of amendments of different quality at annually doses of 2.5 tC/ha for 20 years on Schists, Marls and Trypalis soils.

## **5.5 DISSOLVED ORGANIC NITROGEN AS AN INDICATOR OF LIVESTOCK IMPACTS ON SOIL BIOCHEMICAL QUALITY**

### **5.5.1 Introduction**

Soil degradation in the Mediterranean and other arid and semi-arid regions of the world is caused mainly by cultivation and grazing (Li et al., 2007). Livestock grazing alone is responsible for 23 % of soil degradation in Europe (RCEP, 1996) and is particularly intense in the Mediterranean region. Free grazing of uncontrolled length and frequency and high stocking densities are responsible for the de-vegetation of many areas within this region. The Greek island of Crete represents a characteristic case of land degradation resulting from intensive grazing (Hill et al., 1998). Since Greece joined the European Communities in 1981, grazing in mountainous regions has expanded due to subsidies that became available through the Common Agricultural Policy (Hill et al., 1998). A consequence of de-vegetation due to overgrazing has been a decrease in organic matter (litter) input to soil and a decrease of aggregate size and stability making soils more susceptible to erosion and to organic matter losses (Bastida et al., 2006).

DON has been found to be decoupled from the production of DOC in such soils and has proportionally more labile soluble organic matter (Ghani et al., 2007). However, detailed information on the nature, bioavailability, and fate of the mobilized dissolved OM following a change in landuse such as de-vegetation is still lacking (Akagi and Zsolnay, 2008). Mediterranean watersheds appear to export a larger fraction of nitrogen in organic form compared to watersheds of continental Europe and North America. However, no systematic analysis of existing data has been made to date. The objective of this work was to test the hypothesis that livestock grazing (and the resulting de-vegetation) degrades soil quality and enriches surface and ground waters with DON by examining data from 3 different scales.

## 5.5.2 Methodology

### *Soil studies*

Scrub and/or herbaceous vegetation associations (codes 321-324, according to the CLC 2000 database) covered 57.6% of the watershed area (130 km<sup>2</sup>), 70% of which was found at mountainous areas (700-2100 m altitude) where Limestones of the Plattenkalk units are found. The mean slope of this area is 20.4±8.1% and it is considered to be the most vulnerable. The soil type in the headwaters corresponded to calcaric Leptosols (or lithosols) also known as Rendzinas. Leptosols is one of the four major soil types of Europe that cover approximately 9% of its surface area and are very common in high altitudes in the Mediterranean (FAO, 1998). Soil surface samples (from 0-15 cm depth), composite of five representative subsamples, were taken from de-vegetated grazing lands (DVs) and native vegetated (shrubs such as phrygana) lands (NVs) not affected from grazing, in the Koiliaris River headwaters region named Bolikas (Municipality of Chania, Crete, Greece). Triplicate samples of DVs and NVs were collected at an altitude of 1500-1550 m (DV1-3 and NV1-3). Soil samples were oven dried at 40 °C, sieved to 2 mm, and stored in a cool-dry place until further analysis. Soils were analyzed, in triplicates, for the following physico-chemical and microbial parameters: porosity and dry bulk density (Nikolaidis et al., 1999), pH and conductivity (measured in a 1:2.5 soil to water ratio, using a Orion 9107 pH meter), soil texture (Bouyoucos, 1936), soil organic carbon (Walkley-Black acid dichromate digestion technique, Santi et al., 2006) and total kjeldahl nitrogen (Hach digestahl digestion apparatus; Nessler method, 8075), acid-hydrolysable carbohydrates (acid hydrolysis with H<sub>2</sub>SO<sub>4</sub> and measurement with the phenol-sulfuric acid procedure; Piccolo et al., 1996), dehydrogenase activity (Chu et al., 2007), total bacteria/fungi counts and species richness.

Total bacterial counts were cultured on Peptone Yeast Agar plates and population levels of total culturable fungi in each soil sample were obtained by culturing on rose Bengal medium at 25 °C using the pour plate method. Microbial colonies were incubated at 37 °C for 48 h and at 22 °C for 72 h, respectively and were observed with countable plates of the highest dilution being enumerated. Plates with 30-300 colonies were selected for enumeration. The isolated bacteria were identified depending on their biochemical characteristics using the standardized identification systems API 20E and API 20NE (BioMérieux, 69280 Marcy-l'Étoile, France). Fungal colonies growing in agar that formed distinctive and consistently recognizable colonies, on the

basis of coloration, morphology, and sporulation were observed after 3, 4, and 5 days, and total colonies were recorded on the 5<sup>th</sup> day. All microbial analysis was conducted in fresh samples.

The 2 M KCl extraction scheme was run in duplicates for the estimation of exchangeable mineral N (EMN) content and potential mineralizable N (PMN) of soils; NO<sub>3</sub>-N and NH<sub>4</sub>-N (Nikolaidis et al., 1999), as well as potential soluble organic nitrogen (PSON) and carbon (PSOC) (Burton et al., 2007). Soils were extracted with KCl in a 1:5 soil-to-solution ratio; shaken at 200 rpm and incubated for 1 h at 20 °C (EMN) and for 1 week at 40 °C (Nikolaidis et al., 1999). PMN was calculated as the difference between incubated and non-incubated samples. PSON and PSOC were considered the dissolved organic nitrogen and carbon of the 1 week extracted pool. The extracted pools were filtered through a 0.45 µm Nylon filter and analyzed using a Hack 2010 spectrophotometer for NO<sub>3</sub>-N (Cadmium Reduction Method, 8039), NH<sub>4</sub>-N (Salicylate Method, 10023), TKN (Kjeldahl digestion technique; Nessler method, 8075) and dissolved organic carbon by a TOC analyzer (Shimadzu 5050), after the removal of inorganic carbon by air sparging for 10 min. Regarding the NO<sub>3</sub>-N measurement calibration curves were prepared for Cl<sup>-</sup> interference.

The size and composition of the soluble pools (operationally defined as the water or salt extracted pool) (Burton et al., 2007) could indicate the magnitude of soil degradation and the potential impacts to surface and ground waters. The specific UV absorbance (SUVA) aromaticity index, has been suggested as the most reliable zero-order UV-visible absorption index for the measurement of DOC aromaticity by many studies which have identified differences between landuses or among soil profiles (Corvasce et al., 2006; Hur et al., 2006; Kalbitz, 2001; Weishaar et al., 2003) and could be indicative of the organic pool's composition and was measured in this study. The specific UV absorbance at 280 nm (SUVA<sub>280</sub> or DOC Aromaticity Index) was estimated for the leachates. The 280 nm was selected since the tail of the NO<sub>3</sub>-N peak has been reported to be measurable, to a greater extent at λ=254 than at λ=280 (Weishaar et al., 2003). UV spectra of leachates were recorded with a UV-Vis spectrophotometer (Shimadzu UV mini 1240) in 1 cm quartz cuvettes, with scanning from 200 to 300 nm. Standard sample volume of 3 mL was used in the measurement. The pH of soil leachates was always in the range 2–8.6 while the concentration of Fe<sup>+3</sup> (1,10 Phenanthroline method, 8146 for Fe<sup>+2</sup> and FerroVer Method, 8008 for total iron) was lower than 0.5 mg/L and NO<sub>3</sub>-N was lower than 9 mg/L, which are the lower reported limits for measurable interferences (Dilling and Kaiser, 2002; Weishaar et al., 2003).

The t-test was used to calculate the significance of observed differences between the means of the variables of the samples. Statistical significance refers to  $P \sim 0.05$  unless otherwise stated.

*Landuse load apportionment in 5 Greek mixed landuse watersheds*

Based on previous published modeling studies using procedures described in Nikolaidis et al. (2009), the nitrogen load from different landuses (urban, agricultural, forest, open areas, open waters and precipitation) from five different size, mixed landuse watersheds in Greece, including Koiliaris River Basin, was apportioned (Table 5.16). The open areas correspond to areas grazed by livestock. Krathis is a small (149 km<sup>2</sup>), pristine river basin located in northern Peloponnese. It is a temporary river flowing in the Korinthian Gulf (Tzoraki et al., 2007). Evrotas has a watershed area of 2417 km<sup>2</sup> and is located in southern Peloponnesus (Nikolaidis et al., 2006). Acheloos is a large (5639 km<sup>2</sup>), permanent river, located in the southwestern part of Greece (Nikolaidis et al., 2004). Axios is a large (25000 km<sup>2</sup>), transboundary, permanent flow river located 83% in the Former Yugoslav Republic of Macedonia, 12% in Greece, and the remaining in Bulgaria, Serbia, and Montenegro (Nikolaidis et al., 2009).

**Table 5.16 Landuse load apportionment calculations.**

	Landuse	Area (km <sup>2</sup> )		TDN (t/y)		DIN (t/y)		DON (t/y)		DON/TDN
AKSIOS	TOTAL	24407	%	108921	%	57398	%	51523	%	0.47
	URBAN	397	1.6	826	0.8	266	0.5	560	1.1	0.68
	AGRICULTURAL	17580	72.0	60444	55.5	35684	62.2	24760	48.1	0.41
	FOREST	5041	20.7	10473	9.6	3372	5.9	7100	13.8	0.68
	OPEN AREAS	1295	5.3	36984	34.0	18013	31.4	18971	36.8	0.51
	OPEN WATERS	94	0.4	194	0.2	62.5	0.1	132	0.3	0.68
ACHELOOS	TOTAL	5639		24643		10211		14433		0.59
	URBAN	15.6	0.3	81.9	0.3	32.4	0.3	49.4	0.3	0.60
	AGRICULTURAL	918.	16.3	4720	19.2	2817	27.6	1902	13.2	0.40
	FOREST	1740	30.9	5319	21.6	1713	16.8	3606	25.0	0.68
	OPEN AREAS	2737	48.5	13825	56.1	5423	53.1	8401	58.2	0.61
	OPEN WATERS	228	4.0	698	2.8	225	2.2	473	3.3	0.68
EVROTAS	TOTAL	2417		10566		7087		3480		0.33
	URBAN	28.4	1.2	333	3.2	158	2.2	175	5.0	0.53
	AGRICULTURAL	910	37.6	6723	63.6	5637	79.6	1086	31.2	0.16
	FOREST	327	13.5	576	5.5	186	2.6	391	11.2	0.68
	OPEN AREAS	1147	47.5	2926	27.7	1103	15.6	1822	52.4	0.62
	OPEN WATERS	4.8	0.2	8.4	0.1	2.7	0.0	5.7	0.2	0.68
KRATHIS	TOTAL	149		369		151		218		0.59
	URBAN	0.3	0.2	12.7	3.4	6.3	4.2	6.5	3.0	0.51
	AGRICULTURAL	36.7	24.6	115	31.1	64.4	42.7	50.5	23.1	0.44
	FOREST	28.1	18.8	57	15.4	18.4	12.2	38.7	17.7	0.68
	OPEN AREAS	84.0	56.3	184	49.9	61.8	41.0	122.6	56.1	0.66
	OPEN WATERS	0.1	0.1	0.2	0.1	0.1	0.0	0.1	0.1	0.68

### 5.5.3 Results

#### *N balance of karstic System*

The Koiliaris River Basin in Crete was selected to study the effects of livestock grazing on water quality because it offers a unique morphologic situation due to its karstic hydrogeology draining the upland grazing areas through the karstic springs. The main contributor to the Koiliaris River flow (136 million m<sup>3</sup>/y) was the Stilos karstic spring (109 million m<sup>3</sup>/year) (see Figures 5.6 and 5.7). The spring recharges a karst area (85 km<sup>2</sup>) with thin skeletal soils largely de-vegetated due to grazing (Kourgialas et al., 2010). DIN concentrations of the karstic flow were similar to rain water (0.91±0.33 mg/L). On the other hand, rain water had an average DON concentration of 1.2 mg/L, while the spring DON concentration was 3.40 mg/L. A mass balance analysis on nitrogen species was conducted for the Koiliaris karstic system (Figure 5.21). The spring DON flux (374 t/y) was the main contributor to river DON export (438 t/y). Approximately 25000 sheep/goats were grazing in the karstic highlands of Koiliaris River. The annual dry manure production was estimated to be 5550 t DM/y, assuming 0.222 t/head y. The annual nitrogen production from manure was estimated to be 175 t N/y (Sorensen and Jensen, 1995). The input of DON from precipitation was 161 t N/y bringing the total estimated DON load to be 336 t N/y. The input load was of the same order of magnitude as the spring DON fluxes suggesting that DON was acting as a conservative substance. Mass balance analyses on Ammonia-N and Nitrate-N suggested different behavior of these species compared to DON. The net Ammonia-N load (assuming 0.433 urine production t/head y and 0.79 % urine nitrogen content) was estimated at 61 t N/y while the spring flux at 2.8 t N/yr suggesting a 95% reduction, most likely due to nitrification (Hoogendoorn et al., 2010; Emerick et al., 1959). Similarly, the Nitrate-N load was estimated at 114 t N/y and the spring flux at 69.8 t N/y. The mass balance of the inorganic N loads was expected, however the question is why the organic N is behaving as a conservative substance. In analyzing this question, one can identify two possible mechanisms for DON (Nikolaidis and Bidoglio, 2011): the Mineralization-Immobilization-Turnover and Direct routes. We postulated that these two mechanisms did not operate in the degraded soils of the karst for the following reasons. A hypothesis could be developed if we consider the semi-arid, cold climatic conditions occurring at the site where the no rain period extends up to 6-7 months and the rain-snow conditions the remaining 5-6 months. During the no-rain period, the sheep and goat excreta are being dehydrated and physically aged. Mineralization is a function of the micro-

organisms present for degradation, whose taxa depend on the organic input to the soil. We can assume then that livestock degraded soils have typical organisms (mostly bacteria) that degrade aerobically organic mater similar to those found in wastewater treatment plants. These organisms degrade effectively the carbonaceous organic matter by converting a fraction of organic carbon to CO<sub>2</sub> and the remaining to cell biomass. This biomass also contains the organic nitrogen which can be mineralized to ammonia by anearobic bacteria following the acid fermentation pathway. We conclude our hypothetical analysis that the thin soils, the hot-dry and cold-wet conditions and the flashy nature of the system are not conducive for the appropriate bacterial population to develop for anaerobic fermentation of organic nitrogen. Along the same lines, direct plant uptake of organic nitrogen has been found to be important mechanism in cool and wet climates which is consistent with the high altitude micro-climate of the area. However, the limited aerial extent of plants minimizes the significance of this mechanism.

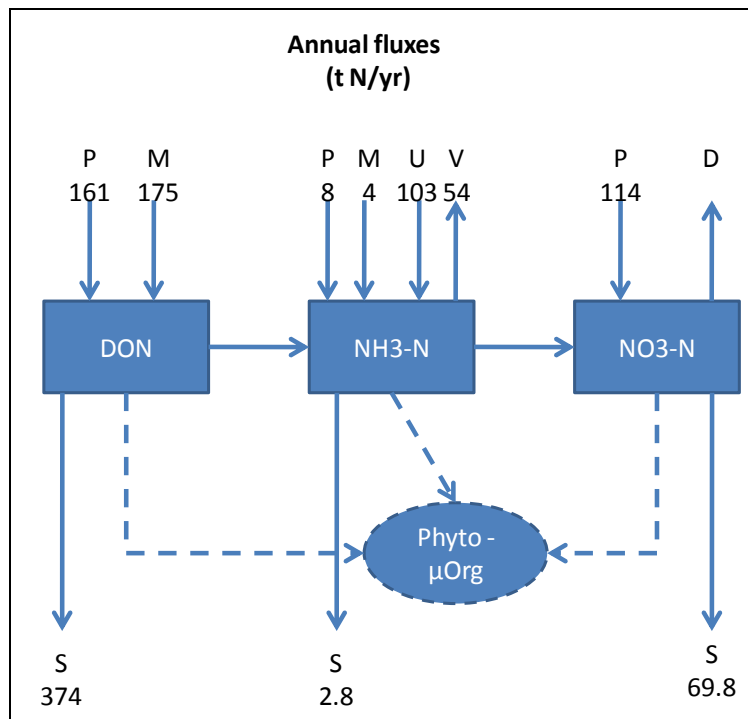


**Figure 5.21 Annual fluxes of Nitrogen in the karstic system discharging Stilos spring, where, P = Precipitation flux, M= Manure flux, U = Urine flux, V= Volatilization, flux D= Denitrification flux, and S= Spring flux (taken from Stamati et al., 2011).**

### Soil biochemical quality

A comparison of the soil quality parameters of de-vegetated (DVs) and naturally vegetated (NVs) soils is presented in Tables 5.17 and 5.18. The OC and TKN density (t/ha) in DVs was found to be 36.3% and 25.5% lower as compared with the adjacent NVs. Similar patterns were found by Albaladejo et al., (1998) in Spain. The acid-hydrolysable carbohydrates were statistically the same between the DVs and NVs. Dehydrogenase activity as a general measurement of microbial activity suggested that de-vegetated lands exhibited more than two times lower activity ( $33.2 \pm 21.8$  mg TPF/kg) compared to vegetated soils ( $72.0 \pm 17.5$  mg TPF/kg). In addition, bacteria counted at 22°C to 37°C were statistically the same among DVs and NVs. NVs exhibited double fungi counts and greater fungi species richness compared to DVs, but the differences were not statistically significant.

**Table 5.17 Physicochemical characteristics of soil samples (standard deviation in parenthesis).**

ID	Altitude	Bulk density	Texture <sup>1</sup>	pH	Cond.	OC	TKN	C/N	Carbon-Carbohy-drates	Dehydro-genase activity
	m	Kg/m <sup>3</sup>			μS/cm	%	%		mg/kg	mg TPF/kg
<b>DV</b>	1483 (29)	914 (24)	SL/L	7.08 (0.44)	114 (36)	3.9 (1.1)	0.42 (0.11)	9.4 (0.3)	432 (92)	33.2 (21.8)
<b>NV</b>	1513 (40)	857 (30)	CL	7.64 (0.07)	205 (18)	6.5 (0.5)	0.60 (0.18)	11.2 (2.0)	440 (195)	79.1 (17.5)

<sup>1</sup> CL(Clay Loam), SL(Sandy Loam), L (Loam)

EMN and PMN were 4.6 and 2.8 times higher in NVs (Figure 5.22). These results were in line with Thompson et al., (2005) who found the mineralized nitrogen of bare soils to be 2 times lower than that of vegetated soils. The PSOC was also 3.2 times higher in NVs ( $341 \pm 27$  mg C/kg soil) compared to DVs ( $106 \pm 17$  mg C/kg soil). Xie and Steinberger, (2001) also found a 2 to 2.5 decrease in this pool of de-vegetated grazing lands. On the other hand, the PSON was statistically the same. DON was the predominant N species in both extracted soluble nitrogen pools (7-day and 1 day extraction) in DVs compared to NVs. PSON as a percent of total soluble nitrogen in 7-day extracted pool, was following the pattern  $NV(21 \pm 5\%) < DV(49 \pm 7\%)$ . The DOC-

to-DON ratio of the extracted pools of the DVs was lower ( $1.24 \pm 0.08$ ) compared to NVs ( $3.14 \pm 0.08$ ) indicating different composition of the OM pools. Finally, the DOC aromaticity was found to be significantly lower in de-vegetated lands ( $0.957 \pm 0.366$  L/mg C m) compared to vegetated ( $2.155 \pm 0.136$  L/mg C m), confirming our hypothesis. DOC aromaticity observed in DVs was in the lower range of values observed in the literature (Akagi and Zsolnay, 2008, Corvasce et al., 2006).

**Table 5.18 Bacteria species richness, bacteria and fungi populations in colony forming units (CFUs), and count ratio of fungi to bacteria for soil samples.**

	DV1	DV2	DV3	NV1	NV2	NV3
<b>Species richness (Bacteria)</b>	4	6	2	4	2	2
<b><u>oxidase negative</u></b>						
<i>Burkholderia cepacia</i>		1		1		
<i>Stenotrophomonas maltophilia</i>		1				
<i>Pasterella pneumophila</i>		1		1	1	1
<i>Pasterella pneumophila/Mannheimia haemolytica</i>	1		1			
<i>Pseudomonas oryzihaditans</i>	1	1		1		
<i>Mannheimia haemolytica</i>		1				
<i>Serratia rubidaea</i>		1				
<b><u>oxidase positive</u></b>						
<i>Pseudomonas fluorescens</i>	1			1		1
<i>Burkholderia cepacia</i>	1		1		1	
<b>Species richness (Fungi)</b>	7	7	8	7	11	14
<b>Microbial populations in Colony Forming Units (CFUs)</b>						
<b>Fungi (F)</b>	1.2E+04	2.2E+04	4.2E+04	6.0E+04	6.8E+04	4.1E+04
<b>Bacteria (B) cultured at 37°C</b>	4.8E+05	2.8E+05	4.7E+05	1.8E+05	2.1E+05	1.3E+05
<b>Bacteria (B) cultured at 22°C</b>	8.8E+04	1.5E+06	9.1E+05	3.2E+06	1.1E+06	6.7E+05
<b>F (CFUs)/B (CFUs) ratio</b>	0.025	0.014	0.046	0.018	0.059	0.062

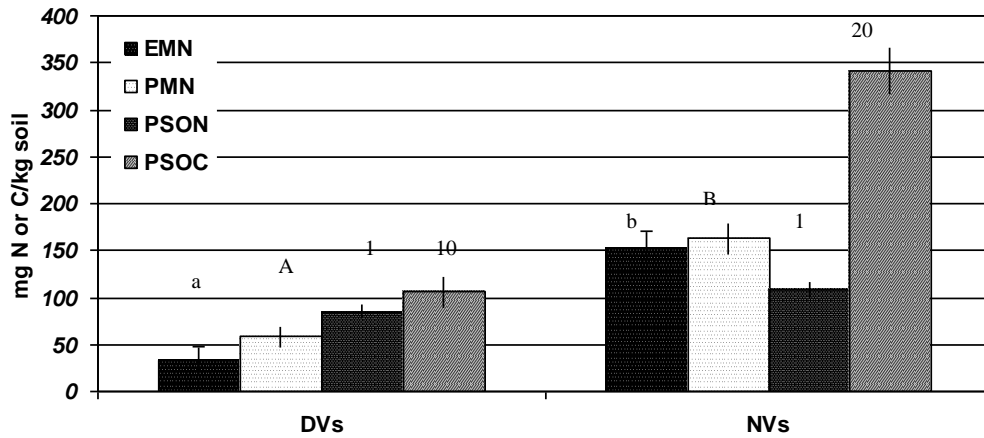


Figure 5.22 Exchangeable Mineral Nitrogen (EMN), Potential Mineralizable Nitrogen (PMN), Potential Soluble Organic Nitrogen (PSON), and Potential Soluble Organic Carbon (PSOC) of soil samples. Values followed by the same letter or number under the same series label are not significantly different ( $p < 0.05$ ) (taken from Stamati et al., 2011).

*Livestock grazing intensity and DON export*

Based on previous published studies, the nitrogen load from five different size, mixed landuse watersheds in Greece was apportioned and related the export of nitrogen species from the watersheds. A comparison of the annual dissolved organic nitrogen (DON) river export versus livestock DON input (normalized to the grazing land area) is presented in Figure 5.23 and the load calculations are presented in the supporting information. River DON export was found to be linearly correlated with livestock DON load that is input to the watershed for five basins in Greece.

Finally, the patterns of dissolved nitrogen export from Mediterranean watersheds were compared to forested and mixed landuse watersheds from other climatic regions reported in the literature in order to elucidate the differences in response at a larger scale. River water in mixed agricultural watersheds exhibited different patterns of dissolved inorganic nitrogen (DIN) versus DON-to-TDN ratio as compared to forested watersheds and mixed watersheds of other climates (Figure 5.24, Table A5.5 in the Appendix). Forested watersheds had low DIN concentrations and high DON-to-TDN ratio while mixed landuse watersheds of Mediterranean with significant livestock grazing contribution exhibited higher DIN and DON-to TDN ratios

compared to other watersheds, providing additional evidence that DON could be a reliable indicator of livestock grazing impacts.

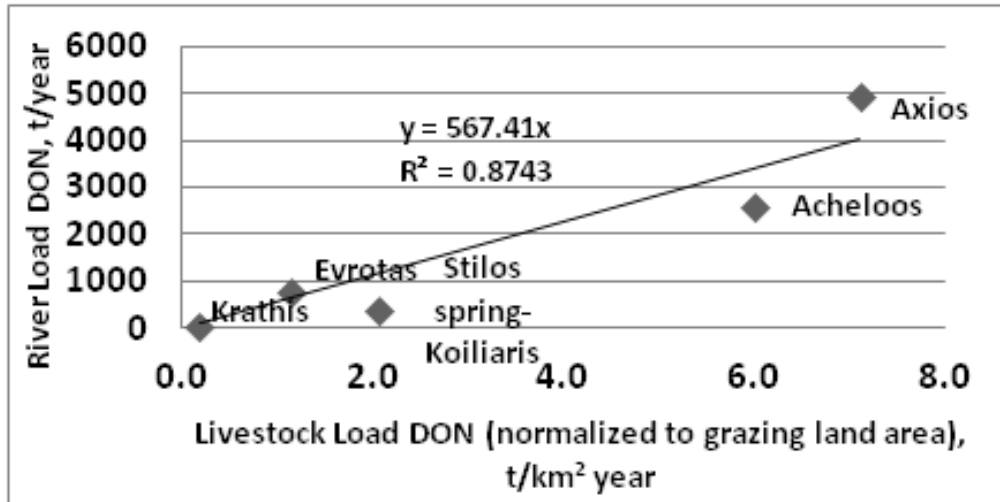


Figure 5.23 A comparison of the annual dissolved organic nitrogen (DON) river export versus livestock DON input (normalized to the grazing land area) for five rivers of Greece (taken from Stamati et al., 2011).

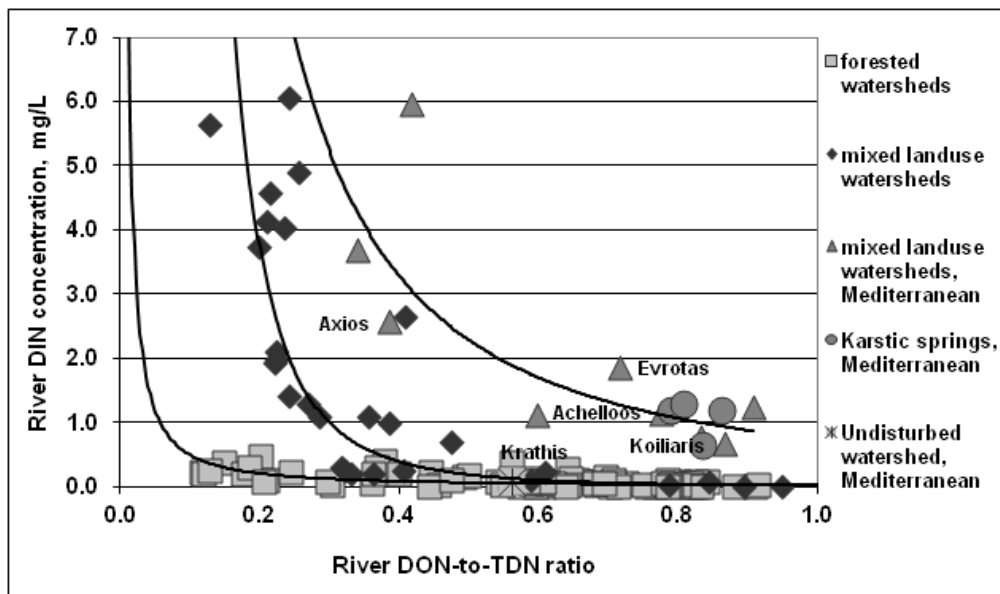


Figure 5.24 River concentration of dissolved inorganic nitrogen (DIN) relatively to the DON/TDN ratio in different watershed types (See detailed data in Table A5.5 in the Appendix) (taken from Stamati et al., 2011).

Overall, this study provided evidence linking the DON export from river basins to livestock grazing intensity and the resulting decrease in vegetation. A linear relationship between DON export and livestock N load was obtained for five Greek basins suggesting a mechanism that operate regional scales. The de-vegetation of grazing lands in Koiliaris River highland calcareous leptosols was shown to be a primary factor causing the decline of soil biochemical quality. De-vegetated soils presented lower decomposition potential as compared to vegetated soils. Mineralization and plant uptake appeared to be restricted and leaching of soluble low aromaticity organic matter was favored. The evidence provided by this study suggested that DON can be used as a reliable indicator for livestock grazing impacts to soil biochemical quality.

## 5.6 LITERATURE CITED

- Akagi, J., Zsolnay Á., 2008. Effects of long-term de-vegetation on the quantity and quality of water extractable organic matter: Biogeochemical implications. *Chemosphere* 72, 1462-1466.
- Albaladejo, J., Martinez-Mena, M., Roldan, A., Castillo, V., 1998. Soil degradation and desertification induced by vegetation removal in a semi arid environment. *Soil Use and Management* 4, 1-5.
- Banwart, S., Bernasconi, S.M., Bloem, J., Blum, W., Brandao, M., Brantley, S., Chabaux, F., Duffy, C., Kram, P., Lair, G., Lundin, L., Nikolaidis, N., Novak, M., Panagos, P., Ragnarsdottir, K.V., Reynolds, B., Rousseva, S., de Ruyter, P., van Gaans, P., van Riemsdijk, W., White, T., Zhang, B., 2011. Assessing Soil Processes and Function in Critical Zone Observatories: hypotheses and experimental design. *Vadose Zone Journal* 10, 974-987.
- Bastida, F., Moreno, J.L., Hernández, T., García, C., 2006. Microbiological activity in a soil 15 years after its devegetation. *Soil Biology and Biochemistry* 38, 2503-2507.
- Burton, J., Chen, C., Xu, Z., Ghadiri, H., 2007. Soluble organic nitrogen pools in adjacent native and plantation forests of subtropical Australia. *Soil Biology and Biochemistry* 39, 2723-2734.
- Bouyoucos, G.J., 1936. Directions for making mechanical analysis of soils by the hydrometer method. *Soil Science* 4, 225-228.
- Chappell, N.A., Ternan, J.L., Bidin, K., 1999. Correlation of physicochemical properties and sub-erosional landforms with aggregate stability variations in a tropical ultisol disturbed by forestry operations. *Soil and Tillage Research* 50, 55-71.
- Chu, H., Lin, X., Fujii, T., Morimoto, S., Yagi, K., Hu, J., Zhang J., 2007. Soil microbial biomass, dehydrogenase activity, bacterial community structure in response to long-term fertilizer management. *Soil Biology and Biochemistry* 39, 2971-2976.
- Corvasce, M., Zsolnay, A., D'Orazio, V., Lopez, R., Miano, T.M., 2006. Characterization of water extractable organic matter in a deep soil profile. *Chemosphere* 62, 1583-1590.
- Déqué, M., Drevet, C., Braun, A., Cariolle,.: The ARPEGE/IFS atmosphere model: a contribution to the French community climate modeling. *Climate Dynamics*, 10 (4-5), 249-266, 1994.
- Dilling, J., Kaiser, K., 2002. Estimation of the hydrophobic fraction of dissolved organic matter in water samples using UV photometry. *Water Resources* 36, 5037-5044.
- Dimoyiannis, D.G., Tsadilas, C.D., Valmis, S., 2008. Factors affecting aggregate instability of Greek agricultural soils. *Commun. Soil Science and Plant Analysis* 29, 1239-1251.
- Elliott, E.T., 1986. Aggregate structure and carbon, nitrogen, and phosphorus in native and cultivated soils. *Soil Science Society of America Journal* 50, 627-633.
- Emerick, R.J., Embry, L.B., Olson, O.E., 1959. Effect of sodium silicate on the development of urinary calculi and the excretion of various urinary constituents in sheep. *Journal of Animal Science* 18, 1025-1030.
- FAO 1998. World Reference Base for Soil Resources. <http://www.fao.org/ag/agl/agll/wrb/>
- Ghani, A., Dexter, M., Carran, R.A., Theobald, P.W., 2007. Dissolved organic nitrogen and carbon in pastoral soils: the New Zealand experience. *European Journal of Soil Science* 58, 832-843.
- Hendershot, W.H. and M. Duquette. 1986. A simple barium chloride method for determining cation exchange capacity and exchangeable cations. *Soil Biology and Biochemistry* 50, 605-608.
- Hill, J., Hostert, P., Tsiourlis, G., Kasapidis, P., Udelhoven, Th., Diemer, C., 1998. Monitoring 20 years of increased grazing impact on the Greek island of Crete with earth observation satellites. *Journal of Arid Environments* 39, 165-178.
- Hoogendoorn, C.J., Betteridge, K., Costall, D.A., Ledgard, S.F., 2010. Nitrogen concentration in the urine of cattle, sheep and deer grazing a common ryegrass/cocksfoot/white clover pasture New Zealand. *Journal of Agricultural Research* 53, 235 - 243.
- Hur, J., Williams, M.A., Schlautman, M.A., 2006. Evaluating spectroscopic and chromatographic techniques to resolve dissolved organic matter via end member mixing analysis. *Chemosphere* 63, 387-402.

- Idowu, O.J., 2011. Relationships between aggregate stability and selected soil properties in Humid Tropical environment. *Commun. in Soil Science and Plant Analysis* 34, 695-708
- IPCC, 2007. Climate change 2007: The physical science basis. In: Solomon, S., Qin, D. Manning, M., Chen, Z., Marquis, M., Averyt, K.B., Tignor, M., Miller, H.L. (Eds), Contribution of working group I to the fourth assessment report of the intergovernmental panel on climate change. Cambridge University Press.
- Jacob, D., 2001. The role of water vapor in the atmosphere. A short overview from a climate modeller's point of view. *Physics and Chemistry of the Earth*, 26A, 523-527.
- Kalbitz, K., 2001. Properties of organic matter in soil solution in a German fen area as dependent on landuse and depth. *Geoderma* 104, 203-214.
- Kazakis, G., Ghosn, D., Vogiatzakis, I.N., and Papanastasis, V.P., 2007. Vascular plant diversity and climate change in the alpine zone of Lefka Ori, Crete. *Biodiversity and Conservation* 16, 1603-1615.
- Kjellström, E., Bärring, L., Gollvik, S. and Hansson, U, 2005. A 140-year simulation of European climate with the new version of the Rossby Centre regional atmospheric climate model (RCA3). *Rep. Meteorol Climatol*, 108, SMHI, Norrköping, Sweden.
- Kourgialas, N.N., Karatzas, G.P., and Nikolaidis, N.P. 2010. An integrated framework for the hydrologic simulation of a complex geomorphological river basin. *Journal of Hydrology* 381, 308-321.
- Krull, E.S., Skjemstad, J.O., Baldock, J.A., 2004, Functions of Soil Organic Matter and the effect on soil properties. GRDC report, Project CSO 00029.
- Li, X.G., Wang, Z.F., Ma, Q.F., Li, F.M., 2007. Crop cultivation and intensive grazing affect organic C pools and aggregate stability in arid grassland soil. *Soil and Tillage Research* 95, 172-181.
- Moraetis, D., Efstathiou, D., Stamati, F.E., Tzoraki, O., Nikolaidis, N.P., Schnoor, J.P., Vozinakis, K. 2010. High frequency monitoring for the identification of hydrological and bio-geochemical processes in a Mediterranean river basin. *Journal of Hydrology* 389, 127-136.
- Moraetis, D., Stamati, F., Kotronakis, E., Fragia, T., Paranychnianakis, N. and Nikolaidis, N. P.: Identification of hydrologic and geochemical pathways using high frequency sampling, REE aqueous sampling and soil characterization at Koiliaris Critical Zone Observatory. *Applied Geochemistry* 26, S101-S104, 2011.
- Nikolaidis, N.P., Chheda, P., Lackovic, J.A., Guillard, K., Simpson, B., Pedersen, T., 1999. Nitrogen mobility in biosolid-amended glaciated soils. *Water Environmental Resources* 71, 368-376.
- Nikolaidis, N., Skoulikidis, N., Karageogis, A., 2004. Pilot implementation of EU policies in Acheloos River basin and coastal zone, Greece. *Proceedings of International Symposium on Water Resources Management: Risks and Challenges for the 21st Century*, Izmir Turkey, 2 to 4 September.
- Nikolaidis, N., Skoulikidis, N., Tsakiris, K., Kalogerakis, N., 2006. Preliminary management plans of Evrotas River watershed and coastal zone. Technical report 242pp +Index 79pp. In: Nikolaidis N., N. Kalogerakis, N.Skoulikidis, K. Tsakiris, (Eds), 2005-2009. *Environmental friendly technologies for rural development*. Life-Environment project, LIFE05ENV/Gr/000245 EE (Envi-Friendly).
- Nikolaidis, N., Karageorgis, A., Kapsimalis, V., Drakopoulou, P., Skoulikidis, N., Behrendt, H., Levkov, Z., 2009. Management of nutrient emissions of Axios River catchment: Their effect in the coastal zone of Thermaikos Gulf, Greece. *Ecological Modeling* 220, 383-396.
- Nikolaidis, N.P., Bidoglio, G., 2011. Modeling of soil organic matter and structure dynamics: A synthesis review, *Geoderma* (under revision).
- Nikolaidis, N.P., 2011, Human impacts on soils: Tipping points and knowledge gaps. *Applied Geochemistry* 26, S230-S233.
- Nikolaidis, N.P., Bouraoui, F., Bidoglio, G., Hydrologic and geochemical modeling of a karstic Mediterranean watershed, *Hydrology and Earth System Sciences Discussion* (under revision).
- Piccolo, A., Zena, A., Conte, P., 1996. A comparison of acid hydrolyses for the determination of carbohydrates in soils. *Commun. Soil Science and Plant Analysis* 27, 2909-2915.
- RCEP., 1996. Sustainable Use of Soil. 19th report of the Royal Commission on Environmental Pollution. Cmnd 3165, HMSO, London.

- Roeckner, E., 2003. The atmospheric general circulation model ECHAM5. Part 1: Model description, p. 127. Max Planck Institute for Meteorology Rep. 349, Hamburg, Germany, 127pp.
- Rojas, R., Feyen, L., Dosio, A., Bavera, D., 2011. Improving pan-european hydrological simulation of extreme events through statistical bias correction of RCM-driven climate simulations, *Hydrology and Earth System Sciences Discussions* 8, 3883-3936.
- Santi, C.A., Certini, G., D'Acqui, L.P., 2006. Direct Determination of organic carbon by dry compustion in soils with carbonates. *Comm. in Soil Science and Plant Analysis* 37, 155-162.
- Soil Sampling and Methods of Analysis, M. R. Carter and E. G. Gregorich, Eds., pp. 71-80, CRC Press, Taylor and Francis, Boca Raton, Fla, USA, 2nd edition, 2008
- Sorensen, P., Jensen, E.S., 1995. Mineralization of carbon and nitrogen from fresh and anaerobically stored sheep manure in soils of different texture. *Biology and Fertility of Soils* 19, 29-35.
- Stamati, F.E., Nikolaidis, N.P., Venieri, D., Psillakis, E., Kalogerakis, N., 2011. Dissolved organic nitrogen as an indicator of livestock impacts on soil biochemical quality. *Applied Geochemistry* 26, 340-343.
- Stamati, F., Nikolaidis, N., Bozinakis, K., Papamastorakis, D., Kritsotakis M., 2006. Stochastic Modeling of the Karstic System of Western Apokoronas in Crete. In VIII International Conference Protection and Restoration of the Environment, Vol. VIII, Chania, Greece, pp. 184-192.
- Thompson, D.B., Walker, L.R., Landau F.H., Stark L.R., 2005. The influence of elevation, shrub species, and biological soil crust on fertile islands in the Mojave Desert, USA. *Journal of Arid Environments* 61, 609-629.
- Tzoraki, O., Nikolaidis, N., Amaxidis, Y., Skoulikidis, N., 2007. In stream biogeochemical processes of a temporary river. *Environmental Science and Technology* 41, 1225-1231.
- Van Meijgaard, E., Van Ulft, L.H., Van De Berg, W.J., Bosveld, F.C., Van Den Hurk, B.J.J.M., Lenderink, G. and Siebesma, A.P.: The KNMI regional atmospheric climate model RACMO, version 2.1 KNMI-publication TR-302 KNMI, de Bilt, The Netherlands, 2008.
- Wan, Y., Lin, E., Xiong, W., Li, Y., Guo, L., 2011. Modeling the impact of climate change on soil organic carbon stock in upland soils in the 21st century in China. *Agriculture Ecosystems and Environment* 141, 23-31.
- Weishaar, J.L., Aiken, G.R., Bergamaschi, B.A., Fram, M.S., Fujii, R., Mopper, K., 2003. Evaluation of specific Ultraviolet Absorbance as an indicator of the chemical composition and reactivity of dissolved organic carbon. *Environmental Science and Technology* 37, 4702-4708.
- Xie, G., Steinberger, Y., 2001. Temporal patterns of C and N under shrub canopy in a loessial soil desert ecosystem. *Soil Biology and Biochemistry* 33, 1371-1379.



## 6. CONCLUSIONS

---

Current management of soil has been recognized to be unsustainable. In the next 20-50 years, the pressures on soil and its core service functions are predicted to further increase, due to climate change (droughts, extreme precipitation events) and competing demands from production systems to provide food, biofuel and timber. It is of prime importance to re-evaluate current agricultural practices and develop alternative sustainable soil farming management systems that protect ecological functions of soils. There is urgent need for tools and methodologies that will give reliable predictions for climate change effects and restoration management to evaluate alternatives. This dissertation was dedicated to contribute to the improvement of our understanding of the mechanisms of nutrient cycling and organic matter protection/loss in soils and provide tools that can be used to assist the sustainable functioning of soil critical zone.

Most model simulations of soil organic carbon (SOC) turnover do not account for the inherent uncertainties due to input data, initial conditions, and model parameters with very few exceptions. In this dissertation, a Monte-Carlo fashion methodology for RothC model parameter estimation, through initialization and calibration with field derived physical fractionation data, assessment of the uniqueness of solution, sensitivity analysis and quantification of uncertainties in modeling results was developed. The methodology was validated with field data at various soil types and lithologies, climatic conditions (Budyco's Radiational Index of Dryness from 3.94-Desert to 0.96-Forest), and landuse conversions (native land to cropland, cropland to set-aside from crop production). Calibrated decomposition rate constants greatly varied from the default RothC values, suggesting that the model should not be used without calibration. The sensitivity analysis suggested that the most sensitive parameters were the humus (HUM) and resistant plant material (RPM) decomposition rate constants as well the plant litter input and the RPM initial pools in the sites where it was not field measured with physical fractionations. Sensitivity greatly depended on the available data for the calibration of the parameters. The total uncertainty of the simulated carbon stock change after 100 years of cultivation or as fallow land was found to be in the eleven cases examined as high as 22% to 122% of the total change. The uncertainty was smaller in the sites with available field measured particulate organic carbon

(POC) data and information about the plant input. The analysis showed that the resulting uncertainties are important; encumbering our ability to accurately predict landuse change effects even in the absence of climate change impacts. Chronosequence data and field measurements POC are important, since the model needs calibration and therefore its inverse use for the estimation initial conditions of native lands for example is not appropriate. The results emphasized the necessity of obtaining accurate plant input data and other physical soil parameters as well as quantifying the variability of initial conditions in order to reduce the uncertainty of carbon turnover projections and determine more accurate the variability of carbon transformation rate constants as a function of climatic conditions.

The average rate of carbon loss after the conversion of a native land to cropland found to decline under a logarithmic pattern and varied from 1 to 11 t/ha the 1<sup>st</sup> year and 0.27 to 0.85 t/ha y after 100 years of cultivation in the climatic gradient simulated. The time for the soil to reach a new stable carbon content also varied from more than 100 years (Tibet, Desert) to 20-30 (Ethiopia, Forest). The Net C to C amended ratio as an index of the effectiveness of carbon addition was found to vary greatly between soil types, climatic conditions and amendment type. For example after 100 years of application (2.5 t C/ha y) of an amendment with composition 30/60/10 (DPM/RPM/HUM, the respective RothC pools) the ratio was found to vary from 0.07 to 0.39. The percentage sequestered in the HUM fraction also varied from 39.8% to 83.1%. The results indicate that reliable long term model simulations are important for the design of long-term sustainable agricultural practices like the appropriate quantity and quality of carbon addition under different climatic regimes and soil types for the effective carbon sequestration and humus increase.

The estimation of the temperature coefficient Q10 as an index of the 'apparent' temperature sensitivity of the RPM and HUM RothC carbon pools revealed that it was lower for the HUM pool as compared with the RPM, particularly in the lower temperature ranges (5-15 °C) and should not be consider identical in the model. The protection of SOM through aggregation and sorption to clays, which greatly varies with soil type, clay content and other parameters, is considered to be responsible for the observed pattern. The function used in RothC for the correction of the decomposition rate due to temperature was found to systematically underestimate decomposition at low temperatures and overestimate decomposition at high temperatures in accordance with the reports of other authors. Worth noting, however, is that

Q10 for the HUM pool at low temperatures was found lower than the RothC Q10 value and therefore the decomposition rate in this case is overestimated. These results indicated the importance of the inclusion of physical protection i.e. aggregation in carbon model with a deterministic manner.

Therefore, a coupled soil carbon, aggregation, and structure turnover (CAST) model was developed. The model was based on the current knowledge of the proposed mechanism in the relevant scientific literature that suggests that macro-aggregates are formed around particulate organic matter, followed by the release of micro-aggregates. The CAST model constitutes the first attempt in the scientific literature for the modeling of this mechanism. A simplified mechanistic N model was also developed. The developed CAST model was successfully used for the simulation of carbon, aggregate, and structure turnover in cropland to set-aside from crop production conversions of Critical Zones Observatories in Greece (fine textured Mediterranean) and Iowa (coarse textured humid continental). A more deterministic explanation of the saturation level of the different carbon pools and soil structure (porosity and bulk density) were obtained. The soil system reached maximum macro-aggregation/porosity and minimum bulk density after 7 and 14 years in Greece and Iowa, respectively. Afterwards, macro-aggregate disruption presented a constant seasonal pattern and any further SOC increase was due to micro-aggregation resulting in the increase of bulk density and decrease of porosity towards a stable value. The Nitrogen modeling revealed that the presence of fungi was related with macro-aggregation. The CAST model can assist in revealing primary factors that influence organic matter, aggregation, and structure turnover in different ecosystems and in describing the response of the soil system to management practices, landuse changes, and climate change in order to design and optimize the appropriate measures/practices.

Finally in this dissertation the soil status of Koiliaris River Basin Critical Zone Observatory was evaluated by assessing the primary factors of soil aggregation in the soils of the basin, quantifying the effects of landuse and climate changes and evaluating the effects of over-grazing to soil biochemical quality and water quality. A soil survey (29 samples) was conducted based on a soil mapping typology approach in order to assess primary control factors of soil aggregation in the basin. Principal component analysis revealed that there are two major soil groups which can be described by 15 soil parameters. Soils in Group-1 were primarily from regions where Schists was the parent material as well as from Marls with sandy texture and acidic pH and were found

in elevations lower than 550 m. Soils in Group-2 were mostly derived from the alluvial plain (some from alkaline calcareous Marls also) and the semi-mountainous region where the Limestones of the Trypalis units are found. Most soils were croplands, cultivated with olive groves (elevation 9-383 m) and there were also as a sub-group of shrublands on limestones (592-1098 m). Group-1 was distinguished from Group-2 by its lower content in macro-aggregates which was found to be primarily related to the lower eCEC and the sandier texture (more coarse sand, less silt and clay). All the soils in Group-1 and six out of the sixteen soils in Group-2 exhibited WSA-250 lower than the limit value of 60% which indicates agronomically valuable soils (Banwart et al., 2011). The content of the soils in macro-aggregates as revealed by the multi regression analysis was adequately described by 7 parameters for Group-1: BD, pH, TKN, particles >1000 $\mu$ m, eCEC, BS\_Na-BaCl<sub>2</sub>, and PMN and 11 parameters for Group-2: BD, pH, TKN, particles >1000  $\mu$ m, particles <53  $\mu$ m, particles <2  $\mu$ m, eCEC, BS\_Na-BaCl<sub>2</sub>, PMN, N-1hour (KCl extracted), and K-BaCl<sub>2</sub>.

The effect of the climate change predicted by the IPCC scenario A1B -which puts a balanced emphasis on all energy sources- on SOC stocks of cultivated soils of three lithologies (Schists, Marls, Trypalis limestones) was assessed by the simulation with RothC. The results for the present scenario (1990-2010) were compared with the results for the decades 2010-2030 and 2030-2050 given the local decadal climatic variability. It was found that less carbon sequestered due to climate change (simulation of shrublands to croplands conversions) will correspond to 1.7% to 4.1% of the initial SOC stock, while the carbon stock change due to landuse change under the present scenario (1990-2010) was 12% to 28% of the initial SOC. On the other hand, the climate change effects in 50 year old olive grove fields were estimated to be 2-3% of the initial SOC, while the change of stock due to cultivation for 20 years under the present scenario was estimated to be 1.7% to 8.9%. The amount of carbon (t/ha) that was not sequestered due to climate change was predicted to be 1.5-3 t C/ha for 20 years. The results emphasize that management effects and particularly landuse change effects are such high that may hamper our ability to detect climate change effects.

Finally, the hypothesis that livestock grazing (and the resulting de-vegetation) that takes place in the highlands of Koiliaris River Basin degrades soil quality and enriches surface and ground waters with DON was examined with field data from 3 different scales. The study provided evidence linking the DON export from river basins to livestock grazing intensity; a linear

relationship was obtained for five Greek basins suggesting a mechanism that operates at regional scales. Mass balance calculations of N loads indicated that organic N is behaving as a conservative substance. De-vegetated soils had lower C and N content, similar bacterial count, but lower microbial activity, lower fungi counts and species richness and lower mineralizable nitrogen compared to naturally vegetated soils. DON was the predominant N species in both extracted soluble nitrogen pools. Mineralization and plant uptake appeared to be restricted and leaching of soluble low aromaticity organic matter was favored. DON could be used as a reliable indicator for livestock grazing impacts to soil biochemical quality.

The innovation of this dissertation can be summarized in the following:

- 1.** Development and evaluation with field data (various soil types and lithologies, climatic conditions, and landuse conversions) of a comprehensive Monte-Carlo fashion methodology for RothC model parameter estimation, through initialization and calibration with field derived physical fractionation data, assessment of the uniqueness of solution, sensitivity analysis and quantification of uncertainties in modeling results. Most model simulations of SOC turnover do not account for the inherent uncertainties due to input data, initial conditions, and model parameters with very few exceptions.
- 2.** Simulate the carbon loss and the uncertainty of the predictions under an international climatic gradient of landuse conversions. Estimate the Net C to C amended ratio as an index of the effectiveness of carbon addition under the different soil types, climatic conditions for various amendment types. Estimation of the temperature factor Q<sub>10</sub> as an index of the 'apparent' temperature sensitivity of the RPM and HUM RothC carbon pools. Although many scientists have reported that there are differences between the apparent temperature sensitivity due to factors like aggregation and the sensitivity introduced by the commonly used equations for temperature corrections this is the first time quantified with data from a climatic gradient.
- 3.** Development and evaluation with field data of a coupled carbon, aggregation, and structure (CAST) model that simulates the concept that suggests that macro-aggregates are formed around particulate organic matter, followed by the release of micro-aggregates. This conceptual model has been suggested extensively in the scientific literature but this was the first time that it was modeled.

4. Comprehensive analysis and development of multi linear equations to adequately predict aggregate stability in the two major soil groups identified in Koiliaris soils by bulk soil parameters. Most studies aiming to predict aggregate stability have correlated it only to SOC content, while few studies that have used more soil parameters have not yield to high predictability.
5. Quantify the effects of climate change on SOC stocks and compare them with the respective effects of landuse changes and management practices in three lithologies of Koiliaris River Basin with the use of the developed methodology for RothC calibration and initializatin. RothC has been used similarly with other carbon models to predict climate change effects on soils mostly without calibration of its rate constants and without being initialized with field data.
6. Provided evidence linking the DON export from river basins to livestock grazing intensity; Suggest DON as a reliable indicator for livestock grazing impacts to soil biochemical quality in the Mediterranean geo-environment.

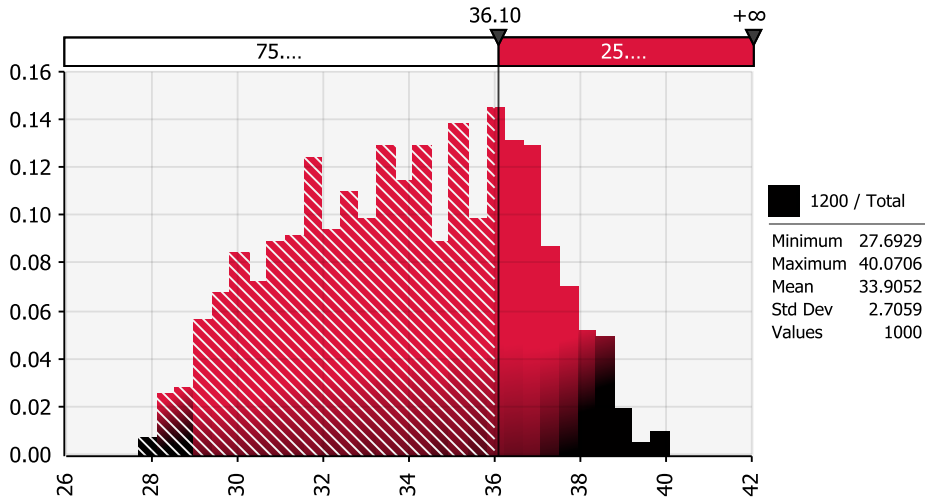
The major direct research interests for future work can be summarized in the following issues:

1. Enhancement of the utility of the CAST model to test hypotheses by its deterministic coupling with the N and P cycles, plant growth, as well soil fauna (food web dynamics) as well the addition of sub layers in order to account for the whole soil profile.
2. Evaluate the CAST model with field data of different soil types and climatic regions.
3. Development of a methodology for the estimation of the composition in terms of modeling pools (e.g. DPM/RPM/HUM ratio for RothC model) of various types of soil amendments and field evaluation of their effectiveness on carbon sequestration and aggregation. Comprehensive life cycle analysis for the estimation of the real benefits.
4. Design of the studies needed to obtain the appropriate data to develop better equations to correspond for the apparent sensitivity of decomposition to temperature and moisture.
5. Use geostatistics to estimate distributed values for soil parameters indicative of soil quality and develop a soil quality/degradation assessment methodology to relate the status of soils to specific soil functions and threats.
6. Examine the role of clay mineralogy in the aggregate stability/soil properties relation.
7. Study of the Nitrogen cycling in degraded de-vegetated grazing lands with undisturbed column studies.

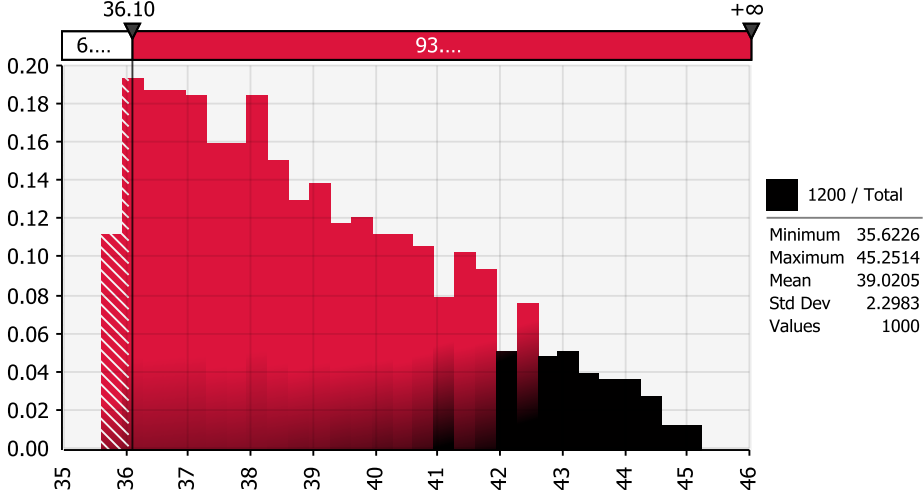
## 7. APPENDIX

---

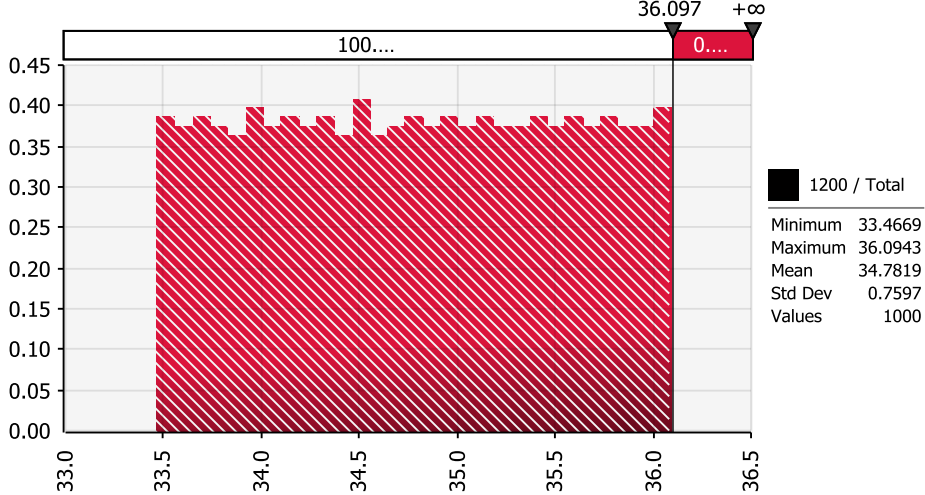
The distribution of SOC output due to the uncertainty of model parameters



The distribution of SOC output due to the uncertainty of litter input and clay content

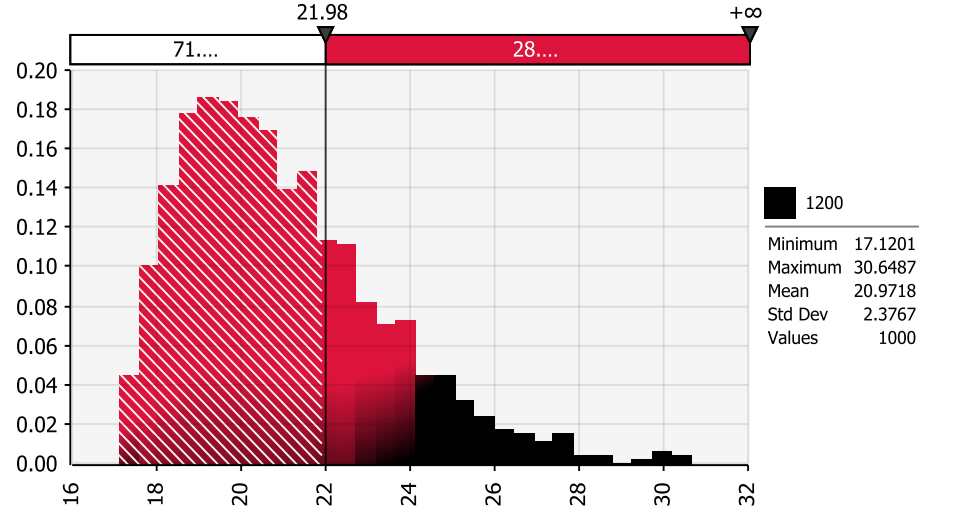


The distribution of SOC output due to the uncertainty of initial conditions

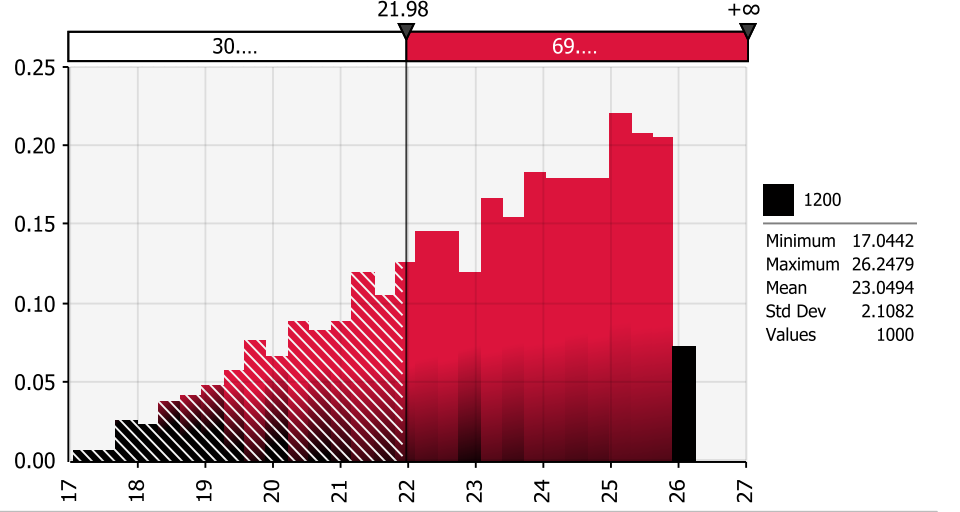


(a)

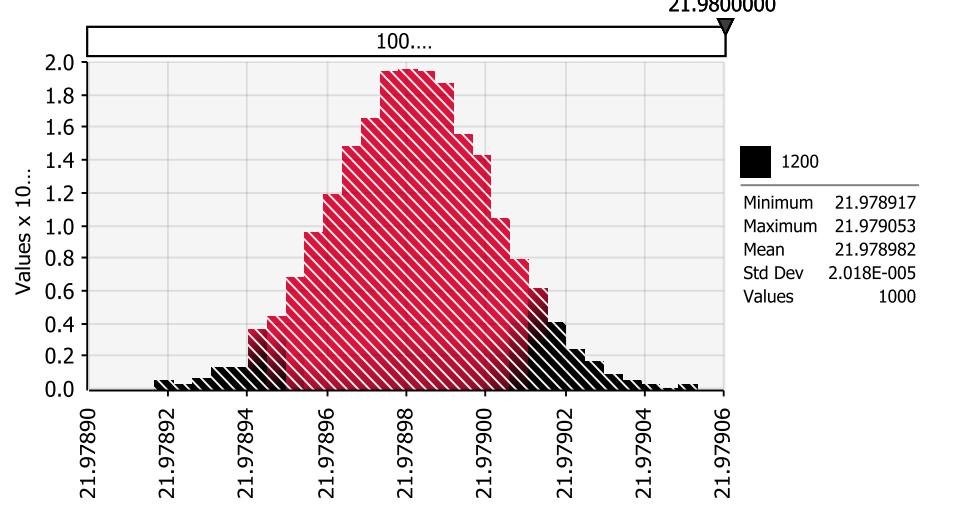
The distribution of POC output due to the uncertainty of model parameters



The distribution of POC output due to the uncertainty of litter input and clay content

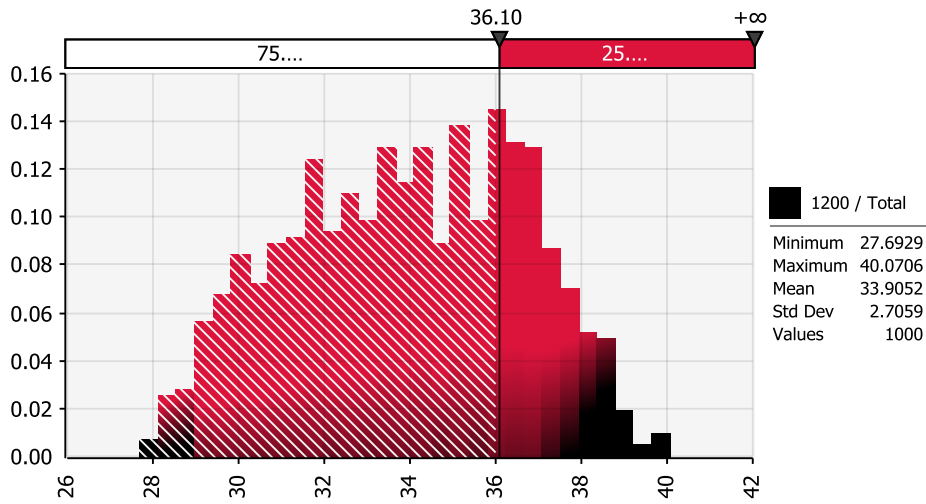


The distribution of POC output due to the uncertainty of initial conditions

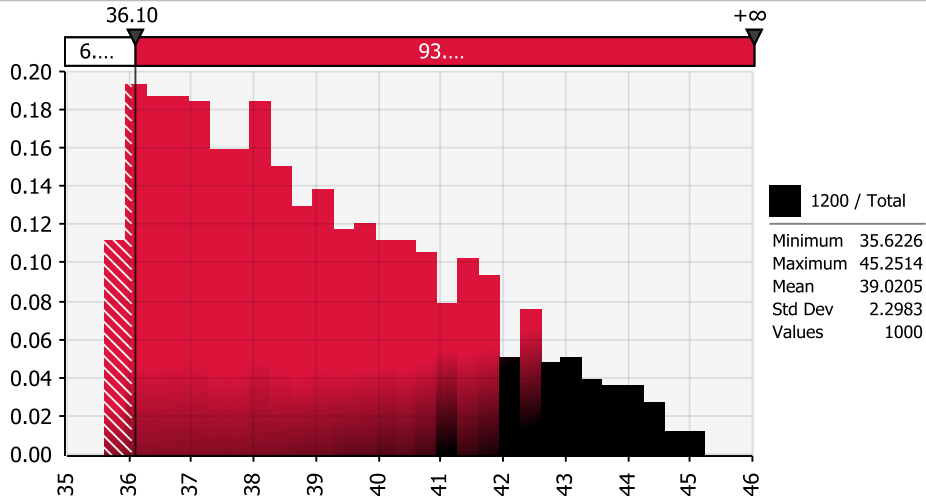


(b)

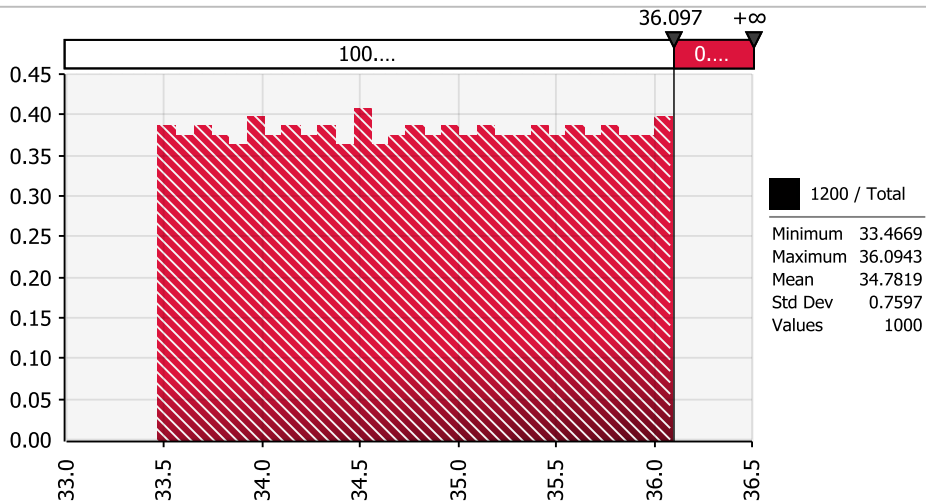
The distribution of SOC output due to the uncertainty of model parameters



The distribution of SOC output due to the uncertainty of litter input and clay content

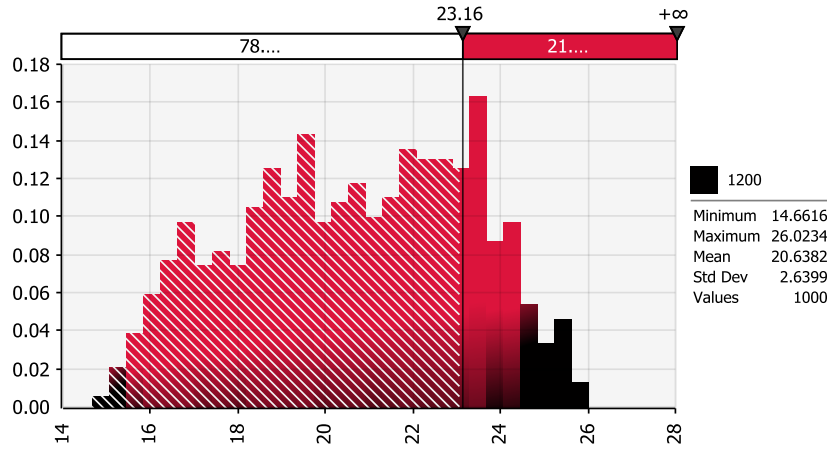


The distribution of SOC output due to the uncertainty of initial conditions

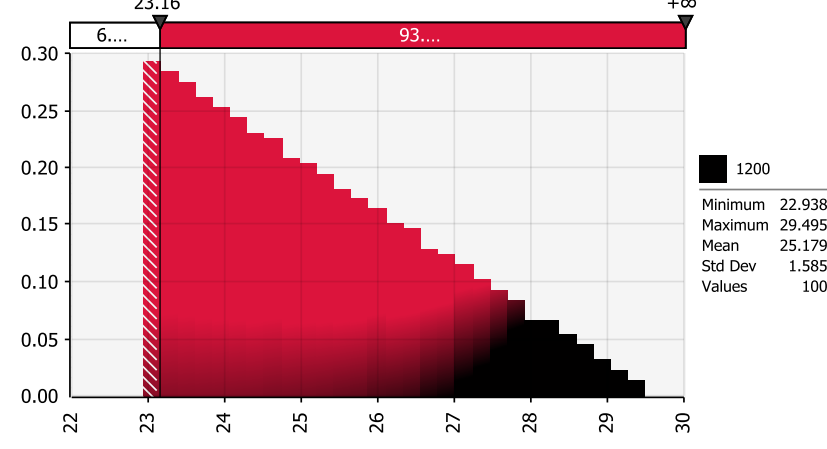


(c)

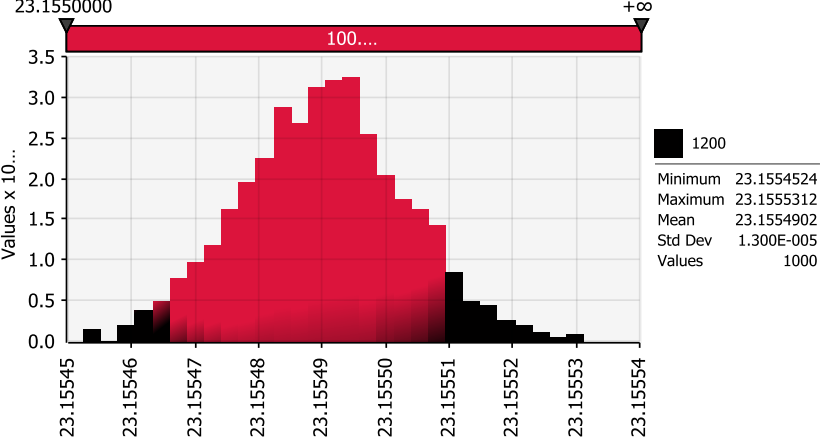
The distribution of POC output due to the uncertainty of model parameters



The distribution of POC output due to the uncertainty of litter input and clay content



The distribution of POC output due to the uncertainty of initial conditions



distribution below the value of the optimum solution and the right (dark shaded histogram bars) indicates the area of the distribution below the value of the optimum solution. The percentage covered in each area is given in the bars at the top of each plot.

(d)

Figure A2.1 The output distributions by the Monte-Carlo simulations for the calculation of the uncertainty due to initial conditions, input data, and model parameters for 100 y of simulation in a) Greece and b) Iowa for soil organic carbon (SOC) and Particulate organic carbon (POC). The x-axis indicates the SOC or POC content in t C/ha. The value of the optimum solution for SOC and POC is indicated in the top of the plot separating the distribution in two parts: the left part (light shaded histogram bars) indicates the area of the

**Table A3.1 Details on natural vegetation as well crop type and crop management for the six sites.**

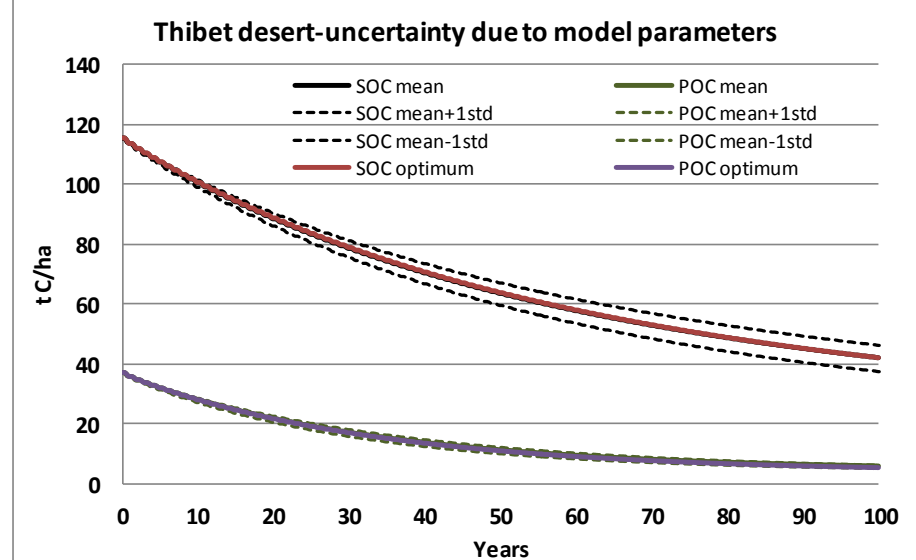
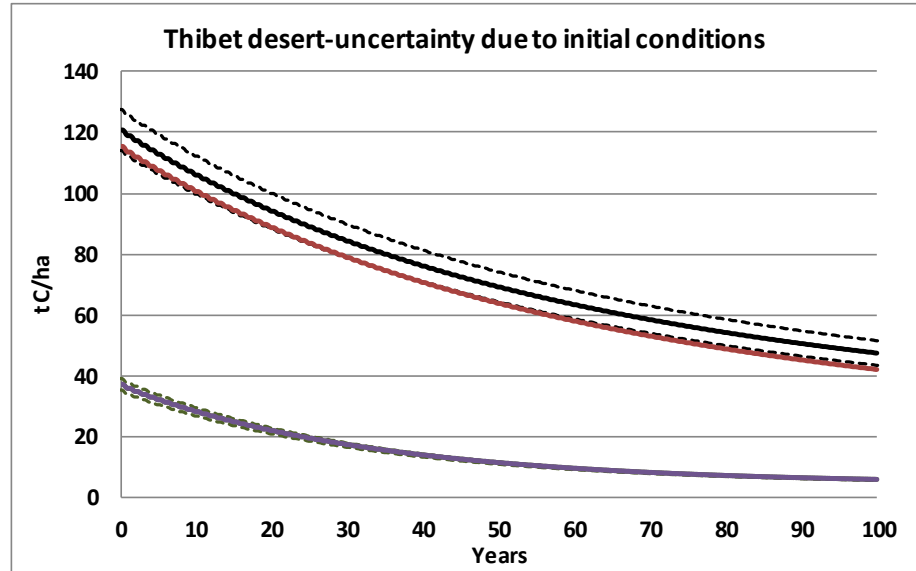
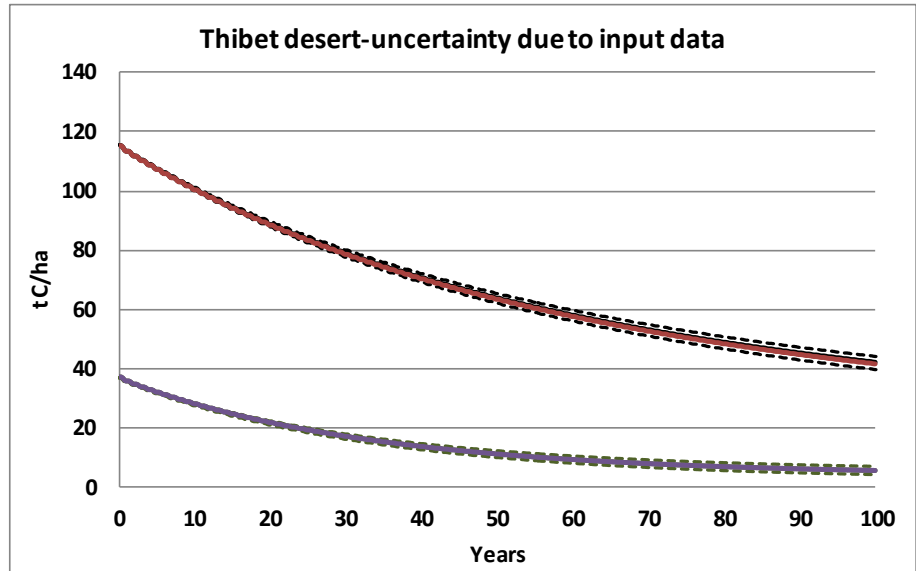
Reference	Li et al (2009), Tibet-Desert	Frank et al (2006), North Dakota-Semiarid	Wu et al (2004), China-Steppe	Evrendilek et al (2004), Turkey-Steppe	Ashagrie et al (2007), Ethiopia-Steppe	Vagen et al (2006), Madagascar-Forest
<b>Natural vegetation</b>	Kobresia capillifolia, Potentilla acaulis, Artemisia frigida and Heteropappus altaicus	Typical Northern Great Plains mixed-grass prairie ecosystem dominated by blue grama [Bouteloua gracilis (H.B.K.) Lag. ex Griffiths], needle-and-thread (Stipa comata Trin. and Rupr.), Carex (Carex spp.), Kentucky bluegrass (Poa pratensis L.), little bluestem [Schizachyrium scoparium (Michx.) Nash], side-oats grama [Bouteloua curtipendula (Michx.) Torr.], and western wheatgrass [Pascopyrum smithii (Rybd.) Lovell].	Forest	Chrysopogon gryllus, Festuca ovina, Bothriochloa ischaemum, Globularia trichosantha, Plantago lagopus, Lotus corniculatus, and Teucrium polium	A Podocarpus falcatus dominated mixed natural forest (ca. 3000–4000 years)	Rainforest
<b>Crops/ Crop Management</b>	spring wheat (Triticum aestivum), barley (Hordeum vulgare), canola (Brassica campestris) and vegetable pea (Pisum sativum) were grown without regular crop rotations --Fertilized, Conventional ploughing (about 15 cm), above ground biomass removed for hay or fuel	Spring wheat was seeded in late April --Fertilization: 67 kg N ha <sup>-1</sup> (NH <sub>4</sub> NO <sub>3</sub> ). Triple superphosphate 11 kg P ha <sup>-1</sup> with pre- and post-emergent herbicides	panic millet (Panicum italicum L.) or beans (Phaseolus L.). --35–70 kgNha <sup>-1</sup> as urea or ammonium nitrate and 9.7–16.1 kg P ha <sup>-1</sup> as superphosphate, till to a 20 cm depth with a plough in spring and autumn and hand cultivate to a depth of about 5 cm with a hoe for weeding 3–5 times during the growing season. Straw removed along with grain	Continuous barley (Hordeum vulgare L.) and wheat (Triticum aestivum L.) in a rotational manner --Conventional tillage practices	Maize, bread- wheat, faba bean, and sorghum --Fertilized with di- ammonium phosphate annually depending on the crops' fertiliser requirement. conventionally cultivated using a traditional oxen- drawn implement (Maresha).	Dryland crops: rice varieties (Oryza sp.), cassava (Manihot esculenta), maize (Zea mays), beans (Phaseolus sp.), potatoes (Solanum tuberosum), sweet potatoes (Ipomoea batatas),vegetable and fruit production in some areas. --Conventional practices
<b>Cultivation period</b>	Jun-Sep	May-Jul	Jan-Dec	Jan-Dec	Jan-Dec	Jan-Dec

Table A3.2 Mean monthly meteorological data used for the application of the ROTHC model in the six sites (taken from the Local Climate Estimator-New LocClim 1.10, Grieser, 2006 according to the coordinates and elevation given in the manuscripts).

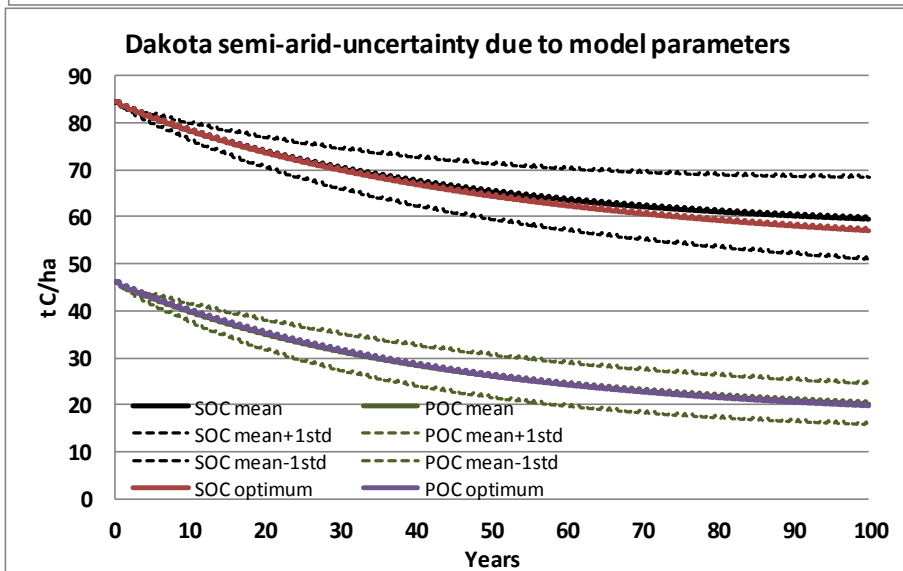
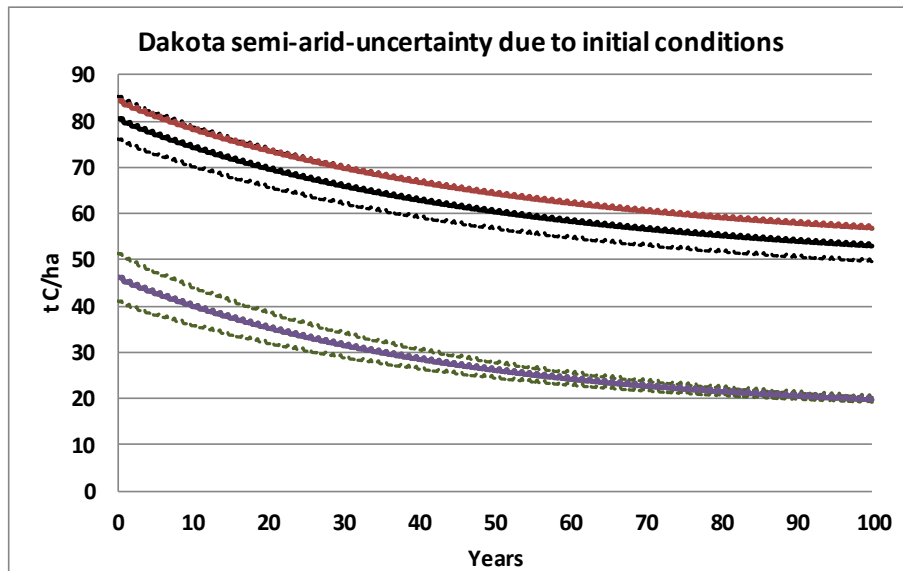
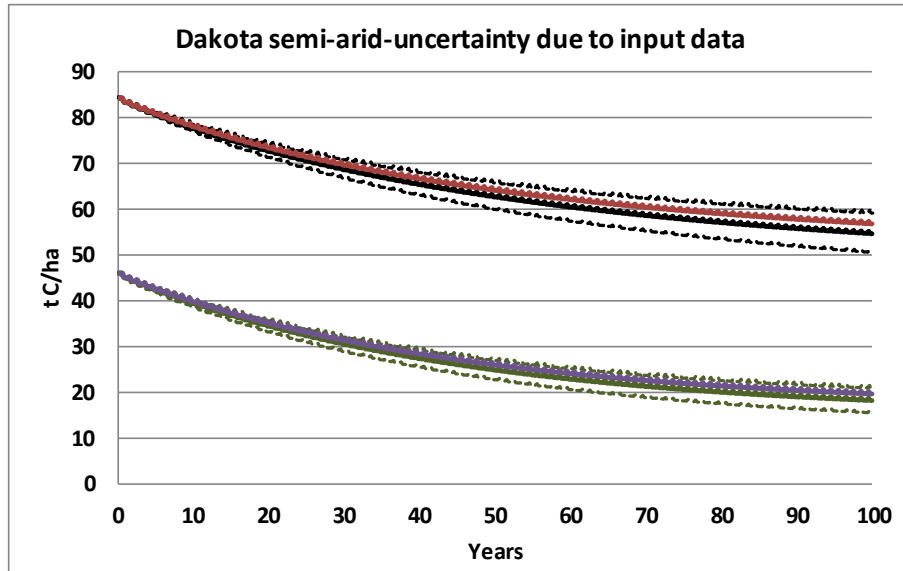
Month	Li et al (2009), Tibet-Desert			Frank et al (2006), North Dakota-Semiarid			Wu et al (2004), China-Steppe		
	Temp	Rain	PET	Temp	Rain	PET	Temp	Rain	PET
	°C	mm	mm	°C	mm	mm	°C	mm	mm
1	-9.2	2	27	-12.2	8	7	-6.4	4	30
2	-6.6	3	39	-8.9	8	10	-2.3	7	35
3	-0.2	8	76	-2.1	12	38	7.4	18	63
4	6.2	14	118	5.9	43	80	11.3	30	87
5	11.5	29	150	12.5	57	129	17.2	41	124
6	15.1	41	160	18.0	75	147	20.8	76	144
7	17.4	56	162	21.2	60	180	23.7	151	128
8	16.9	66	148	20.2	49	171	21.2	126	113
9	11.8	43	103	13.5	41	103	16.5	72	84
10	5.7	14	73	7.5	24	78	9.8	38	65
11	-1.7	4	41	-1.5	11	31	4.0	17	41
12	-7.8	1	26	-9.7	9	11	-5.2	6	31
<b>Annual</b>	4.9	279	1122	5.4	397	985	9.8	586	944
Month	Evrendilek et al (2004), Turkey-Steppe			Ashagrie et al (2007), Ethiopia-Steppe			Vagen et al (2006), Madagascar-Forest		
	Temp	Rain	PET	Temp	Rain	PET	Temp	Rain	PET
	°C	mm	mm	°C	mm	mm	°C	mm	mm
1	3.5	127	34	12.1	41	97	20.7	295	115
2	4.8	87	39	13.3	82	96	20.6	243	99
3	8.3	89	66	14.0	108	110	20.2	230	95
4	12.5	67	90	14.1	146	103	19.0	82	79
5	16.6	65	130	13.3	131	104	16.7	37	63
6	21.1	29	150	12.6	130	92	14.8	27	49
7	24.7	9	169	12.1	191	80	13.8	22	51
8	24.7	4	156	11.8	187	84	14.3	23	66
9	20.7	16	123	12.3	189	83	15.8	33	84
10	15.3	49	82	12.3	84	98	18.5	59	109
11	9.6	86	46	11.8	30	94	20.0	196	112
12	5.0	124	29	11.1	14	90	20.6	282	122
<b>Annual</b>	13.9	752	1112	12.6	1333	1131	17.9	1529	1046

Table A3.3 Sensitivity coefficients (the absolute value of the ratio:  $(\Delta Y/Y)/(\Delta x/x)$ ) for RothC model parameters for  $\pm 10\%$  and  $\pm 50\%$  change of the calibrated values for the six sites.

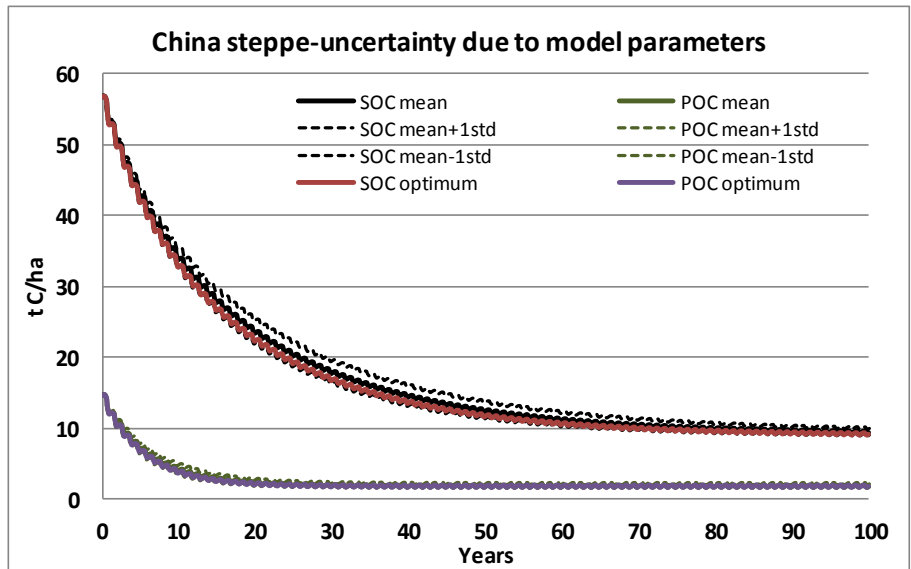
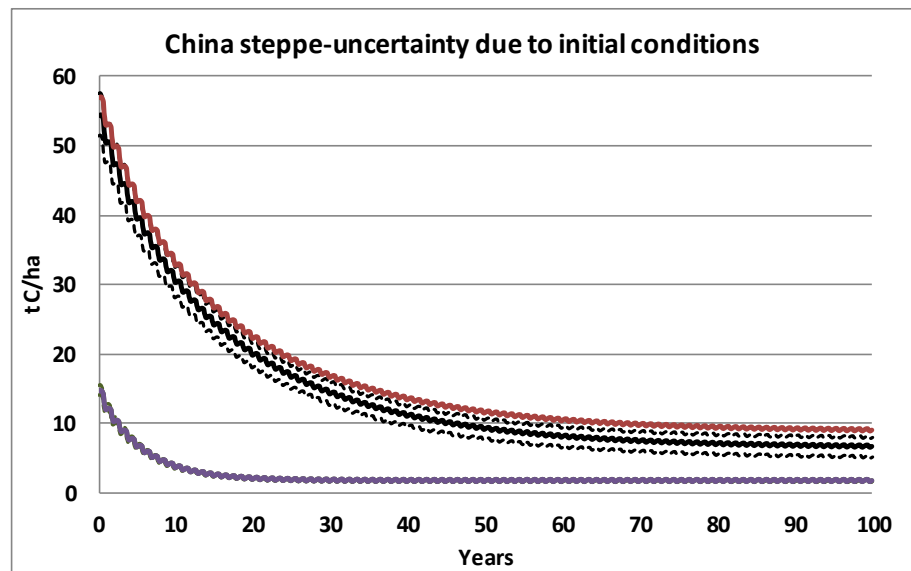
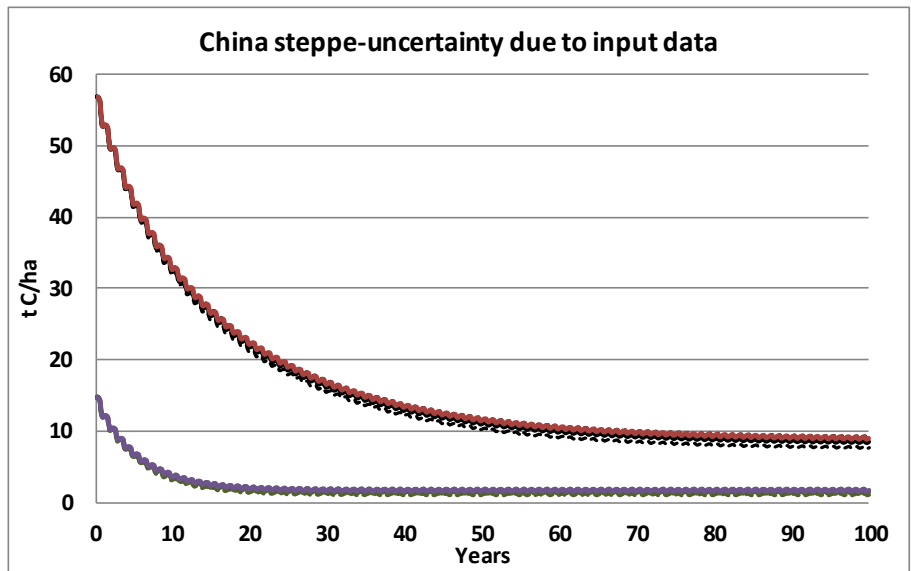
	Li et al (2009), Tibet-Desert								Frank et al (2006), North Dakota-Semiarid							
	SOC				POC				SOC				POC			
	-10%	+10%	-50%	+50%	-10%	+10%	-50%	+50%	-10%	+10%	-50%	+50%	-10%	+10%	-50%	+50%
<b>total plant input</b>	0.045	0.045	0.045	0.045	0.149	0.149	0.149	0.149	0.164	0.164	0.164	0.164	0.268	0.268	0.268	0.268
<b>DPM/RPM ratio</b>	0.016	0.014	0.021	0.012	0.085	0.075	0.114	0.062	0.063	0.055	0.084	0.045	0.163	0.145	0.219	0.118
<b>BIO%</b>	0.027	0.027	0.026	0.027	0.000	0.000	0.000	0.000	0.044	0.045	0.043	0.046	0.000	0.000	0.000	0.000
<b>DPM</b>	0.002	0.002	0.003	0.001	0.009	0.008	0.017	0.006	0.005	0.004	0.008	0.003	0.012	0.009	0.021	0.007
<b>RPM</b>	0.166	0.152	0.198	0.129	0.870	0.796	1.048	0.672	0.230	0.216	0.263	0.191	0.600	0.562	0.686	0.496
<b>BIO</b>	0.030	0.026	0.042	0.020	0.000	0.000	0.000	0.000	0.023	0.019	0.036	0.014	0.000	0.000	0.000	0.000
<b>HUM</b>	0.202	0.195	0.216	0.182	0.000	0.000	0.000	0.000	0.062	0.061	0.064	0.059	0.000	0.000	0.000	0.000
<b>RPM initial</b>									0.178	0.178	0.178	0.178	0.732	0.732	0.732	0.732
	Wu et al (2004), China-Steppe								Evrendilek et al (2004), Turkey-Steppe							
	SOC				POC				SOC				POC			
	-10%	+10%	-50%	+50%	-10%	+10%	-50%	+50%	-10%	+10%	-50%	+50%	-10%	+10%	-50%	+50%
<b>total plant input</b>	0.284	0.284	0.284	0.284	0.996	0.996	0.996	0.996	0.209	0.209	0.209	0.209	0.740	0.740	0.740	0.740
<b>DPM/RPM ratio</b>	0.071	0.063	0.096	0.051	0.546	0.484	0.736	0.394	0.055	0.049	0.074	0.040	0.397	0.353	0.533	0.288
<b>BIO%</b>	0.163	0.164	0.162	0.165	0.000	0.000	0.000	0.000	0.074	0.075	0.073	0.076	0.000	0.000	0.000	0.000
<b>DPM</b>	0.006	0.004	0.011	0.003	0.036	0.028	0.080	0.019	0.009	0.007	0.016	0.005	0.062	0.050	0.112	0.037
<b>RPM</b>	0.145	0.117	0.285	0.085	1.052	0.848	2.091	0.615	0.197	0.162	0.312	0.116	1.351	1.099	2.189	0.774
<b>BIO</b>	0.040	0.032	0.078	0.023	0.000	0.000	0.000	0.000	0.061	0.052	0.090	0.039	0.000	0.000	0.000	0.000
<b>HUM</b>	0.899	0.734	1.415	0.513	0.000	0.000	0.000	0.000	0.368	0.346	0.419	0.307	0.000	0.000	0.000	0.000
<b>RPM initial</b>									0.207	0.207	0.207	0.207	0.260	0.260	0.260	0.260
	Ashagrie et al (2007), Ethiopia-Steppe								Vagen et al (2006), Madagascar-Forest							
	SOC				POC				SOC				POC			
	-10%	+10%	-50%	+50%	-10%	+10%	-50%	+50%	-10%	+10%	-50%	+50%	-10%	+10%	-50%	+50%
<b>total plant input</b>	0.265	0.265	0.265	0.265	0.749	0.749	0.749	0.749	0.437	0.437	0.437	0.437	1.000	1.000	1.000	1.000
<b>DPM/RPM ratio</b>	0.066	0.059	0.087	0.048	0.427	0.380	0.566	0.312	0.049	0.044	0.065	0.036	0.539	0.480	0.717	0.393
<b>BIO%</b>	0.178	0.181	0.171	0.189	0.000	0.000	0.000	0.000	0.376	0.377	0.373	0.379	0.000	0.000	0.000	0.000
<b>DPM</b>	0.003	0.002	0.006	0.002	0.018	0.015	0.035	0.011	0.006	0.005	0.011	0.003	0.073	0.058	0.132	0.039
<b>RPM</b>	0.260	0.204	0.470	0.137	1.632	1.272	2.996	0.849	0.090	0.073	0.161	0.054	0.965	0.790	1.737	0.579
<b>BIO</b>	0.017	0.013	0.033	0.010	0.000	0.000	0.000	0.000	0.021	0.017	0.038	0.013	0.000	0.000	0.000	0.000
<b>HUM</b>	0.110	0.108	0.114	0.104	0.000	0.000	0.000	0.000	0.836	0.677	1.362	0.472	0.000	0.000	0.000	0.000
<b>RPM initial</b>									0.071	0.071	0.071	0.071	0.000	0.000	0.000	0.000



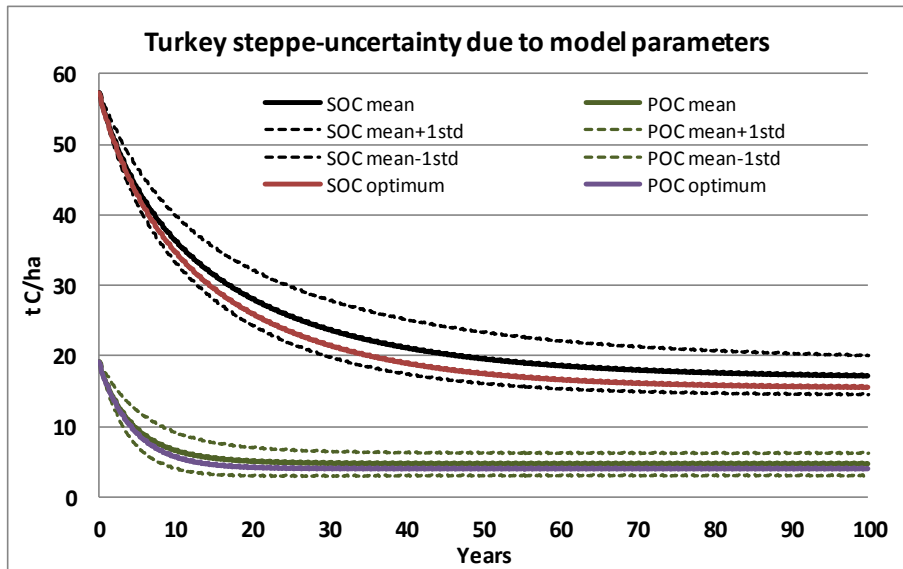
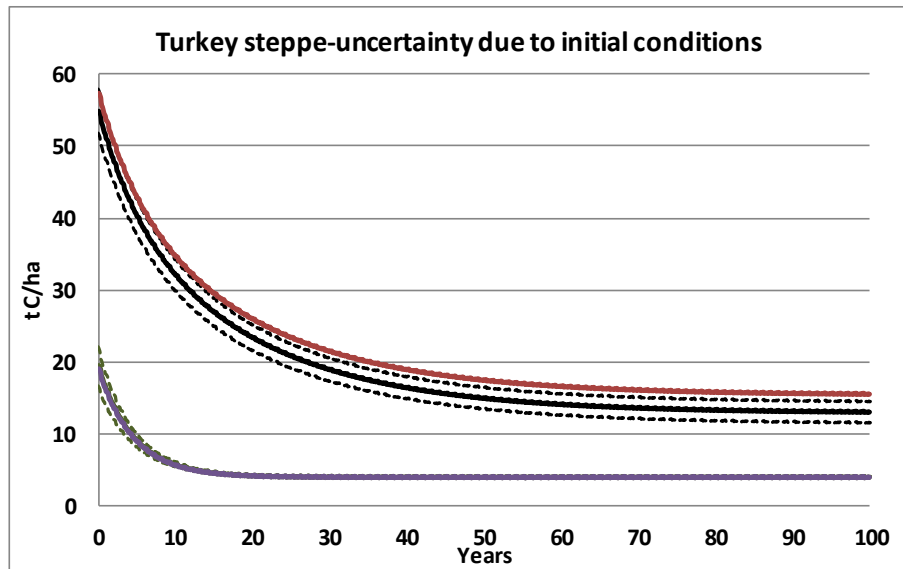
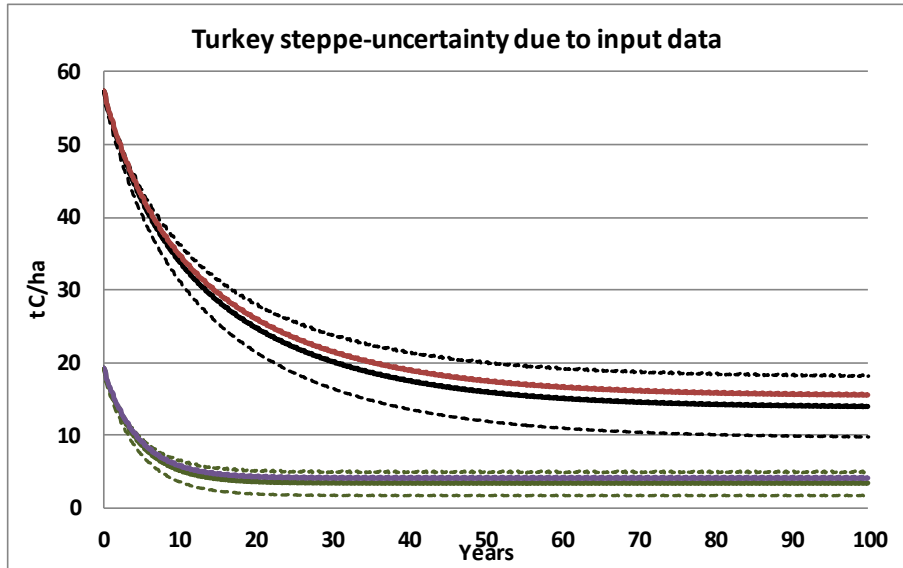
(a)



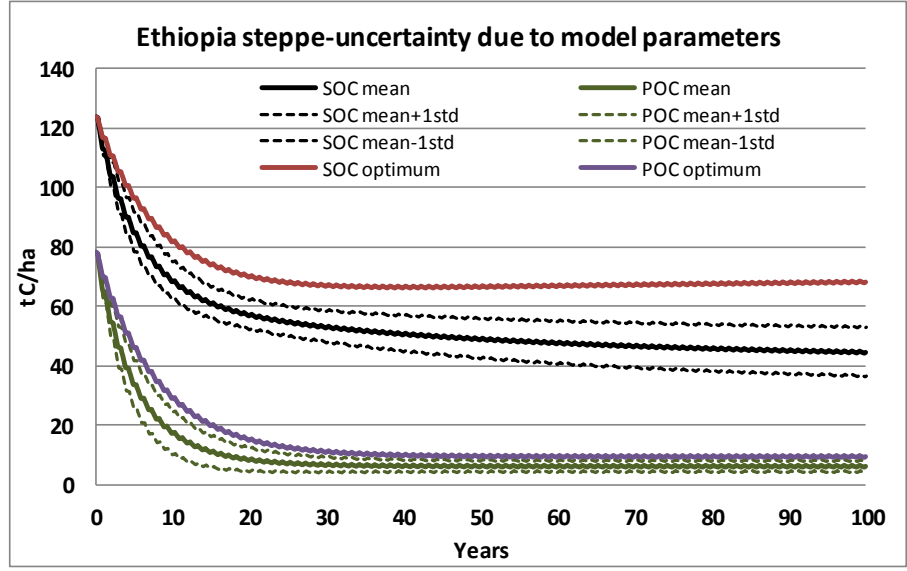
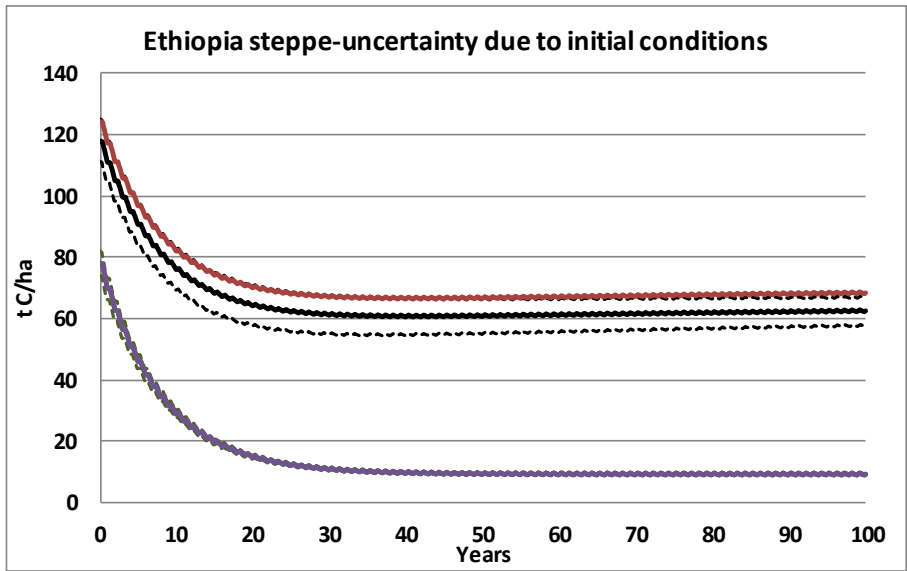
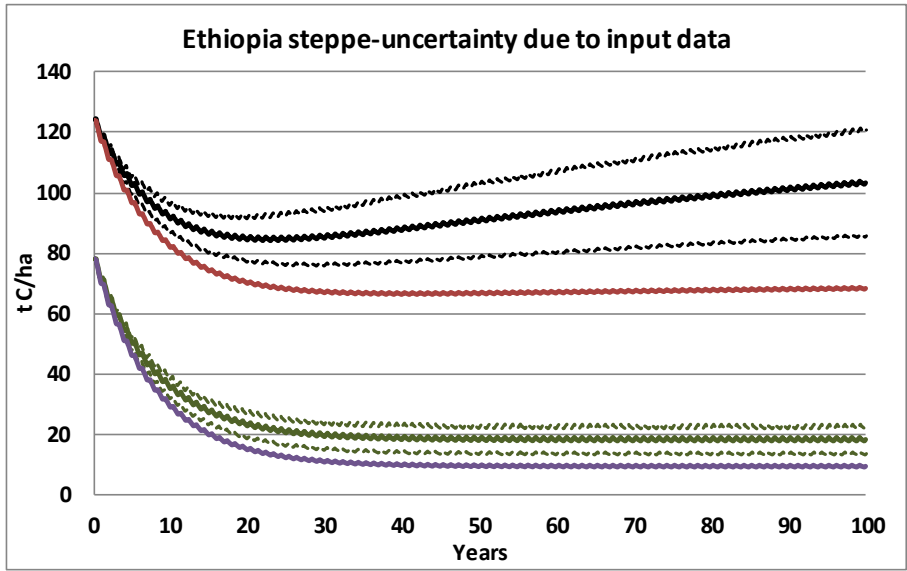
(b)



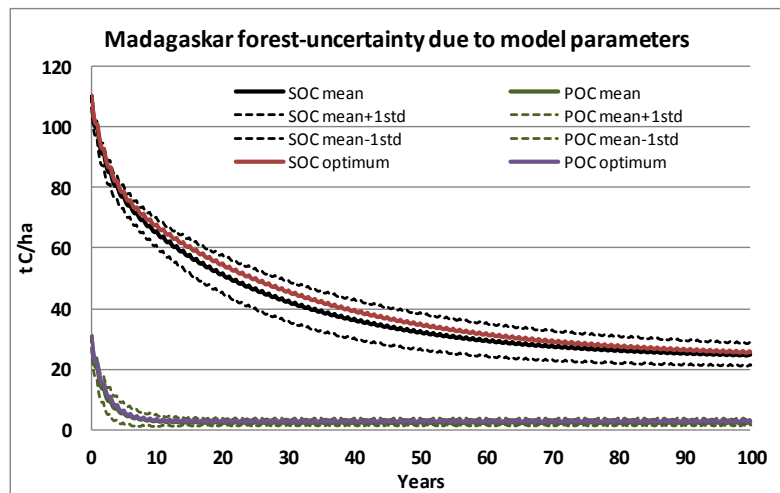
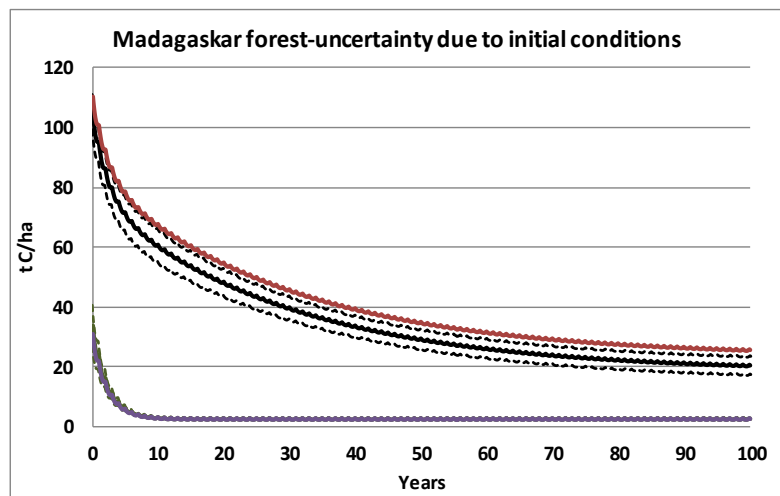
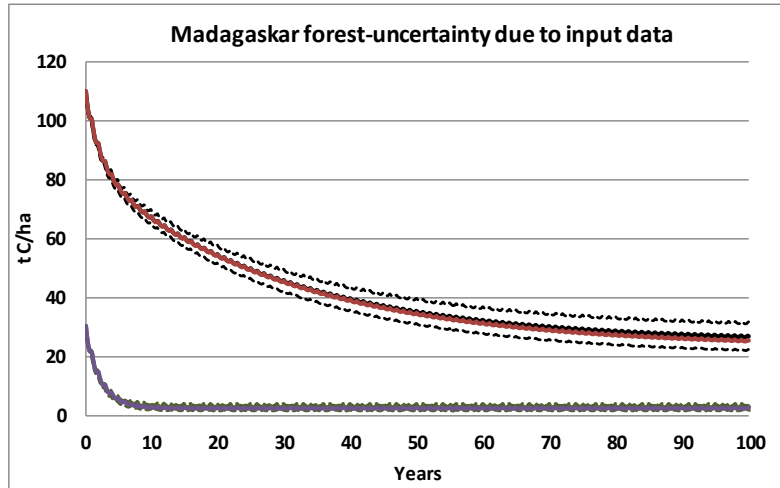
(c)



(d)



(e)



(f)

Figure A3.1 Uncertainty of total organic carbon (SOC) and particulate organic carbon (POC) due to model parameters, input data, and initial conditions compared with the optimum solution (calibration) for a) Tibet-Desert, b) Dakota-semi-arid, c) China-steppe, d) Turkey-steppe, e) Ethiopia-steppe, and f) Madagascar-forest.

**Table A5.1 The 15 soil properties used in the PCA analysis (the 12 first samples correspond to soil Group-1 and the latter 16 in soil Group-2).**

PC4	PC3	PC2	PC1	Soil ID	Land cover	Geologic formation	Altitude	<53µm	Al-ox	Fe-ox	Fe-ox/F-d	K-BaCl2	N-1hour	pH	<2 µm	>1000µm	WSA-250	BD	TKN	eCEC	BS_Na-BaCl2	PMN	
							m	%	%	%	-	cmol/kg	mgN/kg	-	%	%	%	g/cm <sup>3</sup>	%	cmol/kg	%	mgN/kg	
				1	41A	Scrub and herbaceous	Limestones (Plattenkalk)	166	72.5	0.34	0.33	0.87	0.30	3.5	7.49	17.6	1.4	46.6	1.27	0.15	3.89	0.76	66.8
				2	49A	Olive groves	Marls	135	63.1	0.09	0.10	0.95	0.10	4.8	8.13	20.6	14.2	50.0	1.13	0.16	5.74	0.33	49.2
				3	K3	Olive groves	Schists	550	32.2	0.11	0.17	0.22	0.03	3.4	6.47	7.1	31.1	25.0	1.23	0.12	2.74	0.86	63.1
				4	9A	Olive groves	Calcaric Marls	383	51.9	0.61	0.38	0.73	0.10	3.7	7.87	13.4	20.4	33.7	1.15	0.23	6.01	0.54	93.1
				5	37A	Scrub and herbaceous	Schists	371	36.7	0.28	0.25	0.24	0.07	2.3	6.01	13.5	31.5	24.9	1.14	0.08	0.92	1.67	20.3
				6	16A	Scrub and herbaceous	Calcaric Marls	219	40.8	0.21	0.23	0.26	0.21	3.5	5.99	13.3	32.0	34.8	1.19	0.10	2.25	0.71	41.2
				7	10B	Olive groves	Limestones (Trypalis)	351	46.4	0.20	0.20	0.20	0.21	7.5	7.33	22.7	19.3	49.8	0.96	0.14	2.90	0.50	70.8
				8	37E1	Olive groves	Schists	400	31.0	0.16	0.20	0.16	0.01	4.0	4.85	8.2	42.6	12.7	1.34	0.12	0.53	3.91	25.4
				9	37E2	Olive groves	Schists	400	59.9	0.18	0.25	0.21	0.16	9.5	5.72	17.0	18.9	13.9	1.20	0.30	0.83	3.71	52.8
				10	6A	Olive groves	Marls	409	48.5	0.13	0.38	0.48	0.13	6.6	6.35	8.7	12.0	54.8	1.14	0.17	1.54	2.36	76.6
				11	K4(3)	Olive groves	Limestones (Plattenkalk)	465	60.0	0.36	0.30	0.72	0.19	12.2	4.70	12.1	22.5	31.1	1.26	0.20	1.22	1.81	39.7
				12	25F	Olive groves	Schists	290	39.8	0.13	0.37	0.52	0.28	9.4	6.53	10.9	24.3	28.6	1.20	0.13	1.98	1.38	51.9
PC4	PC3	PC2	PC1																				
				1	4B	Scrub and herbaceous	Limestones (Trypalis)	582	83.4	1.26	0.30	0.29	0.19	10.6	7.72	21.0	1.0	90.5	0.97	0.49	9.71	0.27	108.3
				2	52A	Scrub and herbaceous	Limestones (Plattenkalk)	1098	51.0	1.25	0.60	0.92	0.17	17.1	6.95	12.0	6.9	66.3	0.92	0.42	7.70	0.23	99.9
				3	6B	Olive groves	Marls	383	51.6	0.36	0.31	0.55	0.16	9.7	7.86	12.9	25.1	44.2	1.08	0.31	7.03	0.18	143.0
				4	9B	Scrub and herbaceous	Calcaric Marls	383	43.1	0.53	0.43	0.69	0.11	7.4	7.68	9.5	27.9	47.6	1.09	0.34	8.68	0.50	120.0
				5	12A	Olive groves	Alluvial	42	74.1	0.39	0.30	0.86	0.98	5.6	8.10	30.7	4.0	56.3	1.20	0.25	10.23	0.26	57.6
				6	26B	Fruit trees-orange trees	Alluvial	9	59.0	0.34	0.34	1.06	0.84	8.8	8.05	20.8	14.7	62.0	1.18	0.31	10.48	0.37	126.1
				7	5A	Fruit trees-orange trees	Alluvial	17	59.9	0.22	0.35	0.59	0.36	8.9	7.94	25.2	8.6	59.9	1.14	0.23	7.12	0.34	96.1
				8	20B	Olive groves	Marls	56	79.9	0.06	0.10	0.49	0.60	4.0	7.82	35.2	5.0	61.3	1.06	0.25	8.87	0.35	37.1
				9	10F	Olive groves	Limestones (Trypalis)	375	76.9	0.27	0.31	0.74	0.59	8.2	7.59	28.7	1.4	69.7	1.19	0.36	8.20	0.28	83.9
				10	12F	Olive groves	Alluvial	42	68.4	0.55	0.49	0.86	1.05	11.4	7.64	32.0	8.1	56.7	1.15	0.29	10.75	0.21	72.5
				11	12A	Olive groves	Alluvial	46	72.6	0.61	0.60	0.75	0.88	11.9	7.49	38.3	5.3	76.1	1.16	0.25	9.81	0.22	83.8
				12	5B	Fruit trees-orange trees	Alluvial	9	54.7	0.22	0.35	0.90	0.81	12.6	7.07	15.8	2.9	67.2	1.11	0.27	7.65	0.31	104.0
				13	K4(1+2)	Olive groves	Limestones (Plattenkalk)	465	66.7	0.44	0.41	0.87	0.55	15.8	4.72	26.8	16.1	65.7	1.21	0.14	5.97	0.37	92.6
				14	12B	Olive groves	Alluvial	43	72.8	0.67	0.40	0.48	0.36	7.0	6.91	38.4	4.1	57.0	1.20	0.18	6.13	0.64	49.7
				15	4A	Scrub and herbaceous	Limestones (Trypalis)	308	73.5	0.83	0.51	0.71	0.91	8.9	7.67	32.1	3.1	77.7	1.10	0.29	8.81	0.20	80.1
				16	51A	Scrub and herbaceous	Limestones (Trypalis)	748	82.9	1.06	0.54	0.52	0.68	14.8	7.65	32.2	1.8	72.7	1.08	0.34	10.58	0.22	82.7

**Table A5.2 Mean monthly meteorological data used for the calibration (long average 1960-2010) and the climate change scenarios for the station of Samonas.**

Month	Samonas (1960-2010)			Samonas (1990-2010)					
	Temp	Rain	PET	Temp	Rain	PET			
	(°C)	(mm)	(mm)	(°C)	(mm)	(mm)			
1	10.2	224	44	10.4	203	45			
2	10.2	155	47	10.3	134	47			
3	11.9	132	70	12.3	100	71			
4	14.9	51	97	15.2	48	98			
5	19.0	19	147	19.5	17	151			
6	23.5	8	197	24.1	4	203			
7	25.6	1	223	26.3	1	232			
8	25.4	1	197	26.2	2	206			
9	22.6	24	138	23.1	23	142			
10	19.0	110	96	19.7	75	100			
11	15.2	135	62	15.4	136	63			
12	11.9	196	47	11.9	199	47			
<b>Annual</b>	17.4	1056	1363	17.9	942	1406			
Month	BCA-RCA (2010-2030)			ECHAM-RACMO (2010-2030)			ECHAM REMO (2010-2030)		
	Temp	Rain	PET	Temp	Rain	PET	Temp	Rain	PET
	(°C)	(mm)	(mm)	(°C)	(mm)	(mm)	(°C)	(mm)	(mm)
1	10.6	179	46	10.5	197	45	10.6	220	45
2	10.6	148	48	10.4	141	47	10.0	143	46
3	12.6	112	73	12.0	103	70	11.7	115	69
4	15.5	30	100	15.5	49	100	15.2	51	98
5	19.9	17	154	19.6	18	152	19.3	14	149
6	24.8	6	213	24.5	4	209	24.4	4	207
7	26.6	10	236	26.4	1	233	26.5	1	234
8	27.4	39	221	26.3	2	207	26.5	3	209
9	23.4	1	145	24.2	25	152	24.2	21	151
10	20.2	81	103	19.9	123	101	20.1	105	103
11	15.4	133	62	15.3	156	62	15.3	150	62
12	12.2	188	48	12.4	210	48	12.2	202	48
<b>Annual</b>	18.3	943	1448	18.1	1029	1427	18.0	1030	1421
Month	BCA-RCA (2030-2050)			ECHAM-RACMO (2030-2050)			ECHAM REMO (2030-2050)		
	Temp	Rain	PET	Temp	Rain	PET	Temp	Rain	PET
	(°C)	(mm)	(mm)	(°C)	(mm)	(mm)	(°C)	(mm)	(mm)
1	10.9	188	46	12.1	169	50	12.1	204	50
2	10.5	133	48	11.9	115	52	11.6	111	51
3	13.0	82	74	14.0	97	79	13.4	99	76
4	16.3	38	105	16.6	39	107	16.2	34	105
5	21.7	14	171	21.2	8	167	21.2	12	166
6	26.5	8	235	25.9	4	225	25.7	4	224
7	28.3	-45	262	28.0	0	255	28.1	1	256
8	28.6	-1	236	28.0	2	227	27.8	2	225
9	24.0	-11	150	24.6	24	155	24.5	22	153
10	21.5	52	111	21.9	33	114	21.8	77	113
11	16.1	129	65	17.2	125	69	17.1	146	69
12	13.3	192	51	13.4	181	52	13.5	171	52
<b>Annual</b>	19.2	778	1554	19.6	797	1551	19.4	881	1541

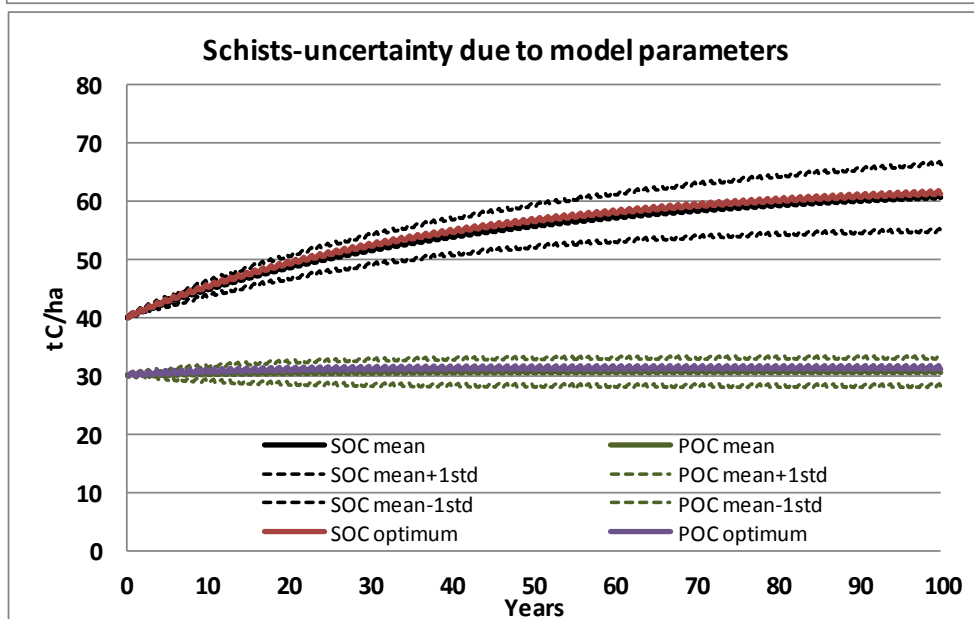
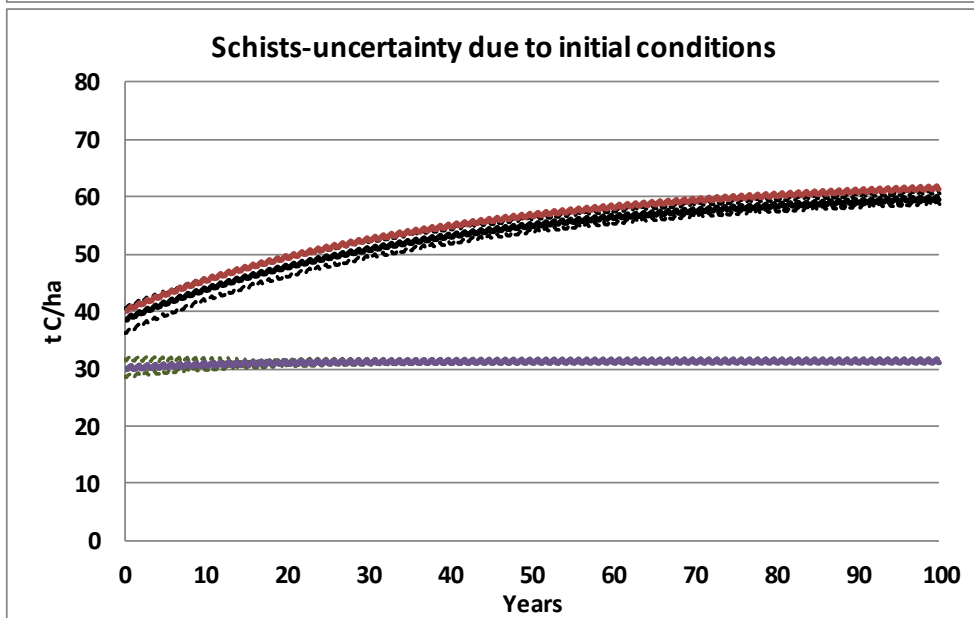
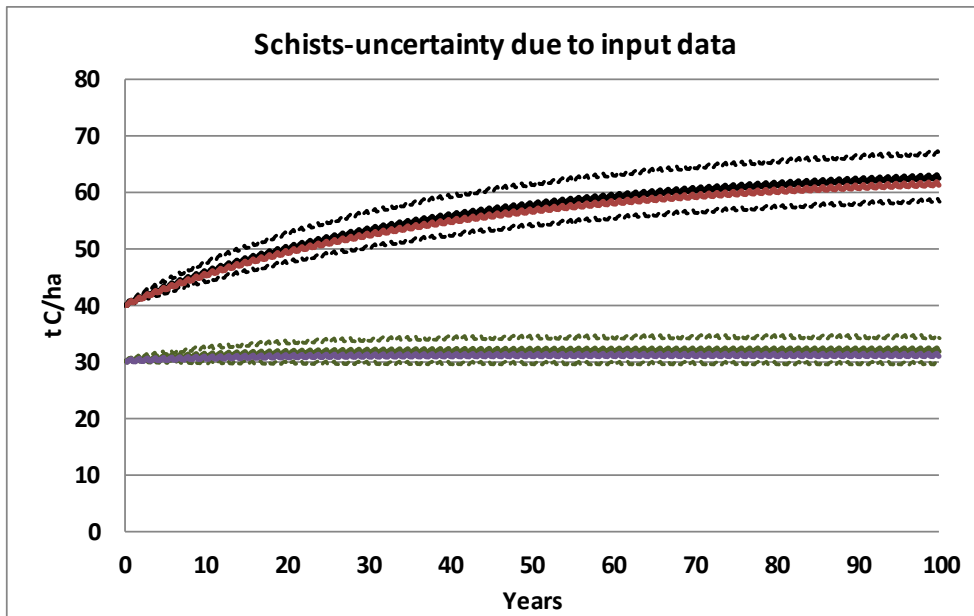
**Table A5.3 Monthly and annual decomposition rates<sup>a</sup> (1/y) for resistant plant material (RPM) and humus (HUM) soil organic pools of ROTHC model for the Greek and Iowa sites.**

	Schists		Marls		Trypalis	
	RPM	HUM	RPM	HUM	RPM	HUM
<b>1</b>	0.078	0.029	0.082	0.034	0.086	0.024
<b>2</b>	0.078	0.029	0.082	0.034	0.086	0.024
<b>3</b>	0.096	0.036	0.101	0.041	0.105	0.029
<b>4</b>	0.060	0.022	0.063	0.026	0.066	0.018
<b>5</b>	0.036	0.014	0.038	0.016	0.040	0.011
<b>6</b>	0.048	0.018	0.051	0.021	0.053	0.015
<b>7</b>	0.054	0.020	0.057	0.023	0.059	0.017
<b>8</b>	0.053	0.020	0.056	0.023	0.059	0.016
<b>9</b>	0.046	0.017	0.048	0.020	0.050	0.014
<b>10</b>	0.100	0.037	0.105	0.043	0.110	0.031
<b>11</b>	0.133	0.050	0.140	0.058	0.146	0.041
<b>12</b>	0.095	0.036	0.100	0.041	0.105	0.029
<b>annual</b>	0.073	0.027	0.077	0.032	0.080	0.022

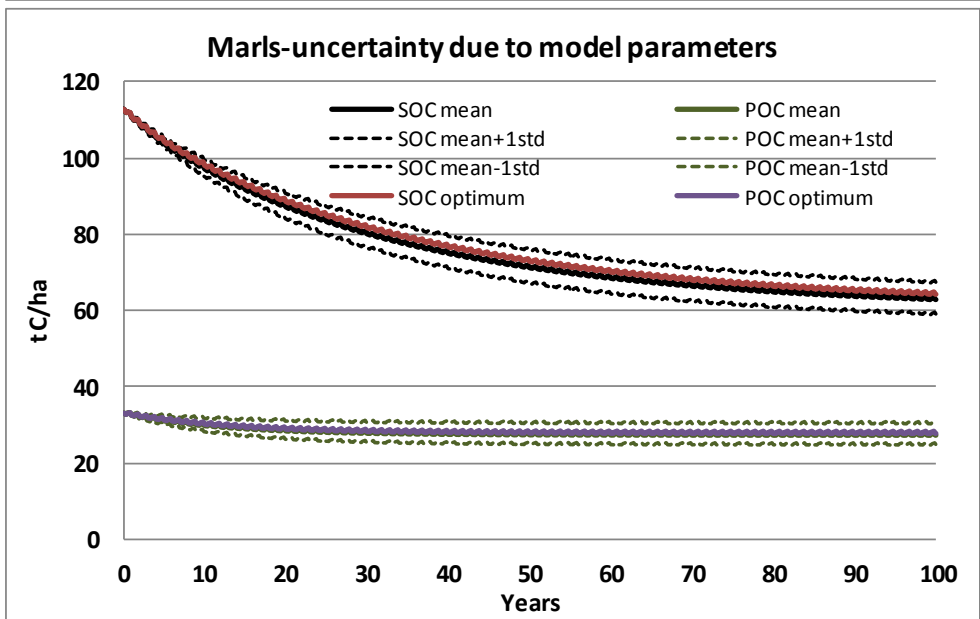
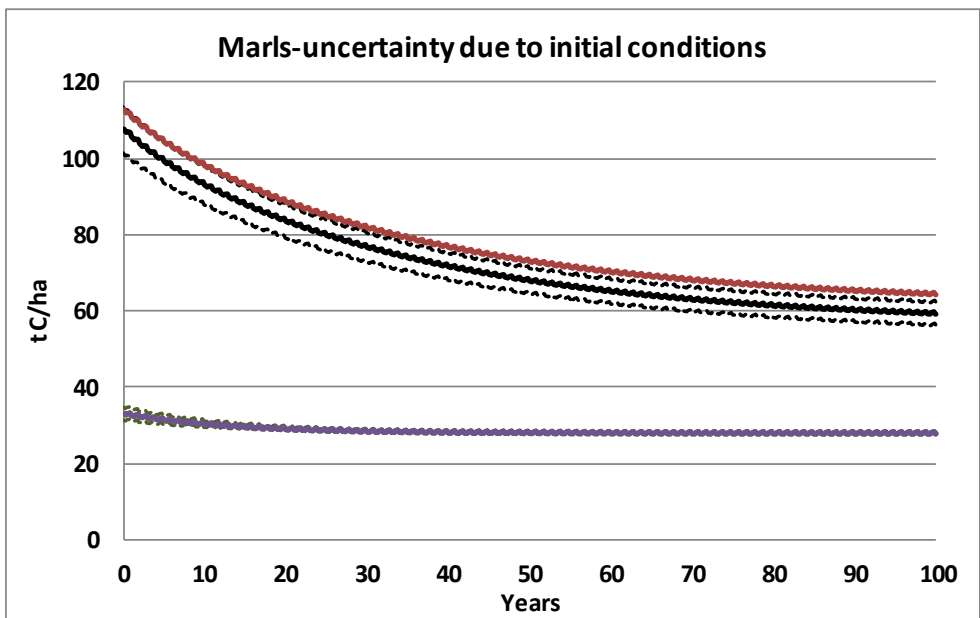
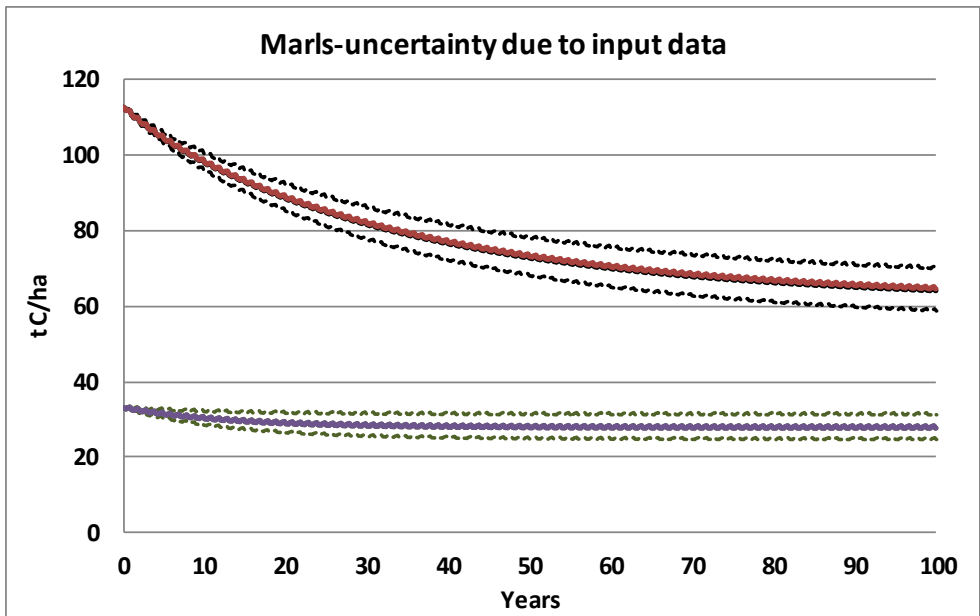
<sup>a</sup>Decomposition rates constant multiplied by the rate modifying factor for temperature (a), the topsoil moisture deficit rate modifying factor (b), and the soil cover factor (c).

Table A5.4 Sensitivity coefficients (the absolute value of the ratio:  $(\Delta Y/Y)/(\Delta x/x)$ ) for ROTHC model parameters for  $\pm 10\%$  and  $\pm 50\%$  change of the calibrated values for the three shrubland to cropland conversions (for the 50 year of the conversion used for the calibration in all sites) for both soil organic carbon (SOC) and particulate organic carbon (POC).

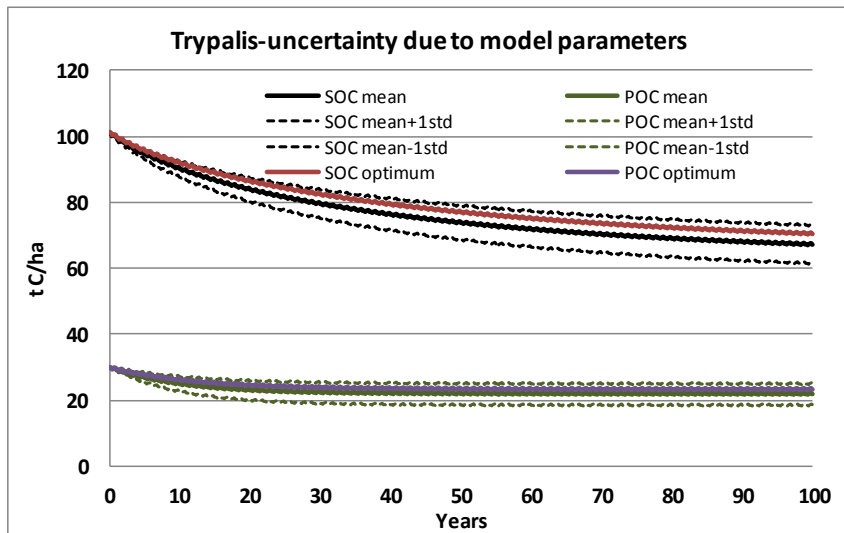
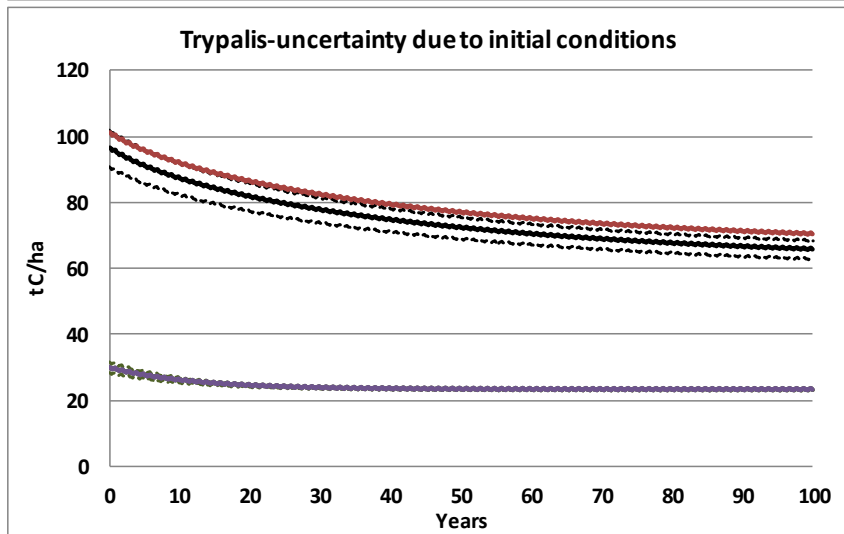
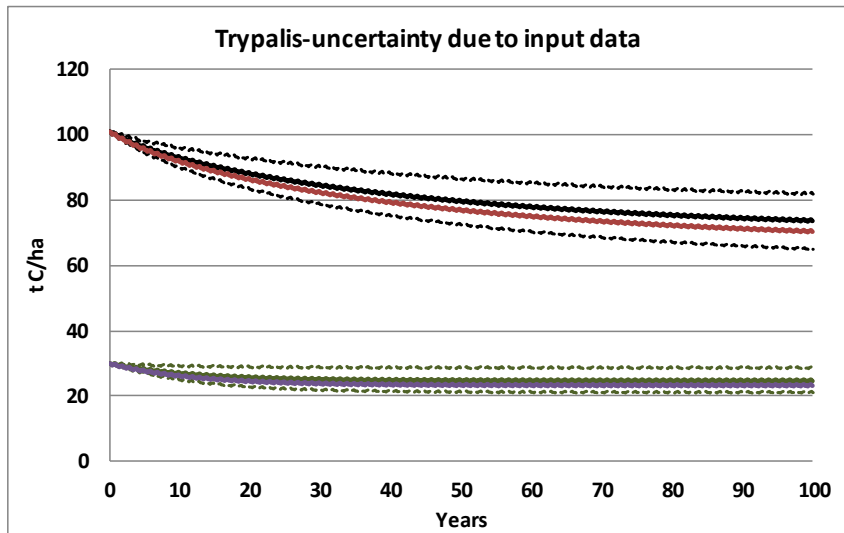
	Schists							
	SOC				POC			
	(-10%)	(+10%)	(-50%)	(+50%)	(-10%)	(+10%)	(-50%)	(+50%)
total plant input	0.871	0.871	0.871	0.871	0.976	0.976	0.976	0.976
DPM/RPM ratio	0.300	0.267	0.396	0.220	0.576	0.514	0.761	0.422
BIO%	0.231	0.234	0.227	0.239	0.000	0.000	0.000	0.000
DPM	0.008	0.006	0.015	0.004	0.014	0.011	0.027	0.007
RPM	0.545	0.457	0.847	0.341	1.049	0.876	1.644	0.652
BIO	0.028	0.023	0.050	0.017	0.000	0.000	0.000	0.000
HUM	0.202	0.187	0.240	0.161	0.000	0.000	0.000	0.000
	Marls							
	SOC				POC			
	(-10%)	(+10%)	(-50%)	(+50%)	(-10%)	(+10%)	(-50%)	(+50%)
total plant input	0.597	0.597	0.597	0.597	0.975	0.975	0.975	0.975
DPM/RPM ratio	0.214	0.190	0.285	0.156	0.586	0.521	0.780	0.427
BIO%	0.196	0.198	0.193	0.202	0.000	0.000	0.000	0.000
DPM	0.006	0.005	0.012	0.003	0.016	0.012	0.031	0.008
RPM	0.392	0.326	0.621	0.242	1.071	0.889	1.714	0.657
BIO	0.022	0.018	0.039	0.013	0.000	0.000	0.000	0.000
HUM	0.462	0.409	0.602	0.327	0.000	0.000	0.000	0.000
RPM initial								
	Trypalis							
	SOC				POC			
	(-10%)	(+10%)	(-50%)	(+50%)	(-10%)	(+10%)	(-50%)	(+50%)
total plant input	0.563	0.563	0.563	0.563	0.981	0.981	0.981	0.981
DPM/RPM ratio	0.170	0.150	0.227	0.123	0.600	0.532	0.803	0.434
BIO%	0.229	0.232	0.223	0.238	0.000	0.000	0.000	0.000
DPM	0.005	0.004	0.010	0.003	0.019	0.015	0.036	0.010
RPM	0.306	0.253	0.496	0.187	1.079	0.890	1.767	0.655
BIO	0.021	0.017	0.038	0.013	0.000	0.000	0.000	0.000
HUM	0.415	0.380	0.500	0.321	0.000	0.000	0.000	0.000



(a)



(b)



(c)

Figure A5.1 Uncertainty of total organic carbon (SOC) and particulate organic carbon (POC) due to model parameters, input data, and initial conditions compared with the optimum solution (calibration) for the shrubland to cropland conversions of a) Schists, b) Marls, and c) Trypalis geologic substrate.

**Table A5.5 Concentrations of dissolved inorganic nitrogen (DIN) and DON/TDN ratio, as well as precipitation for the rivers presented in Figure 5.10 in Chapter 5.**

No ID	Watershed type/Site name	DIN, mg/L	DON/TDN ratio	Prec, mm	Reference
<b>Forested watersheds</b>					
1	Shenandoah National Park (SNP), Virginia	0.379	0.15	133	Buffam et al., 2001
2	streams in the Blue Ridge Mountains, SNP, Virginia	0.232	0.12	133	Buffam et al., 2001
3	Peabody tributary, USA	0.021	0.82	183	Goodale et al. (2000)
4	Encampment river, USA	0.095	0.80	400	Lewis (2002)
5	Red Butte creek, USA	0.101	0.78	400	Lewis (2002)
6	Upper Kugaruk, USA	0.005	0.91	400	Peterson et al. (1992)
7	Vallecito creek, USA	0.091	0.82	400	Lewis (2002)
8	Wet Bottom creek, USA	0.085	0.67	500	Lewis (2002)
9	Finland	0.287	0.64	590	Mattsson et al., 2009
10	Castle Creek, USA	0.049	0.83	600	Lewis (2002)
11	Kiamichi River, USA	0.070	0.82	630	Lewis (2002)
12	LB4, New England	0.222	0.44	1040	Campbell et al. (2000)
13	LB6, New England	0.409	0.38	1040	Campbell et al. (2000)
14	LB8, New England	0.163	0.70	1040	Campbell et al. (2000)
15	Popple Creek, USA	0.090	0.84	1050	Lewis (2002)
16	France	0.480	0.20	1100	Mattsson et al., 2009
17	South Pennines, UK	0.369	0.56	1107	Helliwell et al., 2007
18	Cache Creek, USA	0.116	0.66	1200	Lewis (2002)
19	Elder creek, USA	0.052	0.73	1200	Lewis (2002)
20	Young Womans creek, USA	0.083	0.66	1200	Lewis (2002)
21	Husted creek, USA	0.046	0.46	1250	Cairns and Lajtha (2005)
22	Little Pool creek, USA	0.016	0.61	1250	Cairns and Lajtha (2005)
23	Vinemaple creek, USA	0.009	0.77	1250	Cairns and Lajtha (2005)
24	Soda creek, USA	0.212	0.18	1270	Cairns and Lajtha (2005)
25	Whiteroek creek, USA	0.114	0.21	1280	Cairns and Lajtha (2005)
26	Wolf creek, USA	0.308	0.18	1280	Cairns and Lajtha (2005)
27	Scape Ore Swamp, USA	0.071	0.82	1300	Lewis (2002)
28	Filtering Sun brook, USA	0.207	0.12	1320	Cairns and Lajtha (2005)
29	Hensley creek, USA	0.021	0.57	1320	Cairns and Lajtha (2005)
30	Barringer creek, USA	0.254	0.13	1330	Cairns and Lajtha (2005)
31	Falling creek, USA	0.123	0.64	1400	Lewis (2002)
32	Falcon Nile creek, USA	0.019	0.44	1450	Cairns and Lajtha (2005)
33	New creek, USA	0.005	0.83	1460	Cairns and Lajtha (2005)
34	Gibbs brook-D, USA	0.039	0.64	1470	Goodale et al. (2000)
35	Lafayette brook-A, USA	0.062	0.62	1470	Goodale et al. (2000)
36	Trout creek, USA	0.014	0.60	1470	Cairns and Lajtha (2005)
37	Lafayette brook-B, USA	0.051	0.61	1480	Goodale et al. (2000)
38	Taylor creek, USA	0.012	0.64	1480	Cairns and Lajtha (2005)
39	Longbow creek, USA	0.044	0.30	1490	Cairns and Lajtha (2005)
40	Slide creek, USA	0.078	0.30	1490	Cairns and Lajtha (2005)
41	CP, New England	0.029	0.80	1495	Campbell et al. (2000)
42	Minam River, USA	0.051	0.79	1500	Lewis (2002)
43	Sipsey Fork, USA	0.055	0.59	1500	Lewis (2002)
44	SR, New England	0.243	0.24	1515	Campbell et al. (2000)
45	Zealand valley-A, USA	0.025	0.68	1520	Goodale et al. (2000)
46	Hidden stream, USA	0.010	0.70	1600	Cairns and Lajtha (2005)
47	Upper Twin creek, USA	0.139	0.60	1600	Lewis (2002)
48	HB6, New England	0.049	0.68	1710	Campbell et al. (2000)
49	Mournes, UK	0.310	0.37	1714	Helliwell et al., 2007
50	Little Boulder creek, USA	0.083	0.21	1730	Cairns and Lajtha (2005)
51	West Fork Three creek, USA	0.053	0.36	1730	Cairns and Lajtha (2005)

52	HB8, New England	0.085	0.60	1735	Campbell et al. (2000)
53	Little Wildcat brook-A, USA	0.014	0.82	1740	Goodale et al. (2000)
54	HB7, New England	0.078	0.54	1745	Campbell et al. (2000)
55	Rocky branch-C, USA	0.014	0.83	1750	Goodale et al. (2000)
56	HB9, New England	0.045	0.80	1755	Campbell et al. (2000)
57	Hale brook, USA	0.023	0.55	1760	Goodale et al. (2000)
58	Elephant head, USA	0.012	0.88	1800	Goodale et al. (2000)
59	Gibbs brook-A, USA	0.016	0.79	1830	Goodale et al. (2000)
60	Slide brook, USA	0.018	0.75	1870	Goodale et al. (2000)
61	Snowdonia, UK	0.127	0.56	1902	Helliwell et al., 2007
62	Amazon, Perú-Brazil-Colombia-Venezuela	0.166	0.49	2000	Lewis et al. (1999)
63	Caroní, Venezuela	0.046	0.75	2000	Lewis et al. (1999)
64	Andrews creek, USA	0.043	0.91	2000	Lewis (2002)
65	WS8 (H.J. Andrews Exp. Forest), USA	0.091	0.61	2083	Vanderbilt et al. (2002)
66	Galloway, UK	0.099	0.71	2127	Helliwell et al., 2007
67	Caura, Venezuela	0.048	0.78	2200	Lewis et al. (1999)
68	Negro, Brazil	0.042	0.79	2200	Lewis et al. (1999)
69	Solimoes, Brazil	0.200	0.36	2400	Lewis et al. (1999)
70	Toronja, Puerto Rico	0.055	0.71	2400	Lewis et al. (1999)
71	WS2 (H.J. Andrews Exp. Forest), USA	0.009	0.71	2477	Vanderbilt et al. (2002)
72	WS9 (H.J. Andrews Exp. Forest), USA	0.007	0.78	2477	Vanderbilt et al. (2002)
73	Madeira, Brazil	0.176	0.50	2500	Lewis et al. (1999)
74	Japurá, Colombia	0.102	0.47	2800	Lewis et al. (1999)
75	Juruá, Brazil	0.202	0.40	2800	Lewis et al. (1999)
76	Icacos, Brazil	0.093	0.58	3940	Lewis et al. (1999)
77	Sonadora, Puerto Rico	0.063	0.69	4100	Lewis et al. (1999)
<b>Mixed landuse watersheds</b>					
78	Wales	0.224	0.61	960	Mattsson et al., 2009
79	Sopchoppy, USA	0.078	0.84	1300	Fu and Winchester (1994)
80	Sawmill brook, USA	0.252	0.41	1360	Wollheim et al. (2005)
81	Orinoco, Venezuela-Brazil	0.112	0.59	1400	Lewis et al. (1999)
82	Quebrada El Jobo, Costa Rica	0.303	0.32	2400	Newbold et al. (1995)
83	Quebrada Marilyn, Costa Rica	0.257	0.32	2400	Newbold et al. (1995)
84	Quebrada Zompopa, Costa Rica	0.218	0.36	2400	Newbold et al. (1995)
85	Tempisquito, Costa Rica	0.209	0.33	2400	Newbold et al. (1995)
86	Tempisquito Sur, Costa Rica	0.006	0.89	2400	Newbold et al. (1995)
87	Braço do Mota, Brazil	0.037	0.79	2754	Williams and Melack (1997a)
88	Carter creek, USA	0.011	0.95	1339	Wollheim et al. (2005)
89	Great Lakes, USA Agri-7	0.690	0.47	790	Neilsen et al. (1980)
90	Great Lakes, USA Agri-11	3.750	0.20	790	Neilsen et al. (1980)
91	Great Lakes, USA Agri-10	2.650	0.41	790	Neilsen et al. (1980)
92	Great Lakes, USA Agri-5	4.570	0.21	860	Neilsen et al. (1980)
93	Great Lakes, USA Agri-14	0.990	0.39	890	Neilsen et al. (1980)
94	Great Lakes, USA Agri-4	4.030	0.23	910	Neilsen et al. (1980)
95	Great Lakes, USA Agri-3	5.640	0.13	940	Neilsen et al. (1980)
96	Great Lakes, USA Agri-6	2.110	0.22	990	Neilsen et al. (1980)
97	Great Lakes, USA Agri-1	6.050	0.24	760	Neilsen et al. (1980)
98	Great Lakes, USA Agri-13	4.900	0.26	760	Neilsen et al. (1980)
99	Great Lakes, USA Agri-2	1.090	0.36	890	Neilsen et al. (1980)
100	Denmark	4.138	0.21	810	Mattsson et al., 2009
101	Blackstone, USA	1.928	0.22	1190	Nixon et al. (1995)
102	Moshassuck, USA	1.302	0.27	1190	Nixon et al. (1995)
103	Pawtuxet, USA	1.981	0.22	1190	Nixon et al. (1995)
104	Taunton, USA	1.408	0.24	1190	Nixon et al. (1995)

<b>105</b>	Woonasquatucket, USA	1.101	0.28	1200	Nixon et al. (1995)
<b>Mixed landuse watersheds, Mediterranean</b>					
<b>106</b>	South-east Spain	1.233	0.91	418	Lorit-Herrera et al., 2009
<b>107</b>	Aksios	2.578	0.39	600	Nikolaidis et al., 2009
<b>108</b>	Achelous	1.124	0.60	1091	Nikolaidis et al., 2004
<b>109</b>	Anapodaris	3.693	0.34	-	Skoulikidis kai Gritzalis, 2006
<b>110</b>	Kelefina-Oinountas (Basaras-Klada subbasin)	0.685	0.87	800	Nikolaidis et al., 2006
<b>111</b>	Magoulitsa (Tripi, before subbasin Evrotas)	1.152	0.78	800	Nikolaidis et al., 2006
<b>112</b>	Brontamas (Evrotas main River)	1.873	0.72	1000	Nikolaidis et al., 2006
<b>113</b>	Koiliaris, South Greece, Crete	0.78	0.83	1100	Moraetis et al., 2010
<b>114</b>	Subbasin (Keramianos stream) with surface runoff	5.956	0.42	1100	Moraetis et al., 2010
<b>Karstic springs, Mediterranean</b>					
<b>115</b>	Skortsinos springs (Evrotas)	1.196	0.86	800	Nikolaidis et al., 2006
<b>116</b>	Vivari springs (Evrotas)	1.201	0.79	800	Nikolaidis et al., 2006
<b>117</b>	Vordonia (Evrotas after springs)	1.28	0.81	800	Nikolaidis et al., 2006
<b>118</b>	Stilos springs (Koiliaris River)	0.66	0.84	1100	Moraetis et al., 2010
<b>Undisturbed watershed, Mediterranean</b>					
<b>119</b>	Krathis, North Peloponnesse	0.073	0.56	950	Tzoraki et al., 2007

### Literature cited in Table A5.5

- Alvarez-Cobelas, M., D. G. Angeler, and S. Sánchez-Carrillo. 2008. Export of nitrogen from catchments: a world-wide analysis. *Environ. Pollut.* 156:161–169.
- Buffam, I., Galloway, J.N., Blum, L.K., McGlathery, K.J., 2001. A stormflow/baseflow comparison of dissolved organic matter concentrations and bioavailability in an Appalachian stream. *Biogeochemistry* 53, 269–306.
- Campbell, J.L., Hornbeck, J.W., McDowell, W.H., Buso, D.C., Shanley, J.B., 2000. Likens G.E.. Dissolved organic nitrogen budgets for upland forested ecosystems in New England. *Biogeochemistry* 49, 123–142.
- Helliwell, R.C., Coul, M.C., Davies, J.J.L., Evans, C.D., Norris, D., Ferrier, R.C., Jenkins, A., Beynolds, B., 2007. The role of catchment characteristics in determining surface water nitrogen in four upland in the UK. *Hydrol. Earth Syst. Sci.* 11, 356–371.
- Lorite-Herrera, M., Hiscock K., Jiménez-Espinosa, R., 2009. Distribution of Dissolved Inorganic and Organic Nitrogen in River Water and Groundwater in an Agriculturally-Dominated Catchment, South-East Spain. *Water Air Soil Pollut.* 198, 335–346.
- Mattsson, T., Kortelainen, P., Laubel, A., Evans, D., Pujo-Pay, M., Räike, A., Conan, P., 2009. Export of dissolved organic matter in relation to landuse along a European climatic gradient. *Sci. Total Environ.* 407, 1967–1976.
- Moraetis, D., Efstathiou, D., Stamati, F.E., Tzoraki, O., Nikolaidis, N.P., Schnoor, J.P., Vozinakis, K. High frequency monitoring for the identification of hydrological and bio-geochemical processes in a Mediterranean river basin. *J. Hydrol.* 389, 127–136.
- Neilsen, J.G.H., Culley, J.L., Cameron D.R., 1980. Nonpoint Runoff from agricultural watersheds into the Great Lakes. *J. Great Lakes Res.* 6, 195–202.

- Nikolaidis, N., Skoulikidis, N., Karageogis, A., 2004. Pilot implementation of EU policies in Acheloos River basin and coastal zone, Greece. Proceedings of International Symposium on Water Resources Management: Risks and Challenges for the 21st Century, Izmir Turkey, 2 to 4 September.
- Nikolaidis, N., Skoulikidis, N., Tsakiris, K., Kalogerakis, N., 2006. Preliminary management plans of Evrotas River watershed and coastal zone. Technical report 242pp +Index 79pp. In: Nikolaidis N., N. Kalogerakis, N. Skoulikidis, K. Tsakiris, (Eds), 2005-2009. Environmental friendly technologies for rural development. Life-Environment project, LIFE05ENV/Gr/000245 EE (Envi-Friendly).
- Nikolaidis, N., Karageogis, A., Kapsimalis, V., Drakopoulou, P., Skoulikidis, N., Behrendt, H., Levkov, Z., 2009. Management of nutrient emissions of Axios River catchment: Their effect in the coastal zone of Thermaikos Gulf, Greece. *Ecol. Model.* 220, 383-396.
- Peterson, B.J., Corliss, T., Kriet, K., Hobbie, J.E., 1992. Nitrogen and phosphorus concentrations and export for the upper Kuparuk River on the North Slope of Alaska in 1980. *Hydrobiologia* 240, 61-69.
- Soulaidis, N., and Gritzalis, K., 2006. Pilot study of the application of the Directive 2000/60 to a temporary River- Estimation of the ecological condition of Anapodaris temporary stream with biological and hydrochemical criteria. Final Report. HCMR pp145
- Tzoraki, O., Nikolaidis, N., Amaxidis, Y., Skoulikidis, N., 2007. In stream biogeochemical processes of a temporary river. *Environ. Sci. Technol.* 41, 1225-1231.

References of data taken and from: Alvarez-Cobelas et al., (2008)

- Cairns, M.A., Lajtha, K., 2005. Effects of succession on nitrogen export in the West-Central Cascades, Oregon. *Ecosystems* 8, 583-601.
- Fu, J.M., Winchester, W., 1994. Sources of nitrogen in three watersheds of northern Florida, USA: mainly atmospheric deposition. *Geochim. Cosmochim. Ac.* 58, 1581-1590.
- Goodale, C.L., Aber, J.D., McDowell, W.H., 2000. The long-term effects of disturbance on organic and inorganic nitrogen export in the White Mountains, New Hampshire. *Ecosystems* 3, 433-450.
- Lewis Jr., W.M., 2002. Yield of nitrogen from minimally disturbed watersheds of the United States. *Biogeochemistry* 57/58, 375-385.
- Lewis Jr., W.M., Melack, J.M., McDowell, W.H., McClain, M., Richey, J.E., 1998. Nitrogen yields from undisturbed watersheds in the Americas. *Biogeochemistry* 46, 149-162.
- Newbold, J.D., Sweeney, B.W., Jackson, J.K., Kaplan, L.A., 1995. Concentrations and export of solutes from six mountain streams in Northwestern Costa Rica. *J. N. Am. Benthol. Soc.* 14, 21-37.
- Nixon, S.W., Granger, S.L., Nowicki, B.L., 1995. An assessment of the annual mass balance of carbon, nitrogen, and phosphorus in Narragansett Bay. *Biogeochemistry* 31, 15-61.
- Vanderbilt, K.L., Lajtha, K., Swanson, F.J., 2002. Biogeochemistry of unpolluted forested watersheds in the Oregon Cascades: temporal patterns of precipitation and stream nitrogen fluxes. *Biogeochemistry* 62, 87-117.
- Williams, M.R., Melack, J.M., 1997. Atmospheric deposition, mass balances, and processes regulating streamwater solute concentrations in mixed conifer catchments of the Sierra Nevada, California. *Biogeochemistry* 37, 111-144.
- Wollheim, W.M., Pellerin, B.A., Vorosmarty, C.J., Hopkinson, C.S., 2005. N retention in urbanizing headwater catchments. *Ecosystems* 8, 871-884.

